

**MOLECULAR BASIS OF ANTAGONIST
ACTION AT THE P2X1 RECEPTOR**

**Thesis Submitted for the Degree of
Doctor of Philosophy
at the University of Leicester**

By Sam El-Ajouz

Department of Cell Physiology and Pharmacology

University of Leicester

June 2011

Abstract

P2X receptors are ATP-gated cation channels. P2X1 receptors are widely expressed throughout the body and have a range of functional roles, e.g. contraction of mesenteric arteries and regulation of blood clotting. The recent crystallisation of the zebra fish P2X4 receptor has provided a major advance in understanding the molecular basis of receptor properties. However, how agonists or antagonists are co-ordinated and the extent of the proposed ligand binding site have not been addressed at a structural level. A mutagenesis based approach was used to propose a model of the ATP binding site and has highlighted some residues involved in antagonist action at P2X receptors.

The aim of this thesis was to investigate the molecular basis of antagonist action at the P2X1 receptor using site-directed mutagenesis and P2X receptor chimeras. The wild-type, mutant and chimaeric P2X receptors were expressed in *Xenopus laevis* oocytes and the currents were characterised using two electrode voltage clamp. Initially, suramin was shown to act as a competitive antagonist and PPADS as a non-competitive antagonist at the P2X1 receptor. The contribution of residues V74 to G96 to human P2X1 receptor properties were determined using cysteine scanning mutagenesis. This region contains a residue that has been shown to be important in suramin action at the P2X4 receptor (K78) but cysteine mutation of the residues V74 to G96 had either no effect or slightly increased antagonism by suramin or PPADS. Also, a further residue was found to be important in ATP potency (F92) and the use of partial agonists and modification with cysteine reactive methanethiosulfonate (MTS) reagents identified additional residues important in channel activation. Mapping these residues onto a homology model of the P2X1 receptor showed the depth of the agonist binding site and highlighted the importance of the rear/inner cavity of the binding pocket in the gating of the channel subsequent to agonist binding.

The cysteine rich head region of the P2X receptor, which is adjacent to the proposed ATP binding pocket, is absent in the antagonist insensitive Dictyostelium receptors. P2X1 and P2X2 receptors have ~1400-fold difference in sensitivity to a suramin analogue NF449. Chimeras and point mutations in the cysteine rich head region were made between the P2X1 and P2X2 receptors and they identified the region between the third and fourth conserved cysteine residues of the P2X1 receptor as being important in conferring the difference in sensitivity. In particular, the positively charged residues at the base of the cysteine rich head region of the P2X1 receptor accounted for the highly selective antagonism of NF449 at the P2X1 receptor. Additionally, these residues were shown to play a role in the molecular basis of suramin and PPADS action at the P2X1 receptor. Reciprocal chimeras and mutations in the P2X2 receptor produced modest increases in antagonist sensitivity. *In silico* docking models highlighted possible sites of action for NF449 and suramin on the P2X1 receptor showing that the base of the cysteine rich head region may be important in the binding of antagonists. In summary, this research furthered understanding of ligand action at the P2X1 receptor.

Publications

Papers

Roberts, JA, Digby, HR, Kara, M, **El Ajouz, S**, Sutcliffe, MJ & Evans, RJ (2008). Cysteine substitution mutagenesis and the effects of methanethiosulfonate reagents at P2X2 and P2X4 receptors support a core common mode of ATP action at P2X receptors. *J Biol Chem* 283, 20126-36.

El-Ajouz, S, Ray, D, Allsopp, RC & Evans, RJ (2011). Molecular basis of selective antagonism of the P2X1 receptor for ATP by NF449 and suramin; contribution of basic amino acids in the cysteine rich loop. *Br J Pharmacol*, paper in press.

Allsopp, CA, **El-Ajouz, S**, Schmid, R & Evans, RJ (2011). Cysteine scanning mutagenesis (residues E52-G96) of the human P2X1 receptor for ATP; mapping agonist binding and channel gating. *J Biol Chem*, paper in press. (Joint 1st author).

Abstracts

El-Ajouz, S, Allsopp, RC & Evans, RJ. Cysteine scanning mutagenesis of the region Glu52 to Gly96 of the human P2X1 receptor refines a model of the ATP binding site and identifies residues that contribute to channel gating. *Poster presentation at the Purines 2010 conference, Tarragona, Spain and at the UK Purine Club 2010 conference, Nottingham.*

El-Ajouz, S, Allsopp, RC & Evans, RJ. Molecular basis of agonist action at the P2X1 receptor. *Oral presentation at the Young Physiology Symposium 2009, University of Leicester.*

Acknowledgements

Firstly, I would like to give a massive thank you to my exceptional supervisor, Prof. Richard Evans. I started in your lab as an undergraduate project student and your enthusiasm for the P2X1 receptor inspired me to do a PhD. Throughout my time at University you have given me encouragement, good teaching, excellent guidance, but most of all good company. Whenever I have needed a chat, either about my lab work or my personal life, you have always been there for me and given me sound advice. We have had many laughs together, especially with your great sense of humour, and I am so grateful for the opportunity you have given me in life. Also, a huge thank you for being so patient with me during the write up of this thesis, it has been a long journey, but I've got there in the end! I am also grateful to the British Heart Foundation for funding my project and everyone who attended my Lab Talks, especially Steve and Martyn, who gave me expert advice and feedback about my project. Many thanks to Ralf who constructed the homology model of the P2X1 receptor and provided me with many docking models.

I would also like to thank everyone in the lab for providing a stimulating environment. Especially thanks to Jon and Becky for helping me with new techniques, for keeping me company on the rig next to me and for enjoying my random stories. Also, thanks to Manijeh for the preparation of countless trays of oocytes every week! I would like to give a sincere thank you to Catherine who made me feel welcome in the lab when I first started as an undergraduate student, passing her knowledge onto me and also, has always been a good friend throughout my PhD. A big thank you goes to all my friends in CPP, who have kept me entertained at lunch every day and have always put a smile on my face. Especially thanks to Sophie who has been an awesome friend making life at University entertaining and enjoyable.

Also, I would like to say thank you to my gorgeous fiancée Serena, my family and all my friends outside of University. Massive thanks goes to two of my special friends, Brown and Yeomans, who have always given me support and laughter through 'whatsapp' everyday, especially Brown, for our daily chats at 12 o'clock on the dot. Also, I am grateful for the hospitality and friendship Shippers and Sam have given me and Serena during my PhD. I loved the many picnics and roasties we had together. The biggest thank you ever goes to Serena, I have been so lucky to come home to you every day during my PhD. You have patiently been waiting for me to join you in Australia for the past few months and your daily phone calls have been a great source of encouragement and motivation to finish my thesis. I would also like to thank my two sisters, Sara for her strong values in life and Suzy for the endless cups of tea, and my nephew Alex for always waking me up at the crack of dawn!

Finally, I am forever grateful to my parents, Joseph and Maria, who have given me a privileged education and their unconditional love and support every step of the way. I could not have got this far without them. Therefore, I dedicate this thesis to the best parents ever!

Abbreviations

2-meSATP	2- Methylthioadenosine- 5'- O- triphosphate
5-HT	5-hydroxytryptamine
ABC transporter	ATP-binding cassette transporters
ADP	Adenosine diphosphate
AFM	Atomic force microscopy
AMP	Adenosine monophosphate
AMPA	2-amino-3-(5-methyl-3-oxo-1,2- oxazol-4-yl)propanoic acid
ANAPP₃	Arylazido aminopropinyl adenosine triphosphate
Ap5A	P1, P5-di(adenosine-5') pentaphosphate
ASICs	Acid-sensing ion channels
ATP	Adenosine-5'-triphosphate
ATPγS	Adenosine 5'-O-(3-thio) triphosphate
BDNF	Brain-derived neurotrophic factor
BN-PAGE	Blue native polyacrylamide gel electrophoresis
BzATP	3'-O-(4-benzoyl)benzoyl adenosine 5'-triphosphate
cAMP	Cyclic adenosine monophosphate
CMV	Cytomegalovirus
CNS	Central nervous system
DAG	Diacylglycerol
DdP2X	<i>Dictyostelium discoideum</i> P2X
DNA	Deoxyribonucleic acid
DRG	Dorsal root ganglion
DTT	Dithiothreitol
EC₅₀	Half maximal effective concentration

EDTA	Ethylenediaminetetraacetic Acid
EM	Electron microscopy
ENaC	Epithelial sodium channel
ER	Endoplasmic reticulum
FRET	Fluorescence resonance energy transfer
FSEC	Fluorescence-detection size exclusion chromatograph
GABA	Gamma-aminobutyric acid
GPCRs	G-protein coupled receptors
G-protein	Guanosine nucleotide binding protein
HEK	Human embryonic kidney
IC₅₀	Half maximal inhibitory concentration
IP₃	Inositol triphosphate
IVM	Ivermectin
Kir	Inward rectifying potassium channel
KO	Knockout
LTP	Long term potentiation
LGICs	Ligand-gated ion channels
mACh	Muscarinic acetylcholine
MRS2220	Cyclic pyridoxine- α 4,5-monophosphate-6-azo-phenyl-2',5'disulfonate
MRS 2257	pyridoxal-5'-phosphonate 6-azophenyl 3',5'-bismethylenephosphonate
MTS	Methanethiosulfonate
MTSEA	(2-aminoethyl)methanethiosulfonate
MTSES	Sodium (2-sulfonatoethyl) methanethiosulfonate
MTSET	2-(Trimethylammonium)ethyl methanethiosulfonate bromide

NCS-ATP	Sulfhydryl-reactive 8-thiocyano-ATP
NF023	8,8'-(Carbonylbis(imino-3,1-phenylene carbonylimino)bis(1,3,5-naphthalenetrisulfonic acid))
NF279	8,8'-(Carbonylbis(imino-4,1-phenylenecarbonylimino-4,1-phenylenecarbonylimino))bis(1,3,5-naphthalenetrisulfonic acid))
NF449	4,4',4'',4'''-(Carbonylbis(imino-5,1,3-benzenetriylbis(carbonylimino)))
NMDA	N-methyl-D-aspartic acid
P2X	Purinoceptors 2X
P2Y	Purinoceptors 2Y
P-5-P	Pyridoxal-5-phosphate
PCR	Polymerase chain reactions
PGE2	Prostaglandin E2
PKC	Protein kinase C
PPADS	Pyridoxal-phosphate-6-azophenyl-2',4'-disulfonate
PPNDS	Pyridoxal-5'-phosphate-6-(2'-naphthylazo-6'-nitro-4',8'-disulfonate
RNA	Ribonucleic acid
SAD	Single-wavelength anomalous diffraction
SCAM	Substituted cysteine accessibility method
SCG	Superior cervical ganglia
SDS-PAGE	Sodium dodecyl sulfate polyacrylamide gel electrophoresis
SNP	Single-nucleotide polymorphism
TMs	Transmembrane segments/domains
TNP-ATP	[2'(3')-O-(2,4,6-Trinitrophenyl)adenosine 5'-triphosphate]

UDP	Uridine diphosphate
UTP	Uridine 5'- triphosphate
WT	Wild type
zP2X4	zebra fish P2X4.1
α,β-meATP	α,β -methylene ATP

Contents

Chapter 1. Introduction	1
1.1 Preface.....	1
1.2 Adenosine 5'-triphosphate (ATP).....	1
1.3 Purinergic Receptors	2
1.3.1 P1-purinoceptors.....	3
1.3.2 P2-purinoceptors.....	3
1.4 P2Y Receptors	4
1.5 P2X receptors	4
1.6 Cloning, distribution and physiological roles of the P2X receptors	5
1.6.1 P2X1 Receptors	6
1.6.2 P2X2 to P2X7 Receptors.....	9
1.7 Structural insight of the P2X receptor	12
1.7.1 Membrane Topology	12
1.7.2 Trimeric Assembly of P2X receptors	14
1.7.3 Heterotrimeric Receptors – Distribution and physiological roles	16
1.7.4 Tertiary structure of the P2X receptor and the location of agonist action ..	19
1.7.5 Properties of P2X receptors.....	19
1.8 Crystallisation of Zebra fish P2X4 receptor	24
1.8.1 Transmembrane domains and the pore region.....	27
1.8.2 Permeability.....	29
1.8.3 Extracellular loop ATP binding site	30
1.8.4 Model of the ATP binding site	35
1.8.5 Allosteric binding sites	38
1.8.6 Signal transduction	39
1.8.7 Antagonist binding site.....	40
1.8.8 Limitations of the zP2X4 receptor crystal structure	40
1.9 Thesis aims	41
Chapter 2. Materials and Methods	42
2.1 Molecular Biology.....	42
2.1.1 The human P2X1 receptor.....	42
2.1.2 Site-directed mutagenesis.....	43

2.1.3	Generation of chimeric P2X receptors	44
2.1.4	Transformation and plasmid DNA extraction	47
2.1.5	Sequencing	48
2.1.6	mRNA synthesis.....	48
2.2	Expression in <i>Xenopus laevis</i> oocytes	49
2.3	Two-electrode voltage clamp recordings	50
2.3.1	Measurement of agonist sensitivity	50
2.3.2	Characterisation of the effects of the different antagonists	51
2.3.3	Characterisation of the effect of the MTS compounds	51
2.3.4	Data analysis	52
2.4	Molecular modelling.....	52
Chapter 3. Characterisation of Suramin and PPADS.....		54
3.1	Introduction	54
3.1.1	Inhibition of the P2X receptor.....	54
3.1.2	P2 receptor antagonist Suramin.....	55
3.1.3	P2 receptor antagonist PPADS.....	56
3.1.4	Structure of suramin and PPADS.....	57
3.1.5	Aims	57
3.2	Results	58
3.2.1	ATP action at the human WT P2X1 receptor	58
3.2.2	Characterisation of suramin action at WT P2X1 receptor	58
3.2.3	Characterisation of PPADS action at WT P2X1 receptor.....	61
3.3	Discussion.....	68
3.3.1	Suramin acts as a competitive antagonist.....	68
3.3.2	Possible mechanisms of suramin action at the P2X1 receptor.....	71
3.3.3	PPADS acts as a non-competitive antagonist.....	74
Chapter 4. Involvement of region V74 to G96 in P2X1 receptor properties.....		78
4.1	Introduction	78
4.1.1	Aims	80
4.2	Results	81
4.2.1	F92 has a role in ATP potency at the P2X1 receptor	81
4.2.2	Partial agonists identify additional residues involved in agonist action	81

4.2.3	Effects of charged MTS reagents on cysteine mutants	83
4.2.4	Antagonist action at P2X1 receptor mutants	88
4.3	Discussion.....	92
4.3.1	Importance of F92 on ATP potency.....	92
4.3.2	Importance of the residues at the rear/inner cavity of the proposed ATP binding pocket in P2X1 receptor function.....	95
4.3.3	Residues V74-G96 do not have a large involvement in suramin and PPADS action	99
Chapter 5. Role of the cysteine rich loop on antagonist action.....		102
5.1	Introduction	102
5.1.1	The cysteine rich head region of the P2X receptor	102
5.1.2	Suramin analogues are selective P2X1 receptor antagonists	103
5.1.3	Physiological uses of NF449.....	106
5.1.4	Site of action of NF449	107
5.1.5	Aims	107
5.2	Results	108
5.2.1	Cysteine rich head region does not play a major role on ATP potency	108
5.2.2	Cysteine rich head region is important in NF449 sensitivity	111
5.2.3	Smaller sub-divided chimeras revealed the importance of the base region in NF449 sensitivity.....	113
5.2.4	The importance of the basic amino acids in the region C132 to C149 on NF449 sensitivity.....	116
5.2.5	NF449 sensitivity is partially recovered at the reciprocal mutations in the P2X2 receptor	125
5.3	Discussion.....	131
5.3.1	The involvement of the cysteine rich head region on P2X1 receptor properties	131
5.3.2	The importance of basic amino acids at the base of head region in determining NF449 sensitivity	132
5.3.3	NF449 interacts with different parts of the cysteine rich head region	134
5.3.4	Molecular docking of NF449 at the P2X1 receptor	137
Chapter 6. Role of cysteine rich head region on suramin and PPADS action		143
6.1	Introduction	143

6.1.1	Molecular basis of Suramin action at the P2X receptor.....	143
6.1.2	Molecular basis of PPADS action at the P2X receptor.....	144
6.1.3	Aims.....	145
6.2	Results.....	146
6.2.1	Suramin action at the P2X1 and P2X2 receptors.....	146
6.2.2	The cysteine rich head region contributes to suramin sensitivity.....	146
6.2.3	Basic amino acids at the base of the cysteine rich head region contribute to suramin sensitivity at the P2X1 receptor.....	149
6.2.4	Suramin sensitivity is partially recovered at the reciprocal mutations in the P2X2 receptor.....	151
6.2.5	PPADS sensitivity at the WT P2X1 and P2X2 receptor.....	154
6.2.6	Cysteine rich head region also plays a role in PPADS sensitivity.....	154
6.2.7	Basic amino acids at the base of cysteine rich head region also contribute to PPADS sensitivity at the P2X1 receptor.....	156
6.2.8	PPADS action on the reciprocal mutations in the P2X2 receptor.....	160
6.3	Discussion.....	163
6.3.1	Role of the base of the cysteine rich head region in suramin action.....	163
6.3.2	PPADS may coordinate with the base of the cysteine rich head region....	165
6.3.3	Top and middle regions of the cysteine rich head region contribute to both suramin and PPADS sensitivity.....	166
6.3.4	Molecular docking of Suramin at P2X1 receptor.....	169
6.3.5	Proposed site of PPADS action.....	173
Chapter 7. General discussion.....		175
References.....		185

Chapter 1. Introduction

1.1 Preface

P2X receptors for ATP provide potential therapeutic targets for a range of diseases. This thesis is focused on understanding the molecular basis of ligand action at the P2X1 receptor. The introduction provides a historical background to the concept of purinergic transmission, the classification of P2X receptors, their subtypes, the basic structure of P2X receptors, the crystallisation of the zebra fish P2X4 receptor and the proposed mode of ligand action.

1.2 Adenosine 5'-triphosphate (ATP)

ATP was initially identified by Lohmann and Fiske in 1929 through the isolation of hexose phosphates from muscle extracts. Subsequently, ATP was known to be the universal carrier of bioenergy in cells. The structure of ATP has an adenine base, ribose sugar and a tail consisting of 3 phosphate groups (Figure 1.1; Baddiley *et al.*, 1949). The release of energy from ATP is generated through the hydrolysis of the covalent bond between the second and the third phosphate group, forming adenosine diphosphate (ADP).

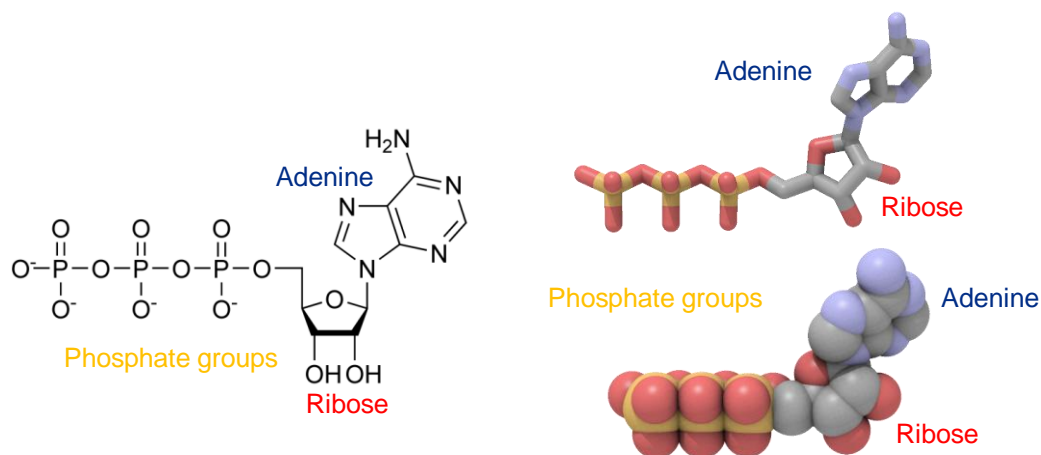


Figure 1.1 Structure of ATP. ATP consists of 3 phosphate groups, a ribose and an adenine. The molecular structure is on the left panel and the .pdb of ATP is in sticks and in spheres on the right panel.

The first evidence that ATP can have an extracellular role in muscular contraction was provided in 1929 by Drury and Szent-Gyorgyi. Extracellular adenine compounds, such as ATP and adenosine, were injected into dogs and guinea-pigs and caused bradycardia and heart block (Drury and Szent-Gyorgyi, 1929). Subsequent studies investigated the

action of extracellular ATP. The vasodilator effects caused by the arterial injection of spinal root extracts were thought to be due to ATP or ADP (Holton *et al.*, 1954). An ultraviolet absorption spectrum indicated the existence of ATP in the spinal root extracts and when ATP or ADP were injected into the rabbit ear artery, prolonged vasodilatation was observed (Holten *et al.*, 1954). In 1959, Holton further suggested that nerves were the source of ATP. During mechanical and electrical stimulation of the great auricular nerves in rabbits, ATP was liberated from the nerve terminal resulting in vasodilatation (Holton, 1959). In the late 1950s, ATP and noradrenaline were shown to be present in sympathetic nerves and ATP was suggested to be the chemical energy supply for the maintenance of membrane permeability (Caldwell *et al.*, 1957; Schumann, 1958). Initially, ATP was thought to be released from nerves and be involved in processes such as muscle contraction (Davies, 1963). However, it is now known that ATP is not just released from nerves and the increase in extracellular ATP can be achieved in various ways. For example, ATP can be released from damaged cells, cells under shear stress, cell death, neuronal vesicles, via ATP-binding cassette (ABC) transporters and from platelets (Bodin *et al.*, 2001). Once ATP is released into the extracellular environment, ecto-ATPases can break it down to ADP. ATP has also been shown to be co-released in the nervous system with classical transmitters such as GABA (Jo and Schlichter, 1999) and acetylcholine (Salgado *et al.*, 2000).

1.3 Purinergic Receptors

In 1972, the concept of ATP acting as a neurotransmitter on purinoceptors was proposed due to the presence of non-adrenergic and non-cholinergic responses (Burnstock, 1972). Nerve stimulation of the guinea pig taenia coli, which are smooth muscle on the gut, still evoked a response when the adrenergic and cholinergic evoked responses were antagonised by guanethidine and atropine (Burnstock, 1972). The response was mimicked following ATP application raising the idea that nerves can release ATP into the gastrointestinal tract and act at a receptor for ATP. This was termed the purinergic receptor, which could be stimulated by nucleotide molecules. In the late 1970s, the purinergic receptors were divided into two classes, nucleosides acting on the P1-purinergic receptors and nucleotides on the P2-purinergic receptors (Burnstock *et al.*, 1978). The sub-classification was based on the different potencies of ATP, ADP, AMP, and adenosine at

the receptors. In subsequent work, different subdivisions within these types of purinoceptors were classified according to their molecular structure, sensitivity to different agonists and their tissue distribution. The P1-purinoceptors, known as the adenosine receptors (A_1 , A_{2A} , A_{2B} and A_3), are sensitive to adenosine and the P2-purinoceptors (P2X and P2Y) are sensitive to ATP and/or ADP (Abbracchio *et al.*, 1994).

1.3.1 P1-purinoceptors

The P1-purinoceptors, which are more commonly referred to as adenosine receptors, were initially subdivided into two different types of receptors, A1 and A2. This was due to the differences in the action of adenosine on glial cells in a perinatal mouse brain (van Calker *et al.*, 1979). Adenosine either caused inhibition (through A1 receptors) or stimulation (through A2 receptors) of cyclic adenosine monophosphate (cAMP) production (van Calker *et al.*, 1979). Four different adenosine receptors have now been cloned (A_1 , A_{2A} , A_{2B} and A_3) which are all metabotropic G-protein coupled receptors (Fredholm *et al.*, 1994). These receptors have been shown to couple to different G-proteins having different effector systems, such as; (i) A_1 coupling to G_i causing a decrease in cAMP production, (ii) A_{2A} coupling to G_s causing an increase in cAMP production, (iii) A_{2B} coupling to G_s and G_q causing an increase in cAMP and inositol triphosphate (IP_3) production and (iv) A_3 coupling to G_i and G_q causing a decrease in cAMP production but an increase in IP_3 production (Ralevic and Burnstock, 1998). The adenosine receptors are expressed in a wide variety of cell types leading to a range of functions, for example; (i) A_1 receptors are expressed in cardiac muscle causing bradycardia (Belardinelli *et al.*, 1995), (ii) A_{2B} receptors are expressed in the airways leading to bronchoconstriction (Pauwels and Joos, 1995) and (iii) A_3 receptors are expressed in the brain and can modulate behaviour (Jacobson *et al.*, 1993).

1.3.2 P2-purinoceptors

Review of the literature suggested that the P2-purinoceptors could be divided into two types of receptors (Burnstock and Kennedy, 1985). This was determined based on different rank orders of agonist potency of ATP analogues and the different antagonist activity (Burnstock and Kennedy, 1985). Early work supported this idea by showing that the different types of P2-purinoceptors had different properties and functions (Bertrand *et*

al., 1987). This was due to the comparison of ATP and an analogue of ATP, 2-methylthioadenosine triphosphate (2-methylthio ATP), on insulin secretion and the flow rate in a rat pancreas (Bertrand *et al.*, 1987). A P2Y subtype, which is on the beta cell of the pancreas, was shown to mediate insulin secretion and a P2X subtype, which is on the vascular bed of the rat pancreas, was shown to mediate vasoconstriction (Bertrand *et al.*, 1987).

1.4 P2Y Receptors

The P2Y receptor family are seven transmembrane domain receptors that are coupled to G-proteins. After their classification in 1985 by Burnstock and Kennedy, the first P2Y family members were cloned in 1993 by Webb *et al.* and Lustig *et al.* from an embryonic chick brain and mouse neuroblastoma cells (Webb *et al.*, 1993; Lustig *et al.*, 1993). Subsequent work cloned a total of 8 different P2Y subtypes, which can be broadly subdivided into G_q-coupled receptors (P2Y1, P2Y2, P2Y4 and P2Y6) and G_i-coupled receptors (P2Y12, P2Y13 and P2Y14) (Dubyak, 2003).

The G_q-coupled subtypes activate phospholipase C, which hydrolyses phosphatidylinositol 4,5-bisphosphate (PIP₂) to IP₃ and 1,2-diacylglycerol (DAG), and the G_i-coupled subtypes inhibit adenylate cyclase decreasing cAMP production. The P2Y11 subtype is one exception that was found to not only activate G_q but also G_s. This G-protein activates adenylate cyclase increasing cAMP production. Depending on what subtypes of the P2Y receptor are present they can be stimulated by nucleotides such as ATP, ADP, uridine 5'-triphosphate (UTP), uridine diphosphate (UDP) and UDP-glucose. P2Y receptors are expressed in the vascular system, brain, heart and the immune system. Knock out mice have identified the involvement of P2Y4 receptors in epithelial tissues in airway cells (Dubyak, 2003) and P2Y1 and P2Y12 receptors in platelet aggregation (Foster *et al.*, 2001; Hechler *et al.*, 2005). Drugs targeting the different P2Y receptor subtypes could potentially be beneficial for cystic fibrosis and anti-thrombotic treatments.

1.5 P2X receptors

P2X receptors were originally classified by Burnstock and Kennedy (1985) based on their sensitivity to the agonist, α,β -methylene ATP. Activation of P2X receptors on

rabbit arterial smooth muscle cells with ATP caused the influx of Na⁺ and Ca²⁺ ions (Benham, 1987). These channels were found to be non-selective for cations as ATP-induced currents were still present in the rat vas deferens smooth muscle after voltage-gated Ca²⁺ and K⁺ currents were eliminated (Nakazawa *et al.*, 1987). Several studies on different tissues highlighted the presence of ATP-gated channels, for example, (i) Benham *et al.* identified ATP-gated channels in arterial smooth muscle cells and in single smooth muscle cells dissociated from rabbit ear artery (Benham and Tsien, 1987, Benham *et al.*, 1987, Benham, 1989), (ii) ATP was found to excite a subpopulation of neurones; in the rat dorsal horn and dorsal root ganglion, and a large number of neurones isolated from various sensory ganglia of the rat and cat (Jahr and Jessell, 1983, Krishtal *et al.*, 1983), (iii) ATP-activated channels were found in neuronal pheochromocytoma PC12 cells, where single channel currents were recorded upon the application of ATP (Nakazawa *et al.*, 1990). These studies indicated that there were most likely to be P2X receptors in a range of cells such as smooth muscle cells of the vas deferens and in neurons of PC12 cells (Westfall *et al.*, 1982, Taylor *et al.*, 1983, Dunn and Blakeley, 1988, Nakazawa *et al.*, 1991, Sela *et al.*, 1991). Subsequently, the different subtypes of P2X receptors were isolated from these cells.

1.6 Cloning, distribution and physiological roles of the P2X receptors

Genes encoding the P2X receptors were isolated by expression cloning from different tissues. The first two subtypes of the P2X receptor were isolated from the vas deferens and pheochromocytoma cells and were named the P2X1 (Valera *et al.*, 1994) and P2X2 receptors (Brake *et al.*, 1994). Subsequently, 5 other subtypes of the P2X receptor family were isolated through PCR and hybridisation (Table 1.1); P2X3 receptors are expressed in the sensory neurones and were isolated from the dorsal root ganglia (Chen *et al.*, 1995), P2X4 receptors were isolated from the rat hippocampus (Bo *et al.*, 1995), P2X5 receptors were isolated from rat celiac ganglia (Collo *et al.*, 1996) and the P2X6 and P2X7 receptors were isolated from rat cervical ganglia (Collo *et al.*, 1996; Surprenant *et al.*, 1996). The P2X receptors are distributed throughout many different tissues (Table 1.1) and to investigate the function of the different P2X receptor subtypes, knockout (KO) mice models were constructed.

Subtype	Isolated Tissue	Distribution
P2X1	Vas deferens (Valera <i>et al.</i> , 1994)	Smooth muscle, heart, platelet, sensory ganglia, cerebellum (Valera <i>et al.</i> , 1994; Kidd <i>et al.</i> , 1995; Collo <i>et al.</i> , 1996; Scase <i>et al.</i> , 1998)
P2X2	Pheochromocytoma cells (Brake <i>et al.</i> , 1994)	Autonomic ganglia, brain, pituitary, sensory ganglia, smooth muscle, retina (Brake <i>et al.</i> , 1994; Chen <i>et al.</i> , 1995; Kidd <i>et al.</i> , 1995; Collo <i>et al.</i> , 1996; Vulchanova <i>et al.</i> , 1996)
P2X3	Dorsal root ganglion (Chen <i>et al.</i> , 1995)	Sensory ganglia, sympathetic neurons (Chen <i>et al.</i> , 1995; Collo <i>et al.</i> , 1996)
P2X4	Hippocampus (Bo <i>et al.</i> , 1995)	Hippocampus, testes, colon, smooth muscle (Bo <i>et al.</i> , 1995; Buell <i>et al.</i> , 1996; Soto <i>et al.</i> , 1996; Wang <i>et al.</i> , 1996)
P2X5	Celiac ganglion (Collo <i>et al.</i> , 1996)	Heart, gut, bladder, autonomic ganglia, spinal cord (Collo <i>et al.</i> , 1996)
P2X6	Superior cervical ganglion (Collo <i>et al.</i> , 1996)	Skeletal muscle, brain, autonomic ganglia (Collo <i>et al.</i> , 1996; Soto <i>et al.</i> , 1996)
P2X7	Superior cervical ganglion (Surprenant <i>et al.</i> , 1996)	Apoptotic cells, macrophages, lymphocytes, skin (Surprenant <i>et al.</i> , 1996)

Table 1.1. Cloning and distribution of the P2X receptor subtypes. The isolated tissue of where each P2X receptor was cloned from and the distribution of the subtypes are listed.

1.6.1 P2X1 Receptors

The P2X1 receptor is known to be expressed in a variety of different tissues and to investigate the function of the P2X1 receptor KO mice have been used. Removing the function of the P2X1 receptor with KO mice highlighted the importance of the P2X1 receptor in the vas deferens for normal male reproductive function (Mulryan *et al.*, 2000). KO mice had a reduction in the male fertility by ~90% compared to the wild-type (WT), with female fertility being unaffected (Mulryan *et al.*, 2000). Also, the contraction of the vas deferens during sympathetic nerve stimulation was reduced by ~60% (Mulryan *et al.*, 2000). This reduction in contraction did not affect the ability of the male mice to copulate but reduced the amount of sperm in the ejaculate (Mulryan *et al.*, 2000). This suggested that drugs targeting the P2X1 receptor could potentially be useful non-hormonal male contraceptive pills.

P2X1 receptors were also present in human platelets and were shown to mediate a rapid phase of ATP-evoked calcium entry (Mackenzie *et al.*, 1996; Vial *et al.*, 1997; Scase *et al.*, 1998).. Megakaryocytes, which are platelet progenitor cells, are known for having a

role in maintaining normal blood platelet count (Kaushansky, 1999). The spleen and bone marrow of P2X1 receptor KO mice were studied using immunohistochemical methods (Vial *et al.*, 2002). Removing the P2X1 receptor did not reduce the number or distribution of megakaryocytes, showing that the P2X1 receptor was not essential for megakaryocyte formation (Vial *et al.*, 2002). However, the ATP-evoked response at megakaryocytes from P2X1 receptor KO mice lacked the initial transient inward current and the inward cation current associated with P2Y-evoked Ca^{2+} release was reduced by approximately 50% (Vial *et al.*, 2002). Also, when the P2X1 and P2Y1 receptors were co-stimulated in human platelets there was a marked acceleration and amplification of the calcium release, highlighting a synergistic interaction between the P2X1 and P2Y1 receptors (Vial *et al.*, 2002). Therefore, during platelet stimulation P2X1 receptors were suggested to have a priming role in the following activation of P2Y1 receptors.

Subsequently, platelets from P2X1 receptor KO mice were used to identify the role of the P2X1 receptor in the response to thrombogenic stimuli (Hechler *et al.*, 2003). When the wall shear rate was elevated, there was a reduced collagen-induced aggregation, secretion of P2X1 receptor KO platelets and a decreased thrombus growth on a collagen-coated surface (Hechler *et al.*, 2003). *In vivo*, removing the function of the P2X1 receptor did not affect the bleeding time of mice suggesting that the P2X1 receptor had little involvement in primary hemostasis (Hechler *et al.*, 2003). However, the mortality of P2X1 receptor KO mice in a model of systemic thromboembolism was reduced, and after laser-induced vessel wall injury the size of the thrombi and the time to remove it were also reduced (Hechler *et al.*, 2003). Interestingly, a study that overexpressed the P2X1 receptor in transgenic mice supported these results (Oury *et al.*, 2003). In models of shear stress and thromboembolism there were increases in platelet aggregation and increases in mortality rates compared to wild-type mice (Oury *et al.*, 2003). Therefore, the P2X1 receptor appeared to play a functional role in the formation of platelet thrombi, especially when shear forces are high.

The P2X1 receptor have also been shown to be involved in the vasoconstriction of mouse mesenteric arteries (Vial and Evans, 2002). α,β -methylene ATP failed to evoke currents and contractions from a range of vascular beds in P2X1 receptor KO arteries.

Also, during nerve stimulation, vasoconstriction was reduced by ~50% in P2X1 receptor KO studies, which was similar to the reduction in vasoconstriction with normal mice in the presence of the non-selective P2X receptor antagonist pyridoxalphosphate-6-azophenyl-2'-5'-disulfonate (PPADS). This demonstrated that the P2X1 receptor may contribute approximately 50% to sympathetic neurogenic vasoconstriction and underlies the P2X receptor phenotype in the artery smooth muscle (Vial and Evans, 2002).

The P2X1 receptor has also been shown to be involved in the contractions of urinary bladder smooth muscle, alongside the muscarinic acetylcholine (mACh) receptors (Vial and Evans, 2000; Heppner *et al.*, 2009). In P2X1 receptor KO mice, the nerve stimulated contractions in bladder smooth muscle were reduced by 30% compared to WT and the contractions were only being mediated by the mACh receptor (Vial and Evans, 2000). A recent study supported the contribution of the purinergic and muscarinic pathways in the contraction of the urinary bladder smooth muscle by using P2X1 receptor KO mice (Heppner *et al.*, 2009). This study also revealed that the P2X1 receptor and mACh receptors shape the time course of the force transients, with the P2X1 receptor contributing to the rapid rise of force and the mACh receptor contributing to duration of the force transient (Heppner *et al.*, 2009). This was due to the P2X1 receptor causing rapid nerve excitability and the mACh receptor having a delayed and longer increase in excitability. Interestingly, removing the function of the P2X1 receptor led to a significant increase in the calcium flashes subsequent to the electrical field stimulation, which caused an increase in the force transient (Heppner *et al.*, 2009). This highlighted a possible inhibitory effect of the P2X1 receptor, which modulated subsequent muscarinic driven contractions by suppressing increases in excitability and force generation post-synaptically (Heppner *et al.*, 2009).

The P2X1 receptor has also been shown to play a role in the autoregulation of arterial tone in kidneys (Inscho *et al.*, 2003). Autoregulatory responses induced by an increase in the renal perfusion pressure were reduced in P2X1 receptor KO mice (Inscho *et al.*, 2003). KO studies have also highlighted the presence of the P2X1 receptor in mouse peritoneal macrophages (Sim *et al.*, 2007) and in the auditory brainstem synapse (Watano *et al.*, 2004). A more recent study highlighted the role of the P2X1 receptor in chemotaxis

in neutrophils (Lecut *et al.*, 2009). In KO mice the rapidly desensitising currents in neutrophils were removed, the neutrophils migrated with a reduced speed and neutrophil recruitment in the mouse peritoneum was impaired (Lecut *et al.*, 2009). Therefore, the P2X1 receptor was shown to be involved in promoting neutrophil chemotaxis and could play a role in host defence and inflammation (Lecut *et al.*, 2009).

The homomeric P2X1 receptor appears to play a role in a range of physiological processes. However, P2X1 receptor subunits are also thought to form heteromeric P2X receptors (see Section 1.7.3) and these channels can highlight additional roles of the P2X1 receptor subunit. Therefore, the developments of drugs targeting the P2X1 receptor could not only act on homomeric P2X receptors but also heteromeric P2X receptors. From the studies described above, drugs targeting the P2X1 receptor could potentially be beneficial for the treatment of several clinical conditions, such as hypertension, stroke and overactive bladders.

1.6.2 P2X2 to P2X7 Receptors

The P2X2 receptor was first cloned by Brake *et al.* (1994) from rat pheochromocytoma PC12 cells and is distributed in various tissues (Table 1.1). Mechanistically, the P2X2 receptor has been shown to be important in various areas, such as; (i) in the carotid body to detect hypoxic conditions, where P2X2 KO mice had a reduced ventilatory response (Rong *et al.*, 2003), (ii) chemosensory transduction by P2X2 receptors is thought to play a role in the detection and identification of different chemical stimuli, such as odorants (Spehr *et al.*, 2004) and taste in the oral cavity (Finger *et al.*, 2005), and (iii) P2X2 receptor KO mice eliminated the response in taste nerves, suggesting that ATP acting on the P2X2 receptor can link the taste buds to the nervous system (Finger *et al.*, 2005). Also, P2X2 receptors are widely expressed in the central nervous system and have been found to play a role in ATP-mediated fast synaptic transmission regulating processes such as learning, memory and sensory integration (Gever *et al.*, 2006).

The P2X3 receptor was cloned by Chen *et al.* (1995) from rat dorsal-root-ganglion sensory neurones and functional P2X3 receptors have been detected in sensory neurons. During cell damage there may be a release of ATP which activates the P2X3 receptor. P2X3 receptor KO mice had normal responses to noxious mechanical and thermal heat but

they were unable to detect the intensity of non-noxious warming stimuli (Souslova *et al.*, 2000). Also, there was a reduction in nerve injury, chronic inflammatory nociception and neuropathetic pain when the function of the P2X3 receptor was removed by using KO mice or selective antagonists (Jarvis *et al.*, 2002; Kennedy *et al.*, 2003). Therefore, drugs targeting the P2X3 receptor could potentially reduce chronic pain and be novel analgesics.

P2X3 receptors could also be a target for the treatment of indigestion (Bian *et al.*, 2003; McIlwrath *et al.*, 2009). Peristalsis was reduced in ileal segments from P2X3 receptor KO mice and the P2X3 receptor was shown to contribute to the detection of distension (Bian *et al.*, 2003). A more recent study confirmed the involvement of the P2X3 receptor in the gut as there were reductions in the inward currents of gastric nodose neurons in P2X3 receptor KO mice (McIlwrath *et al.*, 2009). Also, in response to fluid distension of the oesophagus and stomach there was a blunted response in the gastro-oesophageal sensory neurones of P2X3 receptor KO mice (McIlwrath *et al.*, 2009). Therefore, the P2X3 receptor may contribute to the sensation of fullness or nausea and drugs targeting this receptor could potentially treat dyspeptic symptoms.

The P2X4 receptor was cloned initially from rat hippocampus by Bo *et al.* (1995). The P2X4 receptor was subsequently isolated from DRG cells (Buell *et al.*, 1996) and from rat brain (Seguela *et al.*, 1996). P2X4 receptors have been shown to be associated with inflammatory pain as when they were up regulated in hyperactive glial cells, there was an increased sensitivity to pain, creating tactile allodynia (Tsuda *et al.*, 2003). Subsequent work has shown that in response to peripheral nerve injury P2X4 receptor KO mice lack mechanical hyperalgesia and have reduced brain-derived neurotrophic factor (BDNF) signalling in the spinal cord (Ulmann *et al.*, 2008). Therefore, the P2X4 receptor may contribute to chronic pain through a central inflammatory pathway. Novel drugs targeting the P2X4 receptor could potentially limit microglia-mediated inflammatory responses associated with brain injury and neurodegenerative disorders (Ulmann *et al.*, 2008). A more recent study has shown that the P2X4 receptor is also involved in inflammatory-mediated prostaglandin E2 (PGE2) production (Ulmann *et al.*, 2010). KO mice lack any PGE2 in tissue exudates and do not develop pain hypersensitivity (Ulmann *et al.*, 2010).

The P2X4 receptor has been shown to be involved in nerve injury-induced tactile allodynia (Tsuda *et al.*, 2009). P2X4 receptor KO mice had attenuated pain hypersensitivity to innocuous mechanical stimuli (tactile allodynia) and in a test of neuropathic pain, during injury to the spinal nerve, tactile allodynia was blunted (Tsuda *et al.*, 2009). This highlighted the possibility of a therapeutic benefit of blocking the P2X4 receptor in the treatment of chronic pain, especially tactile allodynia after nerve injury (Tsuda *et al.*, 2009). P2X4 receptor KO studies have further highlighted the role of the P2X4 receptor in; (i) calcium influx into human endothelial cells during fluid shear stress (Yamamoto *et al.*, 2000), (ii) synaptic strengthening and long term potentiation (LTP) (Sim *et al.*, 2006), (iii) flow-sensitive mechanisms that regulate blood pressure and vascular remodelling in the endothelia (Yamamoto *et al.*, 2006), and (iv) ATP-evoked currents produced from peritoneal macrophages (Brone *et al.*, 2007).

The P2X5 receptor was cloned by Collo *et al.* (1996) from rat celiac ganglia. The P2X5 receptor is expressed in areas such as epithelial cells in the nasal mucosa, in the gut and on the skin (Gever *et al.*, 2006). P2X5 receptors are also present in non-melanoma skin cancers and may be associated with the differentiation of the cells to different types of cancer (Greig *et al.*, 2003). There have been no investigations to this date using P2X5 receptor KO mice. The P2X5 receptor is believed form a heterotrimeric channel with P2X1 receptor subunits (see later) and a recent study has shown that most humans only express a non-functional isoform of the P2X5 receptor (Kotnis *et al.*, 2010). This non-functional isoform arises from a single-nucleotide polymorphism (SNP) at the 3' splice of exon 10. Therefore, it may be hard to identify the physiological roles of the P2X5 receptor in humans.

The P2X6 receptor was cloned by Collo *et al.* (1996) from rat superior cervical ganglia. This subtype is expressed in areas such as the sensory ganglia, the thymus and in human salivary gland epithelial cells (Gever *et al.*, 2006). Also, these receptors are the only subtype found to be up regulated during chronic heart failure (Banfi *et al.*, 2005). Novel drugs targeting the P2X6 receptor could reduce this potential pathogenic mechanism in chronic heart failure. There have also been no investigations to this date using P2X6 receptor KO mice.

The P2X7 receptor was cloned by Surprenant *et al.* (1996) from rat brain. This subtype has shown to be expressed in macrophages, monocytes and lymphocytes. P2X7 receptor KO studies have highlighted the role of P2X7 receptors in bone formation and resorption. These receptors are involved in leukocyte function and are important in the inflammatory response of joints (Labasi *et al.*, 2002). Novel drugs targeting the P2X7 receptor could reduce the inflammatory response in arthritis and be used in the management of skeletal disorders such as osteoporosis (Ke *et al.*, 2003). Also, KO studies have shown that the P2X7 receptor may be important in cytokine signalling (Solle *et al.*, 2001) and macrophage function (Le Feuvre *et al.*, 2002). P2X7 receptors can also play a key role in the clearance of pathogens by aiding the movement the cilia in bronchioles (Ma *et al.*, 2006). Therefore, drugs increasing the function of the P2X7 receptor could potentially increase the movement of the cilia and benefit patients with cystic fibrosis.

The use of KO studies has highlighted the role of P2X receptors in native conditions. Combining the data obtained from native and recombinant P2X receptors, they can clearly be divided into different subtypes based on their different properties. The different properties of these channels, including their pharmacological profile, are explained in section 1.7.5.

1.7 Structural insight of the P2X receptor

Characterisation of the P2X receptor showed that the sequence was dissimilar to any other ligand gated ion channels. Initially, to try and determine the structure of the P2X receptor molecular and biochemical studies were carried out. Subsequently, the knowledge obtained from these studies was substantiated with the crystal structure of the zebra fish P2X4 receptor (explained in section 1.8). To begin with the historical perspective of the P2X receptor structure based on its sequence is explained below.

1.7.1 Membrane Topology

Hydrophobicity plots identified two hydrophobic regions (~20 amino acids) long enough to be a transmembrane domain and cross the lipid bilayer (Brake *et al.*, 1994; Valera *et al.*, 1994; North, 1996). This suggested the possibility of two transmembrane domains. If there are two transmembrane domains then the N- and the C-termini could either be intra- or extracellular. The lack of a leader signal peptide on the N-terminus of the

P2X receptor suggested that the termini are intracellular (Brake *et al.*, 1994). Therefore, the P2X receptor was predicted to have a topology of two transmembrane domains, with intracellular N- and C-termini and a large extracellular loop. This topology is similar to the pore-forming subunits of the epithelial sodium channels (Renard *et al.*, 1994) but there is no sequence homology between the epithelial sodium channel and the P2X receptor (North, 1996). The membrane topology of the P2X receptor was further supported by immunofluorescence, glycosylation and mutagenesis studies. For example, Torres *et al.* (1998b) indicated through immunofluorescence studies that the N- and C-termini are intracellular. Anti-bodies only had access to the N- and C-termini epitopes when the cells were permeabilised suggesting that the termini were intracellular (Torres *et al.*, 1998b).

Glycosylation occurs naturally in the endoplasmic reticulum (ER) during protein synthesis, where sugars are added to the protein at asparagine (N) residues. This post translation modification only occurs on the extracellular domain of a protein and relates to protein folding. The P2X receptor mass was greater than the predicted mass suggesting the possibility of post translation modification of the receptor (Valera *et al.*, 1994; Brake *et al.*, 1994). The consensus site for areas of glycosylation is known to be an asparagine – any amino acid (X) – serine or threonine (N-X-S/T). In the predicted extracellular domain of the P2X2 receptor, there were 3 possible N-linked glycosylation sites in the sequence (Brake *et al.*, 1994). By either mutating these sequences or adding the sequence to a part of the protein, glycosylation could be observed from the change in the molecular weight of the protein, which can be detected in a western blot. Glycosylation studies could therefore demonstrate whether a part of the protein is intracellular or extracellular.

Glycosylation studies were first carried out by Torres *et al.* (1998a; 1998b) and Newbolt *et al.* (1998). N-glycosylation scanning mutagenesis, which added the consensus site of glycosylation into the sequence, showed that the regions of the central loop of the P2X2 receptor could be glycosylated and the regions by the termini could not (Torres *et al.*, 1998a). This further indicated that there is an extracellular loop with an intracellular N- and C-termini. Also, the three potential glycosylation sites in the proposed extracellular loop were mutated out of the P2X2 receptor (Torres *et al.*, 1998b). These mutated receptors were not highly expressed on the cell surface and had a reduced molecular

weight, from 70kDa to 55Kda, indicating that these predicted glycosylation sites are on the proposed extracellular loop. Therefore, mutagenesis studies highlighted the sites of glycosylation to include the asparagine residues at positions 182, 239 and 298 in the P2X2 receptor (Torres *et al.*, 1998b). Another study investigated the glycosylation pattern of the P2X2 receptor by adding the consensus site of glycosylation to detect the boundaries of the each end of the extracellular loop (Newbolt *et al.*, 1998). Western blot analysis indicated that glycosylation does not occur close to the proposed transmembrane domains on the intracellular side but does occur on the extracellular region (Newbolt *et al.*, 1998).

Further mutagenesis studies have shown that residues involved in agonist and antagonist action are part of the predicted extracellular loop. For example, mutating the lysine residues at position 68 and 70 in the P2X1 receptor reduced ATP potency (Ennion *et al.*, 2000) and mutating the lysine residue at position 78 in the P2X4 receptor reduced suramin sensitivity (Garcia-Guzman *et al.*, 1997). This suggested that the middle part of the sequence between the transmembrane domains is important in the binding of extracellular drugs (described in more detail later).

The topology of the P2X receptor is distinct to the other two families of the ligand-gated ion channels; the cys-loop superfamily (e.g. nicotinic receptors, 5-HT₃ receptors) and the glutamate cationic channel family (e.g. NMDA receptors). The cys-loop superfamily contains five transmembrane domains with extracellular termini (Rang and Ritter, 1999), and the glutamate cationic channel family contain three transmembrane domains with an intracellular C-terminal and an extracellular N-terminal (Rosenmund *et al.*, 1998). Interestingly, a few channels share a similar topology to the P2X receptor, such as the inward rectifying potassium (Kir) channel (Nichols and Lopatin, 1997), the acid-sensing ionic channels (ASICs) (Saugstad *et al.*, 2004) and the epithelial sodium channel (ENaC) (Snyder *et al.*, 1994). However, these channels have no sequence homology with the P2X receptors.

1.7.2 Trimeric Assembly of P2X receptors

The subunit assembly of the cys-loop superfamily and the glutamate cationic channel family consist of 5 subunits (pentameric) and 4 subunits (tetrameric), respectively (Surprenant *et al.*, 1995). The channels with topological similarity form multimeric

channels and the formation of a functional channel pore in the P2X receptor would unlikely have just one subunit with two transmembrane domains. Bean (1990) suggested that three molecules of ATP are required to bind and open P2X receptors and the P2X receptor could possibly form a multimeric complex. This was due to the concentration-response curve from the ATP-activated channels in rat and bullfrog sensory neurones having a Hill coefficient of ~ 3 (Bean, 1990). Bean (1990) suggested that ATP binds to 3 identical, non-interacting sites in order to activate the channel. Subsequent work on recombinant P2X receptors showed that the Hill coefficients of the concentration-response curves were greater than one (Brake *et al.*, 1995; Evans *et al.*, 1995). This indicated that there is more than one molecule of ATP binding to each P2X receptor and they may form heteromeric channels. Also, novel phenotypes were observed when the P2X2 and P2X3 subunits were co-expressed, suggesting that the P2X receptor forms heteromers of at least two subunits (described in more detail later; Lewis *et al.*, 1995).

To investigate the number of subunits required to form a functional P2X receptor, a study used chemical cross-linking and blue native polyacrylamide gel electrophoresis (BN-PAGE; Nicke *et al.*, 1998). Chemical cross-linking forms covalent bonds between subunits through small reactive reagents targeting primary amines and BN-PAGE can be used to run the isolated multimeric complex on gel showing the molecular mass. The P2X1 and P2X3 subunits were chemically cross-linked and they ran on a gel as a trimer (Nicke *et al.*, 1998). BN-PAGE has also been used to show that the homomeric P2X7 receptor ran on a gel with the size estimated to be a trimer (Kim *et al.*, 2001). Also, chemical cross-linking of P2X2 receptor subunits have shown that they can form high order complexes, consistent with the presence of trimers (Barrera *et al.*, 2005). The stoichiometry of the P2X receptor has been supported by several studies using atomic force microscopy (AFM; Barrera *et al.*, 2005) and electron microscopy (EM) methods (Mio *et al.*, 2005; Young *et al.*, 2008).

AFM technique can be used to analyse single isolated proteins that have not been crystallised and can provide images of protein surfaces. This technique was used to investigate the structure of P2X2 receptors, which were purified from over-expression in human cells (Barrera *et al.*, 2005). Using antibodies agonist the C-termini of the P2X2 receptor complexes AFM images showed that the mean angle between the antibodies on

doubly labelled particles was 123° (Barrera *et al.*, 2005). This provided evidence of the P2X2 receptors forming a trimeric complex. Also, the molecular volume was measured of the imaged particles and it was an average of 409 nm^3 , pointing towards a trimeric structure (expected value of 473 nm^3 ; Barrera *et al.*, 2005). An EM study also investigated the structure of the P2X2 receptor (Mio *et al.*, 2005). Recombinant P2X2 receptors appeared to have a 3D image like a crown-capped inverted three-sided pyramid (Mio *et al.*, 2005). Additionally, the architecture of the P2X4 receptor was investigated using fluorescence resonance energy transfer (FRET) and EM methods (Young *et al.*, 2008). This study showed that the human P2X4 receptor looked like a globular torpedo-like molecule with a compact propeller-shaped ectodomain. This molecule had an estimated molecular mass that was similar to the corresponding masses of a trimeric P2X4 receptor, further supporting the predicted stoichiometry of the receptor (Young *et al.*, 2008). Therefore, the P2X receptor is a third structural class of LGIC, forming as a trimer, with each subunit consisting of two transmembrane domains, intracellular N- and C-termini and a large extracellular loop.

1.7.3 Heterotrimeric Receptors – Distribution and physiological roles

Ion channel diversity can be increased by the mixing of subunits giving rise to function heteromeric channels. For example, voltage dependent K^+ channels can form from Kv1.3 and Kv1.5 subunits leading to pharmacologically distinct channels in macrophages (Villalonga *et al.*, 2007). The combination of different subunits can potentially give rise to channels with different pharmacological properties compared to the homomeric channels. The formation of heteromeric P2X receptors with different properties was first shown by Lewis *et al.* (1995). Co-expression of the P2X2 and P2X3 subtypes showed ATP evoked responses that resembled those in the rat dorsal root ganglion sensory neurons (Lewis *et al.*, 1995). This heteromeric assembly had properties from both subunits (described in section 1.7.5). Also, heteromeric P2X2/3 receptors were shown to be present when interactions between the epitope tags, which labelled the C-terminal of the P2X2 and P2X3 subunits, were detected (Radford *et al.*, 1997). To identify the possible combinations of heterotrimeric formation of the P2X receptors, Torres *et al.*, (1999) used pairwise expression of epitope-tagged subunits and co-immunoprecipitation experiments and the results are summarised in Table 1.2 (Torres *et al.*, 1999).

	P2X ₁	P2X ₂	P2X ₃	P2X ₄	P2X ₅	P2X ₆	P2X ₇
P2X ₁	+	+	+	+	+	+	-
P2X ₂		+	+	-	+	+	-
P2X ₃			+	-	+	-	-
P2X ₄				+	+	+	-
P2X ₅					+	+	-
P2X ₆						-	-
P2X ₇							+

Table 1.2. Co-assembly possibilities of the different P2X receptors. The interaction between two subunits were detected using co-immunoprecipitation using epitope tags. The possible associations are shown. Taken from Torres *et al.*, 1999.

Subsequent studies have also identified possible heteromeric P2X receptors, for example; P2X1/2 receptor (Brown *et al.*, 2002), P2X1/4 receptor (Nicke *et al.*, 2005), P2X1/5 receptor (Le *et al.*, 1999; Surprenant *et al.*, 2000), P2X2/3 receptor (Radford *et al.*, 1997), P2X2/6 receptor (King *et al.*, 2000), P2X4/6 receptor (Le *et al.*, 1998) and P2X4/7 receptor (Guo *et al.*, 2007). Interestingly, the P2X6 subunit is unable to form functional homomeric receptors (Torres *et al.*, 1999). Evidence obtained by chemical analysis and AFM studies have supported this (Aschrafi *et al.*, 2004; Barrera *et al.*, 2005). Chemically cross-linking P2X6 receptor subunits did not form higher order complexes and the mean molecular volume was 143 nm³, which was much lower than the expected value of a trimer of 473 nm³ (Barrera *et al.*, 2005). Assembly of the subunits of the P2X receptor takes place in the ER and the homomeric P2X6 receptor is thought to be retained in the ER (Bobanovic *et al.*, 2002). This is supported by a study that used biochemical and confocal imaging methods to show the P2X6 receptor is not expressed in high amounts on the cell surface and is retained in the ER (Ormond *et al.*, 2006).

Torres *et al.*, (1999) also suggested that the P2X7 receptor could not form a heteromeric P2X receptor. However, a subsequent study provided evidence that there was a structural and functional interaction between the P2X4 and P2X7 subunits, possibly

forming the heteromeric P2X4/7 receptor (Guo *et al.*, 2007). Biochemical and electrophysiological methods showed that the currents were different than the homomeric P2X receptors and the receptors were coimmunoprecipitated in recombinant and native cells (Guo *et al.*, 2007).

P2X1 receptor containing heteromeric channels have been identified in the sympathetic postganglionic neurons from the superior cervical ganglia (SCG) using P2X1 receptor KO mice (Calvert and Evans, 2004). The neurons had a phenotype dominated by P2X2 receptor properties but were also α,β -methylene ATP-sensitive so they could contain heteromeric P2X1/2 receptors (Calvert and Evans, 2004). However, the α,β -methylene ATP-evoked response did not rapidly desensitise and the responses were not increased by high pH, which contrasts previous results obtained for the P2X1/2 receptor by Brown *et al.* (2002). Therefore, the P2X1 heteromeric channel in the SCG neurones may not be the P2X1/2 receptor (Calvert and Evans, 2004). The P2X1 subunits have also been shown to form heteromers with the P2X4 and P2X5 receptors (Le *et al.*, 1999; Nicke *et al.*, 2005). The P2X1/5 receptor has been shown to be expressed in areas such as glial cells (Lalo *et al.*, 2008; Palygin *et al.*, 2010; Ase *et al.*, 2010). The stimulation of neuronal afferents in mice cortical astrocytes were reduced in the presence of a P2X1 receptor selective antagonist, suggesting that the P2X1/5 receptor may contribute to the fast neuronal astroglial signalling at the synaptic level (Palygin *et al.*, 2010). However, the P2X1/5 receptor has not been identified in a human cell line. For example, the attempt to colocalise the P2X1 and P2X5 receptors by immunostaining human cardiac tissue was not successful (Kotnis *et al.*, 2010). Therefore, it is unclear what drugs targeting the P2X1 receptor may do at the P2X1/5 receptor in the human body.

The P2X2/3 receptors were shown to be involved in nociceptive responses and mechanosensory transduction in the urinary bladder (Cockayne *et al.*, 2005). The sensory and sympathetic ganglions neurons from P2X2/P2X3 double KO mice had a minimal response to ATP, the mice had reduced pain-related behaviours and in response to distension there were reduced bladder reflexes (Cockayne *et al.*, 2005). Also, additional studies have used P2X2/P2X3 double KO mice to identify; (i) the role of the P2X2/3 receptor in the carotid body function and in mediating the ventilatory response to hypoxia

(Rong *et al.*, 2003), (ii) the presence of P2X2/3 receptors in mouse otic neurones (Ma *et al.*, 2004), and (iii) the role of the P2X2/3 receptors in the splenic immune system, with KO mice having a compromised immune system and chronic infection (Coutinho-Silva *et al.*, 2005).

1.7.4 Tertiary structure of the P2X receptor and the location of agonist action

Predictions of the tertiary structure of the P2X receptor and the location of the agonist binding site came from several biochemical and mutagenesis studies. In the extracellular domain of mammalian P2X receptors there are 10 conserved cysteine residues and they were proposed to form 5 disulphide bonds. Initial biochemical studies showed that the disulphide bonds do not form between subunits (Nicke *et al.*, 1998). Subsequent studies used a mutagenesis approach and predicted the pairings of the 5 disulphide bonds in the P2X1 and P2X2 receptors (Ennion and Evans, 2002; Clyne *et al.*, 2002). The disulphide bonding of the first 6 cysteine residues are thought to form a cysteine rich loop in the extracellular domain of the P2X receptor. The cysteine rich loop region will be investigated in its involvement to the molecular basis of antagonist action at the P2X1 receptor in Chapters 5 and 6. A more detailed methodology of the proposed pairings is explained in Chapter 5.1.1.

Several mutagenesis studies have also identified conserved residues involved in ATP potency at the P2X1, P2X2, P2X4 and P2X7 receptors (Ennion and Evans, 2000; Jiang *et al.*, 2000; Worthington *et al.*, 2002; Roberts and Evans, 2004, 2006, and 2007; Zemkova *et al.*, 2007; Roberts *et al.*, 2008 and 2009) and these led to a prediction of the residues involved in the ATP binding site. The agonist site of action was suggested to be on the interface between two subunits due to evidence gained from mutagenesis and cross-linking studies (Wilkinson *et al.*, 2006; Marquez-Klaka *et al.*, 2007). These studies and the model of the ATP binding site will be discussed in more detail later in context with the crystal structure of zP2X4 receptor.

1.7.5 Properties of P2X receptors

The different P2X receptor subtypes, both the homomeric and heteromeric channels, have been shown to have a range of different properties. Combining the data obtained from native and recombinant studies the different receptors can clearly be divided

into distinct subtypes. This can help differentiate the P2X subtypes in tissues. The different properties of each subtype can be based on a combination of things, such as the time-course of the ATP-evoked response and the difference in sensitivity to agonists, antagonists, calcium, zinc and pH (Table 1.3 and 1.4).

The P2X receptor is activated by the binding of extracellular ATP causing the influx of cations into the cell. One of the characteristics of the currents produced from each P2X receptor subtype is the time-course of the evoked response. The P2X receptor subtypes have been shown to have different rates of desensitisation, which can be measured as the amount of the decay of the response during the continuous presence of the agonist. For example, the P2X1 and P2X3 receptors are fast desensitising receptors in contrast to the P2X2, P2X4 and P2X7 receptors, which are relatively non-desensitising (Table 1.3; Ralevic *et al.*, 1998). The P2X1 receptor is thought to start desensitising almost as soon as ATP is bound, within 10 milliseconds (ms), and the response decays to 50% of the peak amplitude in ~300 ms (Valera *et al.*, 1994). In contrast to this quick desensitisation, the P2X2 receptor shows no more than 15% decay of the peak amplitude after ATP was applied for two minutes (Evans *et al.*, 1996). Interestingly, when the P2X1 and the P2X2 subunits formed the heteromeric P2X1/2 channel, the time-course of the response showed properties from both subunits (Table 1.4). The resulting inward current showed a biphasic response, with an initial rapid inactivation like the P2X1 receptor but then followed by a slow desensitising current like the P2X2 receptor (Brown *et al.*, 2002).

The understanding of the exact location in the P2X receptor that is involved in the desensitisation of the response is currently unknown. However, several studies have highlighted residues and regions in the P2X receptor that may be important in shaping the time-course of the ATP-evoked response. The protein kinase C (PKC) site is highly conserved throughout the P2X receptor family and mutagenesis of the conserved threonine residue by the C-terminus, which is important in PKC phosphorylation, has shown to affect the desensitisation kinetics of the P2X1 and P2X2 receptors (Boue-Grabot *et al.*, 2000; Ennion and Evans, 2002b). The truncation of the C-terminus or the mutation of T18 in the P2X2 receptor caused the agonist evoked response to have a quicker a desensitisation rate than the wild-type (WT) P2X2 receptor (Boue-Grabot *et al.*, 2000). Also, mutating T18 in

the P2X1 receptor increased the desensitisation of the agonist evoked response (Ennion and Evans, 2002b). Interestingly, mutating this conserved threonine residue in the P2X3 receptor removed the ability of the P2X3 receptor function (Paukert *et al.*, 2001). This highlighted the importance of the conserved threonine close to the N-terminus in P2X receptor kinetics.

The carboxy terminus of the P2X receptor has also been shown to play a role in the desensitisation of the agonist evoked response. The currents produced at splice variants of the rat P2X2 receptor, which had truncated carboxy termini, desensitised quicker than the WT P2X2 receptor (Brandle *et al.*, 1997; Smith *et al.*, 1999). In the P2X2 receptor several residues were shown to be important in shaping the time-course of the agonist evoked response, for example; the 7 amino acid run from V370 (Smith *et al.*, 1999), D349 (Zhou *et al.*, 1998) and V370 (Koshimizu *et al.*, 1998). Also, chimeras that swapped the TM domains of the P2X2 receptor with the P2X1 receptor, produced currents that were quickly desensitising (Werner *et al.*, 1996). Therefore, the time-course of the response appears to involve a combination of residues and regions of the P2X receptor and further investigations are required to highlight specific residues involved in the receptor kinetics at each P2X receptor subtype.

The sensitivity of ATP at the P2X receptor has been shown to be quite varied across the P2X receptor family (Table 1.3 and 1.4). The homomeric P2X1 and P2X3 receptors have been shown to have a high sensitivity to ATP in comparison with other homomeric P2X receptors, with a half effective concentration (EC_{50}) of $\sim 1 \mu\text{M}$ at the P2X1 and P2X3 receptors (Chen *et al.*, 1995; Khakh *et al.*, 2001), 5 to 60 μM at the P2X2 receptor (Brake *et al.*, 1994; Soto *et al.*, 1997), 10-15 μM at the P2X4, P2X5 and P2X6 receptors (Buell *et al.*, 1996; Collo *et al.*, 1996) and $\sim 115 \mu\text{M}$ at the P2X7 receptor (Surprenant *et al.*, 1996). The ATP potency at the different homomeric and heteromeric P2X receptors are shown in Table 1.3 and 1.4.

Homomeric Receptor	Agonist	ATP potency (EC ₅₀)	Antagonist	Desensitising	pH	Calcium	Zinc
P2X1	2-mesATP>ATP >Ap6A> α,β -meATP > $\beta\gamma$ -L-meATP	1	PPADS, Suramin, TNP-ATP, MRS2220, NF023, NF449	Fast	pH6.3: \uparrow pH8.0: N.E.	Increase: N.E.	1-300 μ M: decreased amplitude
P2X2	ATP>2-meSATP >ATP γ S	5-60	PPADS, suramin, reactive blue 2	Slow	pH6.5: \uparrow pH8.0: \downarrow	Increase: reduced amplitude	0.3-30 μ M: 2- 20 fold increase
P2X3	2-meSATP>ATP > α,β -meATP>ATP γ S >Ap3A	1	PPADS, suramin, TNP-ATP, A- 317491	Fast, concentration dependent	pH6.5: \uparrow pH8.3: N.E.	Increase: N.E.	-
P2X4	ATP>ATP γ S>2- meSATP	10	High concentrations of PPADS, suramin	Slow	pH6.5: \uparrow pH8.3 \downarrow	-	10 μ M: increase amplitude
P2X5	ATP=2- meSATP>ATP γ S>2- CIATP	15	PPADS, suramin	Little desensitising	pH6.3: \downarrow pH8.0: N.E.	1.8mM: reduced amplitude	1-100 μ M: increase amplitude
P2X6	ATP> α,β -meATP>2- CIATP>2-meSATP	12	PPADS, suramin	Slow	-	-	-
P2X7	BzATP>ATP>2- meSATP	115	PPADS, suramin, TNP-ATP, KN62, NF279	Little desensitising	-	-	Low concentration: increase amplitude

Table 1.3. Pharmacological profile of the homomeric P2X receptors. Properties of the P2X receptors (P2X1 to 7) to agonists, ATP potency, antagonists, rate of desensitisation and the affect on the ATP-evoked response to pH, calcium and Zinc are summarised. ATP potency is in μ M. N.E. represents no effect.

Heteromeric Receptor	Agonist	ATP potency (EC ₅₀)	Antagonist	Desensitising	pH	Calcium	Zinc
P2X1/2	ATP> Ap6A> α,β -meATP	3.3	-	Fast and slow	pH6.5: \uparrow pH8.0: \uparrow	-	-
P2X1/4	ATP, α,β -meATP	-	PPADS, suramin, TNP-ATP	Slow	-	-	-
P2X1/5	ATP>2-meSATP> α,β -meATP>ADP	0.7	PPADS, suramin, TNP-ATP	Fast and slow	pH6.5: \uparrow pH8.3: N.E.	Increase: N.E.	10 μ M: decrease amplitude
P2X2/3	ATP> α,β -meATP	0.4	PPADS, suramin, TNP-ATP	Slow	pH6.3: \uparrow pH8.3 \downarrow	Increase: reduced amplitude	-
P2X2/6	ATP=ATP γ S>2-meSATP	32	suramin	Fast and slow	pH5.5: \downarrow pH6.3: \uparrow pH8.0: \uparrow	-	1-10 μ M: increase amplitude
P2X4/6	ATP>2-meSATP> α,β -meATP	6	PPADS, suramin, reactive blue 2	Slow	pH6.3: \uparrow pH8.0: N.E.	-	10 μ M: increase amplitude
P2X4/7	BzATP, ATP	-	TNP-ATP, BBG	Little desensitising	-	-	-

Table 1.3. Pharmacological profile of the heteromeric P2X receptors. Properties of the heteromeric P2X receptors (P2X1/2, P2X1/4, P2X1/5, P2X2/3, P2X2/6, P2X4/6 and P2X4/7) to agonists, ATP potency, antagonists, rate of desensitisation and the affect on the ATP-evoked response to pH, calcium and Zinc are summarised. ATP potency is in μ M. N.E. represents no effect.

The sensitivity of the agonist ATP does not only differ between the P2X receptors but other agonists, such as α,β -methylene ATP, and antagonists, such as suramin and PPADS (described in Chapter 3), can contribute to the unique pharmacological profile of each P2X receptor. For example, α,β -methylene ATP is a highly potent agonist at the P2X1 and P2X3 receptors compared to the other P2X receptor subtypes. Interestingly, the heteromeric P2X2/3 receptor is derived from subunits that have differences in their rates of desensitisation and their sensitivity to α,β -methylene ATP (as mentioned above). However, the P2X2/3 receptor showed the properties of non-desensitising time-course of the P2X2 receptor and the α,β -methylene ATP sensitivity of P2X3 receptor (Lewis *et al.*, 1995). Also, the heteromeric P2X4/6 receptor was more sensitive to α,β -methylene ATP and suramin than the homomeric P2X4 and P2X6 receptors (Bobanovic *et al.*, 2002). These studies support the unique channel properties of the heteromeric P2X receptors compared to the homomeric P2X receptors.

The different subtypes of the P2X receptor family also show variations in calcium, zinc and pH sensitivities (Table 1.3 and 1.4). Ions can bind to the extracellular domain of the P2X receptor and act as allosteric modulators. For example, increasing the amount of extracellular protons, by decreasing the pH to 6.3, decreased the ATP-evoked current at the P2X1 receptor by 50% (Stoop *et al.*, 1997). Changing the pH of the extracellular solution appears to affect the P2X receptors in a variety of ways (Table 1.3 and 1.4). Interestingly, the homomeric P2X2 receptor appears to be the most sensitive to the different concentrations of ions. For example, the ATP-evoked response at the P2X2 was dramatically potentiated during acidification and reduced during alkalisation (Stoop *et al.*, 1997). Also, the ATP-evoked response increased at the P2X2 receptor in the presence of higher concentrations of copper and zinc and declined in the presence of extracellular calcium (Xiong *et al.*, 1999; Ding *et al.*, 1999). The residues that were found to be involved in these allosteric binding sites are discussed in context with the crystal structure of the zP2X4 receptor in section 1.8.5.

1.8 Crystallisation of zebra fish P2X4 receptor

Work towards the structural understanding of the P2X receptor came initially from purification studies, AFM and EM techniques (Barrera *et al.*, 2005; Mio *et al.*, 2005;

Young *et al.*, 2008; Mio *et al.*, 2009). The highest resolution data that was obtained from these studies was by using cryo-EM of the P2X2 receptor at 15 Å resolution (Mio *et al.*, 2009). This revealed a 3D structure shaped like a vase, which was a loose assembly of the subunits in a presumed closed state. Subsequently, the P2X receptor was crystallised at 3.1 Å resolution of the zebra fish P2X4 receptor (Kawate *et al.*, 2009). This structure showed the P2X receptor as a trimer, confirming previous topological studies, in a closed, resting state.

The crystallisation of zP2X4 receptor was carried out by Kawate *et al.* (2009) at a 3.1 Å resolution, which reportedly took 7 years to solve (Silberberg and Swartz, 2009). To achieve the final high-resolution crystal structure there was an initial process of finding a potential ortholog to crystallise. This is because the P2X receptors tend to aggregate or dissociate in the presence of detergents commonly used for crystallisation (Kawate *et al.*, 2009). Fluorescence-detection size exclusion chromatograph (FSEC) was used to rapidly determine the stability of 35 P2X orthologs which were transfected in HEK293 cells (Kawate *et al.*, 2009). The most promising candidate was the zebra fish P2X4.1 (zP2X4) receptor. In order to improve the crystallisation process, the receptor was truncated by removing the N- and C-termini. Subsequently, the cysteine residue at position 51 in TM1 (C51F) was mutated to avoid any non-native disulphide bonds forming and the asparagine residues at positions 78 and 187 (N87K and N187R) were mutated to reduce heterogeneity resulting from glycosylation (Kawate *et al.*, 2009). Mutagenesis is not uncommon for the requirement of the membrane proteins to be suitable for 3D crystallisation.

The zP2X4.1 constructs, which were mutated and/or truncated, had lower peak current amplitudes than the full-length wild-type zP2X4 receptor but were functional channels activated by 1 mM ATP (Kawate *et al.*, 2009). Even though the receptor function was different than the wild-type there was still some ion channel function so the structure of the constructs were assumed to only be slightly different from the wild-type. The structures of these “well-behaved” constructs were solved by using single-wavelength anomalous diffraction (SAD) using a gadolinium derivative and then the model was refined by molecular replacement (Kawate *et al.*, 2009).

The crystal structure of the homotrimeric zP2X4.1 receptor has a chalice-like shape showing the extracellular domain protruding ~ 70 Å above the cell surface with the TMs stemming ~ 28 Å through the membrane (Figure 1.2; Kawate *et al.*, 2009). The 3 subunits of the receptor can be seen to be entwined with each other, wrapping around its neighbour in a right-handed twist with 3 vestibules in the centre of the domain (Kawate *et al.*, 2009). Each individual subunit has been given the analogy of a leaping dolphin with the fluke being the TM domains and the main body a β -sandwich domain (Figure 1.2; Kawate *et al.*, 2009). Attached to the main body is the head domain, the dorsal fin, right flipper and the left flipper. The shape of the extracellular domain is unique compared to other channels, including ASICs, glutamate and cys-loop receptors.

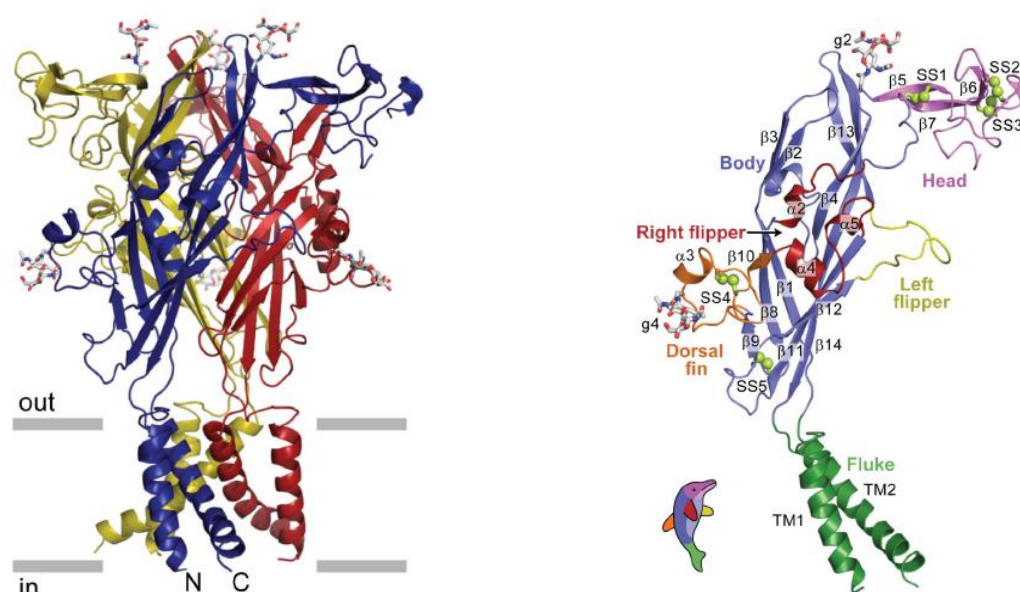


Figure 1.2. Crystallisation of the zP2X4 receptor. Three subunits wrapping around each other in red, yellow and blue (left) and one subunit of the zP2X4 receptor (right), showing the dolphin analogy. The attached glycans are shown in stick representation. Taken from Kawate *et al.* (2009).

The head domain is commonly known as the cysteine rich loop, which contains 3 of the 5 disulphide bonds in the P2X receptor family. The crystallisation of the zP4X4 receptor has supported the predicted pairings of the disulphide bonds, which were suggested by Ennion and Evans (2002) and Clyne *et al.* (2002) (see Chapter 5.1.1 for details). The first 3 disulphide bonds in the sequence of the zP2X4 receptor are located in the head region, 4th is located in the dorsal fin region and the 5th is located in the body region close to the TM domains.

1.8.1 Transmembrane domains and the pore region

The TM domains of the zP2X4 receptor resemble an hourglass formed from 6 α -helices, 2 from each subunit. Interestingly, this shape is similar to those of the acid sensing ion channel (ASIC), which is also a trimer with each subunit containing two TM domains (Gonzales *et al.*, 2009). However, there is no sequence homology between this channel and the P2X receptor. To investigate the contribution of the TM domains prior to the crystallisation of the zP2X4 receptor cysteine scanning mutagenesis studies were carried out (Rassendren *et al.*, 1997; Egan *et al.*, 1998; Jiang *et al.*, 2001; Haines *et al.*, 2001; Li *et al.*, 2008). These studies showed that both of the TM domains contributed to the permeation properties of the P2X receptors. However, there have been some contradicting conclusions about the location of the gate and the structure of the TM domains (see below; Rassendren *et al.*, 1997; Egan *et al.*, 1998). A subsequent study by Li *et al.* (2008) suggested that the TM2 helix lines the central ion conduction pore containing the channel gate and the TM1 helix was peripheral to the pore region (Li *et al.*, 2008). Interestingly, this was supported by the structure of the zP2X4 receptor (Kawate *et al.*, 2009).

The zP2X4 receptor structure has supported many studies that suggested the TM2 forms the ionic pore (Rassendren *et al.*, 1997; Egan *et al.*, 1998; Li *et al.*, 2008). The TM2 was initially investigated to the contribution to the pore of the P2X2 receptor by using the substituted cysteine accessibility method (SCAM; Rassendren *et al.*, 1997; Egan *et al.*, 1998). Mutating the residues to a cysteine allowed the side chain to be covalently modified by reagents such as silver or methanethiosulphonates (MTS) if the residue was accessible. Rassendren *et al.* (1997) used different sized MTS reagents to try and determine the location of the pore and the channel gate. The smaller MTS reagent was found to inhibit the current at two mutated P2X2 receptors, L338C and D349C, but when the MTS reagent was just co-applied with ATP only the mutant D349C had a reduction in the current (Rassendren *et al.*, 1997). This suggested that the channel gate was deep within the TM2 domain, between the residues L338 and D349. Egan *et al.*, (1998) also proposed that TM2 lines pore of the P2X2 receptor. However, in contrast to results obtained by Rassendren *et al.* (1997), the TM2 was thought to form an outward facing loop, rather than being helical, and the residue G242 in the P2X2 receptor is at the apex contributing to the channel gate (Egan *et al.*, 1998). The difference in the secondary structure was proposed due to groups

of linear runs of mutants in the TM2 being affected by silver and MTS reagents without a pattern that resembles an α -helix. Therefore, the TM2 was proposed to cross the membrane in non-helical manner (Egan *et al.*, 1998). However, this is now known to be incorrect as the TM domains form α -helices in the structure of the zP2X4 receptor (Figure 1.2).

To address the conflicting ideas of the location of the pore-forming and gate regions in the P2X receptor, Li *et al.*, (2008), used the SCAM method to generate a clearer picture of the involvement of the TM domains of the P2X2 receptor. This study demonstrated that the central ion conduction pathway is predominately formed by the TM2 domain (Li *et al.*, 2008). The ability of 2-trimethylaminoethyl methanethiosulfonate (MTSET) and silver to access the residue T336C and below was greatly affected by the presence and absence of ATP, suggesting that T336 may be part of the gate of the P2X2 receptor (Li *et al.*, 2008). Interestingly, T336 corresponds to A344 in the zP2X4 receptor and this residue was suggested to be the centre of the gate, which was the narrowest section of the pore (Kawate *et al.*, 2009). The contribution of TM2 has also been supported by single-channel analysis studies of mutants in the TM2 (Cao *et al.*, 2007; Cao *et al.*, 2009). Residues in TM2 were shown to play a role in gating, single-channel conductance and the rectification of the P2X2 receptor.

Li *et al.* (2008) also mutated residues in TM1 of the P2X2 receptor but only one mutant had a modified accessibility with MTSET. Interestingly, after treatment with MTSET this mutant (V48C) had a dramatic slowing of the closing of the channel after ATP was removed suggesting that the TM1 is also involved in the gating of the channel. The small involvement of TM1 suggested that this region was positioned peripheral to TM2 (Li *et al.*, 2008) and this is also supported by the structure of the zP2X4 receptor (Kawate *et al.*, 2009). The involvement of TM1 on the channel properties has also been highlighted in several studies prior to Li *et al.* (2008) (Haines *et al.*, 2001; Li *et al.*, 2004; Rettinger and Schamlzing, 2004). Residues that have a reduction in ATP potency upon their mutation can either be affecting ATP binding and/or gating of the receptor. Alanine mutation of the residues in TM1 of the P2X2 receptor showed 7 mutants with reduced ATP potency highlighting the involvement of these residues in gating of the channel (Li *et al.*, 2004). Also, a chimera, which added the TM1 of the P2X1 receptor into the P2X2

receptor, increased sensitivity to the α,β -methylene ATP suggesting the contribution of this TM domain in channel properties (Haines *et al.*, 2001). Interestingly, the reciprocal chimera, adding in the TM1 of the P2X2 receptor, changed the P2X1 receptor from a desensitising channel to a non-desensitising channel (Rettinger and Schmalzing, 2004). Therefore, the TM2 of the P2X receptors is thought to line the pore of the P2X receptor, containing the channel gate, and TM1 could contribute to the movement of the pore during activation.

1.8.2 Permeability

The binding of ATP to the extracellular domain is thought to induce a conformational change between the subunits, causing the TM domains to move and allowing the influx of cations through the pore of the receptor (Kawate *et al.*, 2009). The crystallisation of the zP2X4 receptor showed the receptor to have a three-fold axis of symmetry that runs the length of the extracellular domain. Between the 3 subunits of the zP2X4 receptor there are three vestibules; the upper, central and extracellular vestibules (Figure 1.3). One possible pathway of the ions in the extracellular solution accessing the TM domains may be through the full length of the extracellular domain through these vestibules, along the three-fold axis of symmetry (Kawate *et al.*, 2009). Even though in the closed structure of the zP2X4 receptor, which shows that it is too narrow (~ 2.3 Å) for ions to pass through, it is thought that upon agonist binding the channel expands these constrictions allowing ions to pass through (Kawate *et al.*, 2009).

Another possibility of the ions passing through the receptor could be an area located directly above the TM domains, which is next to the extracellular leaflet of the membrane bilayer (shown with an orange arrow in Figure 1.3; Kawate *et al.*, 2009). This opening is ~ 8 Å in diameter and is big enough for cations, such as Na^+ , K^+ and Ca^{2+} , to access the channel (Kawate *et al.*, 2009). On the intracellular side of the P2X receptor, the ions have been proposed to exit via an inverted cone-like structure in the intracellular vestibule (Kawate *et al.*, 2009). This region includes the conserved aspartic acid residue at position 357 in the zP2X4 receptor, which has been shown to be important in receptor assembly (Duckwitz *et al.*, 2006).

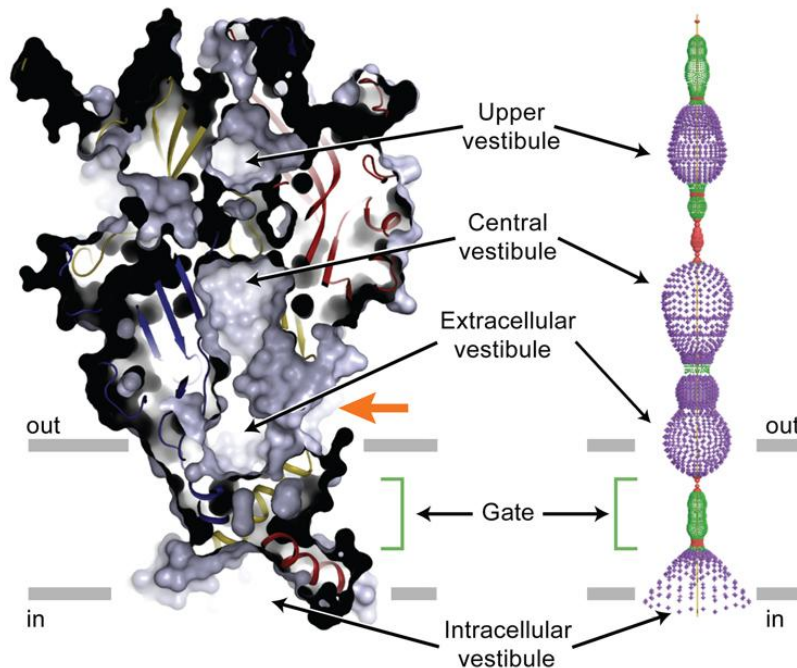


Figure 1.3. Vestibules in the closed, resting state of the zP2X4 receptor. Crystal structure of the zP2X4 receptor (left), showing the location of the three vestibules (upper, central and extracellular) across the three-fold symmetry of the structure. The different radius range of the vestibules from the line of symmetry (right) are shown in different colours with red being $<1.15 \text{ \AA}$, green being $1.15\text{-}2.3 \text{ \AA}$ and purple being $>2.3 \text{ \AA}$. Figure taken from Kawate *et al.*, 2009.

However, further investigations are required to understand the full extent of how the ions pass through the P2X receptor. The crystallisation of the zP2X4 receptor is in its closed, resting state and during activation there may be large conformational changes allowing further possible locations of ion channel access. Previous studies have suggested that many residues in the TM domains are involved in gating of the receptor so there may be widespread conformational changes around the pore region (Li *et al.*, 2004; Silberberg *et al.*, 2005; Silberberg *et al.*, 2007; Cao *et al.*, 2007; Li *et al.*, 2008). For example, a study probed the movements of the P2X4 receptor with ivermectin (IVM), which stabilises the open state of the receptor (Silberberg *et al.*, 2007). Mutation of residues in the TM domains highlighted a range of mutants that weakened IVM binding suggesting that there may be widespread rearrangements of the TM helices during opening of the P2X receptors (Silberberg *et al.*, 2007).

1.8.3 Extracellular loop ATP binding site

The crystallisation of the zP2X4 receptor was an important advance in our understanding of P2X receptors. However, the receptor was crystallised in the absence of

an agonist so there was no direct information of residues that coordinate agonist action. Also, in the extracellular loop there seems to be no sequence homology with any other proteins that contain a consensus motif for ATP binding, for example, the Walker motif (GXXXGKTS/S) that coordinates the phosphate of ATP (Walker *et al.*, 1982). Consequently, over the past decade mutagenesis studies on the residues in the extracellular region have helped to develop an understanding the site of agonist action. The large extracellular loop of the P2X receptor contains ~280 amino acids of which 93 are conserved in at least 6 of the P2X receptor subunits (Vial *et al.*, 2004). Initial studies mutated the conserved basic, aromatic and polar amino acids in the extracellular region and measured the effect on ATP potency (Jiang *et al.*, 2000; Ennion *et al.*, 2000; Roberts and Evans, 2004 and 2006). These initial studies mutated the conserved residues to an alanine residue as this small amino acid is well tolerated.

Studies have also investigated the agonist site of action by using partial agonists (Roberts and Evans, 2004; Roberts *et al.*, 2009). Studies on ionotropic glutamate receptors have used partial agonists to identify whether residues are involved in agonist binding or the subsequent opening of the channel (Armstrong *et al.*, 2003; Jin *et al.*, 2003). The AMPA receptor has been found to have a range of conformational states and crystallographic and biochemical techniques showed that upon the mutation of the leucine at position 650 (L650T) there were effects on the closure of the structure in the presence of the partial agonist kainate and the agonist AMPA (Armstrong *et al.*, 2003). Kainate had a higher efficacy at the mutated receptor, with an increase in the domain closure, and AMPA only acted as a partial agonist, giving partial closure of the “clamshell-shaped” ligand binding core (Armstrong *et al.*, 2003). Also, crystallographic and electrophysiological techniques of the AMPA subtype-glutamate receptor have shown that a series of partial agonists held the receptor in a range of ligand-dependent conformational states (Jin *et al.*, 2003). Therefore, mutants in the P2X receptor that have a change in partial agonist efficacy may be involved in the different conformations of the receptor that contribute to the gating of the channel. Additionally, studies have also investigated the residues involved in ATP potency at the P2X receptor by mutating them to a cysteine (Roberts *et al.*, 2008 and 2009). The introduction of a cysteine residue can allow the side chain to be modified by MTS reagents if they are accessible, which can change the local charge environment.

For the majority of mutants tested there were no effects on ATP potency, however, a few residues have been shown to be important in ATP sensitivity in the P2X1 receptor and in other P2X receptor subtypes (Figure 1.4). These studies have given a prediction of the ATP binding site and they can be mapped onto the crystal structure of zP2X4 receptor highlighting the possible location of the ATP binding site (detailed below).

```

mutants  flye-g--tss-glissvsvKlK-lavtqlpglgpqv--va--Vf-aq-dnsfvvm-nfi
hP2X1 49  FLYEKGYQTSS-GLISSVSVKlKGLAVTQLPGLGPQVWDVADYVFPAQGDNSFVVMTNFI 107
hP2X2 61  FIVQKSYQESETGPESSIITKVKGITTS-----HKVWDVEEYVKPPEGGSVFSIITRVE 115
hP2X4 48  FVWEKGYQETD-SVVSSVTTKVKGVAVTNTSKLGFRIWDVADYVIPAQEENSLFVMTNVI 106

mutants  v-pk-tq-y-a-hp-eg-gi-ke-sg-tp-kakrkaq-ir--k-vaf-ndtvk---ifg-
hP2X1 108  VTPKQTQGYCAEHP-EG-GICKEDSGCTPGKAKRKAQGIRTGKCVAF-NDTVKTCEIFGW 164
hP2X2 116  ATHSQTQGTCEESIRVHNATCLSDADCVAGELDMLGNGLRTGRCVPPYQGPSKTCEVFGW 175
hP2X4 107  LTMNQTQGLCEIP-DATTVCKSDASCTAGSAGTHSNGVSTGRCVAF-NGSVKTCEVAAW 164

mutant   --v-vdddiprpall-----FT-----n-r-lveevnaahm-t-lfhkltlh
hP2X1 165  CPVEVDDDIPRPALLREAENFTLFIKNSISFPRFKVNRRNLVEEVNAAHMKTCLFHKTLH 224
hP2X2 176  CPVEDGASVSQ-FLGTMAPNFTILIKNSIHYPKFHFSKNIADR-TDGYLKRCTFHEASD 233
hP2X4 165  CPVEDDTHVPQPAFLKAAENFTLLVKNNIWYPKFNFSKRNILPNITTTYIKSCIYDAKTD 224

mutants  -l--v-ql-yvvqes-qn-stlaek--vv-itid-h--l-whvrh-r-i-e-hglye---
hP2X1 225  PLCPVFQLGYVVQESGQNFSTLAEKGGVVGITIDWHCDLDWHVRHCRPIYFHGLYE--- 281
hP2X2 234  LYCPIFKLGFIVEKAGESFTELAHKGGVIGVIINWCDLDLPASECNPKYSFRRLDPKH- 292
hP2X4 225  PFCPIFRLGKIVENAGHSFQDMAVEGGIMGIQVNWCNLDRAASLCLPRYSFRRLDTRDV 284

mutants  eknl----NFR-----K-----
hP2X1 282  EKNLSPGFNFRFARHFVE-NGTNYRHLFKVFGIRFDILVDGKAGKFD 327
hP2X2 293  -VPASSGYNFRFAKYYKI-NGTTTRLIKAYGIRIDVIVHGQAGKFS 337
hP2X4 285  EHNVSPGYNFRFAKYYRDLAGNEQRLIKAYGIRFDIIVFGKAGKFD 331

```

Figure 1.4. Sequence alignment of the human P2X1, P2X2 and P2X4 receptors. The amino acids that are conserved in at least 5 mammalian P2X receptor subunits are shown in red (basic), purple (aromatic), green (polar), yellow (glycine/proline) and black (cysteine, valine, alanine, aspartate and glutamate). The top line, labelled mutants, that are in bold and colour are the residues that have been shown to be involved in ATP potency and are shown in the model of the ATP binding site (Figure 1.5). The top line also shows the residues that have been mutated and have no or >10-fold effect on ATP potency (dashes) and the non-conserved residues (lower case). Taken from Evans, 2010.

Charged amino acids

Positively charged residues have been shown to coordinate the negatively charged phosphate tail of ATP; for example, the lysine residue in the Walker motif (Muller *et al.*, 1996) and the arginine residues in the P2Y receptor (Erb *et al.*, 1995). Mutating the 11 conserved positively charged residues in the extracellular loop of the P2X1 receptor highlighted the involvement of K68, K70, R292 and K309 in ATP potency (Ennion *et al.*,

2000). The P2X1 receptor mutants, K68A and K309A resulted in a striking >1400-fold decrease in ATP potency and the mutants K70A and R292A resulted in an ~20- and ~100-fold decrease in ATP potency, respectively (Ennion *et al.*, 2000). The charged residues R292 and K309 have also been mutated to a cysteine in the P2X1 receptor and these mutants had a large reduction in ATP potency (Roberts and Evans, 2007). Also, these two mutants had a reduction in the binding of the radiolabel 2-azido ATP, further suggesting that these residues are directly coordinating ATP (Roberts and Evans, 2007).

The conserved charged basic amino acids were found to also play a role in ATP potency at the P2X2 and the P2X4 receptor (Jiang *et al.*, 2000; Zemkova *et al.*, 2007; Roberts *et al.*, 2008) and the reciprocal residue of K309 in the P2X7 receptor (Worthington *et al.*, 2002). This suggested that there may be a core ATP binding site throughout the P2X receptor family and these positively charged residues may coordinate the negative phosphate tail of ATP. Interestingly, the ATP potency at the cysteine mutants of the reciprocal P2X1 residues K68, K70 and K309 in the P2X4 receptor (Roberts *et al.*, 2008), and K309 in the P2X1 receptor (Roberts and Evans, 2007), were sensitive to modification with differently charged MTS reagents ((2-aminoethyl) methanethiosulfonate hydrobromide (MTSEA) and sodium (2-sulfonatoethyl) methanethiosulfonate (MTSES)). The positively charged MTS reagent, MTSEA, recovered the ATP potency suggesting that the positive charge of the lysine residues are important in binding ATP. Therefore, K68, K70 and K309 could coordinate the negatively charged phosphate tail of ATP. Interestingly, both of the differently charge MTS reagents reduced the ATP potency at the P2X1 receptor mutant R292C, suggesting that this residue may not coordinate the phosphate tail but the aromatic groups of ATP (Roberts and Evans, 2007). The conserved negative charged residues, aspartic acids and glutamic acids, have also been investigated using site site-directed mutagenesis and they have been shown that to not play a role in ATP potency at the P2X1 and P2X2 receptors (Jiang *et al.*, 2000; Ennion *et al.*, 2001).

Aromatic amino acids

Analysis of the other ATP-binding proteins indicated that the aromatic residues may coordinate the action of the adenine group in ATP. For example, aromatic residues coordinate the binding of the adenine ring of ATP in DEAD box helicases (Tanner *et al.*,

2003). Roberts and Evans (2004) mutated the 20 conserved (within at least 6 subtypes) aromatic residues in the extracellular loop of the P2X1 receptor to an alanine. The majority of the mutants had >6-fold decrease in ATP potency but two mutants, F185A and F291A, had an ~10- and ~140-fold decrease in ATP potency, respectively, (Roberts and Evans, 2004). These aromatic residues were also shown to be important in ATP action at the P2X2 and P2X4 receptors, further supporting a core common mode of ATP action at P2X receptors (Zemkova *et al.*, 2007; Roberts *et al.*, 2008). In contrast to alanine mutation of the residue F185, the cysteine mutation of this residue in the P2X1 receptor did not have a decrease in ATP potency but a reduced partial agonist efficacy (Roberts *et al.*, 2009). Also, the ATP-evoked response was not affected in the presence of different charged MTS reagents (Roberts *et al.*, 2009). Therefore, the residue F185 may not directly be involved in agonist binding at the P2X1 receptor but may have regulatory role in ATP binding, facing away from the agonist binding site.

Polar amino acids

Polar amino acids have also been shown to coordinate the binding of the ribose ring in ATP in other ATP-binding proteins (Skorvaga *et al.*, 2002). These polar amino acids may play an important role in the activation of the P2X receptor, including the formation of hydrogen bonds with the agonist stabilising the conformational changes that occur upon activation (Roberts and Evans, 2006). The alanine substituted mutants, T186A and N290A, had an ~6- and ~60-fold decrease in ATP potency, respectively, and a decrease in the efficacy of the partial agonists BzATP (3'-O-(4-benzoyl)benzoyl adenosine 5'-triphosphate) and Ap₅A (P1, P5-di(adenosine-5') pentaphosphate) (Roberts and Evans, 2006). These residues were suggested to be important in the binding of the adenine ring of ATP. Cysteine mutation of N290 also reduced the ATP potency and by even greater amounts in the presence of either negatively or positively charged MTS reagents, suggesting this residue may coordinates the adenine ring of ATP (Roberts and Evans, 2007). The cysteine mutation of T186 in the P2X1 receptor had a reduction in ATP potency and abolished the response to partial agonists (Roberts *et al.*, 2009). Also, the binding of the radioligand 2-azido ATP and the effect on the ATP-evoked current in the presence of the differently charged MTS reagents were decreased at the T186C mutant (Roberts *et al.*, 2009). This suggested that T186 may also be involved in coordination of

the adenine or ribose groups of ATP. Interestingly, the corresponding residues in the P2X2 receptor were also shown to be important in ATP potency, further indicating a core binding site across the P2X receptor family (Jiang *et al.*, 2000; Clyne *et al.*, 2002).

1.8.4 Model of the ATP binding site

Over 120 amino acids in the extracellular loop have been mutated to an alanine or a cysteine residue in the human P2X1 receptor (Figure 1.4). The majority of these mutants have no effect on ATP potency but 8 conserved residues have been shown to play an important role in ATP potency (Evans, 2009). The residues involved in ATP potency are K68, K70, F185, T186, N290, F291, R292 and K309 (P2X1 receptor numbering) have been used to propose a model of the ATP binding site (Figure 1.5). This model was proposed before the crystallisation of the zP2X4 receptor (Roberts *et al.*, 2008). The lysine residues, K69, K70 and K309 are thought to coordinate the negatively charged triphosphate tail of ATP, the aromatic region N290F291R292 are thought to coordinate the binding of the adenine ring and the residues F185 and T186 have a possible regulatory role through hydrogen bonding (P2X1 receptor numbering; Roberts *et al.*, 2006, 2008 and 2009). As mentioned previously, these residues are conserved in the different mammalian P2X subunits and studies investigating the conserved residues in the P2X2, P2X4 and P2X7 receptors have highlighted a common binding site across P2X receptor subunits (Jiang *et al.*, 2000; Worthington *et al.*, 2002; Zemkova *et al.*, 2007; Roberts *et al.*, 2008).

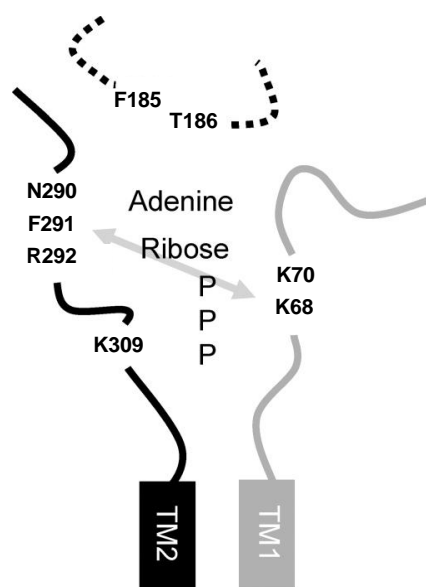


Figure 1.5. Model of the predicted ATP binding site. Residues shown to be involved in ATP potency are shown (P2X1 receptor numbering). The ATP binding site is between two adjacent subunits, TM1 from one subunit, TM2 from another. Dotted line for the FT motif is because these residues it is unclear if these residues are involved in ATP binding and/or gating. The grey arrow represents the disulphide bond that can be formed between the cysteine mutants (Marquez-Klaka *et al.*, 2007). Model is based on data obtained prior to the crystallisation of the zP2X4 receptor. (adapted from Roberts *et al.*, 2008)

Intersubunit ATP binding site

Prior to the crystallisation of the zP2X4 receptor, mutagenesis and cross-linking studies highlighted that the ATP may bind on the interface of two subunits rather than intra-subunit binding (Figure 1.5; Wilkinson *et al.*, 2006; Marquez-Klaka *et al.*, 2007). A disulphide cross-linking approach was used to identify pairs of residues that were in close proximity within the P2X1 receptor (Marquez-Klaka *et al.*, 2007). The 8 residues predicted to coordinate ATP were mutated to cysteine residues and co-expressed in *Xenopus laevis* oocytes. There was a dimer formation between the K68C and F291C mutants, which was observed by using nonreducing SDS-PAGE analysis, and there was a complete cross-link into trimers with the K68C/F291C double mutant (Marquez-Klaka *et al.*, 2007). The cross-linked subunits produced small ATP-activated currents and when these intersubunit disulphide bridges were dissociated, using the reducing agent dithiothreitol (DTT), the ATP-evoked current amplitudes increased by >60-fold. Also, the formation of the disulphide bond between K68C and F291C was prevented in the presence of ATP suggesting that these two residues are in the ATP binding site. Therefore, these lines of evidence suggested that the two residues K68 and F291 are on different subunits and they must be close together forming the ATP binding site (shown by grey arrow in Figure 1.5). These results also supported a previous study by Wilkinson *et al.* (2006), which mutated the reciprocal lysine mutants of K68 and K309 in either P2X2 or P2X3 subunits and were coexpressed human embryonic kidney (HEK) cells. The heteromeric P2X2/3 receptor was formed and due to the failure of a functional channel occurring when both the residues were mutated in the P2X2 subunits, the ATP binding site was suggested to interact with both subunits (Wilkinson *et al.*, 2006). Crystallisation of the zP2X4 receptor has supported the predictions of the location of the predicted ATP binding site on the interface of two subunits (see below).

Mapping the residues onto the homology model of the P2X1 receptor

Crystallisation of the zP2X4 receptor was in the absence of an agonist. However, the 8 conserved residues that were thought to be involved in ATP binding were predicted to be part of the ATP binding site (Kawate *et al.*, 2009). Mapping these residues onto the homology model of the P2X1 receptor (method of how this was formed is described in Chapter 2.4) shows the proposed ATP binding to be located in a deep groove ~45 Å away

from the TM domains on the interface between two subunits (Figure 1.6). This groove is shaped like an open jaw and is surrounded by the head, body, right flipper and dorsal fin domains (Kawate *et al.*, 2009). The 8 conserved residues predicted to be involved in ATP binding can be seen to be in the cavity of this groove of the zP2X4 receptor with K70, K72, F188 and T189 (corresponding to K68, K70, F185 and T186 in the P2X1 receptor) being from one subunit and N296, F297, R298 and K316 (corresponding to N290, F291, R292 and K309 in the P2X1 receptor) from the neighbouring subunit (Figure 1.6; Kawate *et al.*, 2009). This supports the previous predictions that the ATP binding site is on the interface of two neighbouring subunits (Marquez-Klaka *et al.*, 2007).

The residue F185 in the P2X1 receptor has previously been proposed to not directly bind ATP and it may be facing away from the agonist binding site (as explained above; Roberts *et al.*, 2008 and 2009). Interestingly, the crystallisation of the zP2X4 receptor supports this and showed that the residue F188 (reciprocal residue of F185 in the P2X1 receptor) is orientated away from the groove. This suggested that this residue may be important in regulating ATP binding and the subsequent gating of the channel (Kawate *et al.*, 2009).

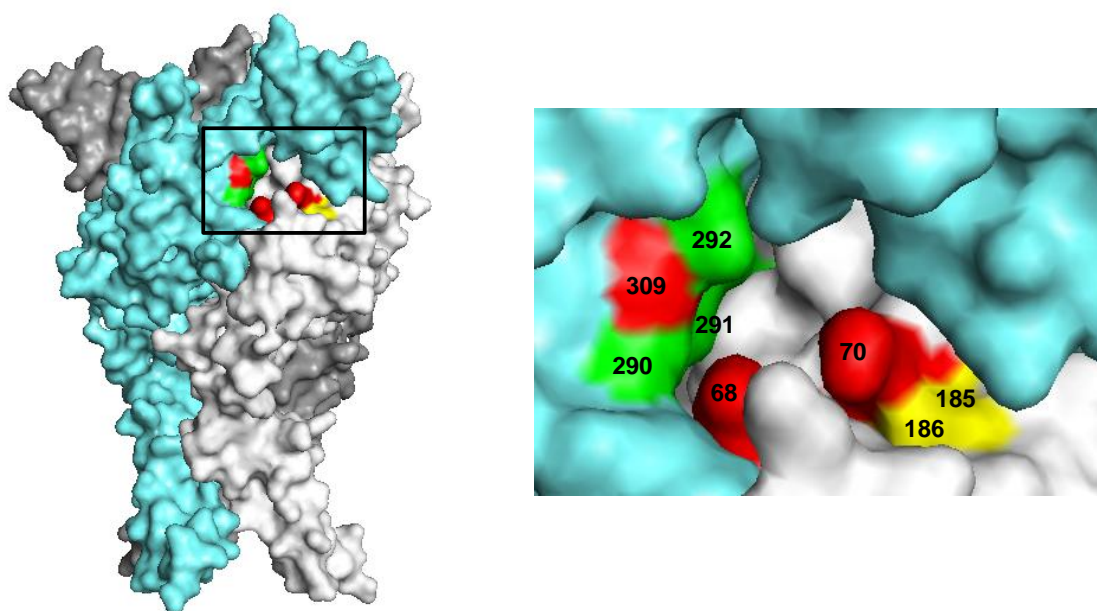


Figure 1.6. Homology model of the P2X1 receptor showing the ATP binding site. The homology model of the human P2X1 receptor is based on the structure of the zP2X4 receptor (as described in Chapter 2.4). The three subunits are shown in white, cyan and dark grey with the black box representing the region of the receptor that may bind ATP. The residues predicted to coordinate ATP are shown in red (K68, K70 and K309), yellow (F185 and T186) and green (N290, F291 and R292).

The location of the predicted ATP binding site in the P2X receptor family is supported by many mutagenesis studies which have been explained above (Ennion *et al.*, 2000; Jiang *et al.*, 2000; Worthington *et al.*, 2002; Roberts and Evans, 2004, 2006 and 2007; Zemkova *et al.*, 2007; Roberts *et al.*, 2009). Studies on the P2X7 receptor also support the model of the ATP binding site (Adriouch *et al.*, 2008; Schwarz *et al.*, 2009). ADP-ribose can be transferred onto proteins from NAD using ATP-ribosyltransferases and the P2X7 receptor can be activated following ADP-ribosylation. Mutagenesis studies showed that mutation of R125 in the P2X7 receptor leads to irreversible receptor activation (Adriouch *et al.*, 2008). Interestingly, the corresponding residue in the zP2X4 receptor is located at the base of the head region of the receptor, adjacent to the predicted ATP binding pocket (Kawate *et al.*, 2009). Therefore, ADP must be able to access the adjacent ATP binding pocket and activate the receptor, supporting previous predictions that the location of R125 in the P2X7 receptor and ATP binding pocket are in similar positions (Adriouch *et al.*, 2008; Schwarz *et al.*, 2009).

Therefore, mutagenesis studies have proposed a model of the ATP binding site, which is supported by Kawate *et al.* (2009), and the residues K68, K70, K309 could coordinate the binding of the phosphate tail of ATP, N209, F291 and R292 could coordinate the aromatic region of ATP, and F185 and T186 have a regulatory role of ATP action (P2X1 receptor numbering).

1.8.5 Allosteric binding sites

The P2X receptors have been shown to be regulated by divalent cations (Table 1.3 and 1.4). Zinc binding sites only appear to be present in the P2X2 receptor and they have been shown to be at the histidine residues 120 and 213 (Clyne *et al.*, 2002; Lorca *et al.*, 2005). Mutagenesis studies in the rat P2X2 receptor of these residues highlighted that these residues are important in zinc potentiation (Clyne *et al.*, 2002; Lorca *et al.*, 2005). The corresponding residues in the zP2X4 receptor are located in the head and the dorsal fin of the structure, which are close to the predicted ATP binding pocket. Interestingly, the reciprocal residue of the histidine at position 120 in the rat P2X2 receptor is R125 in the P2X7 receptor, which has been shown to underlie ATP-ribosylation. This residue is located in the head of a P2X receptor subunit suggesting that this region may be important

regulating P2X receptor properties. A few studies have supported the involvement of the head region in channel properties; (i) the removal of the disulphide bonds upon mutating the conserved cysteine residues to an alanine, affected zinc regulation in the P2X2 receptor (Clyne *et al.*, 2002), (ii) this region was shown to be important in copper regulation in the P2X4 receptor (Coddou *et al.*, 2007), (iii) mutation of a residue in this region (L127A) of the P2X7 receptor affected the efficacy of the partial agonist BzATP (Young *et al.*, 2007), and (iv) a residue in the head region is important in antagonist action in the P2X1 receptor (investigated in Chapters 5 and 6; Sim *et al.*, 2008). Therefore, the cysteine rich head region, which is in close proximity to the ATP binding site, may be important in regulating P2X receptor properties.

1.8.6 Signal transduction

The proposed ATP binding site is ~ 45 Å away from the pore of the P2X receptor. Therefore, there must be residues that are important in translating the signal from the ATP binding site to the pore of the receptor. The region A304 to I328 (rat P2X2 numbering) has been shown to possibly play a role in this signal transduction (Yan *et al.*, 2006; Roberts and Evans, 2007; Young *et al.*, 2008b). From the crystal structure of the zP2X4 receptor this region spans the full length the extracellular domain. Young *et al.* (2008b) showed that mutations in the region R304 to I314 in the rat P2X2 receptor affected N-linked glycosylation at position N298, suggesting that there was a conformational change in the protein (Young *et al.*, 2008b).

Residues around the proposed to ATP binding site should play a role in the transduction of the signal to open to the channel. The radioligand 2-azido ATP can be used to identify residues that are important in ATP binding and/or gating of the channel (Roberts and Evans, 2007; Roberts *et al.*, 2009). Upon the mutation of residues involved in ATP potency, residues that were involved in ATP binding would have decreased 2-azido ATP binding and residues without a decrease in 2-azido ATP binding would be involved in gating of the receptor. The P2X1 receptor mutants N290C and F291C had a larger decrease in ATP potency than the mutant R292C (Roberts and Evans, 2007). However, N290C and F291C mutants did not decrease 2-azido ATP binding as much as the R292C mutant (Roberts and Evans, 2007). This suggested that the residue R292 had a greater role in

agonist binding than the residues N290 and F291. The residues N290 and F291 appear to have a role in both binding of ATP and gating of the P2X1 receptor. Also, the mutant K309C had similar reductions in 2-azido ATP binding as the mutant R292 but a much larger reduction in ATP potency, suggesting that the residue K309 also plays a role in gating in the receptor (Roberts and Evans, 2007). Interestingly, this is supported by a single channel analysis study, which showed that the reciprocal residue of K309 in the P2X2 receptor had a role in gating of channel as well as binding of ATP (Cao *et al.*, 2007). Therefore, residues in the agonist binding pocket also contribute towards the gating of the receptor, subsequent to binding.

1.8.7 Antagonist binding site

Compared to the understanding of agonist action at the P2X receptor, comparatively little is known about the molecular basis of antagonist action. Only a few residues, such as K138 in the P2X1 receptor (Sim *et al.*, 2008), K78 and K249 in the P2X4 receptor (Garcia-Guzman *et al.*, 1997; Buell *et al.*, 1996) and R126 in the P2X7 receptor (Michel *et al.*, 2008), have been shown to be important in antagonist sensitivity. These residues are located in the vicinity of the predicted ATP binding pocket of the zP2X4 receptor. Kawate *et al.* (2009) suggested that the antagonists block ATP from activating the receptor by affecting conformational rearrangements in the receptor. The residues involved in antagonist sensitivity and the concepts of how antagonists could block the P2X receptor will be discussed in more detail in later chapters.

1.8.8 Limitations of the zP2X4 receptor crystal structure

The structure of the zP2X4 receptor has provided a major advance in the understanding of P2X receptors. However, there are a few limitations to this structure which should be discussed. The crystal structure was based on the zP2X4 receptor and the P2X4 receptor is known to be relatively antagonist insensitive compared to the P2X1 receptor (as explained in Chapter 3.1). Therefore, mapping the antagonist site of action on the homology model of the P2X1 receptor, which is based on the zP2X4 receptor, may prove difficult as the homology model may not be in the physiological resting conformation of the P2X1 receptor that is antagonist-sensitive.

In order to improve the crystallisation of the zP2X4 receptor a few structural modifications were carried out. Initially, the receptor was truncated and the N- and C-termini were removed. Also, the receptor was mutated in order to remove the glycosylation sites. Interestingly, even though this receptor was activated by 1 mM ATP, the peak current amplitudes were much smaller than the full-length WT zP2X4 receptor. Therefore, removing the termini and the glycosylation sites could be affecting the conformation of the extracellular loop affecting the gating of the channel and the receptor may not be in the proposed rested, closed state. Additionally, the zP2X4 receptor was crystallised in the presence of gadolinium. This could have held the receptor in a certain conformation preferable for the crystallisation of the receptor. This conformation may be between the physiological resting and activated states of the receptor. Therefore, the conformation of the receptor and the orientation of residues in this structure may be different compared to the actual resting, closed state of the P2X receptor.

1.9 Thesis aims

In this thesis, the residues around the predicted ATP binding pocket and in the cysteine rich loop will be investigated to determine their contribution to the molecular basis of agonist and antagonist action at the P2X1 receptor. This will be carried out by using two-electrode voltage clamp electrophysiology on a combination of mutated and chimaeric P2X receptors. This research will extend the knowledge gained from the crystallisation of the zP2X4 receptor and provide predictions of the antagonist site of action. Providing a better understanding of how antagonists act at the P2X1 receptor can potentially contribute to novel drug design and help towards the treatment of hypertension and stroke.

Chapter 2. Materials and Methods

2.1 Molecular Biology

2.1.1 The human P2X1 receptor

The human P2X1 cDNA was originally isolated and cloned from the human bladder as described by Ennion *et al.* (2000). The vector used to contain the cDNA was a pcDNA3.1 plasmid (Figure 2.1; Invitrogen, Paisley, UK). The pcDNA3.1 plasmid contains an Ampicillin resistance gene, T7 promoters and a *MluI* restriction enzyme site. The presence of the Ampicillin resistance gene allows for appropriate selection of this plasmid in *E.coli*. The T7 promoter allows for efficient protein expression and was located upstream of the restriction sites for P2X1 cDNA sequence cloning. The *MluI* site was present to linearise the plasmid to make the mRNA. The pcDNA3.1 plasmid also had a modified poly(A) tail, protecting the resulting mRNA from exonucleases, adjacent to the 3' untranslated region of the cloned P2X₁ cDNA (Ennion *et al.*, 2000). The human P2X2 cDNA was originally isolated from pituitary gland (Lynch *et al.*, 1999) and was also encoded in a pcDNA3.1 plasmid.

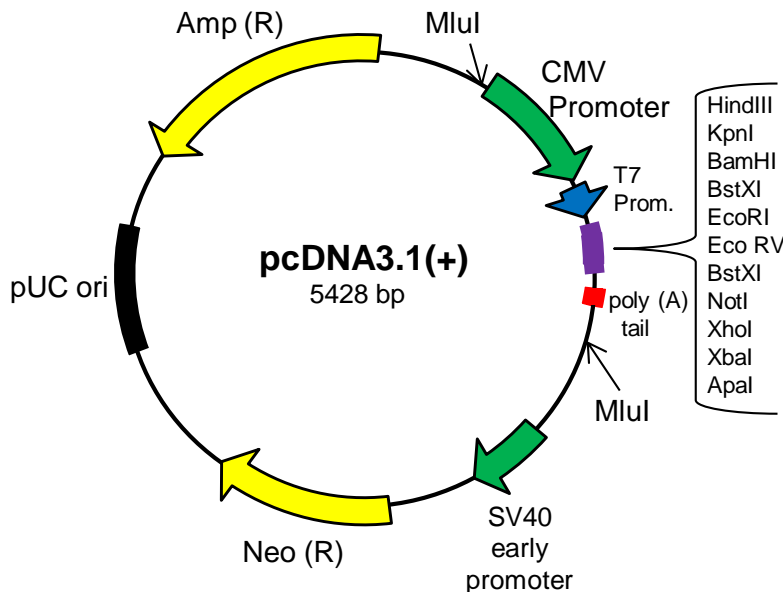


Figure 2.1. pcDNA3.1 plasmid. Plasmid map of pcDNA3.1 showing the human cytomegalovirus (CMV) promoter and the SV40 promoter in green, the modified poly(A) tail in red, the Ampicillin (Amp (R)) and neomycin (Neo (R)) resistance genes in yellow, pUC ori in black (for selection and maintenance in *E.coli*), the T7 promoter in blue and the additional restriction enzymes sites in purple (including EcoRI). The *MluI* restriction sites are labelled with an arrow.

Denaturation	95°C	for 3 minutes	
Denaturation	95°C	for 30 seconds	} 16 cycles
Annealing	55°C	for 60 seconds	
Extension	68°C	for 16 minutes	
	4°C	on hold	

To check if the PCR products were of a correct molecular weight and if there was an adequate amount (pcDNA3.1 plasmid and human P2X1 cDNA ~6600 bp) they were run on a 1% agarose gel. If the PCR failed then there would only be primer dimer bands present. The 1% agarose gel contained TAE buffer 1X (0.4M Tris-acetate, 0.01M EDTA, pH 8.3 ± 0.1) and ethidium bromide (0.5 µg/ml). 8 µl of the products were loaded onto this gel with 2 µl of loading buffer (5X blue juice, Bioline Ltd., U.K.) and run at 100 V for 30 minutes. The molecular weight marker used to quantify the bands was the DNA ladder Hyperladder™ I (Bioline Ltd., U.K.). To see if the PCR products were the correct molecular weight, the gels were visualised on a UV light box. If the PCR reaction did not amplify the sequences, a temperature gradient was used on the PCR machine varying the annealing temperature from 55°C to 75°C.

Finally, the P2X1 and P2X2 receptor plasmid templates were removed by an hour digestion with 10 units of the restriction endonuclease DpnI (Stratagene, Agilent Technologies) at 37°C. The restriction enzyme DpnI specifically digests methylated DNA and the new synthetic DNA generated is not methylated. The plasmid DNA was then transformed into supercompetent cells and then the DNA was isolated, as described in Chapter 2.1.4.

2.1.3 Generation of chimeric P2X receptors

For the generation of chimeric receptors between the P2X1 receptor and the P2X2 receptor, mega-primer-mediated domain swapping was used. Initially, a mega-primer was generated, which contained the smaller of the two receptor components required for the chimera and over-hangs at either side encoding the parent receptor (Figure 2.2). For example, the amplified mega-primer after the first PCR reaction of a P2X1 receptor

chimera, which will replace a section of the P2X1 receptor with the P2X2 receptor, would contain the section of interest of the P2X2 receptor and over-hangs of 25 base pairs of the P2X1 receptor. To generate this mega-primer, forward and reverse primers (Sigma) were designed to encode 25 base pairs of the region of interest and also a 25 base pair overhang corresponding to the desired insertion location with the body of the receptor. In order to generate a P2X1 receptor chimera, the first PCR reaction would initially contain the P2X2 receptor template to amplify the desired region of the P2X2 receptor having P2X1 receptor over-hangs (Figure 2.2). This product was then purified and used as a mega-primer for the second PCR reaction, which contains the P2X1 receptor template, adding the desired region of the P2X2 receptor into the P2X1 receptor, generating the P2X1 receptor chimera (Figure 2.2).

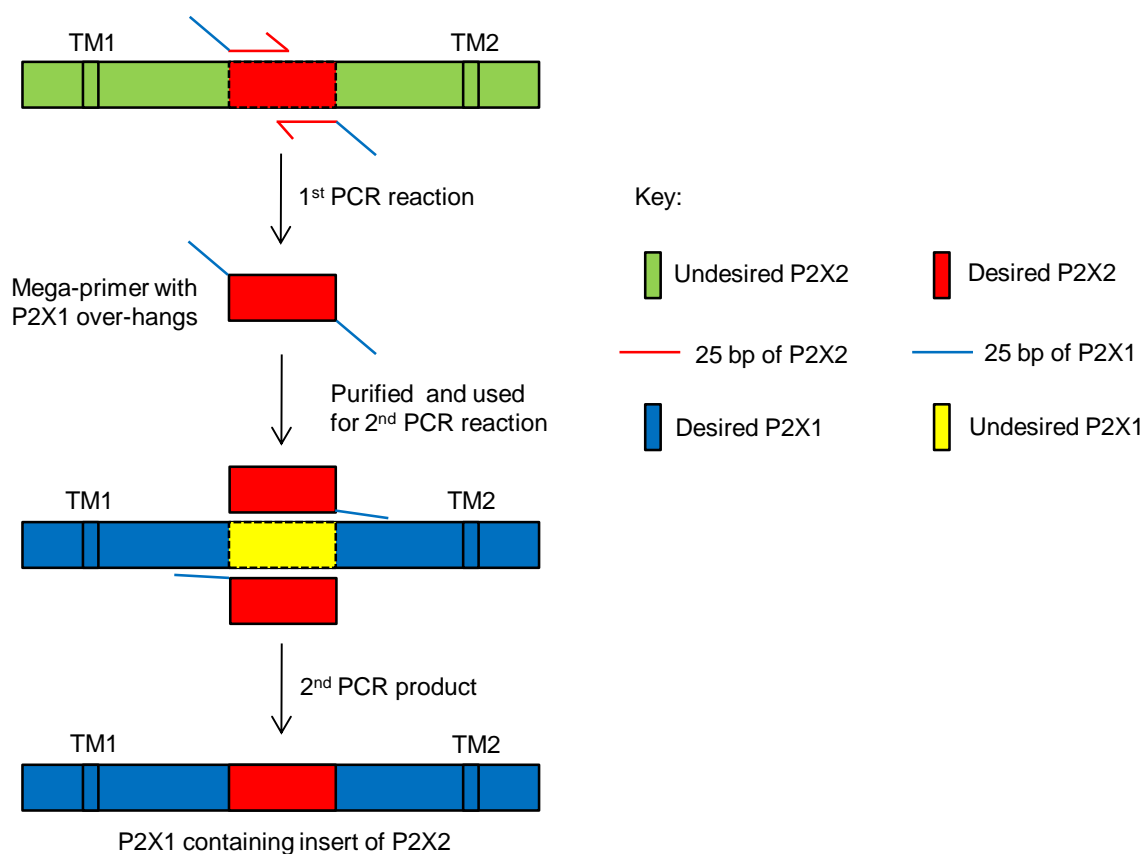


Figure 2.2. Generation of a P2X1 receptor chimera that contains part of the P2X2 receptor. 1st PCR reactions uses forward and reverse primers, which contain 25 base pairs (bp) of the P2X1 receptor and 25 bp of the P2X2 receptor, on the P2X2 receptor template amplifying the region of interest in the P2X2 receptor. This generates a mega-primer, which is purified and then used for the 2nd PCR reaction. The mega-primer amplifies the P2X1 receptor containing the P2X2 receptor region of interesting, generating the P2X1 receptor chimera.

The following steps were undertaken to generate a P2X1 receptor chimera, which contained part of the P2X2 receptor:

(i) First PCR reaction amplified the mega-primer:

1-3 μ l – human P2X2 DNA template (50 ng)

1 μ l – dNTPs (each 200 μ M)

2.5 μ l – Forward primer (250ng)

2.5 μ l – Reverse primer (250ng)

5 μ l – 10X Pfu reaction buffer

1 μ l – Pfu Turbo enzyme (2.5 u) (Agilent Technologies)

37 μ l – Nuclease free water (adjusted if >1 μ l template)

The PCR reactions came to a total volume of 50 μ l

(ii) The PCR reactions were carried out in a Techne Genius thermocycler with the following parameters:

Denaturation	95°C	for 3 minutes	} 30 cycles (high amount of cycles in order to generate a lot of the mega-primer)
Denaturation	95°C	for 30 seconds	
Annealing	55°C	for 60 seconds	
Extension	72°C	for 60 seconds	
Final extension	72°C	for 10 minutes	
	4°C	on hold	

(iii) The PCR product was separated by agarose gel (1%) electrophoresis whereby a band corresponding to the size of the mega-primers could be seen. If the amplifications did not occur then the PCR was re-run using a temperature gradient and the annealing temperatures were varied from 55°C to 75°C.

(iv) The PCR product was treated with DpnI for 1 hour to remove the template DNA leaving the mega-primer, which is the desired insert of the P2X2 receptor with over-hangs of the P2X1 receptor.

(v) The PCR product was purified using a PCR clean-up kit (Qiagen, Sussex, UK).

(vi) The second PCR reaction used 1 μ l of the mega-primer in the presence of the P2X1 receptor template to add the desired insert of the P2X2 receptor into the P2X1 receptor:

1-3 μl – human P2X1 DNA template (50 ng)
 1 μl – dNTPs (each 200 μM)
 1 μl – mega-primer generated in previous step (~30 ng)
 5 μl – 10X Pfu reaction buffer
 1 μl – Pfu Turbo enzyme (2.5 U/ μl) (Agilent Technologies)
 41 μl – Nuclease free water (adjusted if >1 μl template)
 The PCR reactions came to a total volume of 50 μl .

(vii) The PCR reactions were carried out in a Techne Genius thermocycler with the following parameters:

Denaturation	95°C	for 3 minutes	} 16 cycles
Denaturation	95°C	for 30 seconds	
Annealing	55°C	for 1 minute	
Extension	72°C	for 16 minutes	
Final extension	72°C	for 10 minutes	
	4°C	on hold	

(viii) PCR products were again checked on a 1% agarose gel for amplification and then treated with DpnI for 1 hour.

(ix) The PCR product should now consist of the P2X1 receptor chimera plasmid DNA.

In order to generate the reverse chimeras, with the P2X2 receptor containing an insert of the P2X1 receptor, the template DNA used in the first PCR reactions was the P2X1 receptor and in the second PCR reactions was the P2X2 receptor. The plasmid DNA was then transformed into supercompetent cells and then the DNA was isolated, as described below.

2.1.4 Transformation and plasmid DNA extraction

The plasmid DNA was transformed into supercompetent cells, which were grown overnight and then the DNA was isolated. To transform the plasmid DNA into cells, high efficiency XL-1 Blue supercompetent cells (Stratagene, Agilent Technologies) were used. 1 μl of the DpnI treated PCR product was added to 50 μl of the XL-1 Blue supercompetent

cells in a cooled Falcon 2059 tube and incubated on ice for 30 minutes. The transformation occurred with a heat shock, where the tube containing the cells and plasmid DNA were placed in a water bath at 42°C for 45 seconds and then the tube was placed back on ice for 2 minutes. In sterile conditions, 0.5 ml of SOC medium (Invitrogen®) was added to the cells and placed in a 37°C incubator shaking at 250 rpm for 1 hour. SOC medium is a super optimal broth with catabolite repression. 50 µl of the cells in the SOC medium were plated on LB agar Petri dishes (containing 50 µg/ml Ampicillin). These plates were left overnight in a 37°C incubator and the bacteria that were antibiotic resistant were allowed to grow.

The following day 3 distinct colonies were picked for DNA isolation. The colonies were picked from the plate using a sterile pipette tip and each colony was placed into an individual 50 ml sterilin tube (Sterilin Ltd., U.K.) containing 6ml of LB broth and 50 µg/ml Ampicillin. The minicultures were grown over night in a 37°C incubator shaking at 250 rpm. The following day, the cultures that grew were spun down for 5 minutes at 3000 rpm. The plasmid DNA was extracted using a miniprep kit (Wizard plus SV miniprep kit, Promega®), which isolated the plasmid DNA from other genomic DNA and bacterial proteins. This was recovered in 100 µl of nuclease free water. To quantify the DNA, a nanodrop spectrophotometer (Labtech International) was used.

2.1.5 Sequencing

To check to see if the correct mutation was present and that there were no spontaneous mutations present in the mutated P2X receptors, the DNA was sequenced (Protein and Nucleic Acid Chemistry Laboratory sequencing services, University of Leicester). The programme Seqman™ II (DNASTAR) was used to analyse the results obtained from the DNA sequencing. This was also carried out for the DNA of the P2X receptor chimeras.

2.1.6 mRNA synthesis

In order to generate mRNA for the characterisation of the receptor the plasmid DNA from the miniprep that was correctly sequenced was used. 40 µl of the plasmid DNA was incubated at 37°C for 4 hours with 4 µl of the restriction enzyme *MluI* (10 U/µl, Roche) to linearise the DNA. This generated a linear fragment containing the vector T7

RNA polymerase site, the cDNA and the vector poly(A) tail. The DNA may be contaminated with residual RNAs, which may inhibit transcription. Therefore, 1 μ l of proteinase K (20 mg/ml) and 5 μ l of 10% SDS were added and left at 50°C for 1 hour. This was followed with a Phenol/Chloroform/Isoamyl (25:24:1) extraction (1:1 volume) and the DNA was precipitated over night at -20°C using 2x volume of 100% ethanol. The next day, this was centrifuged at 13000 rpm for 1 hour at 4°C and washed twice with 0.5 ml of 70% ethanol. The ethanol was fully removed by drying at 50°C for 5 minutes. The DNA pellet was resuspended into 6 μ l DNAase free water.

To synthesise the mRNA the High Yield Caped RNA Transcription Kit (mMessage mMachine®, Ambion) was used for the T7 promoter. 10 μ l of ribonucleotides (2X NTP/CAP), 2 μ l of 10C Reaction Buffer and 2 μ l of T7 enzyme mix was added to the linear template DNA and incubated at 37°C for 2 hours. To remove the template DNA, 1 μ l of TURBO DNase was added and incubated at 37°C for a further 15 minutes. In order to recover the RNA and remove unincorporated nucleotides and most proteins, lithium chloride precipitation was carried out. 30 μ l of the LiCl precipitation solution (7.5M lithium chloride, 50mM EDTA) was added and stored over night at -20°C. The mRNA pellet was formed by centrifuging at 13000 rpm for 45 minutes and washed once with 1 ml of 70% ethanol. The pellet was dried at 50°C until all the ethanol was removed and resuspended in nuclease free water to give a final concentration of 1.0 μ g/ μ l. The yield was quantified by a nanodrop spectrophotometer (Labtech International).

2.2 Expression in *Xenopus laevis* oocytes

Functional studies of the wild-type, mutant and chimaeric P2X1 and P2X2 receptors were carried out by expressing the RNA in *Xenopus laevis* oocytes. The oocytes were harvested at Stage V of maturity when the pigment shows a distinct animal hemisphere (dark brown) and a vegetal hemisphere (yellow). They were manually defolliculated after being enzymatically dispersed by collagenase (1mg/ml). The oocytes were maintained at 16°C in ND96 buffer (96 mM NaCl, 2 mM KCl, 1.8 mM CaCl₂, 1 mM MgCl₂, 5 mM sodium pyruvate, 5 mM HEPES, pH 7.6) with 50 μ g/ml gentamycin, called the maintenance solution. The *Xenopus laevis* oocytes were injected with 50 nl (50 ng) of the cRNA using an Inject+Matic microinjector (J. Alejandro Gaby, Genève, Switzerland).

The recordings were made 3-7 days later using two-electrode voltage clamp electrophysiology.

2.3 Two-electrode voltage clamp recordings

The two-electrode voltage clamp technique was used on the *Xenopus laevis* oocytes expressing the RNA. The electrodes were made from capillary glass (1.5mm width TW150F-4 World Precision Instruments Inc), which were pulled on an automatic two stage puller (Narishige, Japan), so that the diameter of the tip was about 1 to 2 μ m. They were filled with 3M KCl giving them a resistance of 0.2 to 0.5 M Ω . In contrast to the maintenance solution, the 1.8mM CaCl₂ was replaced with 1.8mM BaCl₂ in the ND96 recording solution. This removed calcium from the solution and reduced the action of endogenous calcium activated chloride channels (Valera *et al.*, 1994). The oocytes were placed into a 2 ml volume recording chamber, which was perfused with the ND96 at a flow rate of ~3 ml / min. The oocytes were voltage clamped at -60mV using the Geneclamp 500B amplifier (Axon Instruments, Union City, CA, U.S.A). The data were digitised with a Digidata 1322A analog to digital converter and collected on a personal computer using pClamp 8.2 acquisition software (Molecular Devices, Menlo Park, CA), which had a sampling frequency of 2kHz and filtering frequency of 10Hz. ATP (+Mg²⁺ salt, Sigma) was applied via a U-tube perfusion system for 3 seconds in 5 minute intervals. This interval time showed reproducible responses as the receptor was able to recover from desensitisation and there was enough time for efficient solution exchange in the U-Tube perfusion system.

2.3.1 Measurement of agonist sensitivity

Concentration-response curves were fitted with the Hill equation: $Y = \frac{[(X)^H \times M]}{[(X)^H + (EC_{50})^H]}$, Y is the response, X is the agonist concentration, H is the Hill coefficient, M is the maximum response and EC₅₀ is the concentration of ATP that evokes 50% of the maximum response. In the figures, concentration-response curves were fitted to the mean normalised data, which showed the peak amplitudes as the maximum response (100%). The EC₅₀ value was also expressed as the pEC₅₀, which is the $-\log_{10}$ of the EC₅₀ value.

2.3.2 Characterisation of the effects of the different antagonists

To study the properties of antagonist action at the P2X1 receptor three different antagonists were used, suramin, PPADS (Pyridoxal-phosphate-6-azophenyl-2',4'-disulfonate) and NF449 (4,4',4'',4'''-[Carbonyl-bis[imino-5,1,3- benzenetriyl bis-(carbonylimino)]]tetrakis-(benzene-1,3-disulfonic acid). To characterise the action of suramin and PPADS at the P2X1 receptor concentration-response curves were constructed in the presence of three different concentrations of the antagonists (Suramin – 1 μ M, 3 μ M, 10 μ M; PPADS – 0.1 μ M, 1 μ M, 10 μ M). The antagonists were bath perfused for at least 5 minutes before their co-application with ATP from the U-tube. This allowed sufficient time for solution exchange around the oocyte.

Schild analysis was used to estimate the pA_2 of suramin. In order to carry out the Schild plot, the dose ratios of the 3 different concentrations of suramin were calculated. The dose ratio (DR) for each concentration of suramin is the EC_{50} of the concentration response curve in the presence of suramin divided by the EC_{50} of the concentration response curve in the absence of suramin. The Schild plot had the $\log_{10}(DR-1)$ on the Y-axis and the $\log_{10}(\text{suramin concentration})$ on the X-axis. The point where the line crosses the X-axis multiplied by -1 (X-intercept x -1) is the pA_2 value.

To investigate the effects of cysteine mutation on antagonist sensitivity, a concentration of antagonist that reduced the EC_{90} concentration of ATP response by half (either 3 μ M suramin or 1 μ M PPADS), was applied to the P2X1 receptor mutants. To characterise the action of suramin, PPADS and NF449 on the mutated and chimaeric P2X1 and P2X2 receptors, varying concentrations of the antagonists were applied to an EC_{90} concentration of ATP. This generated an inhibition curve and allowed an IC_{50} value of the antagonists to be determined for the different receptors.

2.3.3 Characterisation of the effect of the MTS compounds

The different MTS compounds used were MTSES (sodium (2-sulfonatoethyl) methanethiosulfonate) and MTSET [2-(Trimethylammonium) ethyl] methanethiosulfonate Bromide) (Toronto Research Chemicals, Toronto, Canada) MTSES and MTSET. To test the effect of each of the MTS compounds on ATP action at the wild type and cysteine mutants an EC_{50} concentration of ATP was used. An EC_{50} concentration of ATP was used

as this is the most sensitive part of the concentration-response curve. The oocytes were treated with the MTS compounds (1 mM) for 5 minutes before their co-application with ATP through the U-tube. This allowed the MTS compounds to react with the introduced cysteine residue if it is accessible in either the rested (agonist-free) or the active (agonist-bound) states.

With the cysteine mutants that had a change in the response with an EC₅₀ concentration of ATP in the presence of the MTS reagents, full concentration-response curves were generated to see if the ATP potency was affected. It is known the MTS compounds form covalent bonds with cysteine residues and this action should be irreversible. Previous studies have shown that the incubation for 3 hours with the MTS compounds should long enough for the full effects of the compounds (Roberts *et al.*, 2009). Therefore, the oocytes were treated for 3 hours with 1 mM of the MTS compounds prior to full concentration-response curves in the absence of the MTS compounds.

2.3.4 Data analysis

All data are shown as mean \pm standard error of the mean. Any significant differences between wild type and the mutant/chimaeric P2X receptors (e.g. current amplitudes, rise and decay time, hillslope, pEC₅₀ and antagonist and MTS compound results) were calculated by one-way ANOVA followed by Dunnett's test. For comparing two different values, the appropriate Student's t-test was used to $p > 0.05$. The software used was GraphPad Prism 5 (GraphPad Software Inc., San Diego, USA). Everything was repeated at least 3 times with n corresponding to the number of sets of results. The IC₅₀ values of the different antagonists on the mutated and chimaeric P2X receptors were calculated the same as explained in section 2.3.1.

2.4 Molecular modelling

A homology model of the P2X1 receptor was constructed by Ralf Schmid (Department of Biochemistry, University of Leicester). The trimeric assembly of the human P2X1 receptor (residues 33-352) was modelled in Modeller v9.7 (Marti-Renom *et al.*, 2000) based on the zebra fish P2X4 structure (PDBid: 315D) as the template. The target and template share 44% sequence identity and 67% sequence similarity based on a BLAST alignment. The best model chosen, out of the models generated, was selected

based on Modeller's scoring function and external validation via Whatcheck (Hooft *et al.*, 1996) and PROSA (Wiederstein and Sippl, 2007).

The homology model of the P2X1 receptor was then used as the starting structure for ligand docking with ATP, BzATP, suramin and NF449 (also carried out by Ralf Schmid). In preparation for ligand docking, atomic coordinates for ATP were extracted from the protein database (PDBid: 1HCK). Hydrogens were added in Hyperchem 8.0 (Hypercube Inc, Gainesville, FL, U.S.A), using the MM+ force field to generate two alternative protonation states, ATP3- and ATP2-, followed by steepest descent energy minimisation until convergence. In a similar way BzATP, were built and optimised based on the energy minimised ATP structure. Suramin and NF449 were built using Hyperchem 8.0, which were also energy minimized. The ligands were docked into the P2X1 homology model using the GOLD package (Verdonk *et al.*, 2003). The approximate location of the ATP binding site was set based on previous work (Roberts *et al.*, 2008) and was defined as all residues within a 20 Å sphere centered at the F291 backbone nitrogen. The side chains of residues Lys68, Lys70, Arg292 and Lys309 were treated as flexible using the 'flexible side chain - library' option in GOLD to better accommodate the tri-phosphate moiety of ATP. The approximate location of suramin and NF449 were defined from a 20 Å sphere centered at either residue K136 or R180 (classed as the "starting point" in later chapters). The resulting docking poses were ranked by their ChemScores (classed as the "docking scores" in later chapters) and inspected manually. All figures illustrating the homology model of the P2X1 receptor and the molecular modeling results were prepared in PyMOL (Molecular Graphics System, Version 1.2r3, Schrödinger, LLC.).

Chapter 3. Characterisation of Suramin and PPADS

3.1 Introduction

Two non-selective P2 antagonists, suramin and PPADS, have been widely used at P2X receptors over the past 20 years. Initial studies in this thesis have characterised their action at the human P2X1 receptor. The P2X1 receptor is expressed throughout the cardiovascular system and has been shown to have various functional roles including the vasoconstriction of mesenteric arteries, autoregulation of afferent arterioles in the kidney and formation of thrombi (Vial *et al.*, 2002; Inscho *et al.*, 2003; Hechler *et al.*, 2003). Understanding the molecular basis of antagonist action at the P2X1 receptor could contribute to the development of novel drugs benefitting the treatment of hypertension and stroke.

3.1.1 Inhibition of the P2X receptor

In the 1980s, laboratories were interested in characterising the P2X receptor in blood vessels and vas deferens and understanding their role in sympathetic cotransmission (Sneddon and Burnstock, 1984; Stjarne and Astrand, 1984; Allcorn *et al.*, 1986). Interestingly, focus was mainly on the smooth muscle and it is now known that the P2X1 receptor was the subtype present. However, before any useful P2X selective antagonists were identified, researchers relied on the fact that the P2X receptors being investigated had a desensitising phenotype in the presence of the agonist, α,β -methylene ATP. Therefore, to understand the contribution of these P2X receptors in native tissues, the response was abolished by desensitising the receptor using α,β -methylene ATP (Byrne and Large, 1986). This agonist is now known to be inactive at most cloned subunits (Brake *et al.*, 1994; Khakh *et al.*, 1995) and only acts at P2X1 and P2X3 receptors (Evans *et al.*, 1995; Lewis *et al.*, 1995). Another alternative to remove the P2X receptor function, which locked the receptor in a desensitised state, was the use of the photoaffinity label arylazido aminopropinyl adenosine triphosphate (ANAPP₃). However, there were limitations in using ANAPP₃ as it was irreversible and also caused an initial activation of the receptors, like α,β -methylene ATP (Hogaboom *et al.*, 1980). Therefore, there was a requirement for selective P2X receptor antagonists in order to fully understand the functional role of P2X receptors in native tissues.

3.1.2 P2 receptor antagonist Suramin

Suramin (8-[(4-methyl-3-[[3-([3-(2-methyl-5-[(4,6,8-trisulfo-1-naphthyl) carbamoyl] phenylcarbamoyl) phenyl] carbamoyl] amino) -benzoyl] amino} benzoyl] amino] naphthalene-1,3,5-trisulfonic acid) was developed by Bayer in 1916 as an anti-protozoal drug and the formula was published by Fourneau *et al.* (1924). Since then, suramin has been shown to act to inhibit a range of targets, including; (i) enzymes taking part in carbohydrate metabolism (Town *et al.*, 1950), lysozymes (Lominski and Gray, 1961), (ii) calcium transport in the sarcoplasmic reticulum (Layton and Azzi, 1974), (iii) plasma membrane Mg^{2+} -ATPase (Smolen and Weissmann, 1978) and (iv) reverse transcriptase of RNA tumor viruses (De Clercq, 1979). Therefore, suramin can block ATP binding at many enzymes and raised the possibility that suramin might act at the P2X receptor. A study by Dunn and Blakely in 1988 initially tested this possibility and found that suramin could inhibit α,β -methylene ATP induced contractions in the mouse vas deferens (Dunn and Blakeley, 1988). Subsequently, excitatory junction potentials were also shown to be inhibited in isolated guinea-pig vas deferens (Sneddon, 1992). This was the starting point for the use of suramin as a P2X receptor antagonist. Suramin was found to be an effective competitive antagonist of P2X receptors in various native tissues, for example in the; (i) mouse vas deferens (Leff *et al.*, 1990), (ii) rabbit ear artery (von Kugelgen *et al.*, 1990), (iii) rat phaeochromocytoma cells (Nakazawa *et al.*, 1991), (iv) rat vas deferens (Khakh *et al.*, 1994), (v) cat colon (Venkova *et al.*, 1994), and (vi) rat vagus nerve (Trezise *et al.*, 1994). These studies were carried out on native tissues and subsequently suramin was investigated at molecularly defined receptors.

Cloning of P2X receptors has shown that the P2X receptors in native conditions correspond to different molecular subtypes (as explained in Chapter 1). Suramin can antagonise the majority of the P2X receptor subtypes, with the lowest affinity for the P2X4 receptor and the highest for the P2X1 receptor (Table 3.1). Experiments on the human P2X1 receptor found that the suramin could block ATP-induced currents with an IC_{50} value of $\sim 1 \mu M$ and was a competitive and reversible antagonist (Evans *et al.*, 1995; Khakh *et al.*, 1995). Suramin has contributed to the detection and identification of the role of P2X1 receptors in mesenteric arteries and platelets (Lewis and Evans, 2000; Vial *et al.*, 1997).

Antagonists	IC ₅₀ (μM)						
	P2X ₁	P2X ₂	P2X ₃	P2X ₄	P2X ₅	P2X ₆	P2X ₇
Suramin	1 to 5	10	3	178	4	<100	100
PPADS	1	2	1	27.5	3	<100	4.2

Table 3.1. IC₅₀ values in μM of antagonists at different rat P2X receptors. (Data taken from Evans *et al.*, 1995; Bo *et al.*, 1995; Buell *et al.*, 1996; Collo *et al.*, 1996; Soto *et al.*, 1996; Surprenant *et al.*, 1996; Garcia-Guzman *et al.*, 1997).

3.1.3 P2 receptor antagonist PPADS

Pyridoxalphosphate-6-azophenyl-2',4'-disulphonic acid (PPADS) was initially demonstrated by Lambrecht *et al.*, (1992) as an antagonist for P2-purinoceptor-mediated responses in the rabbit vas deferens. PPADS inhibited the P2X receptor at lower concentrations (1-10 μM) compared with suramin (>10 μM) suggesting PPADS had a greater affinity than suramin for the P2X receptors in vas deferens. PPADS was shown not to antagonise other receptors such as α₁-adrenoceptors, histamine H₁- or adenosine A₁-receptors, muscarinic M₁-(M₄-), M₂- and M₃-receptors (Lambrecht *et al.*, 1992; Grimm *et al.*, 1994). Subsequently, PPADS was found to inhibit contractile responses evoked by α,β-methylene ATP; (i) in the rabbit urinary bladder without affecting contractions mediated via muscarinic receptors (Ziganshin *et al.*, 1993), (ii) in the rabbit ear artery and saphenous artery without affecting contractions mediated by noradrenaline or histamine (Ziganshin *et al.*, 1994), (iii) in the guinea-pig isolated vas deferens without affecting contractions mediated by noradrenaline, carbachol or histamine (McLaren *et al.*, 1995). Therefore, PPADS was thought to be a useful P2X receptor antagonist.

Cloning of the different subtypes of the P2X receptor showed that PPADS antagonised various recombinant P2X receptors with PPADS being most effective at the P2X₁ and P2X₃ receptors (Table 3.1; Ralevic and Burnstock *et al.*, 1998; Khakh *et al.*, 2001). The P2X₁ receptor was inhibited by PPADS with an IC₅₀ value of ~1 μM (Khakh *et al.*, 2001; Kim *et al.*, 2001). PPADS is thought to be a slow-acting antagonist at the rat P2X₁ receptor with higher amounts of antagonism at the receptor with longer incubation of PPADS (Khakh *et al.*, 1994). These effects were slowly reversible after a washing-out period of up to 40 minutes (Khakh *et al.*, 1995). A precursor of PPADS, pyridoxal-5-phosphate (P-5-P), has also been shown to be an effective antagonist at the P2X receptor

(Trezise *et al.*, 1994b) and in other proteins P-5-P has been shown to form Schiff bases with lysine residues (Snell and Dimari, 1980). Therefore, the slowly reversible nature of PPADS may be due to the formation of Schiff bases between the P2X receptor and PPADS.

3.1.4 Structure of suramin and PPADS

Suramin has a molecular formula of $C_{51}H_{34}N_6O_{23}S_6$ and the structure of suramin shows symmetry with the centre of the molecule being based around an urea, NH-CO-NH (Figure 3.1A). It contains 8 benzene rings, 4 of which are fused to together to form two naphthyl rings, 4 amide groups in addition to the urea and 6 polysulfonates. There are 3 polysulfonates on each naphthyl ring which gives suramin its negative charge. PPADS has a molecular formula of $C_{14}H_{10}N_3O_{12}P_1S_2$, which contains three charges, one on the phosphate moiety and one on each of the two polysulfonates (Figure 3.1B).

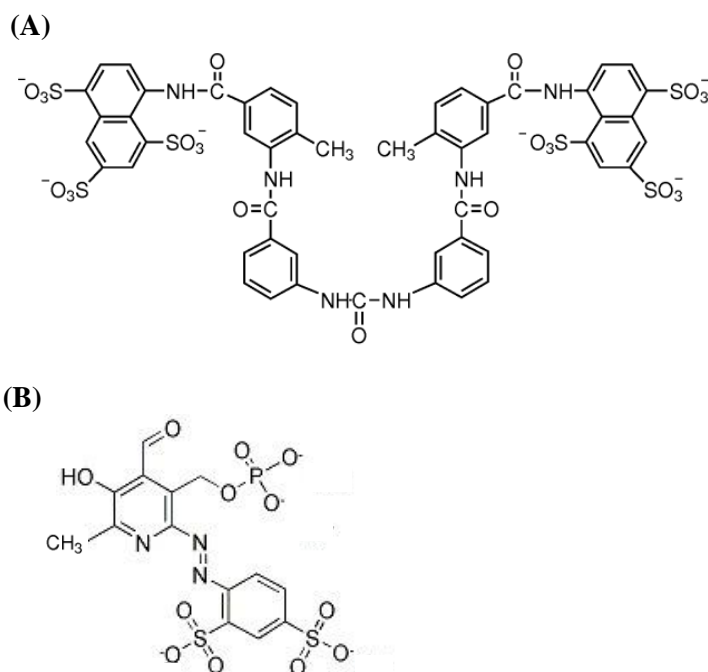


Figure 3.1. Structure of (A) Suramin and (B) PPADS (taken from Sigma-Aldrich and Santa Cruz Biotechnology Inc. websites)

3.1.5 Aims

The aim of this thesis was to understand the molecular basis of antagonist action at the human P2X1 receptor. Initial characterisation of the two antagonists, suramin and PPADS, was carried out to understand the basic pharmacology of these antagonists and

compare how the antagonists act at the P2X1 receptor. Characterisation of these two P2X receptor antagonists led to a prediction of how and where the antagonists may act.

3.2 Results

3.2.1 ATP action at the human WT P2X1 receptor

In this thesis the P2X receptors were expressed in *Xenopus laevis* oocytes and their properties were characterised using two-electrode voltage clamp electrophysiology. ATP evoked concentration-dependent currents at the wild-type (WT) human P2X1 receptor with an EC₅₀ value of ~0.76 μM (pEC₅₀ of 6.15 ± 0.10; Figure 3.2, Table 3.2). The EC₅₀ value is the concentration of the ATP that generates 50% of the maximal response and is used as the measure of ATP potency at the receptors. The ATP potency of the human P2X1 receptor is consistent with previous reports (Evans *et al.*, 1995; Ennion *et al.*, 2000; Roberts *et al.*, 2004, 2006, 2007).

A maximum concentration of ATP (100 μM) was applied to the WT P2X1 receptor and produced a transient inward current that decayed during the 3 second application of ATP. This decay in the presence of agonist corresponds to the closing of the ligand bound receptor and is referred to as desensitisation. The 10-90% rise time of the current was 81 ± 7 ms and the response decayed to 50% during the continued presence of ATP in 465 ± 55 ms (Figure 3.3A). This time-course of the ATP-evoked response was also concentration dependent (Figure 3.3B). Lower concentrations of ATP had slower rise-times and desensitisation compared to the maximum response (Figure 3.2C).

3.2.2 Characterisation of suramin action at WT P2X1 receptor

Suramin has previously been shown to act as a partial agonist at constitutively active P2X2 receptors (Cao *et al.*, 2007). However, suramin (100 μM) had no effect on the holding current when applied on its own at the WT P2X1 receptor. To characterise the action of suramin on the ATP-evoked response, suramin was pre-superfused around the oocyte for 5 minutes before being co-applied with ATP for 3 seconds. For all concentrations of suramin, maximum inhibition of the ATP-evoked response was produced within 5 minutes and this was fully reversed after a 5 minute wash-off period.

Figure 3.2

Figure 3.3

The action of suramin at the WT P2X1 receptor was measured by calculating the ATP potency of the receptor in the presence of different concentrations of suramin (1 μM , 3 μM and 10 μM). Suramin antagonised the ATP-evoked response with a parallel rightward shift in the concentration response curve having no change in the maximum response (Figure 3.5; Table 3.2). The ATP potency of the WT P2X1 receptor decreased by ~ 5 -fold in the presence of 1 μM suramin to an EC_{50} of ~ 4.0 μM , by ~ 15 -fold in the presence of 3 μM suramin to an EC_{50} of ~ 11.3 μM ATP and by ~ 40 -fold in the presence of 10 μM suramin to an EC_{50} of ~ 27.9 μM ATP (pEC_{50} of 5.42 ± 0.07 , 4.99 ± 0.12 and 4.56 ± 0.05 , respectively; Figure 3.4A and 3.5; Table 3.2). To measure the affinity of suramin for the WT P2X1 receptor a Schild plot analysis was carried out. The Schild plot had a slope of 0.9 ± 0.1 and a pA_2 value of 6.72 (Figure 3.5B). This was similar to the value estimated by Ennion *et al.* (2000) of 6.7.

Increasing concentrations of suramin on a defined concentration of ATP not only reduced the ATP-evoked current but also slowed the time-course of the response. For example, the rise-time of the evoked response to 10 μM ATP was reduced in a concentration dependent manner by suramin, with higher concentrations of suramin slowing the rise-time (Figure 3.4B). This is also consistent with the decay-time of the ATP-evoked response but with suramin concentrations higher than 3 μM the current did not desensitise to 50% during the 3 second application of ATP. The rightward parallel shift of the concentration-response curve with similar maximum current amplitudes, the slowing of the time course and the linear relationship (slope of ~ 1) observed in the Schild plot suggested that suramin is acting as a competitive antagonist at the human P2X1 receptor.

3.2.3 Characterisation of PPADS action at WT P2X1 receptor

PPADS is also an antagonist which inhibits P2-receptors (Lambrecht *et al.*, 1992). PPADS (100 μM) had no effect on the holding current when applied on its own at the WT P2X1 receptor suggesting that PPADS does not act as a partial agonist. To characterise the action of PPADS on the ATP-evoked response, PPADS was pre-superfused around the oocyte for 5 minutes before being co-applied with ATP for 3 seconds. For all concentrations of PPADS, maximum inhibition of the ATP-evoked response was produced within 5 minutes and was fully reversed after a 5 minute wash-off period.

Figure 3.4

Figure 3.5

Increasing concentrations of PPADS (0.1 μM , 1 μM , 10 μM and 100 μM) decreased the amplitude of the ATP-evoked response at the WT P2X1 receptor with essentially no effect on the time-course or ATP sensitivity (Figure 3.6 and 3.7). In the presence of 0.1 μM PPADS there was a decrease in the amplitude of the maximum response to ATP (100 μM) by ~15% (Figure 3.6). Increasing the concentration of PPADS further decreased the amplitude of the maximum response by ~60% with 1 μM PPADS, by ~80% with 10 μM PPADS and by ~97% with 100 PPADS μM (Figure 3.6; Table 3.2). The ATP potency at the WT P2X1 receptor in the presence of 0.1 μM and 1 μM PPADS was similar to the WT P2X1 with EC_{50} values of 0.91 μM and 0.69 μM , respectively (pEC_{50} of 6.05 ± 0.07 and 6.22 ± 0.14 ; Figure 3.7A; Table 3.2). However, higher concentrations of PPADS (10 μM and 100 μM) slightly decreased the ATP potency. In the presence of 10 μM and 100 μM PPADS the ATP potency at the WT P2X1 receptor was an IC_{50} of 3.09 μM and 4.56 μM , respectively (pEC_{50} of 5.51 ± 0.03 and 5.35 ± 0.06 ; Figure 3.7; Table 3.2). The reason for the decrease in ATP potency may have been due to the ATP-evoked currents having small amplitudes making it difficult to calculate an accurate EC_{50} .

Increasing concentrations of PPADS did not affect the time-course of the ATP-evoked currents. For example, the rise-times of the responses to 10 μM ATP produced an inward current with similar rise-times in the absence or presence of different concentrations of PPADS (Figure 3.7B). This was also consistent with the decay-time of the responses. The reduction of the maximum response of the concentration-response curves without much change to the time-course or the ATP potency suggested that PPADS is acting as a non-competitive antagonist at the human P2X1 receptor. Therefore, suramin and PPADS most likely have a different molecular basis of action at the human P2X1 receptor.

Figure 3.6

Figure 3.7

Antagonist Concentration (μM)	EC_{50} (μM)	pEC_{50}	Hillslope	Peak Current (nA)
Control	0.76	6.15 \pm 0.10	1.00 \pm 0.14	6311 \pm 373
Suramin:				
1	3.97	5.42 \pm 0.07*	1.03 \pm 0.12	6481 \pm 401
3	11.27	4.99 \pm 0.12**	1.27 \pm 0.16	6109 \pm 514
10	27.89	4.56 \pm 0.05**	1.84 \pm 0.40**	5998 \pm 198
PPADS:				
0.1	0.91	6.05 \pm 0.07	0.78 \pm 0.25	5301 \pm 452
1	0.69	6.22 \pm 0.14	0.98 \pm 0.12	2674 \pm 327**
10	3.09	5.51 \pm 0.03*	0.96 \pm 0.18	1341 \pm 201***
100	4.56	5.35 \pm 0.06*	5.58 \pm 0.89***	178 \pm 21***

Table 3.2. Suramin and PPADS action at the P2X1 receptor. EC_{50} , pEC_{50} , Hillslope and peak current amplitude of the WT P2X1 receptor in the presence of different concentrations of suramin (1, 3 and 10 μM) and PPADS (0.1, 1, 10 and 100 μM). EC_{50} is the concentration of ATP that produces half of the maximum response. pEC_{50} is the $-\log_{10}(\text{EC}_{50})$. $n = 3$ to 5 for all data sets. * $p < 0.05$, ** $p < 0.01$, *** $p < 0.001$. Values are mean \pm S.E.M.

3.3 Discussion

The characterisation of agonist action at the human P2X1 receptor has substantiated previous studies showing that the application of ATP on the P2X1 receptor produces an inward current with an EC₅₀ of ~0.76 μ M. The inward current rapidly desensitises during the 3 second application of a maximal concentration of ATP. These findings are consistent with previous studies on the human P2X1 receptor (Evans *et al.*, 1995; Ennion *et al.*, 2000; Roberts *et al.*, 2004, 2006, 2007). The antagonists, suramin and PPADS, were found to have different characteristics on the ATP-evoked response at the P2X1 receptor, suramin being competitive and PPADS being non-competitive.

3.3.1 Suramin acts as a competitive antagonist

Increasing the concentration of suramin applied to the P2X1 receptor resulted in a rightwards parallel shift in the concentration-response curves. This effect was reversible with inhibition being fully removed after a 5 minute wash-out period. This suggested that suramin is acting as a reversible competitive antagonist at the P2X1 receptor. This was similar to a previous study on the human P2X1 receptor where suramin (1 μ M) shifted the concentration-response curve by almost 10-fold (Evans *et al.*, 1995). To further support competitive antagonism, the Schild plot had a slope of ~1. Also, suramin had a pA₂ value of 6.72 at the human P2X1 receptor, which is consistent with the estimation by Ennion *et al.*, (2000) that was calculated from a single concentration.

These results support previous studies which have shown that suramin acts like a reversible competitive antagonist at the P2X receptors (Leff *et al.*, 1990; Zhong *et al.*, 1998; Surprenant, 1996; Wildman *et al.*, 1998; North, 2002). These studies have used several different methods to highlight the competitive antagonism of suramin; (i) the reduction in contractions in native tissues, (ii) the reduction in the binding of radioligands, and (iii) the reduction in currents produced from recombinant P2X receptors. Experiments on the rabbit isolated ear artery showed that concentration-response curves of α,β -methylene ATP in the presence of increasing concentrations of suramin had a rightward parallel shift with a Schild plot slope of ~1 (Leff *et al.*, 1990). Radioligand binding studies also suggested that suramin is a competitive antagonist by the inhibitory effects of suramin being overcome by increasing concentrations of ATP γ S (Michel *et al.*, 1996) and suramin

competed for binding sites labelled by [^3H] α,β -methylene ATP in rat vas deferens (Khakh *et al.*, 1994). Also, electrophysiological recordings of recombinant P2X receptors showed that suramin had the properties of a competitive antagonist on the agonist-evoked responses (Wildman *et al.*, 1998).

However, a few studies on the P2X receptor suggested that suramin does not have the characteristics of a competitive, contradicting the competitive nature of suramin observed in this chapter (Wong *et al.*, 2000; Trujillo *et al.*, 2006; Guerrero-Alba *et al.*, 2010). Single channel analysis of P2X receptors in outside-out patches from rat hippocampal granule cells showed that the P2X receptor present had a larger conductance than any homomeric P2X receptors (Wong *et al.*, 2000). The P2X receptor present was suggested to be composed of a heteromer made up of P2X4 and P2X6 subunits, or possibly any three of the P2X1, P2X2, P2X4 and P2X6 subunits (Wong *et al.*, 2000). Single channel analysis showed that this receptor had an increase in the single channel conductance and a small reduction in Popen in the presence of suramin, with a decrease in the mean open time, burst length and the total open time per burst (Wong *et al.*, 2000). These results were unusual and were not consistent with simple competitive antagonism. This is because a competitive antagonist should affect the ability of the agonist to bind to the receptor but once the agonist is bound there should not be any affect on the Popen or the channel conductance. The non-competitive nature observed might be the properties of the heteromeric P2X receptor present in these cells, which was not identified. However, suramin has been shown to act as a competitive antagonist at the human P2X1 receptor in this thesis.

A radioligand binding assay showed that suramin did not interfere with [α - ^{32}P]ATP-receptor binding on 1321N1 human glioma cells expressing recombinant P2X2 receptors, suggesting that ATP and suramin do not act the same binding site (Trujillo *et al.*, 2006). However, there could be some non-specific binding of the radioligand to other ATP-binding proteins on the cell surface, giving the impression that suramin did not interfere with [α - ^{32}P]ATP-receptor binding at the P2X2 receptor (see Chapter 6 for the action of suramin on the human P2X2 receptor). In a more recent study, suramin has also been shown to act a non-competitive antagonist on murine myenteric P2X receptors (Guerrero-

Alba *et al.*, 2010). In the presence of suramin (30 μ M) both the ATP potency and the maximum response decreased (Guerrero-Alba *et al.*, 2010). Also, increasing concentrations of ATP did not revert the suramin inhibitory effect (Guerrero-Alba *et al.*, 2010).

One of the issues associated with understanding purinergic pharmacology is agonist stability. ATP is known to be susceptible to breakdown by ectonucleotidases but α,β -methylene ATP is relatively resistant to degradation (Welford *et al.*, 1986 and 1987). This has been shown in single cell studies where ATP was more effective at P2X receptors when the breakdown was controlled but in whole tissue studies the potency of ATP was reduced (Evans and Kennedy, 1994). There was a different rank order of agonist potency at the P2X receptors in single rat tail artery smooth muscle cells (ATP \geq α,β -methylene ATP) compared to the P2X receptors in the rat isolated tail artery (α,β -methylene ATP \gg ATP) (Evans and Kennedy, 1994). Also, suramin is known to inhibit P2X receptors at a similar concentration range to concentrations that inhibit ecto-ATPases (Crack *et al.*, 1994; Humphrey *et al.*, 1995). In native systems, suramin can inhibit the action of ATP but concomitantly increases the ATP concentration by stopping it from being degraded. For example, in the rabbit ear artery, the ATP potency increased in the presence of suramin (Crack *et al.*, 1994). This suggested that inhibition of the P2X receptor by suramin was overcome by the increase of ATP due to the inhibition of the ATPases (Crack *et al.*, 1994). Therefore, careful consideration is needed in whole tissue studies when using unstable ligands.

Suramin has been shown to not only antagonise P2X subtypes (Table 3.1) but also P2Y receptors and other proteins. For example, suramin can inhibit P2Y receptors in smooth muscle cells of guinea-pig taenia caeci (Den Hertog *et al.*, 1989; Hoyle *et al.*, 1990), aortic endothelial cells (Wilkinson *et al.*, 1993) and in rat coronary vasculature (Vials and Burnstock, 1994). At higher concentrations suramin can also, inhibit nicotinic receptors (Allgaier *et al.*, 1995), glutamatergic synaptic transmission (Motin and Bennett, 1995), GABA receptors (Nakazawa *et al.*, 1995) and glutamate receptors, both NMDA (Ong *et al.*, 1997) and AMPA receptors (Nakazawa *et al.*, 1995). Therefore, the generation of antagonists with higher selectivity for the P2X receptor were required.

Selective P2X receptor antagonists have been generated based around the structure of suramin. Some of these antagonists have shown nanomolar sensitivity at the P2X1 receptor compared to other P2X receptor subtypes (see Chapter 5.1 for details; Lambrecht, 1996, Ziyal *et al.*, 1997, Soto *et al.*, 1999; Lambrecht, 2000; Braun *et al.*, 2001; Rettinger *et al.*, 2005). These selective P2X1 receptor antagonists are analogues of suramin and the site of antagonist action at the P2X1 receptor could be similar, which was investigated in this thesis (Chapters 5 and 6).

3.3.2 Possible mechanisms of suramin action at the P2X1 receptor

Crystal structures of other proteins have shown suramin to interact with part of the ATP binding site (Ganesh *et al.*, 2005; Schuetz *et al.*, 2007; Zhou *et al.*, 2008). In one example, suramin competes with ADP-ribose at the human SIRT5 and inhibits SIRT5 NAD⁺-dependent deacetylase activity (Schuetz *et al.*, 2007). Two crystal structures were determined of SIRT5, one in a complex with ADP-ribose and the other with suramin. The superimposition of these two complexes showed that the ends of the suramin and ADP-ribose overlap with the same active site, involving similar residues. Therefore, suramin has been shown to act as a competitive antagonist, competing for a similar site as the agonist, at other suramin-bound complexes.

For suramin to be classified as a competitive antagonist suramin would be thought to compete with ATP for some or all of the residues at its active site. This was supported by suramin acting as a partial agonist at constitutively active P2X2 receptors (Cao *et al.*, 2007). However, studies have shown that the mutation of the residues predicted to be part of the ATP binding site in the P2X1 receptor, have either resulted in only a small reduction (R292A), had no effect (K68A, K70A and K309A) or even increased suramin sensitivity (F291A; Ennion *et al.*, 2000; Roberts and Evans, 2004). Also, mutation of residues that were found to be involved in suramin sensitivity (described in Chapters 4 and 6) did not have a large effect on ATP potency (Garcia-Guzman *et al.*, 1997; Sim *et al.*, 2008). Therefore, it appears for at least the residues tested so far that suramin and ATP do not compete for exactly the same residues at the P2X receptor. To give the appearance of a competitive antagonist at the P2X1 receptor observed in this chapter, suramin could be acting in a variety of ways:

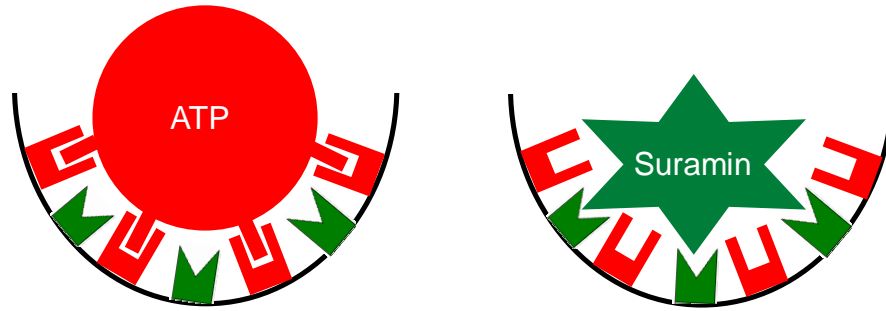


Figure 3.8. Suramin binding in the ATP binding pocket. ATP (red) and suramin (green) could coordinate with distinct residues with either ATP (left) or suramin (right) binding in the agonist binding pocket. Residues involved in ATP binding are in red and residues involved in suramin binding are in green.

- 1) The sites of action for suramin and ATP could overlap with the 2 molecules coordinating with distinct residues in the same region (Figure 3.8). The model shows ATP binding to different residues than suramin in the ATP binding pocket. This would give the appearance of a competitive antagonist.

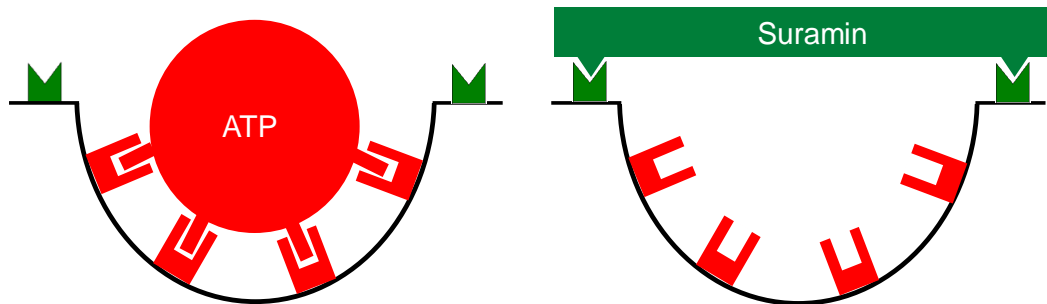


Figure 3.9. Suramin binding over the top of the ATP binding pocket. ATP (red) could coordinate with residues in the binding pocket (left) but the addition of suramin (green) can block ATP access by binding over the top of the ATP binding pocket (right). Residues involved in ATP binding are in red and residues involved in suramin binding are in green.

- 2) Suramin could bind close to the ATP binding site and block access of the ATP molecule from entering its binding pocket (Figure 3.9). This could be a region above the ATP binding pocket and suramin could be acting in an “umbrella” fashion. The model shows ATP binding at its active site and then suramin binding above the active site blocking ATP from entering.

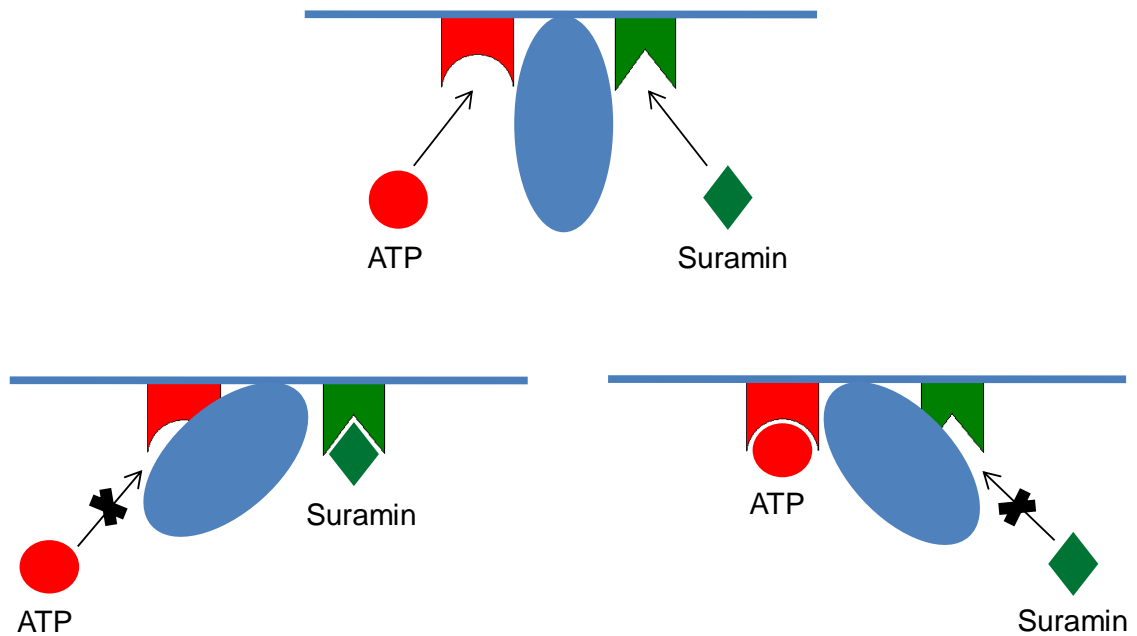


Figure 3.10. Suramin binding at a region adjacent to the ATP binding site causing a conformational change in the receptor. (i) ATP (red) and suramin (green) binding sites are separated by part of the P2X1 receptor (blue). (ii) Suramin binding into its active site, causing a conformational change in the receptor and blocking the ATP binding site. (iii) Increasing the concentration of ATP allows ATP to enter its binding site, causing a conformational change in the receptor, removing suramin from its binding site.

3) The site of action of suramin could be located at a different region of the P2X receptor. This region could be adjacent to the ATP binding pocket and suramin binding could stabilise a certain conformation reducing the ability of the receptor to bind ATP. The conformation change that takes place during suramin binding could move part of the receptor, which blocks ATP from entering its binding pocket (Figure 3.10). The model shows the resting state of the P2X1 receptor when the ATP and suramin binding sites are unoccupied. Suramin binding could cause a conformational change moving part of the P2X1 receptor over the ATP binding site, reducing the access of ATP. Increasing the concentration of ATP allows ATP to enter its active site, reducing suramin binding. This mechanism could also account for the displacement of the radioligands from P2X receptors during increased concentrations of suramin (Michel *et al.*, 1996).

The predicted ATP binding site of the P2X receptors is thought to be conserved throughout the P2X receptor family (as described in Chapter 1.8). For example, residues that have been shown to be involved in ATP potency at the P2X1 receptor appear to be

involved in ATP potency at the P2X2 and P2X4 receptors (Jiang *et al.*, 2000; Roberts and Evans, 2006; Roberts *et al.*, 2008, 2009; Zemkova *et al.*, 2007). This would suggest that there may be a core binding site for ATP throughout the P2X receptor with a few differences in residues between subunits to account for the changes in ATP sensitivity. Suramin may also have a core binding site between the suramin sensitive P2X receptors. However, the residues that have been shown to be involved in suramin sensitivity, for example, K78 in the P2X4 receptor (Garcia-Guzman *et al.*, 1997) and K138 in the P2X1 receptor (Sim *et al.*, 2008), are not conserved in any other P2X receptor subunit. Therefore, to date, there does not appear to be an obvious core binding site for suramin across the P2X receptor family. However, the regions around these residues may play a role in suramin action. The residues in the P2X1 receptor around the corresponding residue of K78 from the P2X4 receptor were investigated in more detail and are described in the next chapter. Also, the region around K138 may also be important in antagonist sensitivity and this region was investigated in Chapters 5 and 6.

3.3.3 PPADS acts as a non-competitive antagonist

In contrast to the competitive nature of suramin, the chemically distinct antagonist, PPADS, had the characteristics of a non-competitive antagonist at the human P2X1 receptor. Increasing the concentration of PPADS decreased the maximum of the concentration response curve without much change in the time-course of the response or the ATP potency. The non-competitive nature of PPADS is consistent with previous observations (Lambrecht *et al.*, 1992). For example, PPADS inhibited the P2X1 receptor that mediated neurogenic excitatory junction potentials and contractions in guinea-pig isolated vas deferens in non-competitive nature (McLaren *et al.*, 1994).

In this chapter, PPADS inhibition was fully reversed at the P2X1 receptor after a 5 minute wash-off period. However, previous studies have shown that PPADS inhibition is long lasting (Khakh *et al.*, 1994; Li, 2000). PPADS produced a long-lasting inhibition of P2X receptors in the bullfrog dorsal root ganglion (DRG) neurons (Li, 2000) and the effects of PPADS on the rat P2X1 receptor were only partially removed after a washing-out period of 40 minutes (Khakh *et al.*, 1994). Also, PPADS was predicted to form a possible Schiff base with a basic amino acid in the P2X1 receptor (Khakh *et al.*, 1994). The reason for the

irreversible or reversible nature of PPADS may be due to the different cell types that were expressing the P2X receptors and/or the subtype that is expressed. For example, the two studies mentioned above were carried out in isolated vas deferens and DRG neurons and in this chapter antagonist action was characterised on *Xenopus laevis* oocytes expressing the human WT P2X1 receptor. In oocytes, there may be a rapid turnover of P2X1 receptors and antagonist-unbound P2X1 receptors could be recycling to the surface in the 5 minute wash-off period. Evidence supporting this has come from experiments using MTS reagents on P2X1 receptor cysteine mutants (data not shown). MTS reagents form a covalent bond with free cysteine residues on the receptor (as explained in the next Chapter), but when the oocytes were incubated for 5 minutes the effects were reversible after a subsequent wash-off period of 5 minutes. This might suggest that P2X1 receptors, which do not have MTS reagents bound, may be coming to the surface of the oocytes. This may be why the effects of PPADS were rapidly reversible in this thesis.

The understanding of how PPADS acts at the P2X1 receptor and the determination of its site of action could contribute towards the design of selective P2X1 receptor antagonists. There is a requirement for subtype selective antagonists as PPADS is not P2X subtype selective (Table 3.1) and can also antagonise P2Y receptors. For example, native studies have shown that PPADS can inhibit P2Y receptors the guinea-pig taenia coli, mesenteric arterial bed and turkey erythrocytes (Ziyal *et al.*, 1994; Windscheif *et al.*, 1994; Boyer *et al.*, 1994). PPADS also inhibits ecto-ATPases, which reduces the hydrolytic activity in cell assays affecting agonist potency (Chen *et al.*, 1996). Taking into account the ability of PPADS to antagonise various P2-purinoceptors and ATPases, there is a further need for antagonists with improved selectivity for the P2X receptor and a reduced ATPase activity.

To improve antagonist selectivity, analogues have been constructed based around the structure of PPADS. MRS 2220 (cyclic pyridoxine- α -4,5-monophosphate-6-azophenyl-2',5'-disulfonate) was found to be a selective antagonist at the P2X1 receptor over other P2 receptors. However, this antagonist was ~10-fold less sensitive at P2X1 receptors compared to PPADS (Jacobson *et al.*, 1998). Further derivatives of PPADS were made with modifications on the sulfophenyl ring and the phosphate moiety. The naphthylazo

derivative PPNDS (pyridoxal-5'-phosphate-6-(2'-naphthylazo-6'-nitro-4',8'-disulfonate) was ~6-fold more potent at P2X1 receptors compared to PPADS (Lambrecht *et al.*, 2000). PPADS can block P2X and P2Y receptors with similar potency but PPNDS had a much higher selectivity for the P2X1 receptors over P2Y1 receptors, up to ~52-fold (Ralevic and Burnstock, 1996; Lambrecht *et al.*, 2000). A study investigating seven PPADS analogues found that the analogues which contained a 5'-phosphonate group, rather than a 5'-phosphate group in the pyridoxal moiety of PPADS, and with the disulphonate groups removed or substituted at the azophenyl moiety were very potent at the rP2X1 receptor (Brown *et al.*, 2001). The most sensitive analogue was MRS 2257 (pyridoxal-5'-phosphonate 6-azophenyl 3',5'-bismethylenephosphonate) with an IC₅₀ of 5 nM at the rP2X1 receptor. These highly sensitive and selective P2X1 receptor antagonists were not investigated in this thesis but they are derived from the antagonist PPADS. Therefore, the understanding of the molecular basis of PPADS action at residue level on the P2X1 receptor (investigated in Chapter 4 and 6) could help towards the development of more sensitive and selective P2X1 antagonists.

The non-competitive nature of PPADS suggested that suramin and PPADS have a different molecular basis of action at the human P2X1 receptor. This is supported by previous studies where point mutations and species homologues had different suramin and PPADS sensitivities (Buell *et al.*, 1996; Garcia-Guzman *et al.*, 1997; Soto *et al.*, 2003). The non-competitive nature observed in this chapter suggests that PPADS could be affecting the gating response subsequent to binding of ATP. PPADS may be binding at the P2X1 receptor structure causing a conformational change affecting the signal that is translated to the pore during gating of the channel. Another possibility is that PPADS is reducing the number of receptors being activated, which would reduce the peak current amplitude of the ATP evoked-response.

In summary, suramin has the characteristics of a competitive antagonist due to the parallel rightwards shift in concentration-response curve. Suramin could be reducing the ability of ATP to bind to its active site either directly or by causing a conformational change in the receptor. Also, PPADS has the characteristics of a non-competitive antagonist due to the reduction of the maximum in the concentration-response curves without affecting

the ATP sensitivity. This suggests that suramin and PPADS most likely have a difference molecular basis of action at the P2X1 receptor. To investigate this in more detail the regions around and adjacent to the proposed ATP binding site have been studied in Chapters 4, 5 and 6.

Chapter 4. Involvement of region V74 to G96 in P2X1 receptor properties

4.1 Introduction

Mutagenesis of conserved residues in the P2X receptor family has given a model of the predicted ATP binding site and this has been substantiated by the crystal structure of the zP2X4 receptor (Chapter 1.8). What was of interest in this thesis was the extent of the agonist binding pocket and in particular, the residues involved in antagonist action. To investigate this, cysteine scanning mutagenesis of the region V74 to G96 has been carried out to identify further residues involved in P2X1 receptor properties, which has refined the model of ATP binding site.

This investigation was started before the crystallisation of the zP2X4 receptor and a linear array of amino acids from V74 to G96 was chosen for a couple of reasons. Firstly, a previous study had highlighted the lysine at position 78 in the P2X4 receptor as being important in suramin sensitivity (Garcia-Guzman *et al.*, 1997) and the corresponding residue in the P2X1 receptor (P78) is incorporated in this region. The antagonist profile is known to be variable across the P2X receptor family (Table 3.1) and this residue and/or the region around it may underlie the molecular differences between the subunits. This region could contain residues which coordinate the antagonists and give antagonists, such as suramin and PPADS, a higher affinity for the P2X1 receptor compared to other P2X receptors. Secondly, this region is linearly close to a couple of residues that have been shown to play an important role in agonist action (K68 and K70). The residues V74 to G96 may contain residues that form part of the ATP binding site and residues that underlie the molecular differences in agonist sensitivity between the subunits.

During the characterisation of this region the crystal structure of the zP2X4 receptor was published (Kawate *et al.*, 2009), which allowed the residues V74 to G96 to be mapped on the homology model of the P2X1 receptor (Figure 4.1). Interestingly, these residues appear to line the rear/inner cavity of the ATP binding pocket and can be divided into two different regions;

- (i) Residues V74-W85 (purple on Figure 4.1) are located above the predicted ATP binding site. This region contains the corresponding residue (P78) which has been shown to play a role in suramin sensitivity in the P2X4 receptor (K78) so it may be important in antagonist action. Interestingly, this region is close to the cysteine rich head region and this region could play a role in antagonist action (Chapters 5 and 6).
- (ii) Residues D86-G96 (green on Figure 4.1) are located at the back of the ATP binding pocket and may interact with ATP and/or the antagonists.

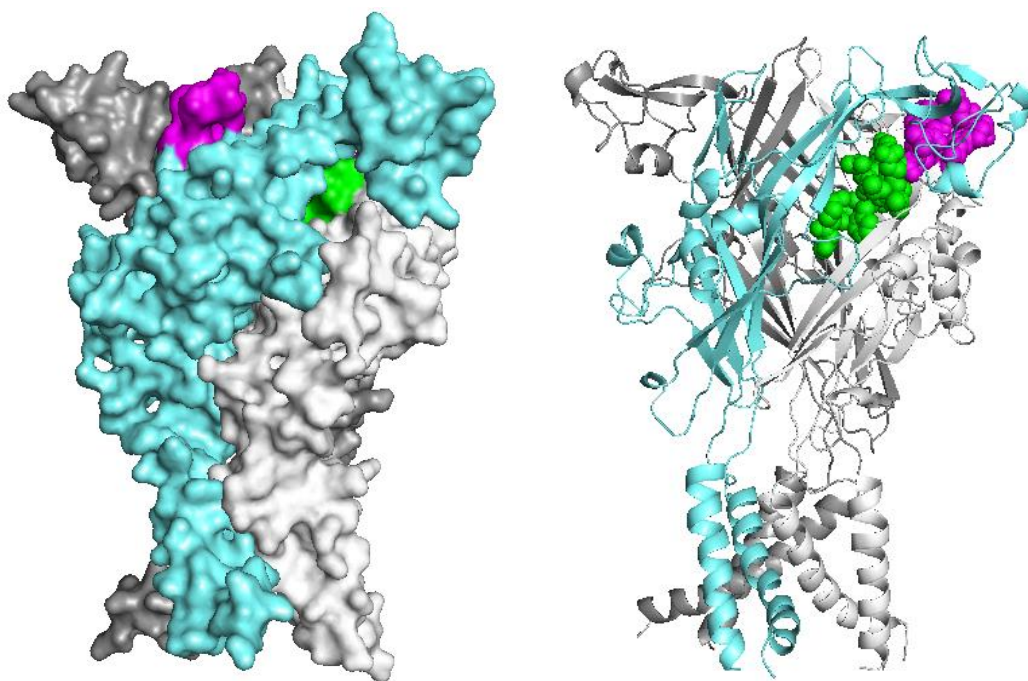


Figure 4.1. Residues V74 to G96 on the homology model of the P2X1 receptor. The homology model of the P2X1 receptor is based on the crystal structure of the zP2X4. Trimeric subunits are in white, grey and cyan in either surface rendering (left) or cartoon (right). In the left panel the residues V74 to W85 are in purple and D86 to G96 are in green in all subunits. In the right panel the third subunit has the residues V74 to W85 in purple spheres, D86 to G96 in green spheres, with the rest of the P2X receptor in cartoon format.

Therefore, this chapter details the importance of the region at the back of the ATP binding site and the region adjacent to the cysteine rich head region on agonist and antagonist action. To investigate this region a systematic unbiased approach was used by using cysteine scanning mutagenesis. This approach has been used in previous studies to identify residues important in the function of acetylcholine receptors (Akabas *et al.*, 1992),

Kir6.2 channels (Trapp *et al.*, 2003) and also P2X receptors (Rassendren *et al.*, 1997; Egan *et al.*, 1998; Jiang *et al.*, 2001; Haines *et al.*, 2001; Roberts and Evans, 2007; Roberts *et al.*, 2008, 2009). One advantage of using cysteine scanning mutagenesis is that the introduced cysteine residue can be modified by MTS reagents. These can change the size and the charge of the side chain of accessible cysteine residues, changing the local charge environment, which is helpful for further characterisation of the receptor.

4.1.1 Aims

The P2X1 receptor residues V74 to G96 are located at the back of the ATP binding site and adjacent to the cysteine rich head region. The roles of these residues in P2X1 receptor properties were determined by using cysteine scanning mutagenesis and investigated with ATP, partial agonists, MTS reagents and antagonists. This highlighted the depth of the agonist binding site, residues associated with channel activation subsequent to agonist binding and residues involved in the molecular basis of antagonist (suramin and PPADS) action. The recent publication of the crystal structure of the zP2X4 receptor allowed the residues to be mapped on the homology model of the P2X1 receptor, which are shown in the discussion, and this substantiated the model of the predicted ATP binding pocket.

4.2 Results

4.2.1 F92 has a role in ATP potency at the P2X1 receptor

The effects of individual cysteine mutation of the residues V74 to G96 on channel properties was determined by expressing the P2X1 mutants in *Xenopus laevis* oocytes and by using two-electrode voltage clamp electrophysiology. Initially, the ATP potency was calculated at the individual P2X1 receptor point mutants by generating concentration-response curves. The majority of mutants tested in the run V74 to Q95 (21/22 mutants) had no change in ATP potency and all of the mutants had a similar peak current amplitudes compared to the WT P2X1 receptor (Figure 4.2D, Table 4.1). However, the ATP potency was reduced by ~120 fold at the F92C mutant, with an EC_{50} value of ~95 μ M (pEC_{50} 4.02 ± 0.42 , $p < 0.001$ compared to WT P2X1; Figure 4.2). Also, the maximum response to ATP (10 mM) of this mutant had a slower time-course of desensitisation (by ~4-fold) during the 3 second application compared to the WT P2X1 receptor (decay-time of 1680 ± 321 ms; Table 4.1). The decrease in ATP potency and change in the time-course highlighted a role of the non-conserved phenylalanine at position 92 in the binding of ATP and/or the subsequent gating of the P2X1 receptor.

4.2.2 Partial agonists identify additional residues involved in agonist action

In other receptors, such as ionotropic glutamate receptors, the effect of point mutation on partial agonist efficacy has been used to highlight further residues involved in channel activation (Armstrong *et al.*, 2003; Jin *et al.*, 2003). These residues were suggested to be involved in gating and the conformational changes of the receptor subsequent to agonist binding. 3'-O-(4-benzoylbenzoyl)-ATP (BzATP) is as potent as ATP at the WT P2X1 receptor but has a reduced efficacy of ~0.5 making it a partial agonist at the P2X1 receptor (Roberts and Evans, 2004). In this chapter the efficacy of BzATP at the WT P2X1 receptor was similar to previous studies, with an efficacy of 0.48 ± 0.02 (Table 4.1). At the majority of mutants from V74C to G96C (15/23 mutants) there was a similar BzATP efficacy as the WT P2X1 receptor (Table 4.1). The mutant which had a reduced ATP potency, F92C, also had a reduced BzATP efficacy of 0.12 ± 0.04 , further highlighting the role of F92 in agonist action (Figure 4.3, Table 4.1). There were 7 other mutants with a decreased BzATP efficacy, which were either decreased by about half (T75C, G81C, W85C, Q95C and G96C) or were almost abolished (Y90C and P93C; Figure 4.3, Table

Figure

4.2.....

4.1). For the mutants with a decrease in the response there was no difference in efficacy between 10 or 100 μM BzATP indicating there had not been a decrease in the potency. The change in efficacy observed with BzATP highlighted additional residues involved in subtle changes in the P2X receptor upon agonist binding.

For the mutants which had a changed BzATP potency, the efficacy of the partial agonists P1, P5-di(adenosine-5') pentaphosphate (Ap5A) and α,β -methylene ATP (α,β -meATP) were also determined. These partial agonists also had a similar potency to ATP and were applied at 100 μM at each of the mutants (Evans *et al.*, 1995; Roberts and Evans, 2004). At the WT P2X1 receptor the efficacy of Ap5A and α,β -meATP was 0.40 ± 0.09 and 0.56 ± 0.09 , respectively (Figure 4.3; Table 4.1). The pattern of changes in efficacy for Ap5A was similar compared to BzATP for the majority of the mutants (decreases in efficacy at mutants G81C, Y90C, F92C, P93C, Q95C and G96C; Figure 4.3). However, there was no change in the efficacy to Ap5A at the mutant W85C compared to the WT P2X1 receptor. Interestingly, the majority of mutants (7/8) with a decreased BzATP efficacy had no change in the efficacy of α,β -meATP (Figure 4.3). Only the mutant F92C had a decreased α,β -meATP efficacy compared to the WT P2X1 receptor (efficacy of 0.19 ± 0.02 ; Figure 4.3).

These results show that partial agonists can reveal subtle changes in properties of the P2X receptor not seen for ATP. The results obtained with the partial agonists can be used to classify mutants into three groups; (i) Mutants with a decrease in ATP potency and efficacy of all partial agonists (F92C). (ii) Mutants with agonist dependent efficacy changes (T75C, G81C, Y90C, P93C, Q95C, G96C; reductions in BzATP and Ap5A efficacy but no effect on α,β -meATP). (iii) Mutants which were least sensitive to partial agonists (W85C; efficacy reduction only for BzATP).

4.2.3 Effects of charged MTS reagents on cysteine mutants

Thiol reactive MTS reagents have previously been used to modify accessible cysteine residues and investigate molecular properties of a range of ion channels including P2X receptors (Akabas *et al.*, 1992; Rassendren *et al.*, 1997). The effects of the negatively charged sodium (2-sulfonatoethyl) methanethiosulfonate (MTSES) and the larger positively charged 2-(Trimethylammonium) ethyl] methanethiosulfonate Bromide

Figure 4.3.....
.....

(MTSET) were tested on the cysteine mutants. The MTS reagents (1mM) were pre-superfused around the oocyte for 5 minutes and then an EC₅₀ concentration of ATP was applied to the WT and mutant P2X1 receptors.

MTSES (1 mM) had no effect on the WT P2X1 receptor currents in response to an EC₅₀ concentration of ATP (Figure 4.4), similar to previous findings (Roberts *et al.*, 2007). This is consistent with the lack of free cysteine residues in the WT P2X1 receptor. For the majority of mutants (18/23) MTSES had no effect on the ATP-evoked response. However, responses were significantly inhibited at the P2X1 receptor mutants P82C, D86C, V87C, P93C and G96C (Figure 4.4; Table 4.1).

Mutants that were reduced by MTSES were investigated further to determine whether ATP sensitivity and responses to a maximal concentration of ATP were also affected. For the mutants P82C and D86C, MTSES reduced the response to a maximal concentration of ATP but had no effect on agonist potency (Figure 4.5, Table 4.2). This suggested that mutating these residues caused an effect on the conformational changes affecting gating of the channel subsequent to agonist binding. In addition to a reduction in the amplitude of currents to a maximal concentration of ATP, MTSES also reduced ATP potency for the P2X1 receptor mutants V87C, P93C and G96C by ~2 to ~4-fold (Figure 4.5, Tables 4.2). This suggested that mutating these residues affected ATP binding and/or gating of the channel.

The effects of a positively charged MTS reagent, MTSET, were also tested at the WT and mutant P2X1 receptors. MTSET (1 mM) had a small effect on the response to an EC₅₀ concentration of ATP increasing it by $10 \pm 8\%$ at WT P2X1 receptors consistent with previous findings (Roberts *et al.*, 2009). For the majority of mutants (22/23) there was no significant change in the response to MTSET compared to the WT P2X1 receptor (Figure 4.4). At the mutant V91C, MTSET potentiated the EC₅₀ concentration of ATP (1 μ M) by $71 \pm 21\%$ and the maximum response to ATP (100 μ M) by $25 \pm 4\%$ (Figures 4.4 and 4.5, Table 4.2 and 4.3). MTSES did not have an effect on the ATP potency of this mutant V91C (Figure 4.5, Table 4.3) suggesting this residue is important in the gating of the channel subsequent to agonist binding.

Figure 4.4

Figure 4.5

4.2.4 Antagonist action at P2X1 receptor mutants

Suramin is a known P2-receptor antagonist (Dunn and Blakeley, 1988) and has been shown to act as a competitive antagonist at the P2X1 receptor. The region V74 to G96 is close to the predicted ATP binding site and a lysine residue at position 78 in the P2X4 receptor has been shown to play a role in suramin sensitivity (Garcia-Guzman *et al.*, 1997). This raised the possibility that this region might be important in mediating antagonist action. The effects on suramin sensitivity were tested on an EC₉₀ concentration of ATP at the WT and mutant P2X1 receptors to standardise the effects of any change in ATP potency. At the WT P2X1 receptor an EC₉₀ concentration of ATP (10 µM) was reduced by 52 ± 2% in the presence of 3 µM suramin. Therefore, testing of the effects 3 µM suramin on an EC₉₀ concentration of ATP at the cysteine mutants provided a sensitive assay to detect any changes in antagonist action compared to the WT P2X1 receptor.

At the majority of mutants there were no changes in suramin sensitivity compared to the WT P2X1 receptor (19/23). However, there was an increase in sensitivity at the four mutants (T75C, Y90C, P93C and Q95C; Figure 4.6). Interestingly, all of these mutants, which had an increase in suramin antagonism, were associated with a decrease in the efficacy of BzATP (Table 4.3). A Schild analysis was carried for the mutant with the greatest increase in suramin sensitivity (Y90C) to observe the change in suramin affinity. Suramin had a pA₂ value of 7.2 at the Y90C, which showed suramin to have a ~3 fold higher affinity at this mutant compared to the WT P2X1 receptor (pA₂ of 6.7; Figure 4.6).

PPADS is another P2-receptor antagonist (Lambrecht *et al.*, 1992) and has been shown to act a non-competitive antagonist (Chapter 3) suggesting that PPADS may act a region adjacent to the predicted ATP binding pocket. PPADS (1 µM) reduced the response to an EC₉₀ concentration of ATP at the P2X1 WT receptor by 44 ± 7%. Therefore, 1 µM PPADS was used to test for any changes in PPADS sensitivity at the P2X1 receptor mutants. Interestingly, there was no change in sensitivity to PPADS for any of the cysteine mutants in the region V74-G96 (Figure 4.6). These results suggested that residues in the region V74-G96 do not make a major contribution on suramin or PPADS action at the P2X1 receptor.

Figure 4.6

Mutant	pEC ₅₀	Peak (nA)	Rise-Time (ms)	Decay-Time (ms)	BzATP Efficacy	Suramin Inhibition (%)	PPADS Inhibition (%)	MTSES (% change)	MTSET (% change)
WT	6.10 ± 0.07	8503 ± 590	81 ± 7	465 ± 55	0.48 ± 0.02	52 ± 2	44 ± 7	5 ± 3	10 ± 8
V74C	5.67 ± 0.10	7362 ± 1572	82 ± 8	327 ± 88	0.30 ± 0.07	71 ± 3	59 ± 5	-5 ± 11	-5 ± 1
T75C	6.07 ± 0.06	10562 ± 429	76 ± 7	476 ± 56	0.01 ± 0.01***	90 ± 4*	45 ± 14	-4 ± 4	-2 ± 2
Q76C	6.02 ± 0.05	5598 ± 636	67 ± 8	255 ± 39	0.31 ± 0.12	62 ± 4	73 ± 6	-8 ± 7	22 ± 7
L77C	6.14 ± 0.12	10263 ± 1277	73 ± 5	452 ± 30	0.27 ± 0.05	42 ± 9	36 ± 6	-18 ± 6	-7 ± 13
P78C	6.14 ± 0.03	9634 ± 1798	72 ± 7	373 ± 17	0.48 ± 0.07	69 ± 2	49 ± 5	17 ± 4	15 ± 10
G79C	6.09 ± 0.03	9888 ± 1057	97 ± 6	418 ± 32	0.24 ± 0.04	48 ± 5	33 ± 5	-4 ± 2	31 ± 6
L80C	6.17 ± 0.02	10328 ± 584	79 ± 14	608 ± 170	0.33 ± 0.02	66 ± 3	38 ± 8	-4 ± 13	17 ± 4
G81C	5.92 ± 0.09	7006 ± 831	67 ± 8	420 ± 91	0.17 ± 0.04***	61 ± 12	78 ± 3	-5 ± 8	-17 ± 8
P82C	6.03 ± 0.02	10055 ± 867	68 ± 12	367 ± 57	0.45 ± 0.09	54 ± 2	38 ± 8	-40 ± 7**	11 ± 6
Q83C	5.97 ± 0.13	6285 ± 1783	84 ± 4	554 ± 39	0.46 ± 0.03	60 ± 8	19 ± 4	-10 ± 7	-21 ± 6
V84C	6.11 ± 0.24	10279 ± 924	73 ± 10	388 ± 35	0.40 ± 0.09	72 ± 10	44 ± 4	-12 ± 7	39 ± 16
W85C	6.04 ± 0.17	8694 ± 917	65 ± 8	511 ± 95	0.12 ± 0.02***	82 ± 6	72 ± 5	-19 ± 9	-3 ± 6
D86C	6.04 ± 0.03	4572 ± 558	76 ± 10	342 ± 107	0.39 ± 0.03	88 ± 3	62 ± 7	-34 ± 4**	-31 ± 7
V87C	6.72 ± 0.09	7773 ± 1345	69 ± 10	369 ± 51	0.50 ± 0.08	53 ± 6	23 ± 9	-38 ± 8**	-24 ± 10
A88C	6.08 ± 0.30	9398 ± 886	70 ± 8	357 ± 59	0.63 ± 0.10	64 ± 6	65 ± 3	-7 ± 2	-2 ± 4
D89C	6.14 ± 0.14	6881 ± 1175	57 ± 2	255 ± 44	0.33 ± 0.04	46 ± 9	87 ± 1	-18 ± 3	12 ± 7
Y90C	5.83 ± 0.05	6741 ± 306	105 ± 11	628 ± 14	0.02 ± 0.01***	95 ± 1**	62 ± 10	-22 ± 5	-8 ± 1
V91C	6.05 ± 0.07	6440 ± 362	80 ± 17	565 ± 101	0.27 ± 0.05	84 ± 1	43 ± 6	-4 ± 14	74 ± 16*
F92C	4.02 ± 0.42***	6032 ± 970	149 ± 24	1680 ± 322***	0.03 ± 0.01***	55 ± 10	83 ± 5	10 ± 2	18 ± 1
P93C	5.64 ± 0.04	6929 ± 343	105 ± 34	863 ± 162	0.04 ± 0.01***	96 ± 0**	70 ± 6	-55 ± 3***	15 ± 9
A94C	6.23 ± 0.01	5930 ± 471	101 ± 12	753 ± 57	0.29 ± 0.04	67 ± 2	81 ± 3	-22 ± 8	40 ± 10
Q95C	5.85 ± 0.10	8213 ± 535	116 ± 30	840 ± 32	0.12 ± 0.02***	90 ± 3*	41 ± 8	-11 ± 4	23 ± 5
G96C	5.28 ± 0.10	7084 ± 563	113 ± 9	789 ± 205	0.13 ± 0.04***	68 ± 11	68 ± 10	-38 ± 4**	12 ± 4

Table 4.1. Summary of effects of cysteine substitution on P2X1 receptor mutants E52C to G96C pEC₅₀ values are shown as calculated from experimental data. pEC₅₀ is -log₁₀ of the EC₅₀. Peak current values are taken from the 1st application of a maximal concentration of ATP (100 μM to 10 mM). For the partial agonist data, values correspond to the efficacy of the partial agonist (100 μM) compared with a maximal concentration of ATP (100 μM to 10 mM). Suramin and PPADS inhibition data is taken from the inhibition of an EC₉₀ concentration of ATP in the presence of an IC₅₀ concentration of the antagonist. MTS data is calculated as a percentage change of the response to an EC₅₀ concentration of ATP in the presence and absence of the MTS reagent (1mM). Conserved residues are shown in a black box. *p<0.05; **p<0.01; ***p>0.001. n = 3–12. Values are mean ± S.E.M.

Mutant	pEC ₅₀		% change of peak response
	Control	With MTSES	
P82C	6.03 ± 0.02	6.16 ± 0.11	-38 ± 2**
D86C	6.04 ± 0.03	5.96 ± 0.19	-28 ± 2**
V87C	6.72 ± 0.09	6.20 ± 0.13*	-50 ± 2**
P93C	5.64 ± 0.04	5.14 ± 0.02***	-39 ± 5*
G96C	5.28 ± 0.10	4.72 ± 0.07***	-30 ± 3**
	Control	With MTSET	
V91C	6.05 ± 0.07	6.29 ± 0.08	25 ± 4*

Table 4.2. Effect of MTSES and MTSET on P2X1 receptor mutants. pEC₅₀ values are calculated from the experimental data in the absence and the presence of MTSES (1mM) or MTSET (1mM). pEC₅₀ is -log₁₀ of the EC₅₀. The change of the peak response is shown as a percentage change of the maximal response of the mutant P2X receptor in the presence of MTSES or MTSET. Conserved residues are shown in a black box. Values are mean ± S.E.M.

Mutant	EC ₅₀	BzATP Efficacy	Suramin Inhibition	MTSES	MTSET
WT	0.73	0.48	48%	↑ 5%	↑ 10%
V74C	-	-	-	-	-
T75C	-	↓	↑	-	-
Q76C	-	-	-	-	-
L77C	-	-	-	-	-
P78C	-	-	-	-	-
G79C	-	-	-	-	-
L80C	-	-	-	-	-
G81C	-	↓	-	-	-
P82C	-	-	-	↓	-
Q83C	-	-	-	-	-
V84C	-	-	-	-	-
W85C	-	↓	-	-	-
D86C	-	-	-	↓	-
V87C	-	-	-	↓	-
A88C	-	-	-	-	-
D89C	-	-	-	-	-
Y90C	-	↓	↑	-	-
V91C	-	-	-	-	↑
F92C	↓	↓	-	-	-
P93C	-	↓	↑	↓	-
A94C	-	-	-	-	-
Q95C	-	↓	↑	-	-
G96C	-	↓	-	↓	-

Table 4.3. Summary of effects of cysteine substitution on P2X1 receptor mutants V74C to G96C. Significant changes are shown with an upwards arrow, indicating an increase in the value, or a downwards arrow, indicating a reduction in the value. Dashes indicate residues that did not have a significant change in the response. pEC₅₀ values are calculated from the concentration-response curves of the mutant P2X1 receptors. The values for partial agonist data, values correspond to the efficacy of BzATP (100 μM) compared with a maximal concentration of ATP (100 μM to 10 mM). Suramin inhibition data is taken from the inhibition of an EC₉₀ concentration of ATP in the presence of an IC₅₀ concentration of the antagonist. MTS data is calculated as a percentage change of the response to an EC₅₀ concentration of ATP in the presence and absence of the MTS reagent (1mM). Conserved residues are shown in a black box.

4.3 Discussion

Cysteine scanning mutagenesis of the residues V74 to G96 has highlighted additional residues involved in P2X1 receptor properties. With the aid of the homology model of the P2X1 receptor (figures shown below) these findings have identified an additional residue involved in ATP potency, giving an indication of the extent of the agonist binding site, and have identified residues at the rear/inner cavity that are important in channel activation. Also, cysteine scanning mutagenesis has ruled out the contribution of the residues V74 to G96 in coordinating the action of suramin and PPADS at the P2X1 receptor.

4.3.1 Importance of F92 on ATP potency

Several previous mutagenesis studies have provided a model of the predicted ATP binding pocket. This model incorporates the positively charged residues K68, K70 and K309, which are thought to bind the phosphates of ATP, N290, F291 and R292 coordinating the adenine ring of ATP and a regulatory role of the F185T186 doublet through polar interactions (P2X1 receptor numbering, as described in Chapter 1.8; Roberts *et al.*, 2009). Investigating the region V74-G96 highlighted an additional residue involved in ATP sensitivity at the P2X1 receptor. Mutating the phenylalanine at position 92 to a cysteine reduced the ATP potency by ~120-fold compared to the WT P2X1 receptor. Mapping the residue F92 onto the homology model of the P2X1 receptor, along with the other residues thought to be part of the ATP binding site, shows F92 to be located at the back of the ATP binding pocket, on the inner/rear cavity of the groove (Figure 4.7A). Aromatic residues have previously been shown to coordinate the adenine ring of ATP in DEAD box helicases and the ribose of ATP in UvrB DNA helicase (Tanner *et al.*, 2003; Theis *et al.*, 1999). Therefore, the phenylalanine at position 92 in the P2X1 receptor could contribute to the binding of the adenine/ribose ring of ATP.

Based on the key residues predicted to be involved in ATP binding, ligand docking was used on the homology model of the P2X1 receptor (carried out by Ralf Schmid, Department of Biochemistry, University of Leicester) to dock ATP at the predicted ATP binding site (Figure 4.7B). The ligand docking solution with the highest docking score is shown in Figure 4.7B. This model predicted that the phosphate tail of ATP is co-ordinated

by the conserved positively charged residues at the receptor surface with the adenine buried within the binding pocket. Interestingly, the residue F92 is shown to be close to the ribose of ATP (Figure 4.7B). The other residues that are predicted to coordinate ATP are; (i) the positively charged residues K68, K70, R292, K309 and the NH₂-amide of N290, which coordinate the partially negative oxygens of the phosphate moiety, (ii) the residues V67, F100, F289 and F291, which form a hydrophobic pocket for the adenine ring, (iii) L69, which donates a hydrogen bond to the ring-oxygen of the ATP-ribose, (iv) A88, which its backbone carbonyl interacts with the 3'-hydroxyl group of the ATP-ribose, and (v) G96 and D97, which coordinate with the amino group of ATP-adenine through two hydrogen bonds from their backbone carbonyls (as explained in Allsopp *et al.*, 2011). Interestingly, the P2X1 receptor mutant G96C has previously been shown to have a ~5-fold decrease in ATP potency compared to the WT P2X1 receptor (Digby *et al.*, 2005). Therefore, this model supports the contribution of the residue F92 in the binding of ATP and the other residues which have found to be important in ATP binding, such as the lysine residues in the P2X1 to P2X4 receptors (Ennion *et al.*, 2000; Jiang *et al.*, 2000; Zemkova *et al.*, 2007; Bodnar *et al.*, 2010). Also, the residues F185 and T186 are shown to be adjacent to the pocket, possibly having a regulatory role in ATP action.

A recent study has shown the docking of ATP on a homology model of the P2X2 receptor in two different possible binding models (Jiang *et al.*, 2011). The ATP binding sites were localised by used a proximity-dependent “tethering” reaction, which caused covalent bonds forming between a thiol-reactive P2X2 agonist (NCS-ATP) and introduced single point cysteine mutants (Jiang *et al.*, 2011). Two different conformations were shown, firstly, with a similar orientation as described above and secondly, the opposite orientation with the phosphates binding deep inside the ATP binding pocket (Jiang *et al.*, 2011). However, the second docking model on the homology of the P2X2 receptor does not show the predicted close proximity of the positively charged residues (K68 and K70, P2X1 receptor numbering) with the negatively charged phosphate tail. Work carried out by Allsopp *et al.*, (2011) used charged MTS reagents to show that reapplying the positive charge at the P2X1 receptor mutants, K68C and K70C, increases ATP sensitivity. This further suggested that these residues are most likely to be close to the negatively charged phosphate tail of ATP. Therefore, docking models with the phosphate tail of ATP

interacting with the positively charged residues have a greater possibility of being correct compared to models that do not.

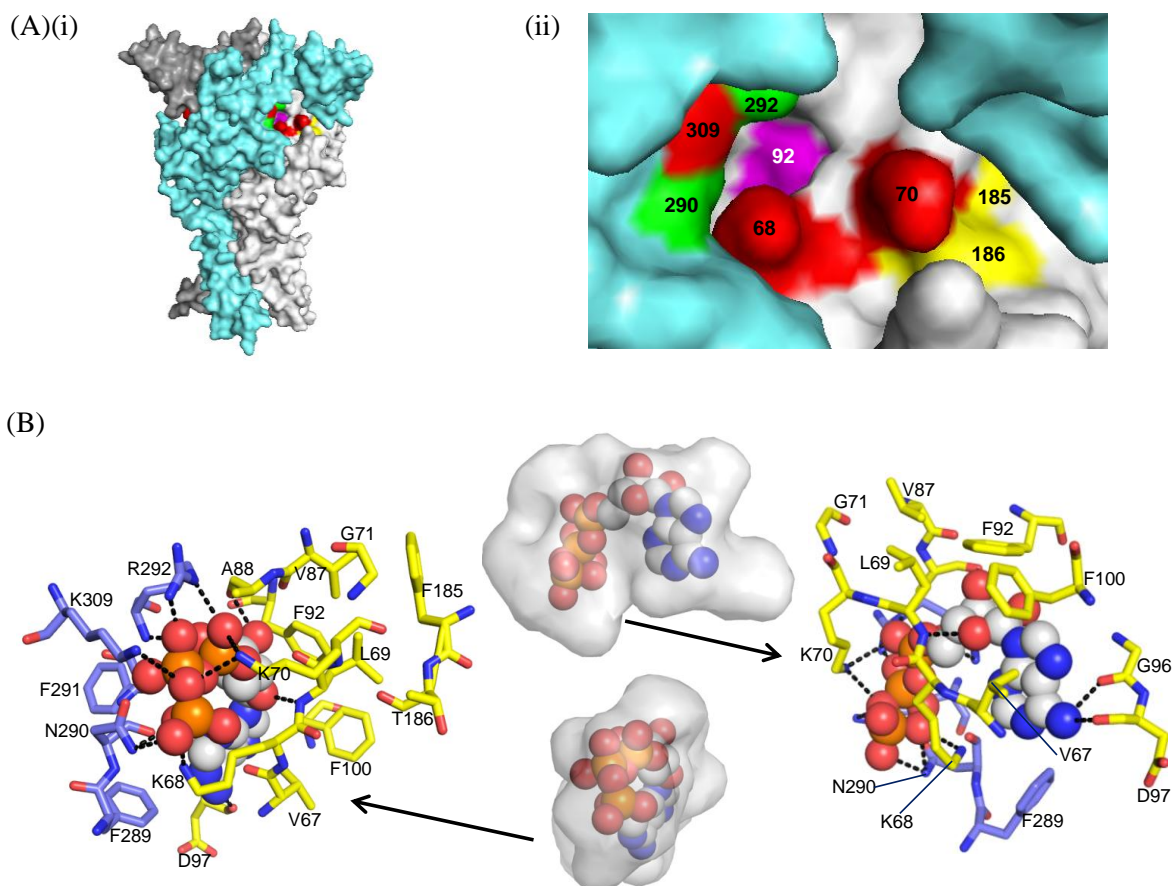


Figure 4.7 Predicted site of ATP action on the homology model of the P2X1 receptor. Homology model of the P2X1 receptor was based on the crystal structure of the zP2X4 receptor and the figures were generated in pymol. **(A)(i)** The location of the residues predicted to coordinate ATP action, with the three subunits as surface rendered in cyan, white and dark grey. **(A)(ii)** Zoomed in on the predicted ATP binding pocket showing the residue F92 (purple) at the rear/inner cavity. Positively charged residues K68, K70 and K309 are in red, F185 T186 are in yellow and N290, F291 and R292 are in green. **(B)** Docking model ATP-binding site (provided by Ralf Schmid) from the front (left) and rear (right) of the receptor. The best scoring docked pose of ATP is shown as spheres. Residues within 3Å of ATP are shown as sticks, the purple and yellow colours are indicating different subunits of the P2X1 trimer. Predicted hydrogen bonds are plotted as dotted lines in black. The central panel illustrates the available space in the ATP binding cavity as determined by hollow for both views. The volume of the cavity is shown as transparent surface representation with the docked ATP in spheres.

The orientation of ATP at the homology model of the P2X1 receptor in its proposed binding site is consistent with data obtained from previous studies (Ralevic *et al.*, 1995; Adriouch *et al.*, 2008). The orientation of ATP with the adenine ring buried in the ATP binding pocket and the phosphate tail facing towards the surface would suggest that

modifications on the phosphate tail of ATP would be tolerated and still activate the channel. Ralevic *et al.* (1995) has shown this, where ATP analogues bearing modifications of the phosphate tail activated the channel. For example, Ap5A which adds an ADP to ATP activates some P2X receptors indicating that bulky substitutions at the phosphate tail end of ATP are possible (Ralevic *et al.*, 1995). If this tail was facing inside the groove then these partial agonists would not likely activate the channel. Also, the P2X7 receptor can be ADP ribosylated and activate the channel suggesting the region around the terminal phosphate is open (Adriouch *et al.*, 2008).

Interestingly, the phenylalanine at position 92 is not conserved throughout P2X receptor family. This suggested that this residue may either be important in ATP binding only at the P2X1 receptor or the residue at this position in each P2X receptor subtype may be regulating the differences in the agonist profile between P2X subtypes. To address this, point mutations of the corresponding residues in the P2X2 and the P2X4 receptors were constructed (data not shown). The introduction of a phenylalanine at the reciprocal positions in the P2X2 (I92F) and P2X4 (K88F) receptors did not change the potency of the receptor compared to the WT receptors. This suggested the phenylalanine at position 92 in the P2X1 receptor is only important for the P2X1 receptor and residues at different positions in the other P2X receptor subtypes (at least P2X2 and P2X4) are important in conferring the changes in their agonist profile. Interestingly, the conserved phenylalanine residue at position 291, which was suggested to coordinate the binding of the adenine ring in the P2X1 receptor, had a >40-fold decrease in ATP potency in the P2X1 receptor but only a modest ~4-fold decrease in the P2X2, 3 and 4 receptors (Roberts *et al.*, 2008; Bodnar *et al.*, 2010). Therefore, it seems that no individual residue plays a major role in coordinating the binding of adenine ring and co-ordination may be by several variant residues in each P2X receptor subunit, such as the non-conserved residue F92 in the P2X1 receptor.

4.3.2 Importance of the residues at the rear/inner cavity of the proposed ATP binding pocket in P2X1 receptor function

This chapter highlighted the back of the ATP binding site as being important in agonist action through the identification of F92 in ATP potency. The cysteine point

mutants were further investigated by looking at partial agonist efficacy of each mutant and the effects of cysteine modification with MTS reagents. This highlighted the importance of the rear/inner cavity of the ATP binding pocket in channel activation. In the region V74-G96 there were 8 P2X1 receptor mutants that had a reduction in BzATP (T75C, G81C, W85C, Y90C, F92C, P93C, Q95C and G96C) and the majority of these mutants had no change in ATP potency (apart from F92C). These residues are clustered around the predicted ATP binding pocket in the homology model of the P2X1 receptor. BzATP has quite large substitutions on the benzoyl groups of the ribose of ring so to see if the predicted ATP binding pocket can accommodate BzATP, docking simulations were carried out (by Ralf Schmid; Figure 4.8). The docking of BzATP on to the homology model of the P2X1 receptor shows that BzATP can be accommodated in the predicted agonist binding pocket (Figure 4.8; ATP is in grey and BzATP is in black). The phosphate moiety of BzATP has a similar orientation with ATP forming polar interactions with K68, K70, N290, R292 and K309 (K68 and K70 are only shown in Figure 4.8). However, the adenine and ribose rings are slightly rotated compared to ATP with the residues Y90, F92, P93 and Q95 being close to the 3'-O-4-benzoyl-benzoyl substituent (as explained in Allsopp *et al.*, 2011). Therefore, BzATP can be accommodated in the predicted agonist binding pocket and has a similar orientation to ATP.

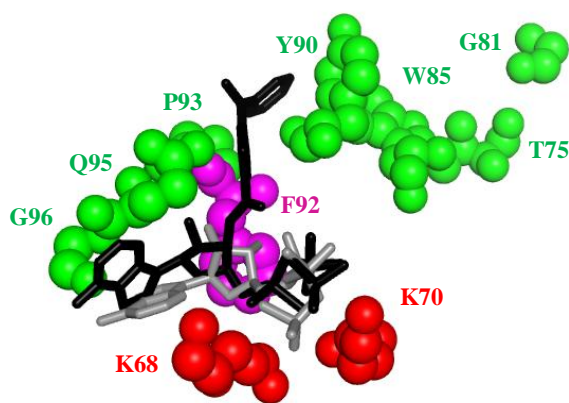


Figure 4.8. Molecular docking of BzATP to the homology model of the P2X1 receptor. The docking models of ATP (in grey) and BzATP (in black) both fit within the proposed ATP binding site in a similar orientation (provided by Ralf Schmid).. Mutants that had modified BzATP efficacy are shown in green, the mutant with a reduced ATP potency and BzATP efficacy in purple (F92), and the residues K68 and K70, which are two residues shown to previously been involved in ATP potency are in red.

The mutants that have a reduced partial agonist efficacy but no reduction in ATP potency are probably not directly interacting with ATP and could be important in channel activation subsequent to ATP binding. Studies on the two other families of ligand gated ion channels (cys-loop and glutamate) have suggested that a reduced partial agonist efficacy is due to an effect on conformational changes in the receptor associated with ligand binding before the channel gating step (Jin *et al.*, 2003; Lape *et al.*, 2008). If the same is true at P2X receptors then these residues at the rear/inner cavity could be contributing to the conformational changes associated with agonist binding. Interestingly, 5/8 of the mutants that had a decreased BzATP efficacy also showed a reduction in the peak response to MTS reagents and/or a modest increase in suramin sensitivity (a more detailed discussion of this is in Chapter 7; Table 4.3). This further highlights the importance of these residues at the back of the ATP binding pocket in the channel properties even though they are not predicted to directly interact with ATP.

Another partial agonist, Ap5A, tested on the region V74C to G96C, had a similar effect on the efficacy (7/8) at the P2X1 receptor mutants. BzATP contains a benzoyl modification of the ribose ring at the aromatic end of ATP but Ap5A has an additional ADP added onto ATP at the phosphate tail end the molecule, meaning that these two partial agonists have structural modifications at either end of the molecule. The reduction in efficacy at these mutants for both partial agonists would, therefore, further support that these residues are not directly involved in agonist binding and are most likely associated with gating subsequent to agonist binding. Also, the ATP pocket can accommodate the addition of ADP onto the ATP molecule, supporting the orientation of ATP. Interestingly, another partial agonist, α,β -meATP, only had a reduced efficacy at the mutant F92C in the region V74C to G96C. Compared to the structure of ATP, this partial agonist only has an addition of a methyl group between the α - and β -phosphates. The greater similarity in structure to ATP at this partial agonist compared to BzATP and Ap5A may be the reason why the changes in the efficacy of α,β -meATP is similar to ATP.

Cysteine scanning mutagenesis allowed the introduced cysteine residues to be modified with MTS reagents, either a negatively (MTSES) or positively (MTSET) charged MTS reagent. In the region V74C to G96C, 5 mutants had a reduced ATP-evoked response

in the presence of MTSES (P82C, D86C, V87C, P93C and G96C), and 1 mutant (V91C) had an increase in the ATP-evoked response in the presence of MTSET. The MTS reagents only caused a change in the peak current amplitude for the mutants P82C, D86C and V91C suggesting that these residues are possibly important in the channel activation subsequent to agonist binding. However, the mutants V87C, P93C and G96C all had a reduction in the ATP potency in the presence of MTSES suggesting these residues may be close to ATP. The modification of the side chain with the negatively charged MTS reagent could be reducing the ability of ATP to bind as well as affecting gating of the channel. Interestingly, mapping these residues on the homology model of the P2X1 receptor shows that the residues V87, P93 and G96 are at the back of the proposed ATP binding site close to F92 (Figure 4.9). Also, the residues P82, D86 and V91 are above the ATP binding site, suggesting that these residues may be important in the conformational changes in the receptor subsequent to agonist binding. Therefore, this further highlighted the importance of the rear/inner cavity of the predicted ATP binding pocket in the activation of the P2X1 receptor.

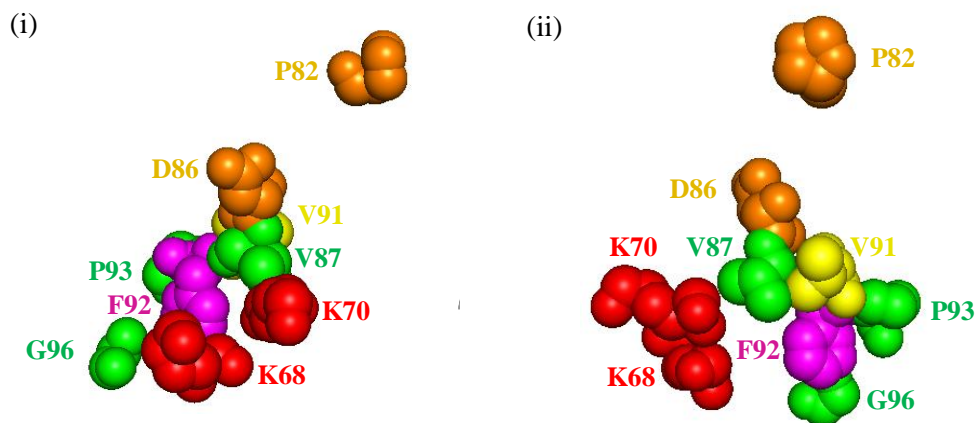


Figure 4.9. Location of the residues that had an effect with MTS reagents upon cysteine mutation on the homology model of the P2X1 receptor. The residues that had an effect in the presence of the MTS reagents are shown above in spheres along with the residues K68 and K70 (red), which have previously been shown to be important in ATP action, and F92 (purple), residues are shown in two conformations; **(i)** a front view of the receptor and **(ii)** rotated clockwise showing a side view. Upon cysteine mutation, the residues that only have a reduction in the peak current amplitude in the presence of MTSES are in orange, the residues that have a reduction in the peak current amplitude and ATP potency are in green and the residue that only has an increase in the peak current amplitude in the presence of MTSET is in yellow.

4.3.3 Residues V74-G96 do not have a large involvement in suramin and PPADS action

The antagonist suramin appeared to act as a competitive antagonist (Chapter 3). However, the residue found to be important in ATP potency (F92), upon its mutation, did not have a reduction in the suramin sensitivity. Also, the mutants K68C and K70C did not have a reduction in suramin sensitivity (Allsopp *et al.*, 2011). This supported previous studies where residues found to be important in ATP potency do not have a reduction in suramin sensitivity (Ennion *et al.*, 2000; Roberts and Evans, 2004). These results suggest that suramin does not act like a competitive antagonist in the way where it competes with ATP for the same residues. Another possibility of suramin antagonism was where the sites overlap (as explained in Chapter 3.3.2). However, point mutagenesis of the residues V74 to G96, which incorporated residues at the back of the ATP binding pocket, did not decrease suramin sensitivity. However, suramin sensitivity increased at 4 mutants (T75, Y90, P93 and Q95). Plotting these mutants on the homology model of the P2X1 receptor shows that they are at the rear/inner cavity of ATP binding pocket (Figure 4.10). Interestingly, these mutants also had a reduction in partial agonist efficacy suggesting that they may be important in the conformational changes of the receptor that occur upon antagonist binding rather than direct interaction (discussed more in Chapter 7). Also, the mutant that appeared to have the highest increase in suramin sensitivity (Y90C) only had a ~3-fold increase in suramin affinity for the mutated P2X1 receptor compared to the WT P2X1 receptor. This further suggested that none of these residues coordinate suramin binding.

A previous study highlighted a lysine residue at position 78 as important in suramin sensitivity in the P2X4 receptor (Garcia-Guzman *et al.*, 1997). However, the mutation of the reciprocal residue in the P2X1 receptor (P78C) did not affect the suramin sensitivity (location shown in Figure 4.10). Interestingly, additional experiments investigated the suramin sensitivity at the P78C mutant in the presence of the charged MTS reagents to see if the addition of charge at this position could affect the action of the negatively charged antagonist. The addition of a negative charge could possibly increase suramin sensitivity and/or a positive charge could decrease suramin sensitivity. However, the P78C mutant in the presence of either of the MTS reagents did not cause a change in the suramin sensitivity (data not shown). Therefore, this further suggested that the residue at position

78 was not involved in suramin binding at the P2X1 receptor and the location of suramin action may be different in the P2X1 and P2X4 receptors.

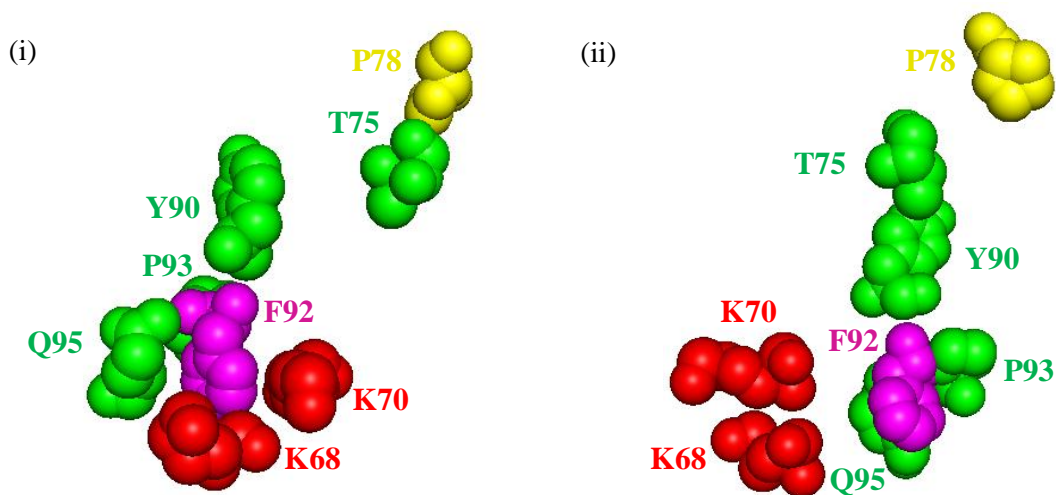


Figure 4.10. Mapping of the residues involved in suramin sensitivity on the homology model of the P2X1 receptor. The residues are shown in spheres. The residues that had an increase in suramin sensitivity upon cysteine mutation are shown in green, two lysine residues that have previously been found to be involved in ATP potency are in red (K68 and K70) and F92 is in purple in two conformations showing (i) a front view of the receptor and (ii) rotated clockwise showing a side view. The reciprocal residue of K78 in the P2X4 receptor is shown yellow (P78).

A recent molecular docking study, modeled an analogue of suramin on the homology model of the P2X2 receptor (Wolf *et al.*, 2011). The antagonist was shown to be docked at the predicted ATP binding pocket and was coordinating with residues predicted to be involved in ATP binding. However, they have not tested their model experimentally so the molecular docking model may not be correct. Also, their model contrast results obtained in this chapter and previous studies that suramin does not act at residues involved in ATP binding (Ennion *et al.*, 2000; Roberts *et al.*, 2004). If suramin and the suramin analogue investigated by Wolf *et al.* (2011) are coordinating in a similar location at the P2X receptor then their docking model would most likely be incorrect.

The results in this chapter suggested that suramin may not be coordinating in the proposed ATP binding site either with residues predicted to be involved in ATP binding or with distinct residues in the ATP binding pocket. Therefore, suramin is most likely either binding over the top of predicted ATP binding pocket and blocking ATP from entering, or acting at a region adjacent to the predicted ATP binding pocket causing a conformational

change in the receptor (see Chapter 3.3.2 for proposed mechanisms). To address this in more detail a region adjacent to the predicted ATP binding was investigated on antagonist action (Chapter 5 and 6).

Individual cysteine mutation of the residues V74 to Y90 in the P2X1 receptor did not affect the PPADS sensitivity compared to the WT P2X1 receptor. This suggested that the molecular basis of PPADS action was not occurring at the rear/inner cavity of the ATP binding pocket or behind the cysteine rich head region. Therefore, the non-competitive action of PPADS would most likely be occurring at a region separate to the proposed ATP binding site. Also, mutants with increased suramin sensitivity did not have a change in PPADS sensitivity compared to the WT P2X1 receptor, supporting a different molecular basis of suramin and PPADS action at the P2X1 receptor. Interestingly, the ATP-evoked currents at the mutant P2X1 receptors that had a small decrease in the amplitude did not have an effect on the time-course of the response. These results further suggest that PPADS does not compete with ATP for the P2X receptor and PPADS may either be decreasing the number of available unbound receptors or affecting the gating of the channel. Therefore, PPADS could also be acting at a different region to ATP and this is investigated in more detail in Chapter 6.

In summary this chapter has used a combination of ATP, partial agonists, MTS reagents and antagonists to expand our understanding of the contribution of the extracellular domain to P2X1 receptor properties. Cysteine scanning mutagenesis of the region V74 to G96 in the P2X1 receptor highlighted a novel residue involved in ATP potency (F92), residues involved in gating of the receptor (rear/inner cavity of predicted ATP binding pocket) and residues that are not essential for suramin or PPADS sensitivity.

Chapter 5. Role of the cysteine rich loop on antagonist action

5.1 Introduction

Suramin appears to be a competitive antagonist (Chapter 3) and a recent molecular *in silico* docking paper, has suggested that suramin analogues bind in the ATP binding site (Wolf *et al.*, 2011). However, 3 lines of evidence suggest that suramin may interact at a region adjacent to the ATP binding pocket, the cysteine rich head region, and not in the ATP binding pocket. Firstly, residues which have been shown to be involved in ATP potency at the P2X1 receptor (K68, K70, F92) are not involved in suramin sensitivity (Chapter 4; Allsopp *et al.*, 2011). Secondly, the residues found to be important in suramin sensitivity (K78 in the hP2X4 receptor and K138 in the hP2X1 receptor) are not located in the proposed agonist binding pocket and one of the residues (K138) is located at the base of the cysteine rich head region (Garcia-Guzman *et al.*, 1997; Sim *et al.*, 2008). Thirdly, commonly used antagonists, e.g. suramin and PPADS, are ineffective at the *Dictyostelium discoideum* P2X (DdP2X) receptors, which do not contain a cysteine rich head region (Fountain *et al.*, 2007; Ludlow *et al.*, 2009). These findings suggests that the cysteine rich head region, which is adjacent to the predicted ATP binding site (Figure 5.2), may be important in suramin sensitivity.

5.1.1 The cysteine rich head region of the P2X receptor

There are 10 conserved cysteine residues in each subunit of the P2X receptor family (excluding DdP2X receptors). This raised the possibility of the cysteine residues forming disulphide bonds and either stabilising inter-subunit dimerisation, like TWIK potassium channels, and/or stabilising the structure within a subunit, like the nicotinic acetylcholine receptor (Lesage *et al.*, 1997; Brejc *et al.*, 2000). Initial biochemical studies showed that disulphide bonds did not form between subunits (Nicke *et al.*, 1998). Subsequent work investigated whether the disulphides formed within a subunit by using a mutagenesis approach and comparing the channel properties (Ennion and Evans, 2002; Clyne *et al.*, 2002). If a disulphide bond was present, mutation that disrupts this bond could have functional consequences affecting channel properties, for example, having changes in the ATP potency, cell-surface expression, maximum current and zinc and pH potentiation (Ennion and Evans, 2002; Clyne *et al.*, 2002). Also, if the disulphide bond is broken, the

free cysteine produced could be probed with the compound, MTSEA-biotin (Ennion and Evans, 2002). The human WT P2X1 receptor was not labelled with MTSEA-biotin suggesting that all the 10 cysteine residues in the extracellular loop are disulphide bonded (Ennion and Evans, 2002). Mutating the individual cysteine residues resulted in MTSEA-biotinylation of the mutants C126A, C132A, C149A, C159A, C217A, and C227A. This provided direct biochemical evidence for at least 3 disulphide bonds in the P2X1 receptor (Ennion and Evans, 2002). Phenotypic comparisons of the mutated P2X receptors proposed the pairings C117-C165 (1-6), C126-C149 (2-4), C132-C159 (3-5), C217-C227 (7-8), and C261-C270 (9-10) in both the P2X1 and P2X2 receptors (P2X1 receptor numbering, numbers in brackets indicate the order of the conserved cysteine residue in the P2X receptor sequence; Ennion and Evans, 2002; Clyne *et al.*, 2002). Since the prediction of the possible disulphide bonds, the publication of the crystal structure of the zP2X4 receptor supported these pairings (Kawate *et al.*, 2009).

The cysteine rich loop of the P2X receptor is incorporated in the head region of the P2X receptor, adjacent to the predicted ATP binding pocket. This region contains the first 6 out of the 10 conserved cysteine residues and is a common feature in the P2X receptor family ranging from algae to human P2X receptors, with the exception of the DdP2X receptors. The DdP2X receptors have >40 amino acids, including conserved cysteine residues 2-5, missing from the receptor (Fountain *et al.*, 2007). Interestingly, the DdP2X receptors are insensitive to a range of antagonists, including suramin and PPADS, and therefore, this region may be important in the structural integrity of the antagonist binding site.

5.1.2 Suramin analogues are selective P2X1 receptor antagonists

Suramin is a non-selective P2-receptor antagonist and inhibits many P2X receptor subtypes, a few P2Y receptor subtypes, and at high concentrations can even inhibit other classes of receptors (as explained in the Discussion of Chapter 3). Thus suramin had limited use as a P2X subtype selective antagonist. To try and generate subtype selective antagonists the laboratory of Lambrecht synthesised a range of suramin derivatives. One of the first suramin analogues with P2X receptor subtype selectivity was the compound NF023 (8,8'-(carbonylbis(imino-3,1-phenylene carbonylimino)bis(1,3,5-naphthalenetri-

sulfonic acid)). This compound was a truncated analogue of suramin, which had two of the p-methylbenzamido groups from the structure of suramin removed (Figure 5.1; Bultmann *et al.*, 1996). Initial studies with the antagonist NF023 were carried out on native P2X1-like receptors in the rat vas deferens, aorta and saphenous arteries (Bultmann *et al.*, 1996; Lambrecht, 1996 and Ziyal *et al.*, 1997). Contractions induced by α - β -methylene ATP were effectively reduced in the presence of NF023. Comparing the antagonist sensitivity at different recombinant P2X receptors, the human and rat P2X1 receptor were the most sensitive to inhibition with IC₅₀ values of 0.24 and 0.21 μ M, respectively (Table 5.1; Soto *et al.*, 1999).

Since the breakthrough of using suramin analogues as potent P2X1 receptor antagonists further analogues of suramin were developed to try and improve their sensitivity and selectivity for the P2X1 receptor. NF279 (8,8'-(carbonylbis(imino-4,1-phenylenecarbonylimino-4,1-phenylenecarbonylimino)) bis(1,3,5-naphthalenetrisulfonic acid)) was designed which was structurally similar to suramin and only had two methyl groups on the benzene moiety removed compared to suramin (Figure 5.1). NF279 antagonist was up to 11-fold more sensitive than NF023 or suramin at inhibiting α , β -methylene ATP evoked contractions in rat vas deferens (Damer *et al.*, 1998). NF279 was also ~10-fold more sensitive (IC₅₀ of 19 nM) at the recombinant rat P2X1 receptor than the antagonist NF023 (Rettinger *et al.*, 2000).

Antagonists	IC ₅₀ (μ M)						
	P2X ₁	P2X ₂	P2X ₃	P2X ₄	P2X ₅	P2X ₆	P2X ₇
Suramin	1 to 5	10	3	178	4	<100	100
NF023	0.21	63	8.5	>100	-	-	-
NF279	0.019	0.77	1.6	>30	-	-	2.8
NF449	0.0003	47	1.8	>300	-	-	40

Table 5.1. IC₅₀ values in μ M of antagonists at the different rat P2X receptors. (Data taken from Evans *et al.*, 1995; Bo *et al.*, 1995; Buell *et al.*, 1996; Collo *et al.*, 1996; Soto *et al.*, 1996; Surprenant *et al.*, 1996; Garcia-Guzman *et al.*, 1997; Rassendren *et al.*, 1997; Virginio *et al.*, 1998; King *et al.*, 1999; Lambrecht, 2000; Rettinger *et al.*, 2005).

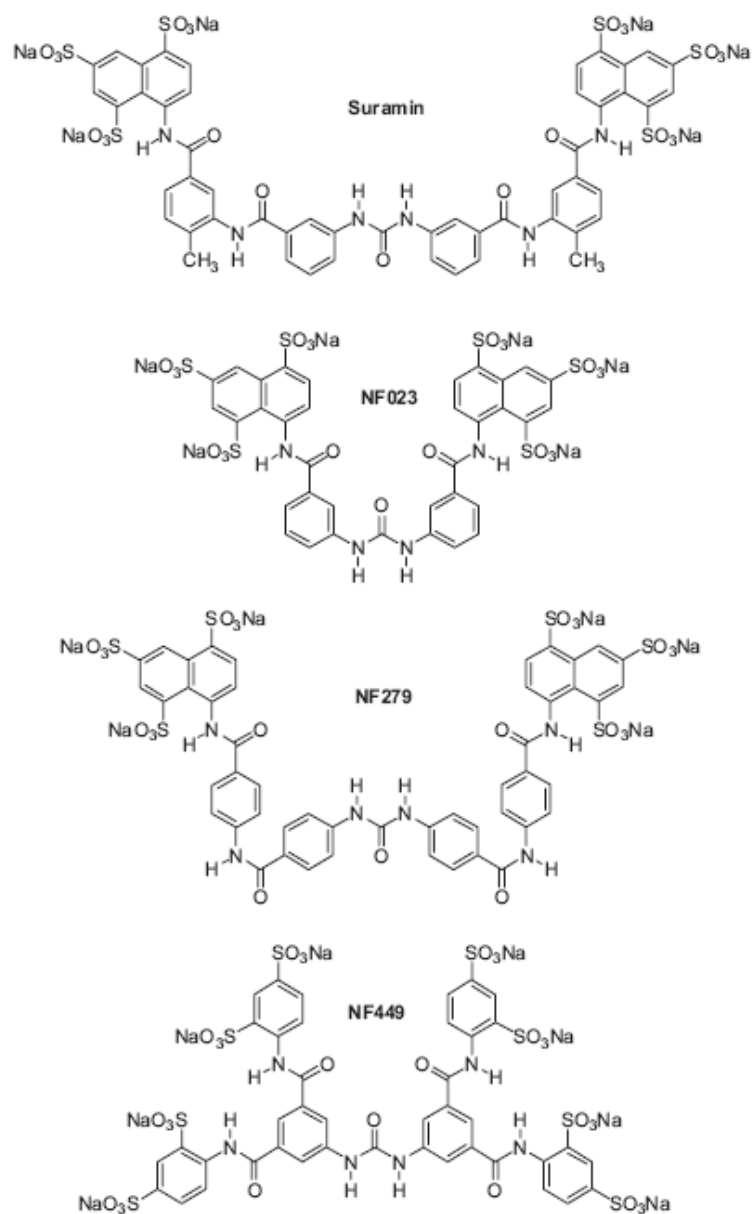


Figure 5.1. Structures of suramin and its derivatives, NF023, NF279 and NF449. (Taken from Kassack *et al.*, 2004).

The antagonists suramin, NF023 and NF279 all have 6 negatively charged polysulfonate groups. The addition of 2 extra polysulfonates (total of 8) resulted in another selective P2X1 receptor antagonist, called NF449 (4,4',4'',4'''-(carbonylbis(imino-5,1,3-benzenetriylbis (carbonylimino)))tetrakis-benzene-1,3-disulfonic acid) (Figure 5.1). Suramin and NF449 both have a central urea group but suramin has 3 polysulfonates at either end of the molecule on 2 naphthyl rings and NF449 has 2 polysulfonates on 4 benzene rings spread around the structure (Figure 5.1; Braun *et al.*, 2001). NF449 was

highly selective and very sensitive at the P2X1 receptor and this could possibly be because of the extra negative charge located around the structure. NF449 inhibited the P2X1 receptor at the lowest concentrations compared to suramin and other suramin analogues inhibiting recombinant rat and human P2X1 receptors at low nanomolar concentrations (IC₅₀ values of 0.3 nM and 0.05 nM, respectively; Braun *et al.*, 2001 and Hulsman *et al.*, 2003). The highly effective P2X1 receptor antagonist was also very selective for the P2X1 receptor compared to other P2X receptor subtypes. For example, compared to the rP2X1 receptor, NF449 was ~170,000-fold less sensitive at the rP2X2 receptor (IC₅₀ of 47 μM), ~6,500-fold less sensitive at the rP2X3 receptor (IC₅₀ of 1.8 μM) and ~1,000,000-fold less sensitive at the rP2X4 receptor and hP2X7 receptor (Table 5.1; Hulsman *et al.*, 2003; Rettinger *et al.*, 2005). Therefore, NF449 is a highly selective antagonist acting at low nanomolar concentrations at the P2X1 receptor.

5.1.3 Physiological uses of NF449

Knockout studies have identified several roles of the P2X1 receptor in animal models (see General Introduction – Chapter 1.6.1). To see if NF449 could be used as a selective P2X1 receptor antagonist *in vivo* the effects of NF449 in animal models were tested. Laser-induced vessel wall injury can be used to induce thrombosis and in the presence of NF449 the size of the thrombi were reduced with decreased intravascular platelet aggregation (Hechler *et al.*, 2005). This was similar to the results observed in the P2X1 receptor knockouts (Hechler *et al.*, 2003) suggesting NF449 was a useful P2X1 receptor antagonist. However, NF449 had a higher potency at recombinant P2X1 receptors compared to native P2X1 receptors (Hechler *et al.*, 2005). The reason for this is not yet known but in native conditions the antagonist might be broken down and/or the antagonist might be acting at non-P2X1 receptor homomers, affecting the antagonist sensitivity. Higher concentrations of NF449 also highlighted the role of the P2X1 receptor in the noncholinergic component of neurogenic contractions of the guinea pig and mouse urinary bladder (Kennedy *et al.*, 2007). Additionally, NF449 has shown that the P2X1 receptor is the predominant P2X subunit functionally expressed in smooth muscle cells of rat small and large pulmonary arteries (Syed *et al.*, 2010).

5.1.4 Site of action of NF449

Species differences in P2X receptor subunit pharmacology have been useful in understanding the general properties of antagonists at the P2X receptor. Studies on mouse P2X1-like currents in peritoneal macrophages and megakaryocytes have shown that suramin is less effective at the mouse compared to human P2X1 receptors (Sim *et al.*, 2007; Ikeda, 2007). Sim *et al.* (2008) compared the differences in suramin and NF449 action between the recombinant mouse and human P2X1 receptors and found that the antagonists were ~10-fold less sensitive at the mouse compared to the human P2X1 receptor. Sequence analysis of the extracellular domain of the P2X1 receptor indicated 4 lysine residues (positions 111, 127, 138, and 148) that are present in the human P2X1 receptor are absent in the mouse P2X1 receptor (Sim *et al.*, 2008). One or more of these positively charged residues could coordinate the action of the negatively charged polysulfonates on the antagonists through electrostatic interactions. The lysine residues in the human P2X1 receptor were mutated to the reciprocal amino acid residue in the mouse P2X1 receptor. The mutant K138E or this mutant together with K111Q, K127Q, and K148N, reduced the sensitivity of suramin and NF449 (by ~10-fold; Sim *et al.*, 2008). Interestingly, when the lysine residue was introduced into the mouse P2X1 receptor at this position (E138K) the sensitivity was increased for both suramin and NF449 (Sim *et al.*, 2008). Therefore, Sim *et al.* (2008) identified a lysine residue at position 138 in the P2X1 receptor that had a role in NF449 antagonism. Interestingly, this residue is incorporated in the cysteine rich head of the P2X1 receptor. However, the rat P2X1 receptor has a similar NF449 sensitivity as the human P2X1 receptor and the reciprocal residue at this position in the rat P2X1 receptor is a negatively charged glutamic acid (Braun *et al.*, 2001 and Hulsmann *et al.*, 2003). Therefore, other residues around this residue in the cysteine rich head region may be important in the sensitivity of NF449.

5.1.5 Aims

The antagonist NF449 has nanomolar sensitivity at the human P2X1 receptor and micromolar sensitivity at the P2X2 receptor (Rettinger *et al.*, 2005). To investigate the role of the cysteine rich head region in NF449 action a series of chimeras and point mutations were generated swapping regions/residues from the P2X1 receptor with the P2X2 receptor. Understanding the molecular basis of a selective P2X1 receptor antagonist could prove

useful in improving selectivity of antagonists at the P2X1 receptor. This could contribute to the generation of antagonists with a reduced side effect profile, greater chemical stability and P2X1 selective antagonists could potentially contribute towards novel drug targets for the treatment of hypertension and stroke. The work investigating the molecular basis of antagonist action at the P2X1 receptor, highlighting the contribution of the cysteine rich head region, is currently in press at the British Journal of Pharmacology (El-Ajouz *et al.*, 2011).

5.2 Results

5.2.1 Cysteine rich head region does not play a major role on ATP potency

Initial experiments to look at the role of the cysteine rich head region on P2X receptor properties were started by a previous Masters student, Debleena Ray. The cysteine rich head region was deleted in the P2X1 receptor but this channel was not functional (data not shown). Therefore, a chimera was constructed as a positive control to see if the cysteine rich head region could be swapped between two different P2X receptor subunits. This was carried out by replacing the cysteine rich head region from the human P2X1 receptor with the human P2X2 receptor, called the P2X1 Cys2(1-6) chimera. The chimera swapped the region between the conserved cysteine residues 1 to 6 (C117-C165, P2X1 numbering; Figure 5.2). In future annotations, “P2X1 Cys2” represents the P2X1 receptor with the cysteine rich loop of the P2X2 receptor. The numbers in the brackets refer to the cysteine residues that the region was swapped at. To determine the contribution of this region on channel properties, initial control experiments were carried out on the human WT P2X1 and P2X2 receptors.

The ATP action at the human P2X1 receptor was described in Chapter 3. The characterisation of the human P2X2 receptor showed 3 differences in the channel properties. The WT P2X2 receptor was ~10-fold less sensitive to ATP than the WT P2X1 receptor (EC_{50} of ~9.1 μ M, pEC_{50} of 5.06 ± 0.09 ; Figure 5.3, Table 1). The peak current amplitude (to 300 μ M ATP) at the WT P2X2 receptor was ~30% smaller than the WT P2X1 receptor (amplitude of -4492 ± 313 nA; Table 1). Finally, there was a marked difference in the time-course of the two P2X receptor subunits. Unlike the P2X1 receptor,

Figure 5.2

Figure 5.3

which rapidly desensitises, the ATP-evoked response at WT P2X2 receptors did not desensitise during a 3 second application of ATP (0 % decay).

The ATP potency at the P2X1 Cys2(1-6) chimera was intermediate between the P2X1 and P2X2 receptor with an EC₅₀ of ~3.4 μM (pEC₅₀ value of 5.48 ± 0.05; Figure 5.3; Table 5.2). The P2X1 Cys2(1-6) chimera also had a similar maximum current amplitude (Table 5.2) but a slower decay time by ~3-fold compared to the WT P2X1 receptor (time to 50% decay of 1305 ± 176 ms; Table 5.2). The small changes in the ATP potency at this chimera may be due to slight conformational changes that occur during the swapping of the cysteine rich head region.

5.2.2 Cysteine rich head region is important in NF449 sensitivity

Suramin has been shown to activate some mutant P2X2 receptors (Cao *et al.*, 2007). This raised the possibility that suramin and its analogue NF449 could act as weak partial agonists. However, initial studies established that NF449 does not act as a partial agonist as when NF449 (1 μM) was applied on its own the holding current of any of the P2X receptors investigated in this chapter was not affected. Due to the differences in the ATP potency between the different P2X receptors studied in this chapter an EC₉₀ concentration of ATP was used to standardise the effects of NF449. The effects of NF449 on the ATP-evoked response was shown to cause maximum inhibition within 5 minutes and was fully reversed after a 5 minute wash-off period for all the P2X receptors investigated in this chapter.

Initially, the sensitivity of NF449 at the human WT P2X1 and P2X2 receptors were characterised. There was an ~1400-fold difference in the sensitivity of NF449 between the WT P2X1 receptor, IC₅₀ of ~1.0 nM, and the WT P2X2 receptor, IC₅₀ of ~1.5 μM (pIC₅₀ of 9.07 ± 0.11 and 5.86 ± 0.09, respectively; Figure 5.4). Therefore, if the cysteine rich head region played an important role in NF449 sensitivity the chimera constructed swapping this region between the P2X1 and P2X2 receptor would have a change in NF449 sensitivity.

To investigate the NF449 sensitivity at the P2X1 Cys2(1-6) chimera an initial concentration of 10 nM of NF449 was used. 10 nM NF449 showed a clear distinction in inhibition between the P2X1 and P2X2 receptor as NF449 (10 nM) reduced the ATP-

Figure

5.4.....

Figure 5.4

evoked response by ~90% at the WT P2X1 receptor and had no effect at the WT P2X2 receptor (Figure 5.5A). Interestingly, there was no inhibition of the ATP-evoked response at the P2X1 Cys2(1-6) chimera with 10 nM NF449, which was similar to the WT P2X2 receptor (Figure 5.5A). Full concentration response curves demonstrated that the P2X1 Cys2(1-6) chimera had an ~300-fold decrease in NF449 sensitivity compared to the WT P2X1 receptor, with an IC_{50} of 0.30 μ M (pIC_{50} value of 6.54 ± 0.07 ; Figure 5.5B; Table 5.2). However, the chimera was ~4-fold more sensitive to NF449 than the WT P2X2 receptor. The decrease in NF449 sensitivity at this chimera highlighted the contribution of the cysteine rich head region in NF449 action at the P2X1 receptor.

5.2.3 Smaller sub-divided chimeras revealed the importance of the base region in NF449 sensitivity

To determine which parts of the cysteine rich head region were important in conferring the change in NF449 sensitivity the cysteine rich head region was sub-divided into 3 smaller chimeras between the P2X1 and P2X2 receptors. Sequence analysis of the two P2X receptor subtypes showed that there were 3 equal sections (16-18 amino acids) between the conserved cysteine residues, which were used as the cross over points for the chimeras (Figure 5.6A and 5.6B). They correspond to the first to third (117 to 132), third to fourth (132 to 149) and fourth to sixth (149 to 165) conserved cysteine residues (P2X1 numbering). Interestingly, mapping these residues onto a homology model of the P2X1 receptor they corresponds to 3 distinct regions, the top (P2X1 Cys2(4-6) chimera), middle (P2X1 Cys2(1-3) chimera) and bottom/base (P2X1 Cys2(3-4) chimera) of the cysteine rich head region (Figure 5.6C).

The 3 sub-divided chimeras were all functional with similar peak current amplitudes to the WT P2X1 receptor (Table 5.2). There was an ~3-fold decrease in the ATP potency for all the chimeras compared to the WT P2X1 receptor. The P2X1 Cys2(1-3), P2X1 Cys2(3-4) and P2X1 Cys2(4-6) chimeras had EC_{50} concentrations of 2.55 μ M, 2.24 μ M and 3.58 μ M (pEC_{50} values of 5.63 ± 0.11 , 5.70 ± 0.16 and 5.47 ± 0.08 ; Figure 5.6D, Table 5.2), respectively. The changes in ATP potency observed with these chimeras were similar to the chimera that swapped the whole of the cysteine rich loop (P2X1 Cys2(1-6) chimera). The time-courses of the maximal responses (300 μ M ATP) at the

Figure

5.5.....

.....

Figure 5.5

Figure 5.6

P2X1 Cys2(3-4) and P2X1 Cys2(4-6) chimera were similar compared to the WT P2X1 receptor. However, the rise time (10% to 90% of the response) at the P2X1 Cys2(1-3) chimera was slowed by ~2 fold, similar to the P2X1 Cys2(1-6) chimera (Table 5.2).

Initial testing with NF449 (10 nM) showed that the sub-divided chimeras had different NF449 sensitivities. NF449 (10 nM) inhibited the ATP-evoked response by ~90% at the P2X1 Cys2(4-6) chimera (top region), by ~50% at the P2X1 Cys2(1-3) chimera (middle region) and by only ~5% at the P2X1 Cys2(3-4) chimera (bottom region; Figure 5.7A). Full inhibition curves highlighted that swapping the top region (P2X1 Cys2(4-6) chimera) of the cysteine head region had no effect on NF449 sensitivity, with an IC_{50} of ~0.69 nM (pIC_{50} of 9.17 ± 0.06 ; Figure 5.7B, Table 5.2). The middle region had a modest contribution to NF449 sensitivity with the P2X1 Cys2(1-3) chimera having an ~20-fold decrease in the NF449 sensitivity compared to WT P2X1 receptor (IC_{50} of 19 nM, pIC_{50} of 7.75 ± 0.11 , Figure 5.7B, Table 5.2). However, the base of the cysteine rich head region made a large contribution to the differences in NF449 sensitivity between the P2X1 and P2X2 receptor (Figure 5.7B). The P2X1 Cys2(3-4) chimera had an ~1800-fold decrease in NF449 sensitivity compared to the P2X1 receptor to an IC_{50} of 1.85 μ M (pIC_{50} value of 5.75 ± 0.08 ; Figure 5.7B, Table 5.2). Interestingly, the NF449 sensitivity at this smaller sub-divided chimera was indistinguishable from the P2X2 receptor and was a further ~5-fold less sensitive to NF449 than the chimera which replaced the whole cysteine rich loop (P2X1 Cys2(1-6) chimera). The decrease of the NF449 sensitivity at the P2X1 Cys2(3-4) chimera suggested that the residues between C132 and C149 in the P2X1 receptor are important for the nanomolar sensitivity of NF449 at the P2X1 receptor.

5.2.4 The importance of the basic amino acids in the region C132 to C149 on NF449 sensitivity

Sequence alignment of the two subunits was used to identify the variant amino acids in the region C132 to C149 (P2X1 receptor numbering) as one or a combination of these were most likely to underlie the phenotypic differences observed between the WT P2X1 receptor and the P2X1 Cys2(3-4) chimera (Figure 5.8A). Out of the 18 amino acids, which were swapped in this region, 11 of them were variant amino acids. The residues predicted to be involved in antagonist action were the positively charged residues. This is

Figure

5.7.....

.....

Figure 5.7

because previous studies have shown that negatively charged antagonists (such as NF449, suramin and PPADS) may coordinate with positively charged basic amino acids (K138 in the P2X1 receptor, Sim *et al.*, 2008, K78 in the P2X4 receptor, Garcia-Guzman *et al.*, 1997, R126 in the P2X7 receptor, Michel *et al.*, 2008). In the region 132-149 there are four basic amino acids in the P2X1 receptor (K136, K138, R139 and K140) that are absent from the P2X2 receptor. Mapping these residues onto the homology model of the P2X1 receptor shows that the side chains of these amino acids face towards the groove below the cysteine rich loop (Figure 5.8Bi) and round the back of the cysteine rich loop, away from the ATP binding pocket (Figure 5.8Bii). The role in ATP and NF449 sensitivity of these non-conserved positively charged residues in the P2X1 receptor were tested by mutating them to the reciprocal residues in the P2X2 receptor (K136E, K138D, R139M and K140L, Figure 5.8A).

The ATP potency of the single point mutations were similar to the WT P2X1 receptor (Figure 5.8C, Table 5.2). The time courses of the maximum response to ATP were similar to the WT P2X1 receptor at the K136E, K138D and R139M mutants but slowed at the K140L mutant. The rise time (10% to 90% of the peak) and the desensitisation of the response (decay time from 100% to 50%) at K140L were slowed by ~2- and ~3-fold compared to the WT P2X1 receptor, respectively (Table 5.2).

NF449 (10 nM) at the single point mutants reduced the ATP-evoked response by ~85% at K136E, R139M and K140L, which was similar to the WT P2X1 receptor but K138D was reduced by ~50% (Figure 5.9B). To see if the mutants K136E, R139M and K140L were more sensitive to NF449 than the WT P2X1 receptor the ~IC₅₀ concentration of NF449 (1 nM) at the WT P2X1 receptor was used. NF449 (1 nM) reduced the currents at these single point mutants by ~50% similar to the WT P2X1 receptor (Figure 5.9B). However, full inhibition curves highlighted an ~10-fold decrease in the NF449 sensitivity at the K138D mutant compared to the WT P2X1 receptor, with an IC₅₀ of 10 nM (pIC₅₀ of 8.02 ± 0.02, Figure 5.9B and 5.9C, Table 5.2). Interestingly in a previous study, removal of the lysine residue at position 138 in the P2X1 receptor showed a similar decrease in NF449 sensitivity (Sim *et al.*, 2008).

Figure 5.8

Figure 5.9

The single point mutants showed that at best there was an ~10-fold decrease in the NF449 sensitivity compared to the WT P2X1 receptor, however, this did not account for the ~1800-fold decrease observed with the P2X1 Cys2(3-4) chimera. This raised the possibility that a combination of charges could be important in conferring the nanomolar sensitivity of NF449 at the P2X1 receptor. To test whether the combination of charges were important, four different P2X1 receptor mutants were constructed in the five amino acid run from K136 to K140. The residues were again swapped to the equivalent residues in the P2X2 receptor (Figure 5.10A)

Interestingly, two of the positively charged residues in the region K136-K140 of the P2X1 receptor were negatively charged residues in the P2X2 receptor (K136E and K138D). The change from positive to negatives at these two residues may have accounted for the change in NF449 sensitivity. Therefore, the double mutant X1-EADRK(2) (KAKRK → EADRK), which replaced the two lysine residues at position 136 and 138 with a glutamic acid and aspartic acid, was initially characterised. The notation gives rise to “X1” being the P2X receptor that the mutant is in, the residues in colour are the residues swapped, residues in black are not changed and the number in brackets is the amount of residues swapped in this region. The ATP potency at this mutant was reduced by ~3-fold with the maximum response having a similar peak current and time-course compared to the WT P2X1 receptor (Figure 5.10, Table 5.2). The sensitivity to NF449 at the double mutant (X1-EADRK(2)) was reduced by ~150-fold with an IC₅₀ of ~150 nM (pIC₅₀ of 6.85 ± 0.10, Figure 5.11, Table 5.2). This mutant was ~15-fold less sensitive compared to the K138D mutant but still did not account for the large reduction in NF449 sensitivity observed with the P2X1 Cys2(3-4) chimera.

Therefore, three further multiple mutations in this region were constructed in the five amino acid run K136 to K140. The two lysine residues at position 136 and 138 along with the additional lysine residue at position 140 were swapped, mutant X1-EADRL(3) (KAKRK → EADRL), the three lysine residues along with the additional arginine residue at position 139 were swapped, mutant X1-EADML(4) (KAKRK → EADML) and the four charged residues along with the additional uncharged alanine residue at position 137 were swapped, mutant X1-ELDML(5) (KAKRK → ELDML; Figure 5.10A). The peak current

Figure

5.10.....

.....

Figure 5.10

amplitudes at all of these mutants were similar to the WT P2X1 receptor (Table 5.2). The X1-EADRL(3) mutant and X1-EADML(4) had an ~3-fold decrease in the ATP potency compared to the WT P2X1 receptor (Figure 5.10 and Table 5.2). However, upon mutation of all 5 amino acids (X1-ELDML(5)), there was an ~10-fold decrease in the ATP potency compared to the WT P2X1 receptor, with an EC₅₀ of ~9.1 μM (pEC₅₀ of 5.05 ± 0.05; Figure 5.10 and Table 5.2). Interestingly, this was similar to the WT P2X2 receptor. The time-course of the peak current was slower at the mutants X1-EADML(4) and X1-ELDML(5) with a maximal concentration of ATP (300 μM). Compared to the P2X1 receptor, the rise times (10% to 90%) were slower by ~2-fold at both mutants and the desensitisation of the response (decay time – 100% to 50%) was slower by ~4-fold at the X1-EADML(4) mutant (Table 5.2).

Removing the additional lysine residue (X1-EADRL(3) mutant) reduced the NF449 sensitivity by a further ~2-fold compared to the double mutant (X1-EADRK(2) mutant) with an IC₅₀ of 0.31 μM (by ~300-fold compared to the WT P2X1 receptor, pIC₅₀ of 6.56 ± 0.12, *p* < 0.001 compared to D138K, Figure 5.11, Table 5.2). Upon mutation of the additional charged arginine residue (X1-EADML(4) mutant) the NF449 sensitivity was reduced by another ~2 fold (by ~600-fold compared to the WT P2X1 receptor) with an IC₅₀ of 0.56 μM (pIC₅₀ of 6.25 ± 0.03, *p* < 0.01 compared to X1-EADRK(2), Figure 5.11, Table 5.2). Mutation of the final additional variant residue, X1-ELDML(5), produced a slightly further decrease in sensitivity (by ~700-fold compared to the WT P2X1 receptor) with an IC₅₀ of 0.70 μM (pIC₅₀ value of 6.16 ± 0.04; *p* < 0.05 compared to X1-EADRL(3), Figure 5.11; Table 5.2). There was a further ~4-fold decrease in the NF449 sensitivity after the removal of the additional positively charged residues compared to the double mutant (*p* < 0.01 compared to X1-EADRK(2)). Therefore, this suggested that the cluster of positively charged residues forming the base of the cysteine rich head region was important in the nanomolar sensitivity of NF449 at the P2X1 receptor. However, the mutant removing these non-conserved basic amino acids in this region had an NF449 sensitivity which was ~2 and ~3-fold more sensitive than the WT P2X2 receptor and the P2X1 Cys2(3-4), respectively. This suggested that other variant amino acids at the base of the cysteine rich loop region may also contribute to the differences in the NF449 sensitivity between the P2X1 and P2X2 receptors.

Figure 5.11

5.2.5 NF449 sensitivity is partially recovered at the reciprocal mutations in the P2X2 receptor

The chimeras and point mutants in the P2X1 receptor identified residues involved in NF449 sensitivity at P2X1 receptors. In order to determine whether these residues solely account for the highly sensitive nature of NF449 at the P2X1 receptor the reciprocal chimera (P2X2 Cys1(3-4)) and mutants in the P2X2 receptor (P2X2 D136K, X2-KLKML(2), X2-KLKMK(3) and X2-KLKRK(4)) were generated. Only the D136K mutant had an effect on ATP potency, which had an ~3-fold increase compared to the WT P2X2 receptor, with an EC₅₀ value of 3.87 μM (pEC₅₀ of 5.43 ± 0.08; Figure 5.12; Table 5.3).

Unlike the shift observed with replacing the base region of the cysteine rich head region of the P2X1 receptor with the P2X2 receptor, the NF449 sensitivity at the reciprocal chimera (P2X2 Cys1(3-4) chimera) was unchanged compared to the P2X2 receptor with an IC₅₀ of 1.1 μM (pIC₅₀ of 5.98 ± 0.09; Figure 5.14, Table 5.3). Also, the single point mutation (D136K) and the double mutant (X2-KLKML(2)) had no effect on NF449 sensitivity with NF449 (1 μM) inhibiting the ATP-evoked response by ~50% similar to the WT P2X2 receptor (Figure 5.13A; Table 5.3). However, the addition of the three lysine residues into the P2X2 receptor (X2-KLKMK(3) mutant) increased the NF449 sensitivity by ~5-fold compared to the P2X2 receptor, with an IC₅₀ of 0.33 μM (pIC₅₀ of 6.46 ± 0.01; Figure 5.13, Table 5.3). This suggested that the positive charge introduced into the P2X2 receptor could slightly increase the NF449 sensitivity towards the P2X1 receptor. However, incorporating the additional charged arginine residue (X2-KLKRK(4) mutant) reduced the NF449 sensitivity back to a similar concentration as the WT P2X2 receptor, with an IC₅₀ of 0.87 μM (pIC₅₀ of 6.08 ± 0.09; Figure 5.14; Table 5.3). The lack of recovery of NF449 sensitivity in the P2X2 receptor with the multiple charge mutants suggested that NF449 does not solely interact with these residues at the base of the cysteine rich head region and other residues seem to contribute towards NF449 action.

Figure 5.12

Figure 5.13

Figure 5.14

Mutant	Peak (nA)	Rise Time (ms)	Decay Time (ms)	ATP pEC ₅₀	ATP EC ₅₀ (μM)	Hillslope	NF449 pIC ₅₀	NF449 IC ₅₀ (nM)
P2X1 WT	6311 ± 373	66 ± 3	495 ± 45	6.15 ± 0.10	0.76	1.00 ± 0.14	9.07 ± 0.11	1.04
P2X2 WT	4492 ± 313	ND	ND	5.06 ± 0.09***	9.09	1.56 ± 0.21	5.86 ± 0.09***	1458
P2X1 Chimeras:								
P2X1 Cys2(1-6)	6937 ± 591	110 ± 14***	1305 ± 176**	5.48 ± 0.05**	3.39	1.96 ± 0.16**	6.54 ± 0.07***	303
P2X1 Cys2(1-3)	6328 ± 183	114 ± 9**	1073 ± 129	5.63 ± 0.11*	2.55	1.65 ± 0.40	7.75 ± 0.11***	19
P2X1 Cys2(3-4)	6299 ± 375	95 ± 7	827 ± 103	5.70 ± 0.16*	2.24	1.67 ± 0.16	5.75 ± 0.08***	1852
P2X1 Cys2(4-6)	5252 ± 343	96 ± 10	581 ± 52	5.47 ± 0.08**	3.58	1.27 ± 0.21	9.17 ± 0.06	0.69
P2X1 Mutants:								
K136E	5646 ± 471	66 ± 5	544 ± 150	5.84 ± 0.01*	1.44	1.66 ± 0.39	ND	ND
K138D	5285 ± 276	75 ± 6	767 ± 154	6.31 ± 0.01	0.49	1.14 ± 0.15	8.02 ± 0.02***	10
R139M	6050 ± 587	108 ± 27	771 ± 106	5.93 ± 0.05	1.18	1.39 ± 0.25	ND	ND
K140L	5553 ± 344	118 ± 9**	1661 ± 474***	5.98 ± 0.07	1.09	1.46 ± 0.31	ND	ND
X1-EADRK(2)	9763 ± 658	98 ± 23	936 ± 215	5.67 ± 0.03**	2.15	1.76 ± 0.07	6.85 ± 0.10***	148
X1-EADRL(3)	5601 ± 373	97 ± 13	1230 ± 244***	5.46 ± 0.02***	3.49	1.32 ± 0.04	6.56 ± 0.12***	308
X1-EADML(4)	5677 ± 385	132 ± 9***	1780 ± 166***	5.58 ± 0.07***	2.68	1.22 ± 0.08	6.25 ± 0.03***	561
X1-ELDML(5)	5123 ± 387	117 ± 25***	757 ± 156	5.05 ± 0.05***	9.06	1.50 ± 0.19	6.16 ± 0.04***	696

Table 5.2. Properties of P2X1 receptor chimeras and mutants. Effects of the P2X1 chimeras and mutants on the peak current, rise time, decay time, ATP potency, Hillslope, NF449 sensitivity and suramin sensitivity. Peak current values taken on the first application of a maximal concentration of ATP. Rise-time represents the time from 10 to 90% of the peak current and decay time represents the time 100% to 50% decay of the current. pEC₅₀ values calculated from the individual concentration response curves. pEC₅₀ is -log₁₀ of the EC₅₀ for ATP. Hill coefficient of the fitted curves is shown. pIC₅₀ calculated from the individual inhibition curves. pIC₅₀ is -log₁₀ of the IC₅₀ for the antagonist. Values are the mean ± S.E.M. Significant differences from WT P2X1 receptors are indicated in bold **p* < 0.05 ***p* < 0.01 ****p* < 0.001 measured by one-way ANOVA, n = 3 to 10, ND, not-determined.

Mutant	Peak (nA)	ATP pEC ₅₀	ATP EC ₅₀ (μM)	Hillslope	NF449 pIC ₅₀	NF449 IC ₅₀ (nM)
P2X2 WT	4492 ± 313	5.06 ± 0.09	9.09	1.56 ± 0.21	5.86 ± 0.09	1458
P2X1 WT	6311 ± 373	6.15 ± 0.10***	0.76	1.00 ± 0.14	9.07 ± 0.11***	1.1
P2X2 chimeras:						
P2X2 Cys1(3-4)	4212 ± 178	5.14 ± 0.06	7.41	1.31 ± 0.16	5.98 ± 0.09	1077
P2X2 mutants:						
D136K	5422 ± 200	5.43 ± 0.08*	3.87	1.04 ± 0.06	ND	ND
X2-KLKML(2)	10782 ± 557	5.33 ± 0.11	5.00	1.48 ± 0.03	ND	ND
X2-KLKMK(3)	3567 ± 212	4.86 ± 0.06	14.07	1.73 ± 0.71	6.46 ± 0.01*	325
X2-KLKRK(4)	3875 ± 185	4.96 ± 0.04	10.95	1.45 ± 0.01	6.08 ± 0.09	868

Table 5.3. Properties of P2X2 receptor chimeras and mutants. Effects of the P2X2 chimeras and mutants on the peak current, ATP potency, Hillslope, NF449 sensitivity and suramin sensitivity. Peak current values taken on the first application of a maximal concentration of ATP. pEC₅₀ values calculated from the individual concentration response curves. pEC₅₀ is -log₁₀ of the EC₅₀ for ATP. Hill coefficient of the fitted curves is shown. pIC₅₀ calculated from the individual inhibition curves. pIC₅₀ is -log₁₀ of the IC₅₀ for the antagonist. Values are the mean ± S.E.M. Significant differences from WT P2X2 receptors are indicated in bold **p* < 0.05 ***p* < 0.01 ****p* < 0.001 measured by one-way ANOVA, n = 3 to 10, ND, not-determined.

5.3 Discussion

The antagonist NF449 has nanomolar sensitivity at the human P2X1 receptor compared to micromolar sensitivity at the human P2X2 receptor. Swapping different parts of the cysteine rich head region from the P2X1 receptor with the P2X2 receptor highlighted the base of the cysteine rich loop as being important for this difference in sensitivity of NF449. The basic amino acid residues at the base of the cysteine rich head region (K136, K138, R139M and K140L) have been shown to play a major role in giving NF449 its nanomolar sensitivity at the P2X1 receptor.

5.3.1 The involvement of the cysteine rich head region on P2X1 receptor properties

The cysteine rich head of the P2X1 receptor is adjacent to the predicted ATP binding site. Swapping regions between the P2X1 and P2X2 receptors and point mutations in the cysteine rich head region only had modest effects on ATP potency. The small changes in ATP potency could have been due to slight localised conformational changes in the receptor. The antagonist, NF449, inhibited the P2X1 receptor at lower concentrations (~1400-fold lower) than the P2X2 receptor. The nanomolar versus micromolar sensitivity of NF449 at the P2X1 and P2X2 receptors is similar with previous studies (Braun *et al.*, 2001; Hulsmann *et al.*, 2003; Kassack *et al.*, 2004 and Rettinger *et al.*, 2005). In this chapter, the most striking observation was the change in NF449 sensitivity during the swapping of regions and residues between the P2X1 and P2X2 receptor.

When the whole of the cysteine rich head region was swapped between the P2X1 and the P2X2 receptor (P2X1 Cys2(1-6) chimera) the NF449 sensitivity was intermediate between the P2X1 and P2X2 receptors. However, when the smaller base region of the cysteine rich head was swapped (P2X1 Cys2(3-4) chimera) there was a much larger decrease in NF449 sensitivity, similar to that of the P2X2 receptor (by ~1800-fold compared to the P2X1 receptor). This suggested that NF449 could be interacting with different parts of the cysteine rich loop. This was supported by the decrease in NF449 sensitivity (by ~20-fold compared to the P2X1 receptor) observed when the middle of cysteine rich loop (P2X1 Cys2(1-3) chimera) was swapped between the subunits. The differences in sensitivities could either be through a direct interaction with NF449 with different parts of the cysteine rich head region and/or conformational changes in the

receptor. The amino acid residues that could be causing these differences in NF449 sensitivity at the different chimeras are discussed below.

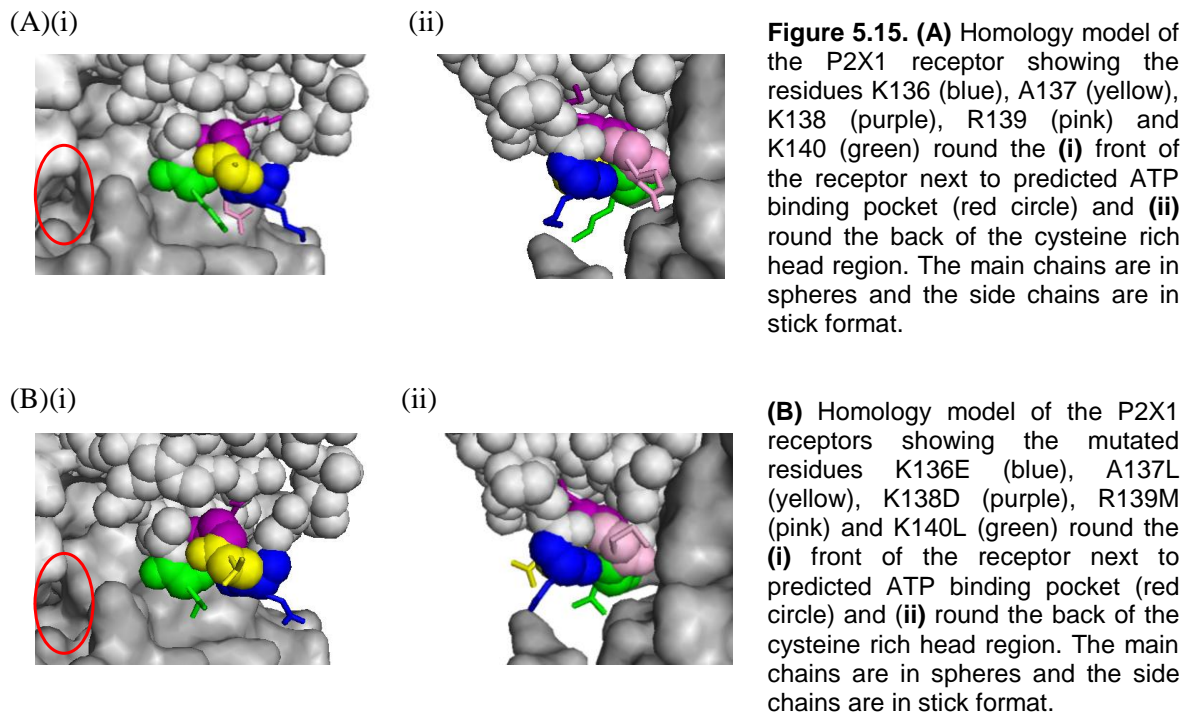
5.3.2 The importance of basic amino acids at the base of head region in determining NF449 sensitivity

This study demonstrated that the four non-conserved positively charged residues at the base of the cysteine rich head region are important for conferring the nanomolar sensitivity of NF449 at the P2X1 receptor. Reversing the charge at one of the residues with the mutant K138D caused a modest ~10-fold decrease in NF449 sensitivity compared to the P2X1 receptor. This is the same as a previous study where the reverse of charge at this position (P2X1 receptor mutant K138E) caused a similar decrease in NF449 sensitivity (Sim *et al.*, 2008). However, it is not just the single charge but the multiplicity of charge at the base of the cysteine rich head region that is important in NF449 sensitivity. The double mutant, which reversed the charge at two residues by swapping two lysine residues with a glutamic acid and aspartic acid, caused a much larger decrease in NF449 sensitivity compared to the WT P2X1 receptor (by ~150-fold). Interestingly, it was not just the presence of these negatively charged residues which changed the NF449 sensitivity as when the other two positive charges at the base of the cysteine rich head region were removed there was a further ~4-fold reduction in NF449 sensitivity. This indicated that it was the cluster of all 4 positively charged residues (K136, K136, R139 and K140) which gave the P2X1 receptor low nanomolar sensitivity to NF449.

The most likely explanation of the importance of the basic amino acids is that they coordinate the binding of the highly charged NF449 molecule through electrostatic interactions, due to NF449 containing 8 negatively charged polysulfonates. This is supported by crystal structures of other suramin binding proteins which show lysine and arginine residues coordinating the binding of its parent molecule suramin (discussed in more detail in Chapter 6.3.1). However, the mutant removing the basic amino acids at the base of the cysteine rich head region (X1-ELDML(5) mutant) was still 2 to 3-fold more sensitive than the P2X2 receptor ($p < 0.05$) and the P2X1 Cys2(3-4) chimera ($p < 0.05$). This suggested that there may either be other variant residues in the base of the cysteine rich head region that contribute to antagonist sensitivity and/or small conformational

changes that occur during the mutation of the P2X1 receptor. To try and predict where the NF449 coordinates at the P2X1 receptor, a series of *in silico* modelling predictions of NF449 binding at the homology model of the P2X1 receptor were carried out. The results showing where and in which orientation NF449 interacts with these positively charged residues at the base of the cysteine rich loop are detailed later (section 5.3.4).

Mapping the region of the X1-ELDML(5) mutant, which caused the largest change in NF449 sensitivity, onto the homology model of the P2X1 receptor allowed structural interpretation of the data. Taking into the account the limitations of the homology model of the P2X1 receptor (explained in Chapter 1.8.9), the side chains of the 5 amino acid residues in the wild type P2X1 receptor can be seen to be facing either the groove underneath the head or away from the ATP binding site (Figure 5.15A). *In silico* mutation to the reciprocal residues introduced from the P2X2 receptor shows that the side chains of the amino acids change in size and orientation (Figure 5.15B). Interestingly, the mutant swapping the additional uncharged residue (X1-ELDML(5) mutant) was less sensitive to NF449 than the mutant removing the positively charged residues (X1-EADML(4) mutant). This may be due to the change in size of the side chains (Figure 5.15). The larger side chain of the leucine may not favour NF449 binding in this region. This suggested that the size of the side chains may also be important in NF449 sensitivity. This may also be the reason why swapping the base of the cysteine rich loop (P2X1 Cys2(3-4) chimera) had a lower sensitivity to NF449 than the X1-ELDML(5) mutant. The changes in the size and orientation of the other variant amino acids may change the conformation of the receptor and affect the binding of NF449. However, there are limitations to this homology model and the orientations of the residues in the resting state of the P2X1 receptor might be slightly different.



5.3.3 NF449 interacts with different parts of the cysteine rich head region

One interesting observation was that one of the smaller sub-divided chimeras (P2X1 Cys2(3-4) chimera) had a greater effect on NF449 sensitivity than the chimera swapping the whole of the region (P2X1 Cys2(1-6) chimera). This suggested there may be interactions with NF449 between the regions in the cysteine rich loop and/or may be due to conformational changes in the receptor. The differences in sensitivity could be due to the addition/removal of charged residues in each region, which could change the local charge environment and affect NF449 binding (Figure 5.16).

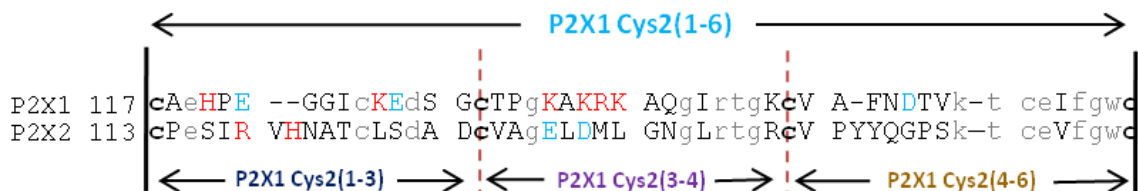


Figure 5.16. Sequence alignment of the human P2X1 and P2X2 receptors of the cysteine rich head region. The amino acid residues of the P2X1 Cys2(1-6) chimera are between the black lines and the P2X1 Cys2(1-3), P2X1 Cys2(3-4) and P2X1 Cys2(4-6) chimeras are between the red dotted lines. The non-conserved residues are in capitals and the charged residues are in red (positive) and cyan (negative). The conserved residues are in grey.

The larger decrease in NF449 sensitivity at the smaller P2X1 Cys2(3-4) chimera compared to the chimera swapping the whole cysteine rich head region (P2X1 Cys2(1-6) chimera) may be due to the presence of the negatively charged residues (E122, E128 and D154). These negatively charged residues are not present in the P2X1 Cys2(1-6) chimera, and this absence may allow the antagonists to inhibit the receptor at lower concentrations than at the P2X1 Cys2(3-4) chimera. Interestingly, the reciprocal residue in the P2X2 receptor of glutamic acid at position 122 in the P2X1 receptor is a positively charged arginine residue. This positively charged residue is present in the P2X1 Cys2(1-6) chimera but absent in the P2X1 Cys2(3-4) chimera. Mapping E122 onto the homology model of the P2X1 receptor the side chain of this residue can be seen to be orientated towards the ATP binding pocket (Figure 5.17). The removal of this negative charge in the P2X1 Cys2(1-6) chimera may allow the NF449 to more readily antagonise the receptor, especially if NF449 is binding over the ATP binding pocket, compared to when the negative charge is present in the P2X1 Cys2(3-4) chimera. To test the contribution of this residue, the P2X1 Cys2(3-4) chimera with the point mutation E122R could be constructed and this may further indicate the role of the local charge environment on NF449 sensitivity.

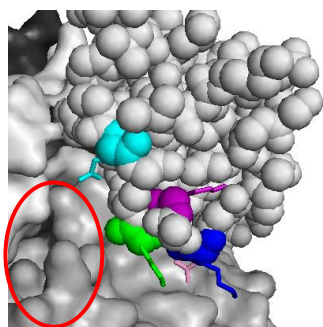


Figure 5.17. Location of E122. Homology of the P2X1 receptor showing the positively charged residues K136 (blue), K138 (purple), R139 (pink), K140 (green) and the negatively charged residue E122 (cyan). The main chains are in spheres and the side chains are in stick format. The predicted ATP binding pocket is shown with a red circle.

Interestingly, the chimera swapping the middle region of the cysteine rich head region (P2X1 Cys2(1-3) chimera) decreased the NF449 sensitivity by ~20-fold compared to the P2X1 receptor. This suggested that NF449 could also interact with the middle region in the P2X1 receptor but compared to the base of the cysteine rich head region, at a lesser extent. Analysing the sequence alignment of the P2X1 and P2X2 receptor, taking into account that positively charged residues may co-ordinate the action of NF449, there are a couple of positive, non-conserved residues (H120 and K127). There is a positively charged lysine residue at positions 127 in the P2X1 receptor, with the reciprocal residue in the

P2X2 receptor being an uncharged leucine residue. This residue can be seen to be facing away from the ATP binding pocket and could play a role if NF449 binds close to this residue (Figure 5.18). To determine whether this residue contributes to NF449 sensitivity in the P2X1 receptor, the sensitivity could be tested at the P2X1 receptor mutant K127L.

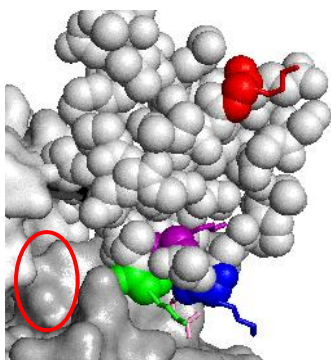


Figure 5.18. Location of K127. Homology of the P2X1 receptor showing the positively charged residues K136 (blue), K138 (purple), R139 (pink), K140 (green) and the positively charged residue K127 (red). The main chains are in spheres and the side chains are in stick format. The predicted ATP binding pocket is shown with a red circle.

The positively charged residues at the base of the cysteine rich head region seemed to play a major role in the difference in NF449 sensitivity between the P2X1 and P2X2 receptor. If the NF449 binding was solely down to these residues then the reciprocal mutations in the P2X2 receptor, which added the positive charge into the P2X2 receptor, would rescue the sensitivity in the P2X2 receptor. However, this was not the case. There was only a partial (~5-fold) recovery in the NF449 sensitivity compared to the P2X2 receptor when 3 lysine residues were introduced into the P2X2 receptor. Also, introducing the additional arginine residue into the P2X2 receptor caused the sensitivity to NF449 to shift back towards that of the P2X2 receptor. The lack of the full rescue of NF449 sensitivity suggested that there may be other residues in different parts of the receptor may also be important in NF449 action. This is supported by the decrease in sensitivity observed with the chimera replacing the middle region of the cysteine rich head region, which as explained previously, had a ~20-fold decrease in NF449 sensitivity compared to the P2X1 receptor.

5.3.4 Molecular docking of NF449 at the P2X1 receptor

Chimeras and point mutants have highlighted the importance of the cysteine rich head region of the P2X1 receptor in the molecular basis of NF499 action. The crystal structure does not provide information on where antagonists might bind so *in silico* docking can be a useful method to predict the site of antagonist action. A previous study has used this method to dock a suramin analogue at the P2X2 receptor, which was shown to interact in the ATP binding pocket (Wolf *et al.*, 2011). *In silico* docking was used to dock NF449 on the homology model of P2X1 receptor (carried out by Ralf Schmid). The molecular model of NF449 was generated and the docking programme was run based around a starting point of a single amino acid. Initially, the starting point was set to K136, which is at the base of the cysteine rich head region. This starting point produced docking models which were over the ATP binding site with high docking scores (example 1). This may be due to the high rate of positively charge residues in the ATP binding site (i.e. K69, K70, R292 and K309). To see if NF449 could bind in a different orientation and whether the best site of action was at the ATP binding site, the starting point was changed to a residue behind the cysteine rich head region. Interestingly, the starting point of R180 pulled NF449 behind and/or below the cysteine rich head region (example 2 and 3). These models also had high docking scores suggesting that *in silico* docking highly depends on where the starting point is.

In silico docking of NF449 has highlighted 3 different orientations of NF449, which all interact with the base of the cysteine rich head region (Figure 5.19). These 3 orientations show NF449 binding in the ATP binding pocket (example 1), in the groove underneath the cysteine rich head region (example 2) and round the back under the cysteine rich head region (example 3; residues predicted to bind ATP are in red, K136 is in blue, K138 is in purple, R139 is in pink and K140 is in green).

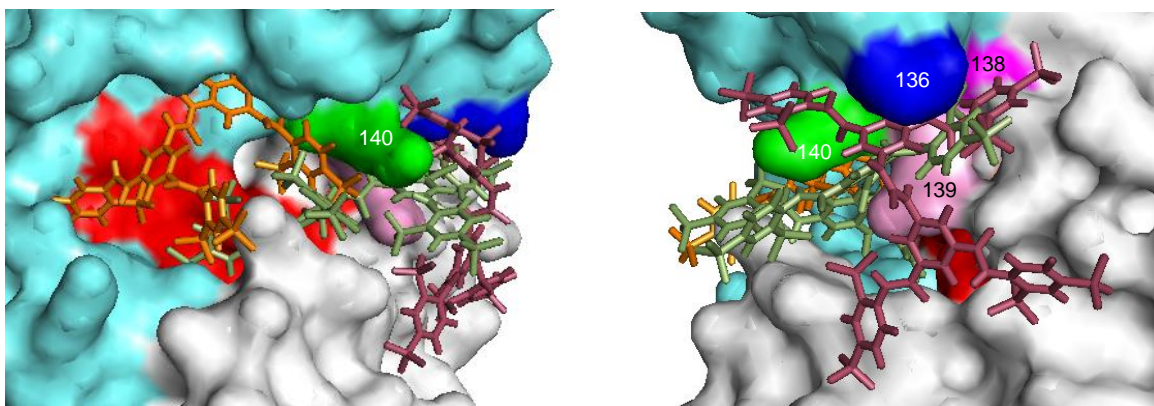


Figure 5.19. Predicted *in silico* docking models of NF449 at the homology model of the P2X1 receptor. Homology model of the P2X1 receptor is based around the crystal structure of the zP2X4 receptor. The 3 subunits as surface rendered in dark grey, cyan and white, the residues involved in ATP potency are coloured in red, K136 is blue, K138 is purple, R139 is pink and K140 is blue. The 3 different docking models of NF449 are shown in orange, green and purple. The P2X1 receptor is shown in two orientations, (i) the front of the receptor and (ii) rotated clockwise showing the back of the cysteine rich head region.

The first *in silico* docking model shows NF449 binding inside the ATP binding pocket of the P2X1 receptor, possibly directly competing with ATP with a few residues in the active site (docking score of 89; Figure 5.20A). There are 6 negatively charged sulphonates on the NF449 molecule and these may coordinate with positively charged lysine, arginine or histidine residues. NF449 appears to be coordinated by K249, K215 and H120 (yellow), the residues in the ATP binding pocket, K68 and K70, and the positively charged residues at the base of the cysteine rich head region, R139 and K140. Interestingly, the lysine residue at 249 has previously been shown to be involved in antagonist action in the P2X4 receptor (Buell *et al.*, 1996). PPADS sensitivity was recovered in the rP2X4 receptor when a lysine was added at this position, E249K (Buell *et al.*, 1996). Also, NF449 appears to be interacting with H120 and interestingly, this residue is swapped with an uncharged serine in the P2X1 Cys2(1-3) chimera. This chimera had an ~20-fold decrease in NF449 sensitivity and the removal of the positive charge at position 122 could reduce the affinity of NF449. This docking model also shows NF449 binding close to the negatively charged E122 residue (orange on Figure 5.20). This residue could contribute to the reason why the chimera swapping the base of the cysteine region has a larger decrease in NF449 sensitivity than the chimera replacing the whole of the cysteine rich region (see section 5.3.3 for more details). However, there are a couple of possible limitations to this first example. Firstly, this docking model suggests NF449 coordinates

with K68 and K70, which in previous studies have shown to not be involved suramin action (as explained before). If NF449 action acts in a similar way to suramin then it is unlikely to bind in this way. Secondly, NF449 does not appear to be close to the residue K138, which had a ~10-fold reduction in NF449 sensitivity upon its mutation (K138D).

Interestingly, the docking model of NF449 coordinating with residues inside the predicted ATP binding pocket is similar to the docking model of a suramin analogue acting on the homology model of the P2X2 receptor (Wolf *et al.*, 2011). However, the *in silico* model proposed by Wolf *et al.* (2011) was not tested experimentally. Also, this model showed the suramin analogue coordinating with residues involved in ATP potency and the reciprocal residues in the P2X1 receptor (K70, R292 and K309) have been shown to not be important suramin action (Ennion *et al.*, 2000; Roberts *et al.*, 2008; Allsopp *et al.*, 2011). Therefore, if suramin and their analogues have a similar molecular basis of action at the P2X receptors the model proposed by Wolf *et al.*, 2011 and the first docking model using NF449 (Figure 5.20A) may not be correct.

The second *in silico* docking model shows NF449 docking in the groove underneath the cysteine head region with part of NF449 entering the ATP binding pocket of the P2X1 receptor (docking score of 86; Figure 5.20B). NF449 appears to be interacting with K68 and K70, which are thought to bind ATP, so it is competing with ATP for part of its active site. Also, NF449 appears to be interacting with K215 and the positively charged residues at the base of the cysteine rich head region. This orientation of NF449 highlights the involvement all four positively charged residues K136, K138, R139 and K140, supporting the prediction that it is the multiple charge in this region that coordinates NF449 binding. However, as mentioned above, ATP and suramin are not thought to coordinate with the same residues at the P2X1 receptor, so NF449 may not bind in this orientation.

The third *in silico* docking model shows NF449 binding round the back and underneath the cysteine rich head region of the P2X1 receptor (docking score of 76; Figure 5.20C). NF449 appears to interacting with the positively charged residues at the base of the cysteine rich loop and the residues R145, R180 and H224. Interestingly, this orientation is

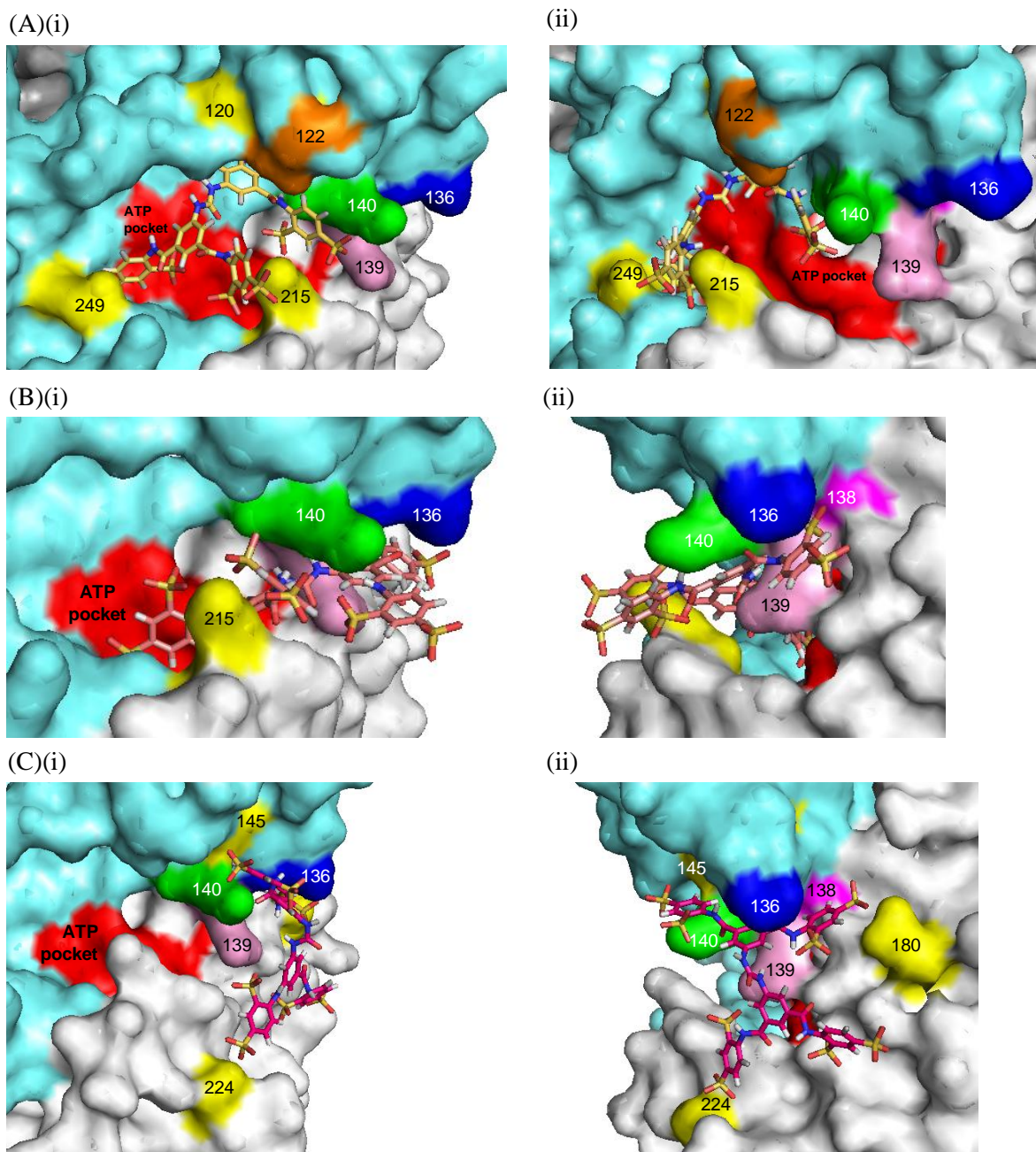


Figure 5.20. *In silico* docking models of NF449 on the homology model of the P2X1 receptor. The 3 subunits as surface rendered in dark grey, cyan and white, the residues involved in ATP potency are coloured in red, K136 is blue, K138 is purple, R139 is pink and K140 is blue. **(A)** NF449 is docked in the proposed ATP binding site, close to the positively charged residues K249, K215 and H120 (yellow) and the negatively charged residue E122 (orange). **(B)** NF449 is docked partly in the proposed ATP binding site, close to the positively charged residue K215 (yellow) and round the back of the cysteine rich head region. **(C)** NF449 is docked round the back of the cysteine rich head region and is close to the positively charged residues R145, R180 and H224 (yellow). The P2X1 receptor is shown in two orientations, **(i)** the front of the receptor and **(ii)** rotated clockwise showing the back of the cysteine rich head region.

the closest to the residue K138 out of the above examples, which was the only single point mutant to have a decrease in NF449 sensitivity. Also, the arginine and histidine residues at position 180 and 224, respectively, are only present in the P2X1 receptor and these positively charged residues, along with the residues at the base of the cysteine rich head region, may be contributing towards the higher sensitivity of NF449 at the P2X1 receptor. The corresponding amino acid in the P2X2 receptor for H224 is a negatively charged aspartic acid and this negative charge could be reducing the affinity of NF449 to bind at the P2X2 receptor, giving its micromolar sensitivity. NF449 in this orientation would not directly compete with ATP for the predicted ATP binding pocket but NF449 could bind round the back of the cysteine rich loop and hold the receptor in a certain conformation. This conformational change could move the cysteine rich head region over the ATP binding pocket, blocking ATP from entering its active site.

Detailed above are 3 different possible orientations of NF449 binding at the homology model of the P2X1 receptor. These models all have high docking scores suggesting that either of these models could be possible. However, these are only 3 models, which were taken from simulations with two different starting points. Simulations using a different starting point could produce even more orientations of NF449 with high docking scores. Therefore, the docking predictions should be tested experimentally. This could be carried out by not only removing the positively charged residues at the base of the cysteine rich loop but also the additional charged residues that NF449 appears to be interacting with. Potentially, this could highlight if any of these docking models are correct. Also, mutants that introduce the positively charged residues into the P2X2 receptor at the different positions predicted to coordinate NF449 action might give the multiple point P2X2 receptor mutant nanomolar sensitivity to NF449.

In summary, what these studies have shown is that the cysteine rich head region appears to play a role in the molecular basis of NF449 action at the human P2X1 receptor. The positively charged residues at the base of the cysteine rich head region (K136, K138, R139 and K140) seem to play a large role in NF449 sensitivity. In comparison, the middle region of the cysteine rich head region appears to play a modest role in the nanomolar sensitivity of NF449 at the P2X1 receptor. *In silico* docking simulations have highlighted 3

possible NF449 sites of action, either binding in the proposed ATP binding site and/or round the back of the cysteine rich head region of the P2X1 receptor.

Chapter 6. Role of cysteine rich head region on suramin and PPADS action

6.1 Introduction

Chimeras and point mutations between the human P2X1 and P2X2 receptors showed that the cysteine rich head region and in particular the basic amino acids at its base (K136-K140) play an important role in determining NF449 sensitivity (Chapter 5). NF449 is a derivative of suramin and it was of interest to see if suramin sensitivity was also affected. Due to the similarities in structure suramin could have a similar mode of action at the P2X1 receptor as NF449. However, the basic amino acids at the base of the cysteine rich head region are not present in other suramin sensitive P2X receptors so suramin may interact with different regions of the cysteine rich loop. PPADS is another P2X receptor antagonist that is structurally distinct from suramin and NF449 and is thought to act in a different way at the P2X1 receptor (Chapter 3 and 4). Interestingly, suramin and PPADS are insensitive at the DdP2X receptors, which do not contain a cysteine rich head region in its structure. Therefore, it was of interest to see if and which parts of the cysteine rich head region play a role in suramin and PPADS sensitivity.

6.1.1 Molecular basis of Suramin action at the P2X receptor

Suramin is effective at low micromolar concentrations at most P2X receptors with the exception of the P2X4 and P2X7 receptors (See Chapter 3.1). Species differences in suramin sensitivity have provided a clue to what residues could be involved in suramin action. Suramin was more sensitive at the hP2X4 receptor compared to the rP2X4 receptor (IC_{50} of $\sim 180 \mu\text{M}$ vs $>500 \mu\text{M}$; Garcia-Guzman *et al.*, 1997). The construction of chimeras between the human and the rat P2X4 receptor identified the region before position 81 in the hP2X4 to be important in suramin sensitivity. A single point mutation in this region, Q78K, replaced the amino acid in the rP2X4 receptor with the reciprocal residue from the hP2X4 and enhanced suramin sensitivity by >50 -fold (Garcia-Guzman *et al.*, 1997). This raised the possibility of the positively charged lysine residue coordinating the action of the negatively charged suramin through electrostatic interactions in the hP2X4 receptor. However, the lysine residue at position 78 in the hP2X4 receptor is not present in other suramin sensitive P2X receptors suggesting this residue is unlikely to be the sole

determinant of suramin sensitivity. Also, the hP2X4 receptor is still >100-fold less sensitive to suramin than the hP2X1 receptor. This indicates that other residues or regions must play a role in the molecular basis of suramin at other suramin-sensitive P2X receptors.

One of the key features of the residues involved in suramin action identified from the differences of sensitivities in species variants is the importance of positive charge. Sim *et al.* (2008) showed that another positively charged residue, a lysine at position 138, contributed to suramin action at the P2X1 receptor. As mentioned in Chapter 5, this residue was identified through the differences in sensitivity between the human and mouse P2X1 receptors. This residue, again, is not conserved in the other suramin sensitive P2X receptors, suggesting that suramin sensitivity may involve different non-conserved residues. These residues could be in the cysteine rich head region.

Suramin appears to act as a competitive antagonist (Chapter 3). However, studies have shown that mutants that have reduced suramin sensitivities do not have an effect on ATP potency (Garcia-Guzman *et al.*, 1997; Sim *et al.*, 2008). Also, residues that are thought to form the ATP binding site do not have a reduction in suramin sensitivity upon their mutation (Chapter 4; Ennion *et al.*, 2000; Roberts and Evans, 2004; Allsopp *et al.*, 2011). Therefore, it appears that ATP and suramin do not interact with the same residues at the P2X receptor (for a more in depth discussion of the possible mechanisms of suramin action see Chapter 3.3.3). Suramin could be binding at a location adjacent to the predicted ATP binding site and due to the similarities in its structure to NF449 the molecular basis of suramin action may also be involved with the cysteine rich head region.

6.1.2 Molecular basis of PPADS action at the P2X receptor

PPADS acts as a non-competitive antagonist at the human P2X1 receptor (Chapter 3) and the P2X1 mutants K68C, K70C and F92C, which reduced ATP potency, did not reduce PPADS sensitivity (Chapter 4; Allsopp *et al.*, 2011). This suggested that PPADS does not coordinate with similar residues as ATP. Also, the antagonist profile at the P2X1 receptor mutants V74C to G96C (investigated in Chapter 4) had different patterns of sensitivity with suramin and PPADS suggesting that these antagonists could have a different molecular basis of antagonist action at the P2X1 receptor compared to each other.

Interestingly, the residues found to be important in PPADS action in previous studies were also positively charged basic amino acids. Sequence analysis of the P2X receptor family identified a lysine residue that is present in PPADS sensitive P2X1 and P2X2 receptors but not in the PPADS insensitive P2X4 receptor (Buell *et al.*, 1996). The reciprocal residue in the rP2X4 receptor was a glutamic acid, E249, and the mutation of this residue to a lysine (E249K) was constructed (Buell *et al.*, 1996). The mutant E249K recovered the sensitivity to PPADS in the rP2X4 receptor highlighting the important of this residue in PPADS sensitivity. PPADS was thought to form a Schiff base with this lysine residue. However, the reverse mutant in the rP2X2 receptor, removing the lysine residue, did not remove the PPADS inhibition and this lysine residue is not present in the PPADS-sensitive P2X3 receptor (Buell *et al.*, 1996). Therefore, there are likely to be other non-conserved residues involved in PPADS action in each PPADS-sensitive P2X receptor subtype.

A recent study identified another positively charged residue involved in PPADS sensitivity using individual point mutations between the hP2X7 receptor and the rP2X7 receptor, which had different PPADS sensitivities (Michel *et al.*, 2008). The positively charged arginine residue at position 126 was found to be important for PPADS sensitivity at the hP2X7 receptor (Michel *et al.*, 2008). Interestingly, this residue is incorporated in the cysteine rich head region. Also, this residue is next to a residue that is important in the site of ADP ribosylation, residue R125, in the hP2X7 receptor (Adriouch *et al.*, 2008). The analogous residue of R125 in the P2X2 receptor, H120, has been found to be important in zinc potentiation (Lorca *et al.*, 2005) suggesting that this region could be important in the channel properties. Also, Garcia-Guzman *et al.* (1997) used a chimeric approach between the PPADS sensitive hP2X4 receptor and insensitive rP2X4 receptor and identified the residues in-between 81 to 183 in the hP2X4 receptor to be important in the PPADS sensitivity. This region incorporates the cysteine rich loop, which further suggests that this region could also be important in the molecular basis of PPADS action.

6.1.3 Aims

To test the role of the cysteine rich head region in suramin and PPADS sensitivity the chimeras and point mutations constructed in the previous chapter were used. It was of interest to see if the parent molecule suramin and the structurally distinct antagonist,

PPADS, were also involved with this region and observe whether this region had a general role in antagonist action. The molecular basis of firstly, suramin and secondly, PPADS action was investigated to see which or if parts of the cysteine rich head region of the P2X1 receptor contribute to antagonist action.

6.2 Results

Suramin has previously been shown to act as a partial agonist at constitutively active P2X2 receptors (Cao *et al.*, 2007). However, in this study suramin (100 μM) or PPADS (100 μM) had no effect on the holding current when applied on its own at any of the WT, chimaeric or mutant P2X receptors suggesting that they do not act as partial agonists. Like for NF449, an EC_{90} concentration of ATP was used for testing antagonist action to account for any differences in the ATP potency. Suramin or PPADS produced maximum inhibition of the ATP-evoked response within 5 minutes and this was fully reversed after a 5 minute wash-off period for all the P2X receptors investigated in this chapter.

6.2.1 Suramin action at the P2X1 and P2X2 receptors

Suramin inhibited the ATP-evoked currents at the WT P2X1 receptor with an IC_{50} of $\sim 1.7 \mu\text{M}$ (pIC_{50} of 5.77 ± 0.04 ; Figure 6.1; Table 6.1). This is consistent with previous studies (Ennion *et al.*, 2000). For in depth characterization of suramin action at the P2X1 receptor see Chapter 3. At the WT P2X2 receptor the inhibition was not saturated with the maximum concentration of suramin used. 100 μM of suramin inhibited the ATP evoked currents by $\sim 50\%$, giving an IC_{50} of $\sim 107 \mu\text{M}$ (pIC_{50} of 4.15 ± 0.18 ; Figure 6.1; Table 6.1). These results show that there was an ~ 60 -fold difference between the suramin sensitivity at the WT P2X1 and P2X2 receptors.

6.2.2 The cysteine rich head region contributes to suramin sensitivity

Replacing the cysteine rich loop of the P2X1 receptor with the P2X2 receptor (P2X1 Cys2(1-6) chimera) reduced the sensitivity of suramin by ~ 3 -fold compared to the WT P2X1 receptor, with an IC_{50} of $\sim 5.0 \mu\text{M}$ (pIC_{50} of 5.32 ± 0.06 ; Figure 6.2; Table 6.1). This indicated that the cysteine rich head region also plays a role in suramin sensitivity. Swapping the base of the cysteine rich head region (P2X1 Cys2(3-4) chimera) decreased the suramin sensitivity further towards that of the WT P2X2 receptor with an IC_{50} of ~ 40

Figure 6.1

Figure 6.2

μM (by ~ 25 -fold compared to the WT P2X1 receptor, pIC_{50} of 4.40 ± 0.04 ; Figure 6.2; Table 6.1). This suggested that the base of the cysteine rich head region appears to be playing a role in giving the P2X1 receptor a higher sensitivity to suramin than the P2X2 receptor.

Surprisingly, the chimeras swapping the “middle” and the “top” regions of the cysteine rich head (P2X1 Cys2(1-3) and P2X1 Cys2(4-6) chimeras) increased the suramin sensitivity by ~ 15 -fold and ~ 3 -fold compared to the WT P2X1 receptor, respectively (Figure 6.2). The IC_{50} with suramin at the P2X1 Cys2(1-3) chimera was $\sim 0.12 \mu\text{M}$ (pIC_{50} of 6.91 ± 0.03 ; Figure 6.2; Table 6.1) and at the P2X1 Cys2(4-6) was $\sim 0.56 \mu\text{M}$ (pIC_{50} of 6.27 ± 0.09 ; Figure 6.2; Table 6.1). This suggested that the different regions of the cysteine rich loop all appear to contribute to the sensitivity of suramin at the P2X1 receptor. However, these results were in contrast to what was observed with NF449 sensitivity (Table 6.1; discussed in the General Discussion, Chapter 7).

6.2.3 Basic amino acids at the base of the cysteine rich head region contribute to suramin sensitivity at the P2X1 receptor

In the previous chapter the change in NF449 sensitivity between the P2X1 receptor and the P2X1 Cys2(3-4) chimera was largely due to the non-conserved positively charged residues (K136-K140). Interestingly, suramin has previously been shown to have a direct interaction with lysine and arginine residues in structural studies (Ganesh *et al.*, 2005; Schuetz *et al.*, 2007; Zhou *et al.*, 2008). Therefore, to see if these basic amino acids are also important in the difference in suramin sensitivity between the P2X receptor subtypes the individual and multiple point mutations were investigated. The mutants K136E, R139M and K140L had a similar $\sim 60\%$ inhibition with suramin ($3 \mu\text{M}$) as the WT P2X1 receptor (Figure 6.3B). However, the mutant K138D P2X1 receptor mutant showed an ~ 3 -fold decrease in suramin sensitivity, with an IC_{50} of $\sim 5.6 \mu\text{M}$ (pIC_{50} of 5.26 ± 0.05 ; Figure 6.3; Table 6.1). Interestingly, the mutant K138D was the only mutant to have a reduction in NF449 sensitivity (Table 6.1).

There was a similar sequential decrease in suramin sensitivity compared to NF449 sensitivity with the multiple point mutants that removed the positively charged residues from the P2X1 receptor. The double mutant swapping two positively charged lysine

Figureee

6.3.....

.....

residues with the reciprocal negatively charged residues (X1-EADRK(2) mutant) reduced the suramin sensitivity by ~10-fold compared to the P2X1 receptor with an IC_{50} of ~15 μM (pIC_{50} of 4.85 ± 0.09 , Figure 6.4; Table 6.1). Replacing the additional lysine residue (X1-EADRL(3) mutant) further decreased the suramin sensitivity to an IC_{50} of ~19 μM (pIC_{50} of 4.74 ± 0.08 ; Figure 6.4; Table 6.1). When the arginine as well as the three lysine residues was replaced with the reciprocal residues in the P2X2 receptor (X1-EADML(4) mutant) there was a further ~4-fold decrease in suramin sensitivity (~40-fold decrease compared to the P2X1 receptor) to an IC_{50} of ~70 μM (pIC_{50} of 4.17 ± 0.08 ; $p > 0.01$ compared to X1-EADRL(3), Figure 6.4; Table 6.1). This inhibition was similar to the WT P2X2 receptor. The mutation of the other variant residue in this region (X1-ELDML(5) mutant) had no further inhibition with suramin having an IC_{50} of ~50 μM (pIC_{50} of 4.32 ± 0.07 ; Figure 6.4; Table 6.1). These results suggested that these positively charged residues, which are involved in NF449 sensitivity, also contribute to selectivity of suramin at the P2X1 receptor.

6.2.4 Suramin sensitivity is partially recovered at the reciprocal mutations in the P2X2 receptor

The chimeras and point mutations in the P2X1 receptor identified residues involved in suramin sensitivity at the P2X1 receptor. To test whether these residues are sufficient to account for the differences in the sensitivity of these antagonists between P2X1 and P2X2 receptors, the reciprocal chimeras and mutants in the P2X2 were tested. Interestingly, swapping the base of the cysteine rich head region (P2X2 Cys1(3-4) chimera) increased the suramin sensitivity by ~25 fold, with an IC_{50} of ~4.3 μM (pIC_{50} of 5.37 ± 0.03 ; Figure 6.5; Table 6.1). The suramin inhibition at this chimera was only ~3-fold less sensitive than the WT P2X1 receptor (Figure 6.5). This further suggested that the residues in this region may account for the differences in suramin selectivity between the P2X1 and P2X2 receptors. Reversing the charge with the mutant D136K in the P2X2 receptor caused an ~4-fold increase in the suramin sensitivity compared to the WT P2X2 receptor to an IC_{50} of ~30 μM (pIC_{50} of 4.56 ± 0.18 ; Figure 6.5; Table 6.1). Further reversing the charge difference with the double mutant (X2- KLKML(2)) increased the suramin sensitivity by another ~2-fold with an IC_{50} of ~12 μM (by ~10-fold compared to the WT P2X2 receptor, pIC_{50} of 4.92 ± 0.06 , $p > 0.001$ compared to D136K; Figure 6.5; Table 6.1). Replacing the

Figure 6.4

Figure 6.5

additional lysine residue (X2-KLKMK(3) mutant) increased the suramin sensitivity by a further ~2-fold with an IC_{50} of ~5.9 μ M (by ~20-fold compared to the WT P2X2 receptor, pIC_{50} of 5.37 ± 0.03 , $p < 0.01$ compared to X2- KLKML(2); Figure 6.5; Table 6.1). Interestingly, the suramin sensitivity at this mutant is similar to the P2X2 Cys1(3-4) chimera suggesting that these three lysine residues are important in differences in suramin sensitivity at this chimera (Figure 6.5). Surprisingly, the mutant incorporating the additional charged arginine residue into the P2X2 receptor (X2-KLKRK(4)) reduced the suramin sensitivity back towards WT P2X2 receptor, with an IC_{50} of ~22 μ M (pIC_{50} of 5.37 ± 0.03 ; Figure 6.5; Table 6.1). However, suramin was still ~5-fold more sensitive compared to the WT P2X2 receptor. The increase in suramin sensitivity observed with mutant that added the three lysine residues into the P2X2 receptor is consistent with the effects on NF449 sensitivity. However, this mutant had a larger recovery of suramin sensitivity (~20-fold) towards the P2X1 receptor than observed using NF449 (~5-fold; Table 6.1). These results further supported that the positive charges at the base of the cysteine rich head region are important in the suramin sensitivity at the P2X1 receptor.

6.2.5 PPADS sensitivity at the WT P2X1 and P2X2 receptor

At WT P2X1 receptors, PPADS inhibited ATP-evoked currents with an IC_{50} of ~1.0 μ M (pIC_{50} of 6.02 ± 0.08 ; Figure 6.6; Table 6.1). For a more in-depth characterisation of PPADS at the P2X1 receptor see Chapter 3. There was an ~3-fold difference in PPADS sensitivity at the P2X2 receptor compared to the WT P2X1 receptor with a lower IC_{50} value of ~0.33 μ M (pIC_{50} of 6.48 ± 0.06 ; $p < 0.01$ compared to WT P2X1, Figure 6.6; Table 6.1). Maximum inhibition occurred within 5 minutes of pre-superfusing the oocyte with suramin and was washed off after 5 minutes. Unlike the differences in NF449 and suramin sensitivity at the WT P2X1 and P2X2 receptors there was not a large difference in the PPADS sensitivity between the subtypes (Table 6.1).

6.2.6 Cysteine rich head region also plays a role in PPADS sensitivity

Due to their only being a ~3-fold difference in PPADS sensitivity between the WT P2X1 and P2X2 receptor, the chimeras were not expected to have much of an effect on PPADS sensitivity. However, swapping the cysteine rich head region of the P2X1 receptor with the P2X2 receptor (P2X1 Cys2(1-6) chimera) reduced the PPADS sensitivity by ~10-

Figure 6.6

fold compared to the P2X1 receptor (IC_{50} of $\sim 11 \mu M$, pIC_{50} of 5.01 ± 0.12 ; Figure 6.7; Table 6.1). Surprisingly, the change in PPADS sensitivity did not shift towards the sensitivity of the WT P2X2 receptor and was ~ 30 -fold less sensitive to PPADS compared to the WT P2X2 receptor. Interestingly, swapping the base of the cysteine rich loop (P2X1 Cys2(3-4) chimera) had a similar PPADS sensitivity as the P2X1 Cys2(1-6) chimera, with an IC_{50} of $\sim 15 \mu M$ (decrease of ~ 15 -fold compared to the P2X1 receptor, pIC_{50} of 4.84 ± 0.11 ; Figure 6.7; Table 6.1). This also highlighted the importance of the base of the cysteine rich head in PPADS.

The chimeras swapping the middle and the top regions of the cysteine rich loop (P2X1 Cys2(1-3) and P2X1 Cys(4-6) chimeras) increased the PPADS sensitivity. The P2X1 Cys2(1-3) chimera and P2X1 Cys2(4-6) chimera both increased the PPADS sensitivity by ~ 20 - to ~ 35 -fold compared to the WT P2X1 receptor to an IC_{50} of $\sim 0.05 \mu M$ and $\sim 0.03 \mu M$ (pIC_{50} of 7.36 ± 0.15 and 7.48 ± 0.07 ; Figure 6.7; Table 6.1), respectively. Surprisingly, PPADS was even more sensitive at these chimeras than at the P2X2 receptor. This suggested that the residues introduced from the P2X2 receptor in these regions can potentiate the PPADS sensitivity and could account for the difference in sensitivity between the WT P2X1 and P2X2 receptor. Interestingly, this was similar to suramin action but different to NF449 action at these chimeras (Table 6.1; explained in more detail in the Final Discussion, Chapter 7).

6.2.7 Basic amino acids at the base of cysteine rich head region also contribute to PPADS sensitivity at the P2X1 receptor

The single point mutants K136E, R139M and K140L had no change in PPADS sensitivity and the mutant K138D had an ~ 3 -fold decrease in PPADS sensitivity, with an IC_{50} of $\sim 3.2 \mu M$ (pIC_{50} of 5.54 ± 0.10 ; Figure 6.8; Table 6.1). Interestingly, the multiple point mutations all decreased the PPADS sensitivity by ~ 50 -fold compared to the WT P2X1 receptor. The mutants X1-EADRL(3), X1-EADML(4) and X1-ELDML(5) had IC_{50} values of $\sim 52 \mu M$, $\sim 41 \mu M$ and $\sim 51 \mu M$, respectively (pIC_{50} 's of 4.31 ± 0.09 , 4.41 ± 0.10 and 4.28 ± 0.07 ; Figure 6.9; Table 6.1). This suggested that the positively charged residues also contribute to PPADS action at the P2X1 receptor.

Figure 6.7

Figure 6.8

Figure 6.9

6.2.8 PPADS action on the reciprocal mutations in the P2X2 receptor

The mutants in the P2X1 receptor showed that the positively charged residues are important in maintaining the PPADS sensitivity in the P2X1 receptor residues. The effects on PPADS action were also investigated on the reciprocal mutants in the P2X2 receptor. PPADS sensitivity at the P2X2 Cys1(3-4) chimera was similar to the WT P2X2 receptor with an IC_{50} of $\sim 0.19 \mu\text{M}$ (pIC_{50} of 6.72 ± 0.06 ; Figure 6.10; Table 6.1). Adding a lysine residue into the P2X2 receptor with the mutant, D136K, increased the PPADS potency by ~ 8 -fold compared the WT P2X2 receptor to an IC_{50} of $\sim 0.04 \mu\text{M}$ (pIC_{50} of 7.48 ± 0.21 ; Figure 6.10; Table 6.1). Interestingly, this was >25 -fold more sensitive to PPADS than the WT P2X1 receptor. The reciprocal mutation of the three lysine residues, mutant X2-**KLKMK(3)**, also had a similar PPADS sensitivity compared to the WT P2X2 receptor with an IC_{50} of $\sim 0.19 \mu\text{M}$ (pIC_{50} of 6.73 ± 0.02 ; Figure 6.10; Table 6.1). The mutant adding the additional charged arginine residue into the P2X2 receptor, mutant X2-**KLKRRK(4)**, decreased the PPADS sensitivity by ~ 3 -fold compared to the WT P2X2 receptor to an IC_{50} of $\sim 1.05 \mu\text{M}$ (pIC_{50} of 5.98 ± 0.02 ; Figure 6.10; Table 6.1). Interestingly, this was similar to the WT P2X1 receptor.

The removal of the charged residues in the P2X1 receptor dramatically decreased the PPADS sensitivity but upon the addition of the charged residues into the P2X2 receptor, only the mutant D136K had an increase in the PPADS sensitivity (by ~ 8 -fold). The other mutations did not have a large difference in PPADS sensitivity compared to the WT P2X2 receptor.

Figure 6.10

Mutant	NF449 pIC ₅₀	NF449 IC ₅₀ (nM)	Suramin pIC ₅₀	Suramin IC ₅₀ (μM)	PPADS pIC ₅₀	PPADS IC ₅₀ (μM)
P2X1 WT	9.07 ± 0.11	1.04	5.77 ± 0.04	1.7	6.02 ± 0.08	1.02
P2X2 WT	5.86 ± 0.09***	1458	4.15 ± 0.18***	107	6.48 ± 0.06*	0.33
P2X1 Chimeras:						
P2X1 Cys2(1-6)	6.54 ± 0.07***	303	5.32 ± 0.09	5	5.01 ± 0.12***	11
P2X1 Cys2(1-3)	7.75 ± 0.11***	19	6.91 ± 0.03***	0.12	7.36 ± 0.15***	0.05
P2X1 Cys2(3-4)	5.75 ± 0.08***	1852	4.40 ± 0.04***	40	4.84 ± 0.11***	15
P2X1 Cys2(4-6)	9.17 ± 0.06	0.69	6.27 ± 0.09	0.56	7.48 ± 0.07***	0.03
P2X1 Mutants:						
K136E	ND	1.44	ND	ND	ND	ND
K138D	8.02 ± 0.02***	0.49	5.26 ± 0.05*	5.6	5.54 ± 0.10*	3.2
R139M	ND	1.18	ND	ND	ND	ND
K140L	ND	1.09	ND	ND	ND	ND
X1-EADRK(2)	6.85 ± 0.10***	2.15	4.85 ± 0.09***	15	ND*	ND*
X1-EADRL(3)	6.56 ± 0.12***	3.49	4.74 ± 0.08***	19	4.31 ± 0.09***	52
X1-EADML(4)	6.25 ± 0.03***	2.68	4.17 ± 0.08***	70	4.41 ± 0.10***	41
X1-ELDML(5)	6.16 ± 0.04***	9.06	4.32 ± 0.07***	49	4.28 ± 0.07***	54
P2X2 Chimera:						
P2X2 Cys1(3-4)	5.98 ± 0.09	1077	5.37 ± 0.03***	4.3	6.72 ± 0.06	0.19
P2X2 mutants:						
D136K	ND	ND	4.56 ± 0.01	28	7.48 ± 0.21***	0.04
X2-KLKML(2)	ND	ND	4.92 ± 0.06***	12	ND*	ND*
X2-KLKMK(3)	6.46 ± 0.01*	325	4.60 ± 0.02***	5.9	6.73 ± 0.02	0.19
X2-KLKRK(4)	6.08 ± 0.09	868	5.37 ± 0.06	22	5.98 ± 0.02*	1.05

Table 6.1 Antagonist action at the P2X1 and P2X2 receptor mutants and chimeras. Summary table of the effects of the P2X1 and P2X2 receptor chimeras and mutants on NF449, suramin and PPADS sensitivity. IC₅₀ is calculated from the individual inhibition curves. pIC₅₀ is -log₁₀ of the IC₅₀ for the antagonist. Values are the mean ± S.E. of the mean. Significant differences of the P2X1 receptor mutants and chimeras are measured by one-way ANOVA with the WT P2X1 receptors as the control. Significant differences of the P2X2 receptor mutants and chimeras are measured by one-way ANOVA with the WT P2X2 receptor as the control. Significant differences are indicated in bold (**p* < 0.05 ***p* < 0.01 ****p* < 0.001), *n* = 3 to 10. ND represents not-determined as the antagonist sensitivity was similar to the WT P2X receptor. ND* represents mutants that were not tested with the antagonist.

6.3 Discussion

The cysteine rich head region of the human P2X1 receptor was shown to be important in mediating NF449 sensitivity (Chapter 5). Further investigations have also shown that the sensitivity of both of its parent molecule, suramin, and the structurally distinct antagonist PPADS are in part determined by the base region of the cysteine rich head region. Specifically, the positively charged amino acids at the base (K136, K138, R139 and K140) appear to have a general role in antagonist sensitivity at the P2X1 receptor.

6.3.1 Role of the base of the cysteine rich head region in suramin action

The non-conserved basic amino acids at the base of the cysteine rich head region had an important role in the differences in sensitivity of both suramin and NF449 between the P2X1 and P2X2 receptor. The involvement of similar residues in suramin and NF449 sensitivity was expected due to the structural similarities of the two antagonists.

Suramin is known to block a variety of enzymes and there have been crystal structures published of different suramin bound complexes. One common feature is that suramin is coordinated through positively charged residues. Examples of structures where suramin has been shown to bind to positively charged residues include; (i) inhibition of heparin-binding of vaccinia virus complement control protein (Ganesh *et al.*, 2005), (ii) inhibition of SIRT5 NAD⁺-dependent deacetylase activity, showing suramin bound to positively charged arginine residues (Schuetz *et al.*, 2007), and (iii) the interaction with ecarpholin S, showing suramin to be coordinating with both positively charged lysine and arginine residues (Zhou *et al.*, 2008). Therefore, suramin could likely coordinate with the basic amino acids (K136, K138, R139 and K140) at the base of the cysteine rich head region in the P2X1 receptor.

This study has shown that the cluster of positive charge is important in mediating suramin sensitivity at the P2X1 receptor. This extends the knowledge gained from a previous study (explained in Chapter 5) that only identified the lysine residue at position 138 in the P2X1 receptor as being important in suramin sensitivity (Sim *et al.*, 2008). However, out of the four positively charged residues in the P2X1 receptor, the mutant K138D was the only residue to have reduced suramin sensitivity (Table 6.1). Interestingly,

the chicken P2X1 receptor also had a reduction in the suramin sensitivity and the residue at position 138 was not a lysine residue but an uncharged asparagine residue (Soto *et al.*, 2003). Also, there is an additional lysine residue at the bottom of the cysteine rich head region in the guinea-pig P2X7 receptor, which is ~10-fold more sensitive to suramin compared to the rat and the human isoforms (Fonfria *et al.*, 2008). This suggested that the lysine residue at position 138 could partly contribute to the differences in suramin sensitivity between the different species of the P2X receptor. If the positively charged residue at this position was important in suramin sensitivity, the rat P2X1 receptor would have been predicted to have lower suramin sensitivity than the human P2X1 receptor. This is because the residue at position 138 in the rat P2X1 receptor is a negatively charged glutamic acid. However, this is not the case and suramin and NF449 sensitivities are similar at the rat P2X1 receptor compared to the human P2X1 receptor. This further suggested that the cluster positively charged residues around this residue (K136, R139 and K140) are also important in the antagonist sensitivity.

Suramin is known to be effective at most P2X receptors (Table 3.1). This would suggest that there may be a common site of action at the different suramin-sensitive P2X receptors involving the same residues. However, the positively charged residues, K136-K140, are only present in the P2X1 receptor and are absent in other suramin-sensitive P2X receptors. Also, the lysine residue at position 78 in the human P2X4 receptor, which was also shown to be important in suramin sensitivity, is not present in other P2X receptors (Garcia-Guzman *et al.*, 1997). Therefore, if the residues K136-K140 are key to suramin binding in the P2X1 receptor then suramin does not have a common binding site and different residues/regions could be involved at different P2X receptor subunits. This is different to agonist action where it has been suggested that there is a common binding site between P2X receptor subtypes (Roberts *et al.*, 2008).

The involvement of different residues between P2X receptor subunits in suramin sensitivity was further supported by the data gained using the reciprocal mutants in the P2X2 receptor. The mutant adding the 3 lysine residues into the P2X2 receptor did not fully recover the suramin sensitivity. The sensitivity to suramin at the P2X1 receptor was still ~3-fold more sensitive to suramin than the P2X2 receptor mutant. Also, the mutant

adding the additional arginine residue had similar suramin sensitivity to that of the P2X2 receptor. Therefore, other residues/regions as well as these basic amino acids must be important in the molecular basis of suramin at the P2X1 receptor. Interestingly, this was similar to NF449 action, which only had a partial recovery of NF449 sensitivity with the triple lysine mutant but no recovery with the additional arginine mutant.

6.3.2 PPADS may also coordinate with the base of the cysteine rich head region

The involvement of the base of the cysteine rich head region and the basic amino acids in suramin sensitivity was similar to NF449. This was expected due to the similarities in their structures. The sensitivity of PPADS at the P2X1 and P2X2 receptors were shown to be quite similar, with an ~3-fold higher affinity of PPADS at the P2X2 receptor compared to the P2X1 receptor. This would suggest that chimeras and point mutations swapping regions and residues between the P2X1 and P2X2 receptor should not have a large change in PPADS sensitivity. However, this was not the case and the chimeras and point mutations in the P2X1 receptor had affected PPADS sensitivity. Swapping the middle and the top regions of the cysteine rich head region in the P2X1 receptor with the P2X2 receptor increased PPADS sensitivity compared to both WT P2X receptors (see section 6.3.3) and swapping the bottom region decreased the sensitivity. Interestingly, PPADS sensitivity decreased by ~50-fold when the positively charged residues were removed at the base of the cysteine rich head region from the P2X1 receptor.

Previous studies have highlighted the involvement of positive charge in PPADS sensitivity (Buell *et al.*, 1996; Michel *et al.*, 2008). For example, the sensitivity of PPADS was recovered in the rP2X4 receptor when a glutamic acid was replaced with a lysine residue at position 249 and PPADS sensitivity was reduced during the mutation of an arginine residue at position 126 in the P2X7 receptor (Buell *et al.*, 1996; Michel *et al.*, 2008). Therefore, PPADS could also be coordinating with the positively charged residues at the base of the cysteine rich loop. However, these residues at the base of the head region are not positively charged in the P2X2 receptor, which is more sensitive to PPADS compared to the P2X1 receptor. Also, the majority of the mutants introducing the charged residues into the P2X2 receptor did not have a large effect on PPADS sensitivity, with the mutant D138K having the largest difference (~8-fold increase) compared to the P2X2

receptor. Therefore, the involvement of the positively charged residues at the base of the head region on the P2X1 receptor in the molecular basis of PPADS action appears to be complicated. The removal of these residues in the P2X1 receptor may not be affecting PPADS binding directly and could be causing conformational changes that affect the state of the receptor, reducing antagonist action. These ideas will be discussed in more detail in the General Discussion (Chapter 7).

6.3.3 Top and middle regions of the cysteine rich head region contribute to both suramin and PPADS sensitivity

The base of the cysteine rich loop was shown to play an important role in suramin and PPADS sensitivity. However, the smaller sub-chimeras showed that the top and the middle regions of the cysteine rich loop also appeared to have a role in antagonist sensitivity. The chimeras, P2X1 Cys2(4-6) and P2X1 Cys2(1-3) chimera, both had an increase in suramin and PPADS sensitivity. Interestingly, these observations were different to those observed with NF449 (explained in more detail in the Final Discussion, Chapter 7).

The top and the middle regions of the cysteine rich head region could contain residues that result in the P2X2 receptor being more sensitive to PPADS than the P2X1 receptor. Due to the known importance of charge in antagonist sensitivity, the charged amino acids in these other regions could also be contributing to the changes observed in antagonist sensitivity (Figure 6.11). The removing/adding of charged residues could either break/form bonds that help hold the receptor in a certain conformation or alter the binding of the negatively charged antagonists.

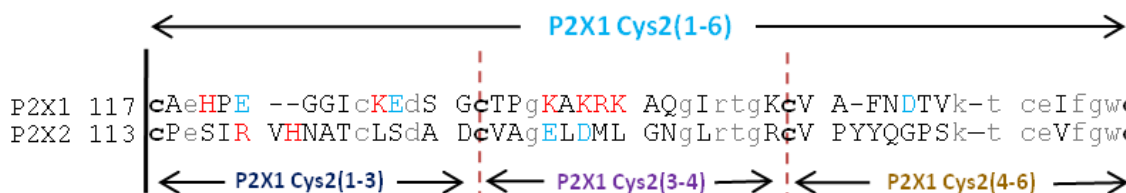


Figure 6.11 Sequence alignment. Sequence alignment of the human P2X1 and P2X2 receptor incorporating the cysteine rich loop. The amino acid residues of the P2X1 Cys2(1-6) chimera are between the black lines and the P2X1 Cys2(1-3), P2X1 Cys2(3-4) and P2X1 Cys2(4-6) chimeras are between the red dotted lines. The non-conserved charged residues are in red (positive) and cyan (negative).

Middle of the cysteine rich head region

The chimera swapping the middle of the cysteine rich head region (P2X1 Cys2(1-3) chimera) had a large increase in suramin and PPADS sensitivity (by ~15- and ~25-fold, respectively). Interestingly, this chimera had a reduction in the NF449 sensitivity (by ~20-fold) further suggesting the different interactions with between the antagonists (see Chapter 7). Sequence analysis of the two subtypes in this region showed that there are two positively charged residues (P2X1 H120 and K127) and two negatively charged residues (P2X1 E122 and E128) in the P2X1 receptor but only two positively charged residues (R118 and H120; Figure 6.11) in the P2X2 receptor. There was an overall reduction of two negatively charged residues in this region, which may account for the increase in the sensitivity of the negatively charged antagonists, suramin and PPADS. Interestingly, the residue at position 122 in the P2X1 receptor was a negatively charged glutamic acid and was replaced by a positively charged arginine residue. Therefore, the removal of a negatively charged residue at this position could remove the possible repulsion between the residue and the antagonist altering the local charge environment. The addition of the added arginine residue could either increase the affinity of negatively charged antagonists, help transduce the inhibition effect of the antagonists or affect the conformational of the receptor increasing the antagonist sensitivity. The side chain of the residue 122 can be seen to be facing towards the predicted ATP binding site (Figure 6.12), where competitive antagonists like suramin could be binding. Therefore, due to the change in the charge at position 122, this residue could most likely be the reason for the increase antagonist sensitivity. Interestingly, this residue has also been highlighted as the possible reason why the P2X1 Cys2(1-6) chimera does not have a reduced NF449 sensitivity as the P2X1 Cys2(3-4) chimera (see Chapter 5.3.3 and below).

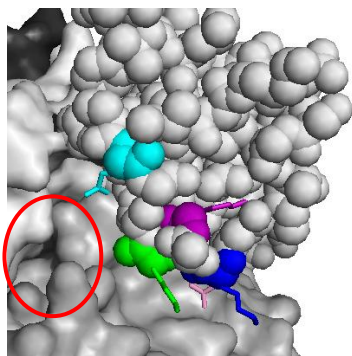


Figure 6.12. Location of E122. Homology of the P2X1 receptor showing the positively charged residues K136 (blue), K138 (purple), R139 (pink), K140 (green) and the negatively charged residue E122 (cyan). The main chains are in spheres and the side chains are in stick format. The predicted ATP binding pocket is shown with a red circle.

To test the contribution of the charged amino acids in this region, point mutations of these amino acids could be constructed in the P2X1 and P2X2 receptor. One example would be to construct the point mutant E122R and the prediction would be that the inhibition is increased for suramin and/or PPADS.

The importance of middle region of the cysteine rich head region in PPADS sensitivity is supported by a previous study, which identified a residue in this region as important in PPADS sensitivity (Michel *et al.*, 2008). This residue was R126 in the hP2X7 receptor, which was identified through differences in species sensitivities (Michel *et al.*, 2008). The corresponding residue in the P2X1 receptor is an uncharged glycine residue and swapping the region around this residue, increased in PPADS sensitivity (P2X1 Cys2(1-3) chimera) showing that this region also contributes to the molecular basis of PPADS action.

Top of the cysteine rich head region

The chimera swapping the top region of the cysteine rich head region (P2X1 Cys2(4-6) chimera) also had an increase in suramin and PPADS sensitivity. Interestingly, this chimera did not have a change in NF449 sensitivity, further highlighting the difference in the molecular basis of suramin and PPADS action compared to NF449 at the P2X1 receptor (discussed in more detail in the Final Discussion, Chapter 7). This region only has one charged amino acid in both of the subtypes and this was the negatively charged aspartic acid at position 154 in the P2X1 receptor (Figure 6.11). The swapping of D154 to the reciprocal uncharged glycine residue in the P2X2 receptor with the P2X1 Cys2(4-6) chimera may affect the local charge environment important for the action of the antagonists. The removal of a negative charge may either allow the positively charged suramin and/or PPADS to bind with a higher affinity directly or cause a conformational change in the receptor. The positioning of this residue in the homology model of the P2X1 receptor shows that this residue is at the top of the cysteine rich head region, which may play a role in antagonist action if the antagonist wraps around the back of the head of the P2X1 receptor (Figure 6.13).

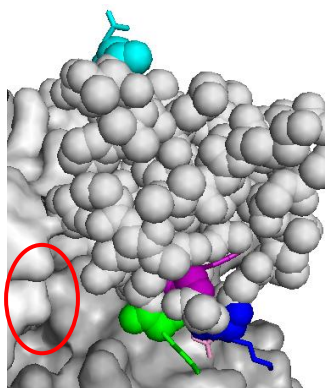


Figure 6.13. Location of D154. Homology of the P2X1 receptor showing the positively charged residues K136 (blue), K138 (purple), R139 (pink), K140 (green) and the negatively charged residue D154 (cyan). The main chains are in spheres and the side chains are in stick format. The predicted ATP binding pocket is shown with a red circle.

Interestingly, the P2X1 Cys2(4-6) chimera only had one negatively charged residue removed compared to the WT P2X1 receptor, whereas, the P2X1 Cys2(1-3) chimera had two (Figure 6.11). This may account for the reason why the P2X1 Cys2(1-3) chimera was ~5-fold more sensitive to suramin than the P2X1 Cys2(4-6) chimera. Additionally, the removal of the negatively charged residues (E122, E128 and D154) in the chimera swapping the whole cysteine rich loop (P2X1 Cys2(1-6) chimera) could be the reason it was more sensitive to NF449, suramin and PPADS compared to the P2X1 Cys2(3-4) chimera (as explained in Chapter 5.3.3). These negatively charged residues are not present in the P2X1 Cys2(1-6) chimera, and this absence may allow the antagonists to inhibit the receptor at lower concentrations than at the P2X1 Cys2(3-4) chimera.

6.3.4 Molecular docking of Suramin at P2X1 receptor

Chimeras and point mutations have highlighted the role of the cysteine rich head region of the P2X1 receptor in the molecular basis of suramin action. In particular, the positively charged residues at the base of the region are important in suramin sensitivity. To predict the involvement of these residues in the binding of suramin at the P2X1 receptor, *in silico* docking simulations were carried out. The molecular model of suramin was generated and docking simulations were ran on the homology model of the P2X1 receptor (carried out by Ralf Schmid). Two different starting points were used (as explained in Chapter 5.3.4) and three examples of the fits are detailed below, all with similar docking scores. The three different orientations of suramin binding on the homology model of the P2X1 receptor shows suramin binding over the top of the ATP binding pocket (purple), going into the ATP binding pocket (orange), and round the back of the cysteine rich head region (green) (Figure 6.14).

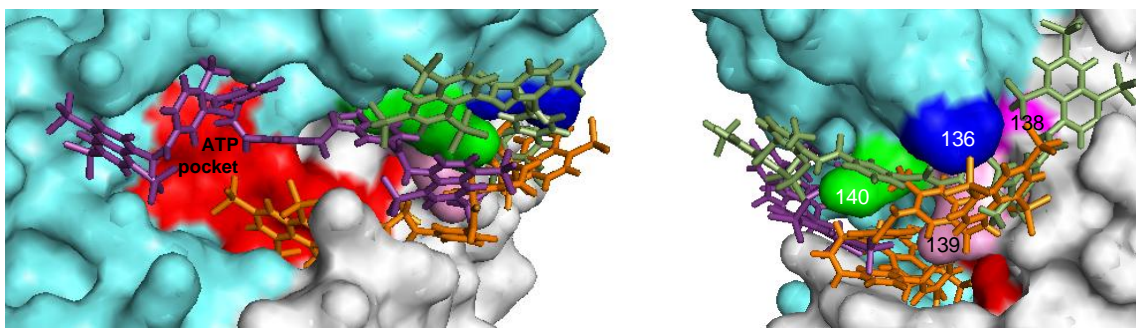


Figure 6.14. Predicted *in silico* docking models of suramin at the homology model of the P2X1 receptor. Homology model of the P2X1 receptor is based around the crystal structure of the zP2X4 receptor. The 3 subunits as surface rendered in dark grey, cyan and white, the residues involved in ATP potency are coloured in red, K136 is blue, K138 is purple, R139 is pink and K140 is blue. The 3 different docking models of suramin are shown in orange, green and purple. The P2X1 receptor is shown in two orientations, (i) the front of the receptor and (ii) rotated clockwise showing the back of the cysteine rich head region.

The first *in silico* docking model shows suramin binding over the top ATP binding pocket (docking score of 71; Figure 6.15A). This orientation of suramin could block ATP from entering the binding site, preventing ATP from activating the channel (as predicted in Chapter 3.3.2; Figure 3.8). There are 6 negatively charged sulphonates on suramin, with 3 being at either end of the molecule. These charges appear to be interacting with R175 and K249 on one end of the molecule and with K215, R139 and K140 on the end. Interestingly, the lysine residue at 249 has been shown to be involved in antagonist action, where in a previous study PPADS sensitivity was recovered in the rP2X4 receptor with the mutation E249K (Buell *et al.*, 1996). However, this model is not close to K138, which was the only single point mutant to have a decrease in suramin sensitivity. Therefore, this model may be not be correct.

The second *in silico* docking model shows suramin binding underneath the cysteine rich head and entering the ATP binding pocket (docking score 84; Figure 6.15B). The negative charges on suramin appear to be interacting with residues involved in ATP binding (K68 and K70), K215, R180 and the residues at the base of the cysteine rich head region (K136 and K138). Interestingly, when the two lysine residues were mutated (K136EK138D double mutant) there was a large decrease in suramin sensitivity supporting this model. In this model suramin could antagonise the P2X1 receptor by directly competing with ATP for its active site (K68 and K70). However, studies have shown that

mutating K68 and K70 does not reduce suramin sensitivity, suggesting that this model may not be possible (as mentioned previously).

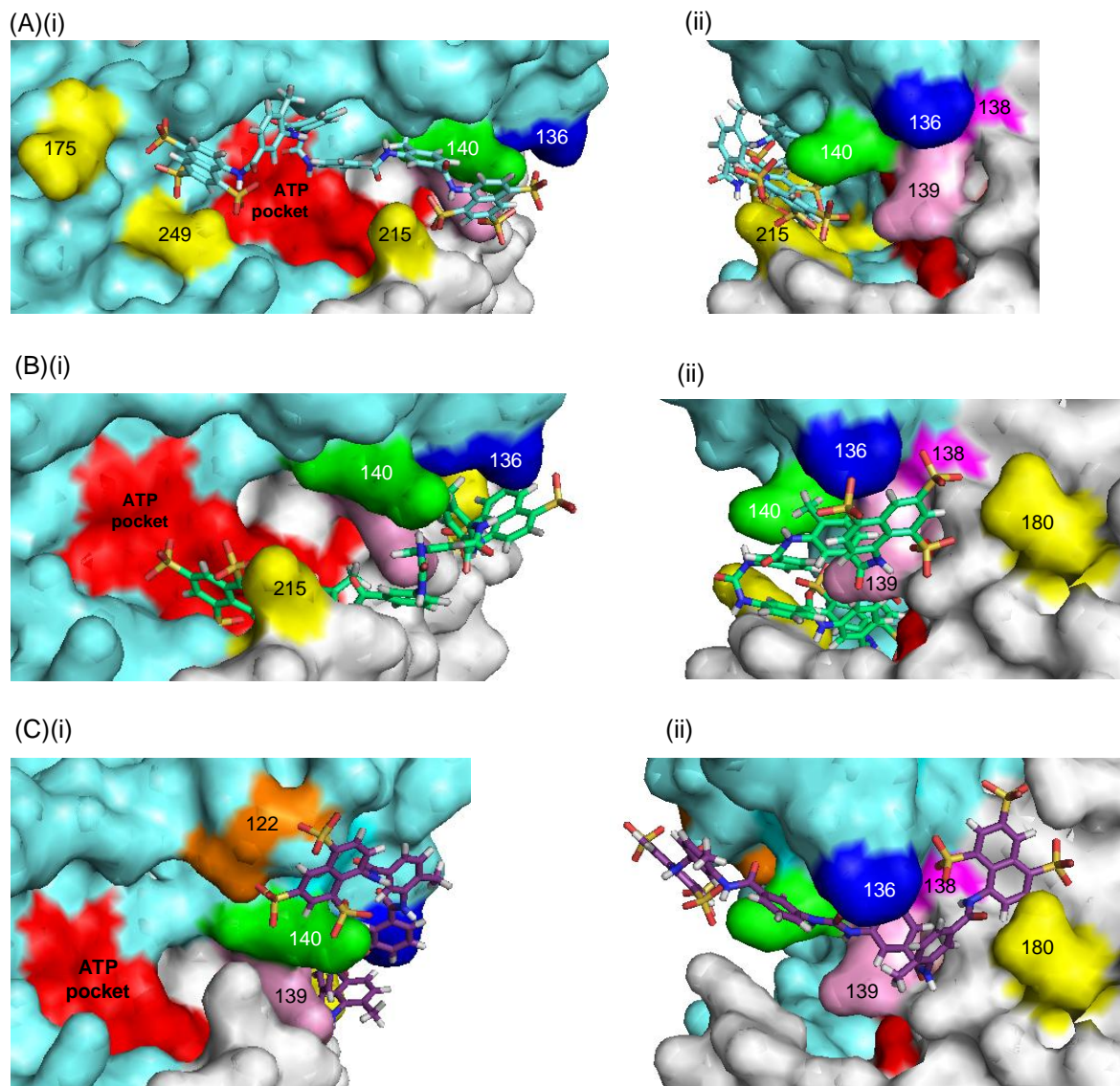


Figure 6.15. *In silico* docking models of suramin on the homology model of the P2X1 receptor. The 3 subunits as surface rendered in dark grey, cyan and white, the residues involved in ATP potency are coloured in red, K136 is blue, K138 is purple, R139 is pink and K140 is blue. **(A)** Suramin is docked over the top of the predicted ATP binding site, close to the positively charged residues K175, K215 and R175 (yellow) and underneath the cysteine rich head region. **(B)** Suramin is docked partly in the proposed ATP binding site, close to the residues K215 and R180 (yellow) and underneath the cysteine rich head region. **(C)** Suramin is docked round the back of the cysteine rich head region and is close to the positively charged residue R180 (yellow). The P2X1 receptor is shown in two orientations, **(i)** the front of the receptor and **(ii)** rotated clockwise showing the back of the cysteine rich head region.

The third *in silico* docking model shows suramin binding underneath and round the back of the cysteine rich loop (docking score of 81; Figure 6.15C). Suramin binding in this orientation would not directly compete with ATP for the predicted ATP binding pocket but hold the receptor in a certain conformation reducing ATP from activating the channel. One possibility is that the conformational change could move the cysteine rich head region over the ATP binding pocket, blocking ATP from entering its active site (as explained in Chapter 3.3.2; Figure 3.10). Suramin appears to interacting with the positively charged residue R180 and the positively charged residues at the base of the cysteine rich head region, in particular K136, K138 and K140. Interestingly, suramin is also close to the residue E122. This negative charge is present in the smaller chimera that replaces the base but absent in the chimera replacing the whole of the cysteine rich region. Therefore, the removal of this negative charge may be reason why suramin can antagonist the chimera replacing the whole of the region at lower concentrations than the smaller chimera (see Section 6.3.3).

The three proposed docking models all have high docking scores but the simulations were based on two starting points. Entering additional starting points in the docking programme could potentially highlight further possible sites of suramin action. Therefore, to see if any of the predicted docking models was the site of suramin action, the models need to be tested experimentally. This can be carried out by generating multiple P2X1 receptor mutants, which remove the positive charge at the base of the cysteine rich head region and the positive charge at the residues that are close to suramin in the docking models. Also, mutants that add all of the positively charged residues into the P2X2 receptor could potentially recover suramin sensitivity highlighting the importance of these residues in suramin action.

Results in this chapter have shown that the positively charged residues at the base of the cysteine rich head region could coordinate suramin binding, with the residue K138 playing a larger role in suramin action. Also, studies have shown that the residues involved in ATP potency do not appear to be involved the molecular basis of suramin action (as previously mentioned). Therefore, the docking models which are not in the proposed ATP binding site and are close to the residue K138 may be correct. From the docking models

shown above, the third example is the closest to K138 and is not in the proposed ATP binding pocket. To support this prediction an experiment testing the suramin sensitivity at a mutant which removed the positively charged residues at the base of the cysteine rich head region and the arginine at position 180 could be carried out.

6.3.5 Proposed site of PPADS action

This chapter has also highlighted the importance of the positively charged residues at the base of the cysteine rich head region of the P2X1 receptor in PPADS sensitivity. These residues could possibly be interacting with PPADS or the removal of these residues could cause a conformational change in the receptor affecting the ability of PPADS to antagonise the receptor (discussed more in Chapter 7). Other residues that have been shown to be important in PPADS sensitivity are the residue 249, which upon the addition of a lysine at position 249 in the P2X4 the PPADS sensitivity is increased (Buell *et al.*, 1996), and the arginine residue at position 126 in the P2X7 (Michel *et al.*, 2008). *In silico* docking was not carried out for PPADS but the residues can be mapped onto the homology model of the P2X1 receptor (K249 and the equivalent residue to R126 in the P2X1 receptor is G123) to get an idea of the possible location of PPADS action (Figure 6.16). These residues appear to be located either side of the proposed ATP binding pocket, with G123 being spatially close to the positively charged residues at the base of the cysteine rich head region. PPADS could be binding across the ATP binding site, restricting the access of ATP to its binding site. This could reduce the number of receptors that are activated giving its non-competitive nature observed at the P2X1 receptor (for more details see the General Discussion, Chapter 7).

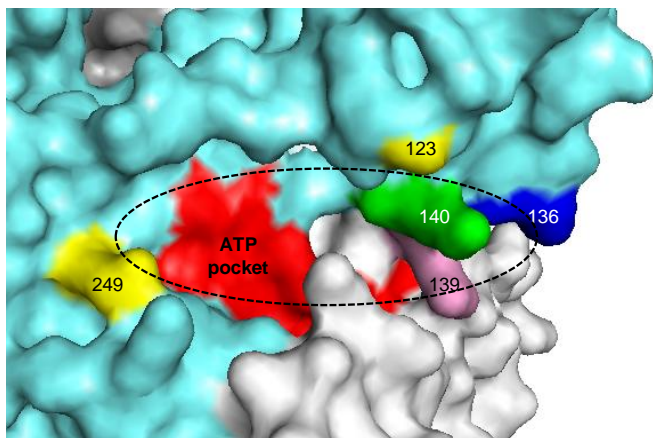


Figure 6.16. Homology model of the P2X1 receptor mapping the residues involved in PPADS sensitivity. The 3 subunits are surface rendered in dark grey, cyan and white. The possible orientation of PPADS is shown by the dotted black circle. Residues previously been shown to be important in PPADS action are K249 and G123 (yellow). G123 is the reciprocal residue of R126 in the P2X7 receptor. Also, the positively charged residues at the base of the cysteine rich loop are shown, which are K136 (blue), K138 (purple), R139 (pink) and K140 (green).

In summary, the cysteine rich loop and in particular the positively charged residues (P2X1 136-140) have been shown to be important in the molecular basis of not only NF449 but also, suramin and PPADS at the P2X1 receptor. This may be due to either the direct coordination with the antagonists and/or conformational changes in the cysteine rich head region reducing antagonist sensitivity. Also, the differences in the sensitivities of the chimeras replacing the top and the middle of the cysteine rich head region have shown that there appears to be a different molecular basis of suramin and PPADS action compared to NF449 action (for more details see Chapter 7).

Chapter 7. General discussion

The main interest of this thesis was the investigation of the molecular basis of antagonist action at the human P2X1 receptor. This was carried out by investigating the residues in the rear/inner cavity of the predicted ATP binding pocket and the cysteine rich head region by using site-directed mutagenesis and P2X receptor chimeras. Drawing these results together, there appears to be some effects on suramin sensitivity at the back of the proposed ATP binding site and a large involvement of the base of the cysteine rich head region in suramin, PPADS and NF449 sensitivity at the P2X1 receptor. Additional to the results obtained on antagonist action, a further residue (F92) was proposed to be part of the ATP binding site in the P2X1 receptor, refining the model of the ATP binding site (Figure 4.7). Also, residues in the rear/inner cavity of the ATP binding pocket have been shown to be involved in channel properties, which could be important in the conformational changes subsequent to agonist binding.

Cysteine scanning mutagenesis of the residues at the rear/inner cavity of the predicted ATP binding pocket, V74C to Y90C, highlighted their contribution to P2X1 receptor properties. Interestingly, the four P2X1 receptor mutants that had an increase in suramin sensitivity also had a decrease in BzATP efficacy (T75C, Y90C, P93C, Q95C). Mutants with an affected partial agonist efficacy, which did not have a decrease in ATP potency, could be involved in the conformational changes of the receptor subsequent to agonist binding (as described in Chapter 4). Therefore, the residues that were shown to be involved in BzATP efficacy and suramin sensitivity could be important in the conformational changes that occur during suramin antagonism. Based on the homology model of the P2X1 receptor these residues are located behind the cysteine rich head region. The cysteine rich head region of the P2X1 receptor has also been shown to be important in suramin sensitivity, in particular, the positively charged residues at the base, K136, K138, R139 and K140 (Chapter 6). These positively charged residues were suggested to be part of the suramin binding site in the P2X1 receptor and suramin could move the cysteine rich head region reducing the ability of ATP to activate the channel. Therefore, the residues T75, Y90, P93 and Q95 could be associated with the conformational changes that occur during suramin antagonism. For example, the cysteine mutation of these residues could

allow the cysteine rich head region to move by greater extent during suramin binding and more readily block ATP from entering the binding pocket. Another possibility is that suramin could bind to the base of the cysteine rich head region affecting the conformation of the agonist binding site. The residues at the rear/inner cavity could be involved in this change.

The residues at the inner/rear cavity of the predicted ATP binding pocket of the P2X1 receptor (V74-G96) were not investigated in their role on NF449 sensitivity. NF449 is a suramin analogue and could be predicted to have a similar molecular basis of action at the P2X1 receptor as suramin. However, studies involving the cysteine rich loop have shown differences and similarities in suramin and NF449 antagonism. For example, the P2X1 receptor chimeras did not all have a similar effect on antagonist sensitivity (Table 7.1). The chimera replacing the middle region of the cysteine rich head region of the P2X1 receptor with the P2X2 receptor (P2X1 Cys2(1-3) chimera) had a decrease in NF449 sensitivity (by ~20-fold) but had an increase in suramin sensitivity (by ~15-fold) compared to the WT P2X1 receptor. In contrast, the multiple point P2X1 receptor mutants, which removed positively charged residues at the base of the cysteine rich loop, had a large decrease in both NF449 and suramin sensitivity (Table 7.1). This suggested that NF449 and suramin could coordinate with the residues at the base of the cysteine rich loop but they could coordinate with different parts of the cysteine rich head region. However, these changes in antagonist sensitivity may not be due to different interactions with the P2X1 receptor but swapping regions of the cysteine rich head could affect the conformation of receptor affecting the antagonist binding site. To investigate whether these antagonists were in different orientations docking models were generated for suramin and NF449 on the homology model of the P2X1 receptor (see below).

(A)	~fold difference in IC ₅₀ compared to WT P2X1		
	NF449	Suramin	PPADS
WT P2X1	1.04 nM	1.7 μM	1.02 μM
WT P2X2	↓ 1400x	↓ 60x	↑ 3x
P2X1 Cys2(1-6)	↓ 300x	↓ 3x	↓ 10x
P2X1 Cys2(1-3)	↓ 20x	↑ 15x	↑ 20x
P2X1 Cys2(3-4)	↓ 1800x	↓ 25x	↓ 15x
P2X1 Cys2(4-6)	-	↑ 3x	↑ 35x
K136E	-	-	-
K138D	↓ 10x	↓ 3x	↓ 3x
R139M	-	-	-
K140L	-	-	-
X1-EADRK(2)	↓ 140x	↓ 10x	N.D.
X1-EADRL(3)	↓ 300x	↓ 11x	↓ 50x
X1-EADML(4)	↓ 540x	↓ 40x	↓ 40x
X1-ELDML(5)	↓ 670x	↓ 30x	↓ 50x
(B)	~fold difference in IC ₅₀ compared to WT P2X2		
	NF449	Suramin	PPADS
WT P2X2	1458 nM	107 μM	0.33 μM
WT P2X1	↑ 1400x	↑ 60x	↓ 3x
P2X2 Cys1(3-4)	-	↑ 25x	↑ 2x
D136K	-	↑ 4x	↑ 8x
X2-KLKML(2)	↑ 2x	↑ 9x	N.D.
X2-KLKMK(3)	↑ 5x	↑ 20x	↑ 2x
X2-KLKRRK(4)	↑ 2x	↑ 5x	↓ 3x

Table 7.1. Antagonist action on chimeras and point mutants in the cysteine rich head region of the P2X receptor. Approximate fold change of the IC₅₀ of the P2X receptor chimeras and point mutants compared to the (A) WT P2X1 receptor and (B) WT P2X2 receptor. The increases in antagonist sensitivity are shown in black and the decreases are shown in red. The dashed lines (-) represents no change in antagonist sensitivity compared to the WT. N.D. represents not determined.

In silico docking predicted several different possible sites of NF449 and suramin action on the homology model of the P2X1 receptor showing 3 different possible fits, with high docking scores (Chapters 5 and 6). Interestingly, these docking models have differences and similarities in the proposed binding sites for NF449 and suramin. These antagonists are symmetrical molecules with a common central urea group but suramin has 3 polysulfonates at either end of the molecule on 2 naphthyl ring and NF449 has 2 polysulfonates on 4 benzene rings spread around the structure (a total of 6 possible negative charges on suramin and 8 on NF449; Figure 5.1). The second docking model examples for each antagonist (Chapters 5 and 6), both appear to have a similar orientation at the P2X1 receptor (Figure 7.1). The central urea group of both antagonists lie

underneath the cysteine rich head region (between R139 and K140) with the rest of the molecule either binding round the back of the cysteine rich head region (near K136 and K138) or inside the predicted ATP binding pocket (near K68 and K70). These two models support the involvement of the multiple charged residues at the base of the cysteine rich head region in coordinating antagonist but they both appear to be coordinating with K68 and K70. Suramin is not thought to coordinate with residues predicted to be involved ATP potency (as mentioned previously) so these docking simulations showing suramin or its analogue, NF449, coordinating with part of the agonist site may be incorrect. Additional docking simulations could be carried out using the homology model of the P2X1 receptor with the positively charged residues in the ATP binding pocket (e.g. K68, K70, R292 and K309) removed. This could refine the model of antagonist action and highlight further possible orientations of suramin and NF449.

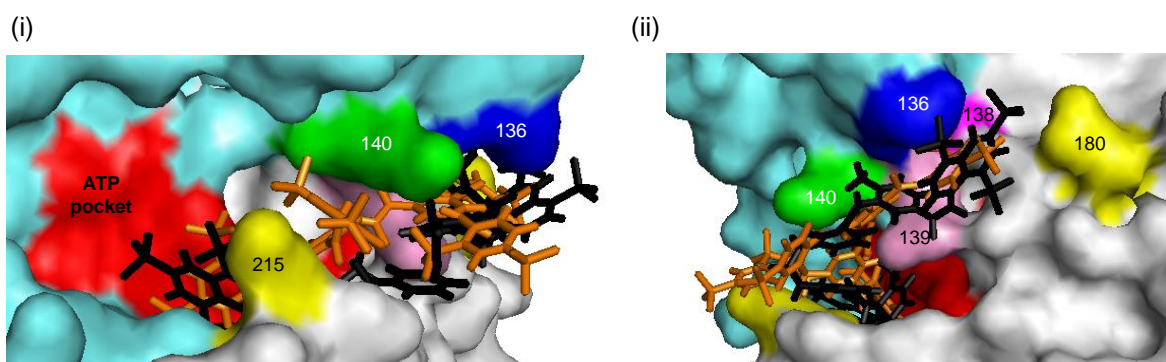


Figure 7.1. *In silico* docking models of NF449 and suramin binding underneath the cysteine rich head region of the P2X1 receptor. NF449 (orange) and suramin (black) are docked on the homology model of the P2X1 receptor. The receptor is in two conformations **(i)** showing the front of the receptor and **(ii)** rotated clockwise showing the side of the cysteine rich head region. They are both docking underneath the cysteine rich head region with the urea core of the antagonists between R139 (pink) and K140 (green) and the ends of the molecule either entering the predicted ATP binding pocket (red) or round the back of the cysteine rich head region near K136 (blue) and K138 (purple). The additional positively charged residues K215 and R180 are shown in yellow.

This thesis has shown that the removal of the multiple positively charged residues at the base of the cysteine rich head region of the P2X1 receptor is required to observe a large decrease in antagonist sensitivity rather than single point mutations. This may be due the highly negatively charged nature of the antagonists. Therefore, to test whether K68 and K70 are important in antagonist sensitivity a multiple point P2X1 receptor mutant, which removed the positive charges in the predicted ATP binding pocket and at the base of the cysteine rich head region, could be constructed. However, this mutant would be hard to test

experimentally as multiple mutation of the positive charges in the ATP binding pocket are also likely to have major effects on agonist action. This suggests that it would be hard to predict whether the models of suramin and NF449 binding with part of the predicted ATP binding are correct.

NF449 is a highly selective P2X1 receptor antagonist acting at low nanomolar concentrations, whereas, suramin acts at low micromolar concentrations at the P2X1 receptor. NF449 contains two additional negatively charged polysulfonates and this might suggest that NF449 coordinates with more positively charged residues on the P2X1 receptor compared to suramin. Interestingly, the third docking examples for suramin and NF449 are both binding behind the cysteine rich head region and the negatively charged polysulfonates of NF449 are close to more positively charged residues than suramin (Figure 7.2). These two structures are both behind the cysteine rich loop, close to R180 and the positively charged residues at the base of the cysteine rich loop but the common core of the molecules appear do dock in different orientations. The differences in the antagonist site of action could be expected as NF449 has a higher affinity than suramin for the P2X1 receptor and the P2X1 receptors chimeras do not have the same effects on suramin and NF449 sensitivity (Table 7.1). For example, the chimera swapping the middle part of the cysteine rich head region (P2X1 Cys2(1-3) chimera) had an increase in suramin sensitivity but a decrease in NF449 sensitivity (Table 7.1). Interestingly, the docking model of suramin shows the molecule binding around the head of the P2X1 receptor close to the middle part of this region (Figure 7.2).

The antagonists binding behind the cysteine rich head region could cause a conformational change in the receptor affecting the ability of ATP to bind in its active site (as explained in Chapter 3.3.2, Figure 3.10). The P2X1 receptor cysteine mutants at the rear/inner cavity of the ATP binding pocket, which had an effect on suramin sensitivity, may be involved in these conformational changes that occur when the antagonists move the cysteine rich head region. Therefore, the docking models in Figure 7.2 appear to correlate with the data obtained in this thesis at a greater extent than the other docking models.

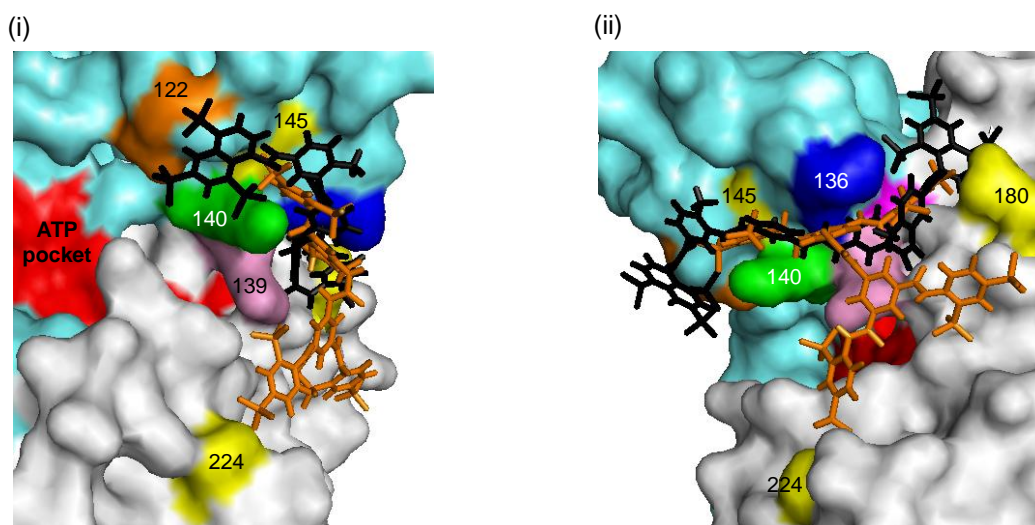


Figure 7.2. *In silico* docking models of NF449 and suramin binding behind the cysteine rich head region of the P2X1 receptor. NF449 (orange) and suramin (black) are docked on the homology model of the P2X1 receptor. The receptor is shown in two conformations **(i)** showing the front of the receptor and **(ii)** rotated clockwise showing the side of the cysteine rich head region. They are both docking behind the cysteine rich head region near the positively charged residues at the base, K136 (blue), K138 (purple), R139 (pink) and K140 (green) and residue R180 (yellow). Additional to these residues NF449 appears to be docking close to the R145 and H224, shown in yellow and suramin close to the E122, shown in orange.

The residues at the inner/rear cavity of the predicted ATP binding pocket of the P2X1 receptor (V74-G96) were also investigated in their contribution to PPADS sensitivity. Individual cysteine mutation of the residues did not affect the sensitivity of PPADS suggesting that suramin and PPADS act differently at the P2X1 receptor. This was expected due to the non-competitive nature of PPADS and the competitive nature of suramin at the P2X1 receptor (Chapter 3). However, the P2X1 receptor chimeras of the cysteine rich head region showed similarities in the changes in sensitivity between suramin and PPADS but differences compared to NF449 (Table 7.1). For example, the P2X1 receptor chimeras replacing the top and middle regions of the cysteine rich head region with the P2X2 receptor both had an increase in suramin and PPADS sensitivity (Table 7.1). In contrast, NF449 sensitivity was decreased at the chimera replacing the middle region and there was no change with the chimera replacing the top region compared to the WT P2X1 receptor. However, all 3 of the antagonists had a large decrease in the sensitivity upon the removal of the positively charged residues at the base of the cysteine rich head region. One possible explanation of these findings is that the three antagonists could all be

coordinating with the base of the head region but have different orientations giving their different properties and affinities at the P2X1 receptor.

A previous study has shown that the mutant E249K in the P2X4 receptor increased PPADS sensitivity but the removal the positive charge in the P2X1 receptor did not decrease PPADS sensitivity (Buell *et al.*, 1996). This thesis has shown that multiple point mutations decreased antagonist sensitivity. Therefore, to observe a possible further decrease in PPADS sensitivity and highlight the role of K249 in the P2X1 receptor, a mutant removing the lysine at position 249 and the other residues involved in PPADS sensitivity could be constructed. Due to the position of the residues that have been shown to be important in PPADS sensitivity, which are either side of the predicted ATP binding pocket, one suggestion of PPADS action was the coordination of PPADS over the top of the predicted ATP binding site reducing the number of receptors activated (as explained in Chapter 6). However, if this was the case PPADS antagonism could be expected to be time dependent and in this thesis, the effects of PPADS saturated after a 5 minute incubation period. Therefore, it is hard to predict the molecular basis PPADS action at the P2X1 receptor. To get a better idea of the possible location of PPADS action, *in silico* docking simulations could be carried out binding PPADS at the homology model of the P2X1 receptor.

The common involvement of the base of the cysteine rich head region in suramin, PPADS and NF449 sensitivity suggested that this area could coordinate all 3 of these antagonists at the P2X1 receptor. Another possibility is that the removal of these positively charged residues at the base of the head could cause a conformational change affecting the ability of the receptor to bind the antagonists at a different location. This can be supported by several lines of evidence; (i) the positively charged residues at the base of the head are not present in other suramin and PPADS sensitive P2X receptors so either there is a different antagonist binding site at each subtype or these residues are important in stabilising the conformation of the P2X1 receptor, (ii) PPADS has a higher sensitivity at the P2X2 receptor compared to the P2X1 receptor but swapping the residues at the base of the head region of the P2X1 receptor with the P2X2 receptor decreased the PPADS sensitivity, and (iii) the reciprocal mutations in the P2X2 receptor, adding positive charge

at the base of the cysteine rich head region, did not fully recover suramin or NF449 sensitivity. This suggested that the antagonists either coordinate with additional variant residues in the P2X1 receptor, the site of antagonist action is in a different location on the P2X2 receptor, or removing these positively charged residues could be causing a conformational change in the P2X1 receptor.

The proposed conformational change in the P2X1 receptor upon the removal of the charged residues at the base of the cysteine rich loop could be putting the receptor into a state that makes the antagonists less able to bind at the P2X1 receptor. One possibility is that the positively charged residues could be forming salt bridges with negatively charged residues on the structure of the P2X1 receptor, stabilising a certain conformation. Interestingly, the positively charged residues at the base of the cysteine rich head region are close to two negatively charged glutamic acids at positions 183 and 185. These residues are located on the body of the P2X1 receptor, which is close to the base of head region. The introduction of the negatively charged residues with the P2X1 receptor mutants K136E and K138D could not only break this salt bridge but repel the head of the receptor away from the body of the receptor. Therefore, the receptor could be cycling between two different conformations, where, in one state it is willing to accept the antagonist and the other it is not willing to accept the antagonist. These mutations could push it towards the state where it is not willing to bind the antagonists at the P2X1 receptor.

The construction of a mutant removing the negative charges at residues E181 or E183 in the P2X1 receptor might also reduce antagonist sensitivity if these residues are important stabilising a particular conformation. Interestingly, NF449 sensitivity has been tested at the individual P2X1 receptor point mutants E181C and E183C and the sensitivity was not reduced suggesting that these salt bridges might not form (data not shown). However, these were replaced with a neutrally charged residue unlike the mutants K136E and K138D. Also, the removal of both possible salt bridges may be necessary to observe a reduction in the antagonist sensitivity. Therefore, future work, either constructing a double mutant and/or mutating the E181 and E183 residues to a positive amino acid, could

highlight the possibility of these positively charged residues at the base of the cysteine rich head region stabilising the P2X1 receptor in a certain conformation.

The removal of the positively charged residues at the base of the cysteine rich head had a large effect on the antagonist action at the P2X1 receptor but in contrast, there were relatively little changes in the ATP potency. If these mutants caused a large enough conformational change in the P2X1 receptor to affect the state of the receptor and reduce antagonist sensitivity, the basic properties of the P2X1 receptor would have also been expected to change. However, the peak current amplitudes of the ATP evoked responses of the mutants were not affected and there were only slight changes in the potency of ATP or the rate of desensitisation of the evoked response. This slight change in the ATP potency and the time-course of the ATP evoked response would suggest that there may be small effects on the conformation of the receptor. However, these effects were not as pronounced as the large changes observed with antagonist sensitivity. For example, NF449 sensitivity decreased by ~540-fold when the four positively charged residues were replaced with the residues in the P2X2 receptor but there was only an ~3-fold decrease in ATP potency. Therefore, mutating the residues at the base of the cysteine rich head region most likely affects the coordination of the antagonists in this region directly rather than affecting the conformation and the state of the P2X1 receptor.

To investigate the possible conformational changes in the P2X1 receptor during antagonist binding a cysteine mutant accessibility approach using MTSEA-biotin could be used. Cysteine mutation could allow MTSEA-biotin to label surface accessible cysteine residues. The biotinylated proteins can then be isolated with streptavidin beads, run on a gel and then probed with a P2X1 receptor antibody. This approach could test the accessibility of the P2X1 receptor mutant cysteine residues in different conditions to test for conformational changes in the protein during antagonist binding. The accessibility of the cysteine residues could be tested in the resting state of the P2X receptor, following activation with ATP (this is likely to move the receptor into the agonist bound desensitised state) and in the presence of the antagonists. The change in accessibility profile of the residues could highlight possible conformational that occur during antagonist binding. This could be tested on the mutants V74C to G96C to highlight any conformational changes that

occur in the proposed ATP binding pocket during antagonist action. Also, mutating the residues at the base of the cysteine rich loop to a cysteine and testing their accessibility could highlight the possible conformational change that occurs during antagonist binding. The change in the accessibility profile could also highlight residues that had their access to the MTSEA-biotin blocked by the antagonist. For example, if the accessibility of any of the cysteine mutants at the rear/inner cavity of the predicted ATP binding pocket is reduced in the presence of the NF449, this could suggest that NF449 might be binding in or over the top of the ATP binding pocket.

The overall results of this thesis have shown the involvement of the residues on the rear/inner cavity of the proposed agonist binding site in channel activation and the residues on the base of the cysteine rich head region in the molecular basis antagonist action at the P2X1 receptor. To conclude, this research furthered understanding of ligand action at the P2X1 receptor.

References

- Abbracchio, MP & Burnstock, G (1994). Purinoceptors: are there families of P2X and P2Y purinoceptors?. *Pharmacol Ther* 64, 445-75.
- Adriouch, S, Bannas, P, Schwarz, N, Fliegert, R, Guse, AH, Seman, M, Haag, F & Koch-Nolte, F (2008). ADP-ribosylation at R125 gates the P2X7 ion channel by presenting a covalent ligand to its nucleotide binding site. *FASEB J* 22, 861-9.
- Akabas, MH, Stauffer, DA, Xu, M & Karlin, A (1992). Acetylcholine receptor channel structure probed in cysteine-substitution mutants. *Science* 258, 307-10.
- Allcorn, RJ, Cunnane, TC & Kirkpatrick, K (1986). Actions of alpha, beta-methylene ATP and 6-hydroxydopamine on sympathetic neurotransmission in the vas deferens of the guinea-pig, rat and mouse: support for cotransmission. *Br J Pharmacol* 89, 647-59.
- Allgaier, C, Wellmann, H, Schobert, A & von Kugelgen, I (1995). Cultured chick sympathetic neurons: modulation of electrically evoked noradrenaline release by P2-purinoceptors. *Naunyn Schmiedebergs Arch Pharmacol* 352, 17-24.
- Allsopp, CA, El-Ajouz, S, Schmid, R & Evans, RJ (2011). Cysteine scanning mutagenesis (residues E52-G96) of the human P2X1 receptor for ATP; mapping agonist binding and channel gating. *J Biol Chem*, paper in press.
- Armstrong, N, Mayer, M & Gouaux, E (2003). Tuning activation of the AMPA-sensitive GluR2 ion channel by genetic adjustment of agonist-induced conformational changes. *Proc Natl Acad Sci U S A* 100, 5736-41.
- Aschrafi, A, Sadtler, S, Niculescu, C, Rettinger, J & Schmalzing, G (2004). Trimeric architecture of homomeric P2X2 and heteromeric P2X1+2 receptor subtypes. *J Mol Biol* 342, 333-43.
- Ase, AR, Bernier, LP, Blais, D, Pankratov, Y & Seguela, P (2010). Modulation of heteromeric P2X1/5 receptors by phosphoinositides in astrocytes depends on the P2X1 subunit. *J Neurochem* 113, 1676-84.
- Baddiley, J, Michelson, AM & Todd, AR (1949). Nucleotides. Part II. A synthesis of adenosine triphosphate. *J Chem Soc*, 582-86.
- Banfi, C, Ferrario, S, De Vincenti, O, Ceruti, S, Fumagalli, M, Mazzola, A, N, DA, Volonte, C, Fratto, P, Vitali, E, Burnstock, G, Beltrami, E, Parolari, A, Polvani, G, Biglioli, P, Tremoli, E & Abbracchio, MP (2005). P2 receptors in human heart: upregulation of P2X6 in patients undergoing heart transplantation, interaction with TNFalpha and potential role in myocardial cell death. *J Mol Cell Cardiol* 39, 929-39.

- Barrera, NP, Ormond, SJ, Henderson, RM, Murrell-Lagnado, RD & Edwardson, JM (2005). Atomic force microscopy imaging demonstrates that P2X2 receptors are trimers but that P2X6 receptor subunits do not oligomerize. *J Biol Chem* 280, 10759-65.
- Bean, BP (1990). ATP-activated channels in rat and bullfrog sensory neurons: concentration dependence and kinetics. *J Neurosci* 10, 1-10.
- Belardinelli, L, Shryock, JC, Song, Y, Wang, D & Srinivas, M (1995). Ionic basis of the electrophysiological actions of adenosine on cardiomyocytes. *FASEB J* 9, 359-65.
- Benham, CD (1989). ATP-activated channels gate calcium entry in single smooth muscle cells dissociated from rabbit ear artery. *J Physiol* 419, 689-701.
- Benham, CD, Hess, P & Tsien, RW (1987). Two types of calcium channels in single smooth muscle cells from rabbit ear artery studied with whole-cell and single-channel recordings. *Circ Res* 61, I10-6.
- Benham, CD & Tsien, RW (1987). A novel receptor-operated Ca²⁺-permeable channel activated by ATP in smooth muscle. *Nature* 328, 275-8.
- Berne, RM (1963). Cardiac nucleotides in hypoxia: possible role in regulation of coronary blood flow. *Am J Physiol* 204, 317-22.
- Bertrand, G, Chapal, J, Loubatieres-Mariani, MM & Roye, M (1987). Evidence for two different P2-purinoceptors on beta cell and pancreatic vascular bed. *Br J Pharmacol* 91, 783-7.
- Bian, X, Ren, J, DeVries, M, Schnegelsberg, B, Cockayne, DA, Ford, AP & Galligan, JJ (2003). Peristalsis is impaired in the small intestine of mice lacking the P2X3 subunit. *J Physiol* 551, 309-22.
- Bianchi, BR, Lynch, KJ, Touma, E, Niforatos, W, Burgard, EC, Alexander, KM, Park, HS, Yu, H, Metzger, R, Kowaluk, E, Jarvis, MF & van Biesen, T (1999). Pharmacological characterization of recombinant human and rat P2X receptor subtypes. *Eur J Pharmacol* 376, 127-38.
- Bo, X, Zhang, Y, Nassar, M, Burnstock, G & Schoepfer, R (1995). A P2X purinoceptor cDNA conferring a novel pharmacological profile. *FEBS Lett* 375, 129-33.
- Bobanovic, LK, Royle, SJ & Murrell-Lagnado, RD (2002). P2X receptor trafficking in neurons is subunit specific. *J Neurosci* 22, 4814-24.
- Bodin, P & Burnstock, G (2001). Purinergic signalling: ATP release. *Neurochem Res* 26, 959-69.

- Bodnar, M, Wang, H, Riedel, T, Hintze, S, Kato, E, Fallah, G, Groger-Arndt, H, Giniatullin, R, Grohmann, M, Hausmann, R, Schmalzing, G, Illes, P & Rubini, P (2010). Amino acid residues constituting the agonist binding site of the human P2X₃ receptor. *J Biol Chem* 286, 2739-49.
- Boue-Grabot, E, Archambault, V & Seguela, P (2000). A protein kinase C site highly conserved in P2X subunits controls the desensitization kinetics of P2X₂ ATP-gated channels. *J Biol Chem* 275, 10190-5.
- Boyer, JL, Zohn, IE, Jacobson, KA & Harden, TK (1994). Differential effects of P2-purinoceptor antagonists on phospholipase C- and adenylyl cyclase-coupled P2Y-purinoceptors. *Br J Pharmacol* 113, 614-20.
- Brake, AJ, Wagenbach, MJ & Julius, D (1994). New structural motif for ligand-gated ion channels defined by an ionotropic ATP receptor. *Nature* 371, 519-23.
- Brandle, U, Spielmanns, P, Osteroth, R, Sim, J, Surprenant, A, Buell, G, Ruppertsberg, JP, Plinkert, PK, Zenner, HP & Glowatzki, E (1997). Desensitization of the P2X₂ receptor controlled by alternative splicing. *FEBS Lett* 404, 294-8.
- Braun, K, Rettinger, J, Ganso, M, Kassack, M, Hildebrandt, C, Ullmann, H, Nickel, P, Schmalzing, G & Lambrecht, G (2001). NF449: a subnanomolar potency antagonist at recombinant rat P2X₁ receptors. *Naunyn Schmiedebergs Arch Pharmacol* 364, 285-90.
- Brejci, K, van Dijk, WJ, Klaassen, RV, Schuurmans, M, van Der Oost, J, Smit, AB & Sixma, TK (2001). Crystal structure of an ACh-binding protein reveals the ligand-binding domain of nicotinic receptors. *Nature* 411, 269-76.
- Brown, SG, Kim, Y, Kim, S, Jacobson, KA., Burnstock, G & King, BF (2001). Actions of a series of PPADS analogs at P2X₁ and P2X₃ receptors. *Drug Dev Res* 53, 281-291.
- Brown, SG, Townsend-Nicholson, A, Jacobson, KA, Burnstock, G & King, BF (2002). Heteromultimeric P2X_{1/2} receptors show a novel sensitivity to extracellular pH. *J Pharmacol Exp Ther* 300, 673-80.
- Buell, G, Lewis, C, Collo, G, North, RA & Surprenant, A (1996). An antagonist-insensitive P2X receptor expressed in epithelia and brain. *Embo J* 15, 55-62.
- Bultmann, R, Wittenburg, H, Pause, B, Kurz, G, Nickel, P & Starke, K (1996). P2-purinoceptor antagonists: III. Blockade of P2-purinoceptor subtypes and ecto-nucleotidases by compounds related to suramin. *Naunyn Schmiedebergs Arch Pharmacol* 354, 498-504.
- Burgard, EC, Niforatos, W, van Biesen, T, Lynch, KJ, Kage, KL, Touma, E, Kowaluk, EA & Jarvis, MF (2000). Competitive antagonism of recombinant P2X_{2/3} receptors by 2', 3'-O-(2,4,6-trinitrophenyl) adenosine 5'-triphosphate (TNP-ATP). *Mol Pharmacol* 58, 1502-10.

- Burnstock, G (1972). Purinergic nerves. *Pharmacol Rev* 24, 509-81.
- Burnstock, G, Campbell, G, Satchell, D & Smythe, A (1970). Evidence that adenosine triphosphate or a related nucleotide is the transmitter substance released by non-adrenergic inhibitory nerves in the gut. *Br J Pharmacol* 40, 668-88.
- Burnstock, G, Cocks, T, Kasakov, L & Wong, HK (1978). Direct evidence for ATP release from non-adrenergic, non-cholinergic ("purinergic") nerves in the guinea-pig taenia coli and bladder. *Eur J Pharmacol* 49, 145-9.
- Burnstock, G & Kennedy, C (1985). Is there a basis for distinguishing two types of P2-purinoceptor?. *Gen Pharmacol* 16, 433-40.
- Byrne, NG & Large, WA (1986). The effect of alpha, beta-methylene ATP on the depolarization evoked by noradrenaline (gamma-adrenoceptor response) and ATP in the immature rat basilar artery. *Br J Pharmacol* 88, 6-8.
- Caldwell, PC & Keynes, RD (1957). The utilization of phosphate bond energy for sodium extrusion from giant axons. *J Physiol* 137, 12-3P.
- Calvert, JA & Evans, RJ (2004). Heterogeneity of P2X receptors in sympathetic neurons: contribution of neuronal P2X1 receptors revealed using knockout mice. *Mol Pharmacology* 65, 139-148.
- Cao, L, Broomhead, HE, Young, MT & North, RA (2009). Polar residues in the second transmembrane domain of the rat P2X2 receptor that affect spontaneous gating, unitary conductance, and rectification. *J Neurosci* 29, 14257-64.
- Cao, L, Young, MT, Broomhead, HE, Fountain, SJ & North, RA (2007). Thr339-to-serine substitution in rat P2X2 receptor second transmembrane domain causes constitutive opening and indicates a gating role for Lys308. *J Neurosci* 27, 12916-23.
- Chen, BC, Lee, CM & Lin, WW (1996). Inhibition of ecto-ATPase by PPADS, suramin and reactive blue in endothelial cells, C6 glioma cells and RAW 264.7 macrophages. *Br J Pharmacol* 119, 1628-34.
- Chen, CC, Akopian, AN, Sivilotti, L, Colquhoun, D, Burnstock, G & Wood, JN (1995). A P2X purinoceptor expressed by a subset of sensory neurons. *Nature* 377, 428-31.
- Chessell, IP, Michel, AD & Humphrey, PP (1998). Effects of antagonists at the human recombinant P2X7 receptor. *Br J Pharmacol* 124, 1314-20.
- Clyne, JD, LaPointe, LD & Hume, RI (2002). The role of histidine residues in modulation of the rat P2X(2) purinoceptor by zinc and pH. *J Physiol* 539, 347-59.

- Cockayne, DA, Dunn, PM, Zhong, Y, Rong, W, Hamilton, SG, Knight, GE, Ruan, HZ, Ma, B, Yip, P, Nunn, P, McMahon, SB, Burnstock, G & Ford, AP (2005). P2X2 knockout mice and P2X2/P2X3 double knockout mice reveal a role for the P2X2 receptor subunit in mediating multiple sensory effects of ATP. *J Physiol* 567, 621-39.
- Coddou, C, Acuna-Castillo, C, Bull, P & Huidobro-Toro, JP (2007). Dissecting the facilitator and inhibitor allosteric metal sites of the P2X4 receptor channel: critical roles of CYS132 for zinc potentiation and ASP138 for copper inhibition. *J Biol Chem* 282, 36879-86.
- Coddou, C, Morales, B, Gonzalez, J, Grauso, M, Gordillo, F, Bull, P, Rassendren, F & Huidobro-Toro, JP (2003). Histidine 140 plays a key role in the inhibitory modulation of the P2X4 nucleotide receptor by copper but not zinc. *J Biol Chem* 278, 36777-85.
- Collo, G, North, RA, Kawashima, E, Merlo-Pich, E, Neidhart, S, Surprenant, A & Buell, G (1996). Cloning OF P2X5 and P2X6 receptors and the distribution and properties of an extended family of ATP-gated ion channels. *J Neurosci* 16, 2495-507.
- Coutinho-Silva, R, Knight, GE & Burnstock, G (2005). Impairment of the splenic immune system in P2X(2)/P2X(3) knockout mice. *Immunobiology* 209, 661-8.
- Crack, BE, Beukers, MW, McKechnie, KC, Ijzerman, AP & Leff, P (1994). Pharmacological analysis of ecto-ATPase inhibition: evidence for combined enzyme inhibition and receptor antagonism in P2X-purinoceptor ligands. *Br J Pharmacol* 113, 1432-8.
- Damer, S, Niebel, B, Czeche, S, Nickel, P, Ardanuy, U, Schmalzing, G, Rettinger, J, Mutschler, E & Lambrecht, G (1998). NF279: a novel potent and selective antagonist of P2X receptor-mediated responses. *Eur J Pharmacol* 350, R5-6.
- Davies, RE (1963). A Molecular Theory of Muscle Contraction: Calcium-Dependent Contractions with Hydrogen Bond Formation Plus Atp-Dependent Extensions of Part of the Myosin-Actin Cross-Bridges. *Nature* 199, 1068-74.
- De Clercq, E (1979). Suramin: a potent inhibitor of the reverse transcriptase of RNA tumor viruses. *Cancer Lett* 8, 9-22.
- Den Hertog, A, Van den Akker, J & Nelemans, A (1989). Suramin and the inhibitory junction potential in taenia caeci of the guinea-pig. *Eur J Pharmacol* 173, 207-9.
- Digby, H, Roberts, JA, Sutcliffe, MJ & Evans, RJ (2005). Contribution of conserved glycine residues to ATP action at human P2X1 receptors: mutagenesis indicates that the unique property of glycine at position 250 is important for channel function. *J Neurochem* 95, 1746-54.

- Ding, S & Sachs, F (1999). Single channel properties of P2X2 purinoceptors. *J Gen Physiol* 113, 695-720.
- Drury, AN & Szent-Gyorgyi, A (1929). The physiological activity of adenine compounds with especial reference to their action upon the mammalian heart. *J Physiol* 68, 213-37.
- Dubyak, GR (2003). Knock-out mice reveal tissue-specific roles of P2Y receptor subtypes in different epithelia. *Mol Pharmacol* 63, 773-6.
- Duckwitz, W, Hausmann, R, Aschrafi, A & Schmalzing, G (2006). P2X5 subunit assembly requires scaffolding by the second transmembrane domain and a conserved aspartate. *J Biol Chem* 281, 39561-72.
- Dunn, PM & Blakeley, AG (1988). Suramin: a reversible P2-purinoceptor antagonist in the mouse vas deferens. *Br J Pharmacol* 93, 243-5.
- Egan, TM, Haines, WR & Voigt, MM (1998). A domain contributing to the ion channel of ATP-gated P2X2 receptors identified by the substituted cysteine accessibility method. *J Neurosci* 18, 2350-9.
- El-Ajouz, S, Ray, D, Allsopp, RC & Evans, RJ (2011). Molecular basis of selective antagonism of the P2X1 receptor for ATP by NF449 and suramin; contribution of basic amino acids in the cysteine rich loop. *Br J Pharmacol*, paper in press.
- Ennion, SJ & Evans, RJ (2002). Conserved Cysteine Residues in the Extracellular Loop of the Human P2X1 Receptor Form Disulfide Bonds and Are Involved in Receptor Trafficking to the Cell Surface. *Mol Pharmacol* 61, 303-311.
- Ennion, SJ & Evans, RJ (2002b). P2X1 receptor subunit contribution to gating revealed by a dominant negative PKC mutant. *Biochemical and Biophysical Research Communications* 291, 611-6.
- Ennion, SJ, Ritson, J & Evans, RJ (2001). Conserved Negatively Charged Residues Are Not Required for ATP Action at P2X1 Receptors. *Biochemical and Biophysical Research Communications* 289, 700-704.
- Ennion, S, Hagan, S & Evans, RJ (2000). The Role of Positively Charged Amino Acids in ATP Recognition by Human P2X1 Receptors. *J Biol Chem* 275, 29361-29367.
- Erb, L, Garrad, R, Wang, Y, Quinn, T, Turner, JT & Weisman, GA (1995). Site-directed mutagenesis of P2U purinoceptors. Positively charged amino acids in transmembrane helices 6 and 7 affect agonist potency and specificity. *J Biol Chem* 270, 4185-8.
- Evans, RJ (2010). Structural interpretation of P2X receptor mutagenesis studies on drug action. *Br J Pharmacol* 161, 961-71.

- Evans, RJ (1996). Single channel properties of ATP-gated cation channels (P2X receptors) heterologously expressed in Chinese hamster ovary cells. *Neurosci Lett* 212, 212-4.
- Evans, RJ & Kennedy, C (1994). Characterization of P2-purinoceptors in the smooth muscle of the rat tail artery: a comparison between contractile and electrophysiological responses. *Br J Pharmacol* 113, 853-60.
- Evans, RJ, Lewis, C, Buell, G, Valera, S, North, RA & Surprenant, A (1995). Pharmacological characterization of heterologously expressed ATP-gated cation channels (P2x purinoceptors). *Mol Pharmacol* 48, 178-83.
- Finger, TE, Danilova, V, Barrows, J, Bartel, DL, Vigers, AJ, Stone, L, Hellekant, G & Kinnamon, SC (2005). ATP signaling is crucial for communication from taste buds to gustatory nerves. *Science* 310, 1495-9.
- Fonfria, E, Clay, WC, Levy, DS, Goodwin, JA, Roman, S, Smith, GD, Condreay, JP & Michel, AD (2008). Cloning and pharmacological characterization of the guinea pig P2X7 receptor orthologue. *Br J Pharmacol* 153, 544-56.
- Ford, KK, Matchett, M, Krause, JE & Yu, W (2005). The P2X3 antagonist P1, P5-di[inosine-5'] pentaphosphate binds to the desensitized state of the receptor in rat dorsal root ganglion neurons. *J Pharmacol Exp Ther* 315, 405-13.
- Fourneau, V, Tréfouel, J, & Vallée, J. (1924). Chemotherapeutic researches in the series "Bayer 205" Ureas of aminobenzoyl-aminonaphthalenesulfonic acids. *Ann. Inst. Pasteur* 38, 81.
- Foster, CJ, Prosser, DM, Agans, JM, Zhai, Y, Smith, MD, Lachowicz, JE, Zhang, FL, Gustafson, E, J., MF, Jr, Wiekowski, MT, Abbondanzo, SJ, Cook, DN, Bayne, ML, Lira, SA & Chintala, MS (2001). Molecular identification and characterization of the platelet ADP receptor targeted by thienopyridine antithrombotic drugs. *J Clin Invest* 107, 1591-8.
- Fountain, SJ, Parkinson, K, Young, MT, Cao, L, Thompson, CR & North, RA (2007). An intracellular P2X receptor required for osmoregulation in *Dictyostelium discoideum*. *Nature* 448, 200-3.
- Fredholm, BB, Abbracchio, MP, Burnstock, G, Daly, JW, Harden, TK, Jacobson, KA, Leff, P & Williams, M (1994). Nomenclature and classification of purinoceptors. *Pharmacol Rev* 46, 143-56.
- Galindo, A, Krnjevic, K & Schwartz, S (1967). Micro-iontophoretic studies on neurones in the cuneate nucleus. *J Physiol* 192, 359-77.
- Ganesh, VK, Muthuvel, SK, Smith, SA, Kotwal, GJ & Murthy, KH (2005). Structural basis for antagonism by suramin of heparin binding to vaccinia complement protein. *Biochemistry* 44, 10757-65.

- Garcia-Guzman, M, Soto, F, Gomez-Hernandez, JM, Lund, PE & Stuhmer, W (1997). Characterization of recombinant human P2X4 receptor reveals pharmacological differences to the rat homologue. *Mol Pharmacol* 51, 109-18.
- Gever, JR, Cockayne, DA, Dillon, MP, Burnstock, G & Ford, AP (2006). Pharmacology of P2X channels. *Pflugers Arch* 452, 513-37.
- Gonzales, EB, Kawate, T & Gouaux, E (2009). Pore architecture and ion sites in acid-sensing ion channels and P2X receptors. *Nature* 460, 599-604.
- Greig, AV, Linge, C, Healy, V, Lim, P, Clayton, E, Rustin, MH, McGrouther, DA & Burnstock, G (2003). Expression of purinergic receptors in non-melanoma skin cancers and their functional roles in A431 cells. *J Invest Dermatol* 121, 315-27.
- Grimm, U, Fuder, H, Moser, U, Bumert, HG, Mutschler, E & Lambrecht, G (1994). Characterization of the prejunctional muscarinic receptors mediating inhibition of evoked release of endogenous noradrenaline in rabbit isolated vas deferens. *Naunyn Schmiedebergs Arch Pharmacol* 349, 1-10.
- Guerrero-Alba, R, Valdez-Morales, E, Juarez, EH, Miranda-Morales, M, Ramirez-Martinez, JF, Espinosa-Luna, R & Barajas-Lopez, C (2010). Two suramin binding sites are present in guinea pig but only one in murine native P2X myenteric receptors. *Eur J Pharmacol* 626, 179-85.
- Guo, C, Masin, M, Qureshi, OS & Murrell-Lagnado, RD (2007). Evidence for functional P2X4/P2X7 heteromeric receptors. *Mol Pharmacol* 72, 1447-56.
- Haines, WR, Migita, K, Cox, JA, Egan, TM & Voigt, MM (2001). The first transmembrane domain of the P2X receptor subunit participates in the agonist-induced gating of the channel. *J Biol Chem* 276, 32793-8.
- Hamilton, SG & McMahon, SB (2000). ATP as a peripheral mediator of pain. *J Auton Nerv Syst* 81, 187-94.
- Hechler, B, Cattaneo, M & Gachet, C (2005). The P2 receptors in platelet function. *Semin Thromb Hemost* 31, 150-61.
- Hechler, B, Lenain, N, Marchese, P, Vial, C, Heim, V, Freund, M, Cazenave, JP, Cattaneo, M, Ruggeri, ZM, Evans, R & Gachet, C (2003). A role of the fast ATP-gated P2X1 cation channel in thrombosis of small arteries in vivo. *J Exp Med* 198, 661-7.
- Heppner, TJ, Werner, ME, Nausch, B, Vial, C, Evans, RJ & Nelson, MT (2009). Nerve-evoked purinergic signalling suppresses action potentials, Ca²⁺ flashes and contractility evoked by muscarinic receptor activation in mouse urinary bladder smooth muscle. *J Physiol* 587, 5275-88.

- Hiratsuka, T, Sakata, I & Uchida, K (1973). Synthesis and properties of N⁶-(2, 4-dinitrophenyl)-adenosine 5'-triphosphate, an analog of ATP. *J Biochem* 74, 649-59.
- Hogaboom, GK, O'Donnell, JP & Fedan, JS (1980). Purinergic receptors: photoaffinity analog of adenosine triphosphate is a specific adenosine triphosphate antagonist. *Science* 208, 1273-6.
- Hollopeter, G, Jantzen, HM, Vincent, D, Li, G, England, L, Ramakrishnan, V, Yang, RB, Nurden, P, Nurden, A, Julius, D & Conley, PB (2001). Identification of the platelet ADP receptor targeted by antithrombotic drugs. *Nature* 409, 202-7.
- Holton, FA & Holton, P (1954). The capillary dilator substances in dry powders of spinal roots; a possible role of adenosine triphosphate in chemical transmission from nerve endings. *J Physiol* 126, 124-40.
- Holton, P (1959). The liberation of adenosine triphosphate on antidromic stimulation of sensory nerves. *J Physiol* 145, 494-504.
- Hooft, RW, Vriend, G, Sander, C & Abola, EE (1996). Errors in protein structures. *Nature* 381, 272.
- Hoyle, CH, Knight, GE & Burnstock, G (1990). Suramin antagonizes responses to P₂-purinoceptor agonists and purinergic nerve stimulation in the guinea-pig urinary bladder and taenia coli. *Br J Pharmacol* 99, 617-21.
- Hulsmann, M, Nickel, P, Kassack, M, Schmalzing, G, Lambrecht, G & Markwardt, F (2003). NF449, a novel picomolar potency antagonist at human P₂X₁ receptors. *Eur J Pharmacol* 470, 1-7.
- Humphrey, PP, Buell, G, Kennedy, I, Khakh, BS, Michel, AD, Surprenant, A & Trezise, DJ (1995). New insights on P₂X purinoceptors. *Naunyn Schmiedebergs Arch Pharmacol* 352, 585-96.
- Ikeda, M (2007). Characterization of functional P₂X₁ receptors in mouse megakaryocytes. *Thromb Res* 119, 343-53.
- Inscho, EW, Cook, AK, Imig, JD, Vial, C & Evans, RJ (2003). Physiological role for P₂X₁ receptors in renal microvascular autoregulatory behavior. *J Clin Invest* 112, 1895-905.
- Jacobson, KA, Kim, YC, Wildman, SS, Mohanram, A, Harden, TK, Boyer, JL, King, BF & Burnstock, G (1998). A pyridoxine cyclic phosphate and its 6-azoaryl derivative selectively potentiate and antagonize activation of P₂X₁ receptors. *J Med Chem* 41, 2201-6.
- Jacobson, KA, Nikodijevic, O, Shi, D, Gallo-Rodriguez, C, Olah, ME, Stiles, GL & Daly, JW (1993). A role for central A₃-adenosine receptors. Mediation of behavioral depressant effects. *FEBS Lett* 336, 57-60.

Jahr, CE & Jessell, TM (1983). ATP excites a subpopulation of rat dorsal horn neurones. *Nature* 304, 730-3.

Jarvis, MF, Burgard, EC, McGaraughty, S, Honore, P, Lynch, K, Brennan, TJ, Subieta, A, Van Biesen, T, Cartmell, J, Bianchi, B, Niforatos, W, Kage, K, Yu, H, Mikusa, J, Wismer, CT, Zhu, CZ, Chu, K, Lee, CH, Stewart, AO, Polakowski, J, Cox, BF, Kowaluk, E, Williams, M, Sullivan, J & Faltynek, C (2002). A-317491, a novel potent and selective non-nucleotide antagonist of P2X3 and P2X2/3 receptors, reduces chronic inflammatory and neuropathic pain in the rat. *Proc Natl Acad Sci U S A* 99, 17179-84.

Jiang, LH, Kim, M, Spelta, V, Bo, X, Surprenant, A & North, RA (2003). Subunit arrangement in P2X receptors. *J Neurosci* 23, 8903-10.

Jiang, LH, Rassendren, F, Spelta, V, Surprenant, A & North, RA (2001). Amino acid residues involved in gating identified in the first membrane-spanning domain of the rat P2X(2) receptor. *J Biol Chem* 276, 14902-8.

Jiang, L, Rassendren, F, Surprenant, A & North, RA (2000). Identification of Amino Acid Residues Contributing to the ATP-binding Site of a Purinergic P2X Receptor. *J Biol Chem* 275, 34190-34196.

Jiang, R, Lemoine, D, Martz, A, Taly, A, Gonin, S, Prado de Carvalho, L, Specht, A & Grutter, T (2011). Agonist trapped in ATP-binding sites of the P2X2 receptor. *Proc Natl Acad Sci U S A* 108, 9066-71.

Jin, R, Banke, TG, Mayer, ML, Traynelis, SF & Gouaux, E (2003). Structural basis for partial agonist action at ionotropic glutamate receptors. *Nat Neurosci* 6, 803-10.

Jo, YH & Schlichter, R (1999). Synaptic corelease of ATP and GABA in cultured spinal neurons. *Nat Neurosci* 2, 241-5.

Kassack, MU, Braun, K, Ganso, M, Ullmann, H, Nickel, P, Boing, B, Muller, G & Lambrecht, G (2004). Structure-activity relationships of analogues of NF449 confirm NF449 as the most potent and selective known P2X1 receptor antagonist. *Eur J Med Chem* 39, 345-57.

Kaushansky, K (1999). The enigmatic megakaryocyte gradually reveals its secrets. *Bioessays* 21, 353-60.

Kawate, T, Michel, JC, Birdsong, WT & Gouaux, E (2009). Crystal structure of the ATP-gated P2X(4) ion channel in the closed state. *Nature* 460, 592-8.

Kennedy, C, Assis, TS, Currie, AJ & Rowan, EG (2003). Crossing the pain barrier: P2 receptors as targets for novel analgesics. *J Physiol* 553, 683-94.

- Kennedy, C, Tasker, PN, Gallacher, G & Westfall, TD (2007). Identification of atropine- and P2X1 receptor antagonist-resistant, neurogenic contractions of the urinary bladder. *J Neurosci* 27, 845-51.
- Khakh, BS, Burnstock, G, Kennedy, C, King, BF, North, RA, Seguela, P, Voigt, M & Humphrey, PP (2001). International union of pharmacology. XXIV. Current status of the nomenclature and properties of P2X receptors and their subunits. *Pharmacol Rev* 53, 107-18.
- Khakh, BS, Humphrey, PP & Surprenant, A (1995). Electrophysiological properties of P2X-purinoceptors in rat superior cervical, nodose and guinea-pig coeliac neurones. *J Physiol* 484 (Pt 2), 385-95.
- Khakh, BS, Michel, A & Humphrey, PP (1994). Estimates of antagonist affinities at P2X purinoceptors in rat vas deferens. *Eur J Pharmacol* 263, 301-9.
- Kidd, EJ, Grahames, CB, Simon, J, Michel, AD, Barnard, EA & Humphrey, PP (1995). Localization of P2X purinoceptor transcripts in the rat nervous system. *Mol Pharmacol* 48, 569-73.
- Kim, M, Spelta, V, Sim, J, North, RA & Surprenant, A (2001). Differential assembly of rat purinergic P2X7 receptor in immune cells of the brain and periphery. *J Biol Chem* 276, 23262-7.
- King, BF, Liu, M, Pintor, J, Gualix, J, Miras-Portugal, MT & Burnstock, G (1999). Diinosine pentaphosphate (IP5I) is a potent antagonist at recombinant rat P2X1 receptors. *Br J Pharmacol* 128, 981-8.
- King, BF, Townsend-Nicholson, A, Wildman, SS, Thomas, T, Spyer, KM & Burnstock, G (2000). Coexpression of rat P2X2 and P2X6 subunits in *Xenopus* oocytes. *J Neurosci* 20, 4871-7.
- Klapperstuck, M, Buttner, C, Nickel, P, Schmalzing, G, Lambrecht, G & Markwardt, F (2000). Antagonism by the suramin analogue NF279 on human P2X(1) and P2X(7) receptors. *Eur J Pharmacol* 387, 245-52.
- Koshimizu, T, Tomic, M, Koshimizu, M & Stojilkovic, SS (1998). Identification of Amino Acid Residues Contributing to Desensitization of the P2X2 Receptor Channel. *J Biol Chem* 273, 12853-12857.
- Kotnis, S, Bingham, B, Vasilyev, DV, Miller, SW, Bai, Y, Yeola, S, Chanda, PK, Bowlby, MR, Kaftan, EJ, Samad, TA & Whiteside, GT (2010). Genetic and functional analysis of human P2X5 reveals a distinct pattern of exon 10 polymorphism with predominant expression of the nonfunctional receptor isoform. *Mol Pharmacol* 77, 953-60.

- Krishtal, OA, Marchenko, SM & Pidoplichko, VI (1983). Receptor for ATP in the membrane of mammalian sensory neurones. *Neurosci Lett* 35, 41-5.
- Labasi, JM, Petrushova, N, Donovan, C, McCurdy, S, Lira, P, Payette, MM, Brissette, W, Wicks, JR, Audoly, L & Gabel, CA (2002). Absence of the P2X7 receptor alters leukocyte function and attenuates an inflammatory response. *J Immunol* 168, 6436-45.
- Lambrecht, G (1996). Design and pharmacology of selective P2-purinoceptor antagonists. *J Auton Pharmacol* 16, 341-4.
- Lambrecht, G, Friebe, T, Grimm, U, Windscheif, U, Bungardt, E, Hildebrandt, C, Baumert, HG, Spatz-Kumbel, G & Mutschler, E (1992). PPADS, a novel functionally selective antagonist of P2 purinoceptor-mediated responses. *Eur J Pharmacol* 217, 217-9.
- Lambrecht, G, Rettinger, J, Baumert, HG, Czeche, S, Damer, S, Ganso, M, Hildebrandt, C, Niebel, B, Spatz-Kumbel, G, Schmalzing, G & Mutschler, E (2000). The novel pyridoxal-5'-phosphate derivative PPNDS potently antagonizes activation of P2X(1) receptors. *Eur J Pharmacol* 387, R19-21.
- Lape, R, Colquhoun, D & Sivilotti, LG (2008). On the nature of partial agonism in the nicotinic receptor superfamily. *Nature* 454, 722-7.
- Lalo, U, Pankratov, Y, Wichert, SP, Rossner, MJ, North, RA, Kirchhoff, F & Verkhratskii, AN (2008). P2X1 and P2X5 subunits form the functional P2X receptor in mouse cortical astrocytes. *Journal of Neuroscience* 28 5473-5480.
- Layton, D & Azzi, A (1974). Suramin: a potent inhibitor of the calcium transport in sarcoplasmic reticulum. *Biochem Biophys Res Commun* 59, 322-5.
- Le Feuvre, R, Brough, D & Rothwell, N (2002). Extracellular ATP and P2X7 receptors in neurodegeneration. *Eur J Pharmacol* 447, 261-9.
- Le, KT, Babinski, K & Seguela, P (1998). Central P2X4 and P2X6 channel subunits coassemble into a novel heteromeric ATP receptor. *J Neurosci* 18, 7152-9.
- Le, KT, Boue-Grabot, E, Archambault, V & Seguela, P (1999). Functional and biochemical evidence for heteromeric ATP-gated channels composed of P2X1 and P2X5 subunits. *J Biol Chem* 274, 15415-9.
- Lecut, C, Frederix, K, Johnson, DM, Deroanne, C, Thiry, M, Faccinetto, C, Maree, R, Evans, RJ, Volders, PG, Bours, V & Oury, C (2009). P2X1 ion channels promote neutrophil chemotaxis through Rho kinase activation. *J Immunol* 183, 2801-9.
- Leff, P, Wood, BE & O'Connor, SE (1990). Suramin is a slowly-equilibrating but competitive antagonist at P2x-receptors in the rabbit isolated ear artery. *Br J Pharmacol* 101, 645-9.

- Lesage, F, Lauritzen, I, Duprat, F, Reyes, R, Fink, M, Heurteaux, C & Lazdunski, M (1997). The structure, function and distribution of the mouse TWIK-1 K⁺ channel. *FEBS Lett* 402, 28-32.
- Lewis, C, Neidhart, S, Holy, C, North, RA, Buell, G & Surprenant, A (1995). Coexpression of P2X2 and P2X3 receptor subunits can account for ATP-gated currents in sensory neurons. *Nature* 377, 432-5.
- Lewis, CJ & Evans, RJ (2000). Lack of run-down of smooth muscle P2X receptor currents recorded with the amphotericin permeabilized patch technique, physiological and pharmacological characterization of the properties of mesenteric artery P2X receptor ion channels. *Br J Pharmacol* 131, 1659-66.
- Li, M, Chang, TH, Silberberg, SD & Swartz, KJ (2008). Gating the pore of P2X receptor channels. *Nat Neurosci* 11, 883-7, DOI: nn.2151 [pii] 10.1038/nn.2151.
- Li, Z, Migita, K, Samways, DS, Voigt, MM & Egan, TM (2004). Gain and loss of channel function by alanine substitutions in the transmembrane segments of the rat ATP-gated P2X2 receptor. *J Neurosci* 24, 7378-86.
- Lominski, I & Gray, S (1961). Inhibition of lysozyme by 'Suramin'. *Nature* 192, 683.
- Lorca, RA, Coddou, C, Gazitua, MC, Bull, P, Arredondo, C & Huidobro-Toro, JP (2005). Extracellular histidine residues identify common structural determinants in the copper/zinc P2X2 receptor modulation. *J Neurochem* 95, 499-512.
- Ludlow, MJ, Durai, L & Ennion, SJ (2009). Functional characterization of intracellular Dictyostelium discoideum P2X receptors. *J Biol Chem* 284, 35227-39.
- Lustig, KD, Shiau, AK, Brake, AJ & Julius, D (1993). Expression cloning of an ATP receptor from mouse neuroblastoma cells. *Proc Natl Acad Sci U S A* 90, 5113-7.
- Lynch, KJ, Touma, E, Niforatos, W, Kage, KL, Burgard, EC, van Biesen, T, Kowaluk, EA & Jarvis, MF (1999). Molecular and functional characterization of human P2X(2) receptors. *Mol Pharmacol* 56, 1171-81.
- Ma, B, Ruan, HZ, Cockayne, DA, Ford, AP, Burnstock, G & Dunn, PM (2004). Identification of P2X receptors in cultured mouse and rat parasympathetic otic ganglion neurones including P2X knockout studies. *Neuropharmacology* 46, 1039-48.
- Ma, W, Korngreen, A, Weil, S, Cohen, EB, Priel, A, Kuzin, L & Silberberg, SD (2006). Pore properties and pharmacological features of the P2X receptor channel in airway ciliated cells. *J Physiol* 571, 503-17.
- MacKenzie, AB, Mahaut-Smith, MP & Sage, SO (1996). Activation of receptor-operated cation channels via P2X1 not P2T purinoceptors in human platelets. *J Biol Chem* 271, 2879-81.

- Marquez-Klaka, B, Rettinger, J, Bhargava, Y, Eisele, T & Nicke, A (2007). Identification of an intersubunit cross-link between substituted cysteine residues located in the putative ATP binding site of the P2X1 receptor. *J Neurosci* 27, 1456-66.
- Marti-Renom, MA, Stuart, AC, Fiser, A, Sanchez, R, Melo, F & Sali, A (2000). Comparative protein structure modeling of genes and genomes. *Annu Rev Biophys Biomol Struct* 29, 291-325..
- McIlwrath, SL, Davis, BM & Bielefeldt, K (2009). Deletion of P2X3 receptors blunts gastro-oesophageal sensation in mice. *Neurogastroenterol Motil* 21, 890-e66.
- McLaren, GJ, Lambrecht, G, Mutschler, E, Baumert, HG, Sneddon, P & Kennedy, C (1994). Investigation of the actions of PPADS, a novel P2x-purinoceptor antagonist, in the guinea-pig isolated vas deferens. *Br J Pharmacol* 111, 913-7.
- Michel, AD, Clay, WC, Ng, SW, Roman, S, Thompson, K, Condreay, JP, Hall, M, Holbrook, J, Livermore, D & Senger, S (2008). Identification of regions of the P2X(7) receptor that contribute to human and rat species differences in antagonist effects. *Br J Pharmacol* 155, 738-51.
- Michel, AD, Lundstrom, K, Buell, GN, Surprenant, A, Valera, S & Humphrey, PP (1996). The binding characteristics of a human bladder recombinant P2X purinoceptor, labelled with [3H]-alpha beta meATP, [35S]-ATP gamma S or [33P]-ATP. *Br J Pharmacol* 117, 1254-60.
- Mihich, E, Clarke, DA & Philips, FS (1954). Effect of adenosine analogs on isolated intestine and uterus. *J Pharmacol Exp Ther* 111, 335-42.
- Mio, K, Kubo, Y, Ogura, T, Yamamoto, T & Sato, C (2005). Visualization of the trimeric P2X2 receptor with a crown-capped extracellular domain. *Biochem Biophys Res Commun* 337, 998-1005.
- Mio, K, Ogura, T, Yamamoto, T, Hiroaki, Y, Fujiiyoshi, Y, Kubo, Y & Sato, C (2009). Reconstruction of the P2X(2) receptor reveals a vase-shaped structure with lateral tunnels above the membrane. *Structure* 17, 266-75.
- Mockett, BG, Housley, GD & Thorne, PR (1994). Fluorescence imaging of extracellular purinergic receptor sites and putative ecto-ATPase sites on isolated cochlear hair cells. *J Neurosci* 14, 6992-7007.
- Motin, L & Bennett, MR (1995). Effect of P2-purinoceptor antagonists on glutamatergic transmission in the rat hippocampus. *Br J Pharmacol* 115, 1276-80.
- Muller, V, Basset, G, Nelson, DR & Klingenberg, M (1996). Probing the role of positive residues in the ADP/ATP carrier from yeast. The effect of six arginine mutations of oxidative phosphorylation and AAC expression. *Biochemistry* 35, 16132-43.

- Mulryan, K, Gitterman, DP, Lewis, CJ, Vial, C, Leckie, BJ, Cobb, AL, Brown, JE, Conley, EC, Buell, G, Pritchard, CA & Evans, RJ (2000). Reduced vas deferens contraction and male infertility in mice lacking P2X1 receptors. *Nature* 403, 86-9.
- Nakazawa, K, Inoue, K, Fujimori, K & Takanaka, A (1991). Effects of ATP antagonists on purinoceptor-operated inward currents in rat pheochromocytoma cells. *Pflugers Arch* 418, 214-9.
- Nakazawa, K, Inoue, K, Fujimori, K & Takanaka, A (1990). ATP-activated single-channel currents recorded from cell-free patches of pheochromocytoma PC12 cells. *Neurosci Lett* 119, 5-8.
- Nakazawa, K, Inoue, K, Ito, K & Koizumi, S (1995). Inhibition by suramin and reactive blue 2 of GABA and glutamate receptor channels in rat hippocampal neurons. *Naunyn Schmiedebergs Arch Pharmacol* 351, 202-8.
- Nakazawa, K & Matsuki, N (1987). Adenosine triphosphate-activated inward current in isolated smooth muscle cells from rat vas deferens. *Pflugers Arch* 409, 644-6.
- Nakazawa, K & Ohno, Y (1999). Neighboring glycine residues are essential for P2X2 receptor/channel function. *Eur J Pharmacol* 370, R5-6.
- Newbolt, A, Stoop, R, Virginio, C, Surprenant, A, North, RA, Buell, G & Rassendren, F (1998). Membrane Topology of an ATP-gated Ion Channel (P2X Receptor). *J Biol Chem* 273, 15177-15182.
- Nichols, CG & Lopatin, AN (1997). Inward rectifier potassium channels. *Annu Rev Physiol* 59, 171-91.
- Nicke, A, Baumert, HG, Rettinger, J, Eichele, A, Lambrecht, G, Mutschler, E & Schmalzing, G (1998). P2X1 and P2X3 receptors form stable trimers: a novel structural motif of ligand-gated ion channels. *Embo J* 17, 3016-28.
- Nicke, A, Kerschensteiner, D & Soto, F (2005). Biochemical and functional evidence for heteromeric assembly of P2X1 and P2X4 subunits. *J Neurochem* 92, 925-33.
- North, RA (1996). P2X receptors: a third major class of ligand-gated ion channels. *Ciba Found Symp* 198, 91-105; discussion 105-9.
- North, RA & Surprenant, A (2000). Pharmacology of cloned P2X receptors. *Annu Rev Pharmacol Toxicol* 40, 563-80.
- Ong, WY, Motin, LG, Hansen, MA, Dias, LS, Ayrout, C, Bennett, MR & Balcar, VJ (1997). P2 purinoceptor blocker suramin antagonises NMDA receptors and protects against excitatory behaviour caused by NMDA receptor agonist (RS)-(tetrazol-5-yl)-glycine in rats. *J Neurosci Res* 49, 627-38.

- Ormond, SJ, Barrera, NP, Qureshi, OS, Henderson, RM, Edwardson, JM & Murrell-Lagnado, RD (2006). An uncharged region within the N terminus of the P2X6 receptor inhibits its assembly and exit from the endoplasmic reticulum. *Mol Pharmacol* 69, 1692-700.
- Oury, C, Kuijpers, MJ, Toth-Zsamboki, E, Bonnefoy, A, Danloy, S, Vreys, I, Feijge, MA, De Vos, R, Vermylen, J, Heemskerk, JW & Hoylaerts, MF (2003). Overexpression of the platelet P2X1 ion channel in transgenic mice generates a novel prothrombotic phenotype. *Blood* 101, 3969-76.
- Palygin, O, Lalo, U, Verkhratsky, A & Pankratov, Y (2010). Ionotropic NMDA and P2X1/5 receptors mediate synaptically induced Ca²⁺ signalling in cortical astrocytes. *Cell Calcium* 48, 225-31.
- Paukert, M, Osteroth, R, Geisler, HS, Brandle, U, Glowatzki, E, Ruppertsberg, JP & Grunder, S (2001). Inflammatory mediators potentiate ATP-gated channels through the P2X(3) subunit. *J Biol Chem* 276, 21077-82.
- Pauwels, RA & Joos, GF (1995). Characterization of the adenosine receptors in the airways. *Arch Int Pharmacodyn Ther* 329, 151-60.
- Radford, KM, Virginio, C, Surprenant, A, North, RA & Kawashima, E (1997). Baculovirus expression provides direct evidence for heteromeric assembly of P2X2 and P2X3 receptors. *J Neurosci* 17, 6529-33.
- Ralevic, V & Burnstock, G (1998). Receptors for purines and pyrimidines. *Pharmacol Rev* 50, 413-92.
- Ralevic, V & Burnstock, G (1996). Relative contribution of P2U- and P2Y-purinoceptors to endothelium-dependent vasodilatation in the golden hamster isolated mesenteric arterial bed. *Br J Pharmacol* 117, 1797-802.
- Ralevic, V, Hoyle, CH & Burnstock, G (1995). Pivotal role of phosphate chain length in vasoconstrictor versus vasodilator actions of adenine dinucleotides in rat mesenteric arteries. *J Physiol* 483 (Pt 3), 703-13.
- Rang, HPD, MM & Ritter JM (1999). *Pharmacology*, London, Churchill Livingstone.
- Rassendren, F, Buell, G, Newbolt, A, North, RA & Surprenant, A (1997). Identification of amino acid residues contributing to the pore of a P2X receptor. *EMBO J* 16, 3446-3454.
- Renard, S, Lingueglia, E, Voilley, N, Lazdunski, M & Barbry, P (1994). Biochemical analysis of the membrane topology of the amiloride-sensitive Na⁺ channel. *J Biol Chem* 269, 12981-6.

Rettinger, J, Braun, K, Hochmann, H, Kassack, MU, Ullmann, H, Nickel, P, Schmalzing, G & Lambrecht, G (2005). Profiling at recombinant homomeric and heteromeric rat P2X receptors identifies the suramin analogue NF449 as a highly potent P2X1 receptor antagonist. *Neuropharmacology* 48, 461-8.

Rettinger, J & Schmalzing, G (2004). Desensitization masks nanomolar potency of ATP for the P2X1 receptor. *J Biol Chem* 279, 6426-33.

Rettinger, J, Schmalzing, G, Damer, S, Muller, G, Nickel, P & Lambrecht, G (2000). The suramin analogue NF279 is a novel and potent antagonist selective for the P2X(1) receptor. *Neuropharmacology* 39, 2044-53.

Roberts, JA, Digby, HR, Kara, M, El Ajouz, S, Sutcliffe, MJ & Evans, RJ (2008). Cysteine substitution mutagenesis and the effects of methanethiosulfonate reagents at P2X2 and P2X4 receptors support a core common mode of ATP action at P2X receptors. *J Biol Chem* 283, 20126-36.

Roberts, JA & Evans, RJ (2007). Cysteine substitution mutants give structural insight and identify ATP binding and activation sites at P2X receptors. *J Neurosci* 27, 4072-82.

Roberts, JA & Evans, RJ (2005). Mutagenesis studies of conserved proline residues of human P2X receptors for ATP indicate that proline 272 contributes to channel function. *J Neurochem* 92, 1256-64.

Roberts, JA & Evans, RJ (2004). ATP binding at human P2X1 receptors. Contribution of aromatic and basic amino acids revealed using mutagenesis and partial agonists. *J Biol Chem* 279, 9043-55.

Roberts, JA, Valente, M, Allsopp, RC, Watt, D & Evans, RJ (2009). Contribution of the region Glu181 to Val200 of the extracellular loop of the human P2X1 receptor to agonist binding and gating revealed using cysteine scanning mutagenesis. *J Neurochem* 109, 1042-52.

Roberts, JA & Evans, RJ (2006). Contribution of conserved polar glutamine, asparagine and threonine residues and glycosylation to agonist action at human P2X1 receptors for ATP. *Journal of Neurochemistry* 96, 843-852.

Rong, W, Gourine, AV, Cockayne, DA, Xiang, Z, Ford, AP, Spyer, KM & Burnstock, G (2003). Pivotal role of nucleotide P2X2 receptor subunit of the ATP-gated ion channel mediating ventilatory responses to hypoxia. *J Neurosci* 23, 11315-21.

Rosenmund, C, Stern-Bach, Y & Stevens, CF (1998). The tetrameric structure of a glutamate receptor channel. *Science* 280, 1596-9.

- Salgado, AI, Cunha, RA & Ribeiro, JA (2000). Facilitation by P(2) receptor activation of acetylcholine release from rat motor nerve terminals: interaction with presynaptic nicotinic receptors. *Brain Res* 877, 245-50.
- Saugstad, JA, Roberts, JA, Dong, J, Zeitouni, S & Evans, RJ (2004). Analysis of the membrane topology of the acid-sensing ion channel 2a. *J Biol Chem* 279, 55514-9.
- Scase, TJ, Heath, MF, Allen, JM, Sage, SO & Evans, RJ (1998). Identification of a P2X1 Purinoceptor Expressed on Human Platelets*1. *Biochemical and Biophysical Research Communications* 242, 525-528.
- Schuetz, A, Min, J, Antoshenko, T, Wang, CL, Allali-Hassani, A, Dong, A, Loppnau, P, Vedadi, M, Bochkarev, A, Sternglanz, R & Plotnikov, AN (2007). Structural basis of inhibition of the human NAD⁺-dependent deacetylase SIRT5 by suramin. *Structure* 15, 377-89.
- Schumann, HJ (1958). [Noradrenalin and ATP content of sympathetic nerves]. *Naunyn Schmiedebergs Arch Exp Pathol Pharmacol* 233, 296-300.
- Schwarz, N, Fliegert, R, Adriouch, S, Seman, M, Guse, AH, Haag, F & Koch-Nolte, F (2009). Activation of the P2X7 ion channel by soluble and covalently bound ligands. *Purinergic Signal* 5, 139-49.
- Seguela, P, Hagehighi, A, Soghomonian, JJ & Cooper, E (1996). A novel neuronal P2x ATP receptor ion channel with widespread distribution in the brain. *J Neurosci* 16, 448-55.
- Sela, D, Ram, E & Atlas, D (1991). ATP receptor. A putative receptor-operated channel in PC-12 cells. *J Biol Chem* 266, 17990-4.
- Silberberg, SD, Chang, TH & Swartz, KJ (2005). Secondary structure and gating rearrangements of transmembrane segments in rat P2X4 receptor channels. *J Gen Physiol* 125, 347-59.
- Silberberg, SD, Li, M & Swartz, KJ (2007). Ivermectin Interaction with transmembrane helices reveals widespread rearrangements during opening of P2X receptor channels. *Neuron* 54, 263-74.
- Silberberg, SD & Swartz, KJ (2009). Structural biology: Trimeric ion-channel design. *Nature* 460, 580-1.
- Sim, JA, Broomhead, HE & North, RA (2008). Ectodomain lysines and suramin block of P2X1 receptors. *J Biol Chem* 283, 29841-6.
- Sim, JA, Chaumont, S, Jo, J, Ulmann, L, Young, MT, Cho, K, Buell, G, North, RA & Rassendren, F (2006). Altered hippocampal synaptic potentiation in P2X4 knock-out mice. *J Neurosci* 26, 9006-9.

- Sim, JA, Park, CK, Oh, SB, Evans, RJ & North, RA (2007). P2X1 and P2X4 receptor currents in mouse macrophages. *Br J Pharmacol* 152, 1283-90.
- Skorvaga, M, Theis, K, Mandavilli, BS, Kisker, C & Van Houten, B (2002). The beta - hairpin motif of UvrB is essential for DNA binding, damage processing, and UvrC-mediated incisions. *J Biol Chem* 277, 1553-9.
- Smith, FM, Humphrey, PP & Murrell-Lagnado, RD (1999). Identification of amino acids within the P2X2 receptor C-terminus that regulate desensitization. *J Physiol* 520 Pt 1, 91-9.
- Smolen, JE & Weissmann, G (1978). Mg²⁺-ATPase as a membrane ecto-enzyme of human granulocytes. Inhibitors, activators and response to phagocytosis. *Biochim Biophys Acta* 512, 525-38.
- Sneddon, P (1992). Suramin inhibits excitatory junction potentials in guinea-pig isolated vas deferens. *Br J Pharmacol* 107, 101-3.
- Sneddon, P & Burnstock, G (1984). ATP as a co-transmitter in rat tail artery. *Eur J Pharmacol* 106, 149-52.
- Snell, EE & Dimari, SJ (1980). Schiff base intermediates in enzyme catalysis. In: Boyer PD, The enzymes (12). Academic, NewYork, 335-370.
- Snyder, PM, McDonald, FJ, Stokes, JB & Welsh, MJ (1994). Membrane topology of the amiloride-sensitive epithelial sodium channel. *J Biol Chem* 269, 24379-83.
- Solle, M, Labasi, J, Perregaux, DG, Stam, E, Petrushova, N, Koller, BH, Griffiths, RJ & Gabel, CA (2001). Altered cytokine production in mice lacking P2X(7) receptors. *J Biol Chem* 276, 125-32.
- Soto, F, Garcia-Guzman, M & Stuhmer, W (1997). Cloned ligand-gated channels activated by extracellular ATP (P2X receptors). *J Membr Biol* 160, 91-100.
- Soto, F, Krause, U, Borchardt, K & Ruppelt, A (2003). Cloning, tissue distribution and functional characterization of the chicken P2X1 receptor. *FEBS Lett* 533, 54-8.
- Soto, F, Lambrecht, G, Nickel, P, Stuhmer, W & Busch, AE (1999). Antagonistic properties of the suramin analogue NF023 at heterologously expressed P2X receptors. *Neuropharmacology* 38, 141-9.
- Souslova, V, Cesare, P, Ding, Y, Akopian, AN, Stanfa, L, Suzuki, R, Carpenter, K, Dickenson, A, Boyce, S, Hill, R, Nebuenis-Oosthuizen, D, Smith, AJ, Kidd, EJ & Wood, JN (2000). Warm-coding deficits and aberrant inflammatory pain in mice lacking P2X3 receptors. *Nature* 407, 1015-7.

- Spehr, J, Spehr, M, Hatt, H & Wetzel, CH (2004). Subunit-specific P2X-receptor expression defines chemosensory properties of trigeminal neurons. *Eur J Neurosci* 19, 2497-510.
- Stjarne, L & Astrand, P (1984). Discrete events measure single quanta of adenosine 5'-triphosphate secreted from sympathetic nerves of guinea-pig and mouse vas deferens. *Neuroscience* 13, 21-8.
- Stoop, R, Surprenant, A & North, RA (1997). Different sensitivities to pH of ATP-induced currents at four cloned P2X receptors. *J Neurophysiol* 78, 1837-40.
- Surprenant, A, Rassendren, F, Kawashima, E, North, RA & Buell, G (1996). The cytolytic P2Z receptor for extracellular ATP identified as a P2X receptor (P2X7). *Science* 272, 735-8.
- Surprenant, A, Schneider, DA, Wilson, HL, Galligan, JJ & North, RA (2000). Functional properties of heteromeric P2X(1/5) receptors expressed in HEK cells and excitatory junction potentials in guinea-pig submucosal arterioles. *J Auton Nerv Syst* 81, 249-63.
- Surprenant, A, Buell, G & North, RA (1995). P2X receptors bring new structure to ligand-gated ion channels. *Trends in Neurosciences* 18, 224-229.
- Syed, NI, Tengah, A, Paul, A & Kennedy, C (2010). Characterisation of P2X receptors expressed in rat pulmonary arteries. *Eur J Pharmacol* 649, 342-8.
- Tanner, NK, Cordin, O, Banroques, J, Doere, M & Linder, P (2003). The Q motif: a newly identified motif in DEAD box helicases may regulate ATP binding and hydrolysis. *Mol Cell* 11, 127-38.
- Taylor, DA, Wiese, S, Faison, EP & Yarbrough, GG (1983). Pharmacological characterization of purinergic receptors in the rat vas deferens. *J Pharmacol Exp Ther* 224, 40-5.
- Theis, K, Chen, PJ, Skorvaga, M, Van Houten, B & Kisker, C (1999). Crystal structure of UvrB, a DNA helicase adapted for nucleotide excision repair. *EMBO J* 18, 6899-907.
- Torres, GE, Egan, TM & Voigt, MM (1999). Hetero-oligomeric assembly of P2X receptor subunits. Specificities exist with regard to possible partners. *J Biol Chem* 274, 6653-9.
- Torres, GE, Egan, TM & Voigt, MM (1998a). Topological analysis of the ATP-gated ionotropic P2X2 receptor subunit. *FEBS Lett* 425, 19-23.
- Torres, GE, Egan, TM & Voigt, MM (1998b). N-Linked glycosylation is essential for the functional expression of the recombinant P2X2 receptor. *Biochemistry* 37, 14845-51.

- Town, BW, Wills, ED, Wilson, EJ & Wormall, A (1950). Studies on suramin; the action of the drug on enzymes and some other proteins. General considerations. *Biochem J* 47, 149-58.
- Trapp, S, Haider, S, Jones, P, Sansom, MS & Ashcroft, FM (2003). Identification of residues contributing to the ATP binding site of Kir6.2. *EMBO J* 22, 2903-12, DOI: 10.1093/emboj/cdg282.
- Trezise, DJ, Bell, NJ, Khakh, BS, Michel, AD & Humphrey, PA (1994). P2 purinoceptor antagonist properties of pyridoxal-5-phosphate. *Eur J Pharmacol* 259, 295-300.
- Trezise, DJ, Kennedy, I & Humphrey, PP (1994b). The use of antagonists to characterize the receptors mediating depolarization of the rat isolated vagus nerve by alpha, beta-methylene adenosine 5'-triphosphate. *Br J Pharmacol* 112, 282-8.
- Trujillo, CA, Nery, AA, Martins, AH, Majumder, P, Gonzalez, FA & Ulrich, H (2006). Inhibition mechanism of the recombinant rat P2X(2) receptor in glial cells by suramin and TNP-ATP. *Biochemistry* 45, 224-33.
- Tsuda, M, Kuboyama, K, Inoue, T, Nagata, K, Tozaki-Saitoh, H & Inoue, K (2009). Behavioral phenotypes of mice lacking purinergic P2X4 receptors in acute and chronic pain assays. *Mol Pain* 5, 28
- Tsuda, M, Shigemoto-Mogami, Y, Koizumi, S, Mizokoshi, A, Kohsaka, S, Salter, MW & Inoue, K (2003). P2X4 receptors induced in spinal microglia gate tactile allodynia after nerve injury. *Nature* 424, 778-83.
- Ulmann, L, Hatcher, JP, Hughes, JP, Chaumont, S, Green, PJ, Conquet, F, Buell, GN, Reeve, AJ, Chessell, IP & Rassendren, F (2008). Up-regulation of P2X4 receptors in spinal microglia after peripheral nerve injury mediates BDNF release and neuropathic pain. *J Neurosci* 28, 11263-8
- Ulmann, L, Hirbec, H & Rassendren, F (2010). P2X4 receptors mediate PGE2 release by tissue-resident macrophages and initiate inflammatory pain. *EMBO J* 29, 2290-300
- Valera, S, Hussy, N, Evans, RJ, Adami, N, North, RA, Surprenant, A & Buell, G (1994). A new class of ligand-gated ion channel defined by P2x receptor for extracellular ATP. *Nature* 371, 516-9.
- Valera, S, Talabot, F, Evans, RJ, Gos, A, Antonarakis, SE, Morris, MA & Buell, GN (1995). Characterization and chromosomal localization of a human P2X receptor from the urinary bladder. *Receptors Channels* 3, 283-9.
- van Calker, D, Muller, M & Hamprecht, B (1979). Adenosine regulates via two different types of receptors, the accumulation of cyclic AMP in cultured brain cells. *J Neurochem* 33, 999-1005.

- Venkova, K, Milne, A & Krier, J (1994). Contractions mediated by alpha 1-adrenoceptors and P2-purinoceptors in a cat colon circular muscle. *Br J Pharmacol* 112, 1237-43.
- Verdonk, ML, Cole, JC, Hartshorn, MJ, Murray, CW & Taylor, RD (2003). Improved protein-ligand docking using GOLD. *Proteins* 52, 609-23
- Vial, C & Evans, RJ (2000). P2X receptor expression in mouse urinary bladder and the requirement of P2X1 receptors for functional P2X receptor responses in the mouse urinary bladder smooth muscle. *Br J Pharmacol* 131, 1489-1495.
- Vial, C, Hechler, B, Leon, C, Cazenave, JP & Gachet, C (1997). Presence of P2X1 purinoceptors in human platelets and megakaryoblastic cell lines. *Thromb Haemost* 78, 1500-4.
- Vial, C, Roberts, JA & Evans, RJ (2004). Molecular properties of ATP-gated P2X receptor ion channels. *Trends Pharmacol Sci* 25, 487-93.
- Vial, C, Rolf, MG, Mahaut-Smith, MP & Evans, RJ (2002). A study of P2X1 receptor function in murine megakaryocytes and human platelets reveals synergy with P2Y receptors. *Br J Pharmacol* 135, 363-72
- Vial, C & Evans, RJ (2002). P2X1 Receptor-Deficient Mice Establish the Native P2X Receptor and a P2Y6-Like Receptor in Arteries. *Mol Pharmacol* 62, 1438-1445.
- Vials, AJ & Burnstock, G (1994). The effect of suramin on vasodilator responses to ATP and 2-methylthio-ATP in the Sprague-Dawley rat coronary vasculature. *Eur J Pharmacol* 251, 299-302.
- Villalonga, N, Escalada, A, Vicente, R, Sanchez-Tillo, E, Celada, A, Solsona, C & Felipe, A (2007). Kv1.3/Kv1.5 heteromeric channels compromise pharmacological responses in macrophages. *Biochem Biophys Res Commun* 352, 913-8.
- Virginio, C, Robertson, G, Surprenant, A & North, RA (1998). Trinitrophenyl-substituted nucleotides are potent antagonists selective for P2X1, P2X3, and heteromeric P2X2/3 receptors. *Mol Pharmacol* 53, 969-73.
- von Kugelgen, I (2006). Pharmacological profiles of cloned mammalian P2Y-receptor subtypes. *Pharmacol Ther* 110, 415-32.
- von Kugelgen, I, Bultmann, R & Starke, K (1990). Interaction of adenine nucleotides, UTP and suramin in mouse vas deferens: suramin-sensitive and suramin-insensitive components in the contractile effect of ATP. *Naunyn Schmiedebergs Arch Pharmacol* 342, 198-205.
- Vulchanova, L, Arvidsson, U, Riedl, M, Wang, J, Buell, G, Surprenant, A, North, RA & Elde, R (1996). Differential distribution of two ATP-gated channels (P2X receptors) determined by immunocytochemistry. *Proc Natl Acad Sci U S A* 93, 8063-7.

- Walker, JE, Saraste, M, Runswick, MJ & Gay, NJ (1982). Distantly related sequences in the alpha- and beta-subunits of ATP synthase, myosin, kinases and other ATP-requiring enzymes and a common nucleotide binding fold. *EMBO J* 1, 945-51.
- Wang, X, Dakshinamurti, K, Musat, S & Dhalla, NS (1999). Pyridoxal 5'-phosphate is an ATP-receptor antagonist in freshly isolated rat cardiomyocytes. *J Mol Cell Cardiol* 31, 1063-72.
- Watanabe, T & Inesi, G (1982). The use of 2',3'-O-(2,4,6-trinitrophenyl) adenosine 5'-triphosphate for studies of nucleotide interaction with sarcoplasmic reticulum vesicles. *J Biol Chem* 257, 11510-6.
- Watano, T, Calvert, JA, Vial, C, Forsythe, ID & Evans, RJ (2004). P2X receptor subtype-specific modulation of excitatory and inhibitory synaptic inputs in the rat brainstem. *J Physiol* 558, 745-57.
- Webb, TE, Simon, J, Krishek, BJ, Bateson, AN, Smart, TG, King, BF, Burnstock, G & Barnard, EA (1993). Cloning and functional expression of a brain G-protein-coupled ATP receptor. *FEBS Lett* 324, 219-25.
- Welford, LA, Cusack, NJ & Hourani, SM (1987). The structure-activity relationships of ectonucleotidases and of excitatory P2-purinoceptors: evidence that dephosphorylation of ATP analogues reduces pharmacological potency. *Eur J Pharmacol* 141, 123-30.
- Welford, LA, Cusack, NJ & Hourani, SM (1986). ATP analogues and the guinea-pig taenia coli: a comparison of the structure-activity relationships of ectonucleotidases with those of the P2-purinoceptor. *Eur J Pharmacol* 129, 217-24.
- Werner, P, Seward, EP, Buell, GN & North, RA (1996). Domains of P2X receptors involved in desensitization. *Proc Natl Acad Sci U S A* 93, 15485-90.
- Westfall, DP, Hogaboom, GK, Colby, J, O'Donnell, JP & Fedan, JS (1982). Direct evidence against a role of ATP as the nonadrenergic, noncholinergic inhibitory neurotransmitter in guinea pig tenia coli. *Proc Natl Acad Sci U S A* 79, 7041-5.
- Wiederstein, M & Sippl, MJ (2007). ProSA-web: interactive web service for the recognition of errors in three-dimensional structures of proteins. *Nucleic Acids Res* 35, W407-10.
- Wildman, SS, King, BF & Burnstock, G (1998). Zinc modulation of ATP-responses at recombinant P2X2 receptors and its dependence on extracellular pH. *Br J Pharmacol* 123, 1214-20
- Wilkinson, GF, Purkiss, JR & Boarder, MR (1993). The regulation of aortic endothelial cells by purines and pyrimidines involves co-existing P2y-purinoceptors and nucleotide receptors linked to phospholipase C. *Br J Pharmacol* 108, 689-93.

- Wilkinson, WJ, Jiang, LH, Surprenant, A & North, RA (2006). Role of ectodomain lysines in the subunits of the heteromeric P2X_{2/3} receptor. *Mol Pharmacol* 70, 1159-63.
- Windscheif, U, Ralevic, V, Baumert, HG, Mutschler, E, Lambrecht, G & Burnstock, G (1994). Vasoconstrictor and vasodilator responses to various agonists in the rat perfused mesenteric arterial bed: selective inhibition by PPADS of contractions mediated via P2x-purinoceptors. *Br J Pharmacol* 113, 1015-21.
- Wolf, C, Rosefort, C, Fallah, G, Kassack, MU, Hamacher, A, Bodnar, M, Wang, H, Illes, P, Kless, A, Bahrenberg, G, Schmalzing, G & Hausmann, R (2011). Molecular determinants of potent P2X₂ antagonism identified by functional analysis, mutagenesis, and homology docking. *Mol Pharmacol* 79, 649-61.
- Wong, AY, Burnstock, G & Gibb, AJ (2000). Single channel properties of P2X ATP receptors in outside-out patches from rat hippocampal granule cells. *J Physiol* 527 Pt 3, 529-47.
- Worthington, RA, Smart, ML, Gu, BJ, Williams, DA, Petrou, S, Wiley, JS & Barden, JA (2002). Point mutations confer loss of ATP-induced human P2X₇ receptor function. *FEBS Lett* 512, 43-6.
- Xiong, K, Peoples, RW, Montgomery, JP, Chiang, Y, Stewart, RR, Weight, FF & Li, C (1999). Differential modulation by copper and zinc of P2X₂ and P2X₄ receptor function. *J Neurophysiol* 81, 2088-94.
- Yamamoto, K, Korenaga, R, Kamiya, A & Ando, J (2000). Fluid shear stress activates Ca²⁺ influx into human endothelial cells via P2X₄ purinoceptors. *Circ Res* 87, 385-91.
- Yan, Z, Liang, Z, Obsil, T & Stojilkovic, SS (2006). Participation of the Lys313-Ile333 sequence of the purinergic P2X₄ receptor in agonist binding and transduction of signals to the channel gate. *J Biol Chem* 281, 32649-59.
- Young, MT, Pelegrin, P & Surprenant, A (2007). Amino acid residues in the P2X₇ receptor that mediate differential sensitivity to ATP and BzATP. *Mol Pharmacol* 71, 92-100.
- Young, MT, Fisher, JA, Fountain, SJ, Ford, RC, North, RA & Khakh, BS (2008). Molecular shape, architecture, and size of P2X₄ receptors determined using fluorescence resonance energy transfer and electron microscopy. *J Biol Chem* 283, 26241-51.
- Young, MT, Zhang, YH, Cao, L, Broomhead, H & Jiang, LH (2008b). Role of the domain encompassing Arg304-Ile328 in rat P2X₂ receptor conformation revealed by alterations in complex glycosylation at Asn298. *Biochem J* 416, 137-43.
- Zemkova, H, Yan, Z, Liang, Z, Jelinkova, I, Tomic, M & Stojilkovic, SS (2007). Role of aromatic and charged ectodomain residues in the P2X₄ receptor functions. *J Neurochem* 102, 1139-50.

- Zhong, Y, Dunn, PM, Xiang, Z, Bo, X & Burnstock, G (1998). Pharmacological and molecular characterization of P2X receptors in rat pelvic ganglion neurons. *Br J Pharmacol* 125, 771-81.
- Zhou, X, Tan, TC, Valiyaveettil, S, Go, ML, Kini, RM, Velazquez-Campoy, A & Sivaraman, J (2008). Structural characterization of myotoxic ecarpholin S from *Echis carinatus* venom. *Biophys J* 95, 3366-80.
- Zhou, Z, Monsma, LR & Hume, RI (1998). Identification of a site that modifies desensitization of P2X2 receptors. *Biochem Biophys Res Commun* 252, 541-5.
- Ziganshin, AU, Hoyle, CH, Bo, X, Lambrecht, G, Mutschler, E, Baumert, HG & Burnstock, G (1993). PPADS selectively antagonizes P2X-purinoceptor-mediated responses in the rabbit urinary bladder. *Br J Pharmacol* 110, 1491-5.
- Ziganshin, AU, Hoyle, CH, Lambrecht, G, Mutschler, E, Bumert, HG & Burnstock, G (1994). Selective antagonism by PPADS at P2X-purinoceptors in rabbit isolated blood vessels. *Br J Pharmacol* 111, 923-9.
- Ziyal, R, Pfaff, O, Windschief, U, BO, X, Nickel, P, Ardanuy, U, Burnstock, G, Mutschler, E & Lambrecht, G (1994). A novel P2-purinoceptor ligand which displays selectivity for the P2X-purinoceptor subtype. *Drug Dev Res* 31 336.
- Ziyal, R, Ziganshin, AU, Nickel, P, Ardanuy, U, Mutschler, E, Lambrecht, G & Burnstock, G (1997). Vasoconstrictor responses via P2X-receptors are selectively antagonized by NF023 in rabbit isolated aorta and saphenous artery. *Br J Pharmacol* 120, 954-60.